Météo-France
Centre National de Recherches Météorologiques

ARPEGE-Climate Version 5.2

Algorithmic Documentation

September 2011

Contents

1

Basic hypotheses and related constants

ARPEGE-IFS is a complex code designed not only for weather forecast or climate simulation, but also for data assimilation, forecast pre- and post-processing. It has been extended, diversified and complexified since 1986 jointly by Météo-France and ECMWF. The present documentation restricts to the description of the French climate version of ARPEGE-IFS. Some features are not compatible with the version used by ECMWF. In this case, we will use the term ARPEGE. Some features are specific to the French climate version, and we will use the term ARPEGE-CLIMAT. The core of the model is cycle 32T0 of ARPEGE-IFS.

ARPEGE-CLIMAT is now an atmosphere-only model. So the calculations concerning the surface boundary layer, vegetation, snow cover and soil are done in SURFEX (SURFace EXternalisée), which is another model. SURFEX simulates the exchanges of momentum, heat, water, carbon dioxide concentration or chemical species between the surface and the atmosphere. It uses the concept of 'tile' to describe the surface (nature, town, sea, water) and can perform different parametrizations. Each surface grid box is made of the four adjacent tiles. The coverage of each of these surfaces is known through the global ECOCLIMAP database. SURFEX receives atmospheric forcing terms, runs the surface schemes, computes the average surface fluxes over the nature, town, sea and water weighted by their respective fraction and sends them back to the atmosphere in addition to radiatives terms. All this information is then used as lower boundary conditions for the atmospheric radiation and turbulent schemes. The present document gives some information about SURFEX and how SURFEX interacts with the atmosphere. The complete documentation on SURFEX (algorithmic and user's guide) is available on the site.

The model relies upon a geometrical assumption: the thin layer approximation, and a certain number of phenomenological assumptions such as the law of perfect gases or the hydrostatic approximation. With these assumptions a set of basic constants is presented here.

1 Astronomical constants

This section follows the last recommendations of the *International Astronomical Union*. It should be noted that the formulas are not valid for dates too far away from the 1st January 2000 (more than one century).

1.1 Calendar

The calendar used is the *Gregorian* calendar. The dates are given in the form:

$$AAAAMMJJ,\ sssss$$

with:

$$\begin{cases} AAAA & \text{year,} \\ MM & \text{month,} \\ JJ & \text{day,} \\ sssss & \text{seconds in the day.} \end{cases}$$

1.2 Time

The length of the day is:

$$d = 86400\ s$$

Time t is expressed in seconds, the date of reference being 20000101.43200 (2451545.0 in *Julian* calendar). It is negative before this date and positive afterward. t is deduced from the calendar date by:

$$t = (JD - 2451545)86400 + sssss$$

with JD, date in the *Julian* calendar (E indicating the integer part):

$$JD = 1720994.5 + K + \mathrm{E}(365.25a) + \mathrm{E}(30.601(m+1)) + JJ$$

and:

$$a = \begin{cases} AAAA, & \text{if } MM > 2 \\ AAAA - 1, & \text{if } MM \leq 2 \end{cases}$$

$$m = \begin{cases} MM, & \text{if } MM > 2 \\ MM + 12, & \text{if } MM \leq 2 \end{cases}$$

$$K = 2 - \mathrm{E}(a/100) + \mathrm{E}(\mathrm{E}(a/100)/4)$$

1.3 Astronomical elements

In the following we set:

$$\theta = t/(dy_j)$$

with:

$$y_j = 365.25 \text{ days}$$

The constants between square brackets are not used in the model; however, we provide them because they form a consistent set with those needed by the model.

	half great axis	e_a	$=$	$149597870000\ m \pm 5\,10^{-5}$
[	excentricity			0.016704 ± 10^{-4}]
[	inclination			$0 \pm 2\,10^{-4}$]
	mean longitude	e_l	$=$	$1.7535 + 6.283076\,\theta$
[	longitude of perihelion			$1.79661 + 0.0000563\,\theta$]
[	longitude of ascending node			6.1937 if $t < 0$, 3.0521 if $t > 0$]
	mean anomaly	e_M	$=$	$6.240075 + 6.283020\,\theta$
	Sun-Earth distance	R_s	$=$	$e_a(1.0001 - 0.0163\sin(e_l)$
				$+0.0037\cos(e_l))$

1.4 Sun trajectory relative to Earth

	mean longitude	l_s	$=$	$4.8951 + 6.283076\,\theta$
	true longitude	L_s	$=$	$4.8952 + 6.283320\,\theta$
				$-0.0075\sin(e_l) - 0.0326\cos(e_l)$
				$-0.0003\sin(2e_l) + 0.0002\cos(2e_l)$
[	true latitude			0]

obliquity	ϵ_s	=	0.409093
declination	δ_s	=	$\mathrm{Asin}(\sin(\epsilon_s)\sin L_s)$
[right ascension			$0 \leq \alpha_s \leq 2\pi$]
[			$\cos(\alpha_s)\cos(\delta_s) = \cos(L_s)$]
[			$\sin(\alpha_s)\cos(\delta_s) = \sin(L_s)\cos(\epsilon_s)$]
equation of time	Et	=	$591.8\sin(2l_s) - 459.4\sin(e_M)$
(true solar time −			$+39.5\sin(e_M)\cos(2l_s)$
mean solar time)			$-12.7\sin(4l_s) - 4.8\sin(2e_M)$

Over the period 1980–2020, the relative accuracy on R_s is of $5\,10^{-4}$, the accuracy on the various angles is of $5\,10^{-4}\ rd$, and that on equation of time is of $10\ s$. These constants implicitly define the length of the sidereal year:

$$y_s = \frac{2\pi\, d\, y_j}{6.283076}$$

and therefore the length of sidereal day:

$$d_s = \frac{d}{1 + d/y_s}$$

and earth rotation:

$$\Omega = \frac{2\pi}{d_s}$$

2 Geometry, geoid

2.1 Geometry

We mentioned in the introduction that the thin layer assumption is the base of Arpege-IFS equations. To make sense, it requires the choice of one surface on which the equations are written.

As we write the momentum equation in vorticity-divergence, the Laplacian operator must have his kernel reduced to constant functions; we suppose moreover than the surface is of revolution around the axis of rotation of the planet.

2.2 Coordinate system

On the horizontal, we use longitude λ varying from 0 to 2π to parametrize the circles of revolution. The East is directed towards increasing longitudes. In the orthogonal direction, we use μ variable from -1 at South pole to $+1$ at North pole (by definition) to parametrize the surface generator.

On the vertical, we use a coordinate η varying from 0 at the top of the fluid to 1 at the bottom. This vertical coordinate has no geometrical significance with the ordinary metrics. The 3d metrics is obtained as the product of horizontal metrics by vertical one.

2.3 Geoid

The preceding assumptions imply that the vertical coordinate does not have any geometrical significance and that gravity is not explicitly used. In place we need two infinitely close equipotential surfaces between which the equations are written. We make the additional assumption that for the description of the Earth, equipotential surfaces are spheres of radius a (average value of the reference ellipsoid):

$$a = 6371229\ m$$

To transform an elevation value into geopotential in $J\,kg^{-1}$, it should be multiplied by the conventional value:

$$g = 9.80665\ m\,s^{-2}$$

If we used an ellipsoid instead of a sphere, gravity would vary with the latitude according to a formula close to that of Clairault, but it would not appear explicitly in the equations and the preceding remarks would remain valid.

Because of the sphericity assumption, the notions of "North, East, longitude ..." used above should not be taken in their geographical meaning since, as we will see further, the pole of the coordinate system is not necessarily in the Arctic.

3 Fundamental constants

light speed	c	=	$299792458\ m\,s^{-1}$
Planck's constant	h	=	$6.6260755\,10^{-34}\ J\,s$
Boltzmann's constant	k	=	$1.380658\,10^{-23}\ J\,K^{-1}$
Avogadro's number	N	=	$6.0221367\,10^{23}\ mol^{-1}$

4 Radiation

Stefan-Boltzmann's constant	σ	=	$\dfrac{2\pi^5 k^4}{15c^2h^3}$
solar constant	I_0	=	$1370\ W\,m^{-2}$

5 Thermodynamics, gas phase

The fluid is a mixture of dry air, of water in gas, liquid and solid phases.

gas constant	$\mathcal{R}$	=	Nk
dry air molar mass	M_a	=	$28.9644\,10^{-3}\ kg\,mol^{-1}$
water vapor molar mass	M_v	=	$18.0153\,10^{-3}\ kg\,mol^{-1}$

$$R_a = \frac{\mathcal{R}}{M_a}\ J\,kg^{-1}K^{-1}$$

$$R_v = \frac{\mathcal{R}}{M_v}\ J\,kg^{-1}K^{-1}$$

It is supposed here that dry air and water vapor are perfect gases. The maximum error is 0.1 %.

$$c_{p_a} = \frac{7}{2}\,R_a$$

$$c_{v_a} = \frac{5}{2}\,R_a$$

These quantities are not constant in the atmosphere. But this assumption is coherent with the approximation of perfect gases, and the error introduced is less than 1 %.

$$c_{p_v} = 4\,R_v$$

$$c_{v_v} = 3\,R_v$$

In the case of water vapor, supposing them constant leads to an error less than 5 %.

If one activates the optional "prognostic physical parametrizations", atmosphere contains also four species: cloud water, cloud ice, rain water and rain ice.

6 Thermodynamics, liquid phase

water molar mass	M_l	=	M_v
massic volume	v_l	=	0

$$c_{p_l} = c_{v_l} = c_l = 4.218\,10^3\ J\,kg^{-1}K^{-1}(\text{value at triple point } T_t)$$

The identity between c_{p_l} and c_{v_l} is very well satisfied and is coherent with the constancy of the massic volume. The fact that c_l is constant is satisfied with less than 1 % error in the temperature range $[0°C, 30°C]$, but the error grows for the negative temperatures and reaches 12.5 % at $-40°C$.

7 Thermodynamics, solid phase

$$M_g = M_l$$

$$v_g = v_l$$

$$c_{p_g} = c_{v_g} = c_g = 2.106\,10^3\ J\,kg^{-1}K^{-1}(\text{value at } T_t)$$

Actually, c_g decreasing linearly with the temperature, the error introduced is 13 % at $-40°C$.

8 Thermodynamics, phase transition

triple point	T_t	=	273.16 K

8.1 Vaporization

$$L_v(T) = L_v(T_t) + (c_{p_v} - c_l)(T - T_t)$$

$$L_v(T_t) = 2.5008\,10^6\ J\,kg^{-1}$$

It is supposed that L_v is independent of the pressure, which is accurate at 0.5 %, and is coherent with $v_l = 0$.

8.2 Sublimation

$$L_s(T) = L_s(T_t) + (c_{p_v} - c_g)(T - T_t)$$

$$L_s(T_t) = 2.8345\,10^6\ J\,kg^{-1}$$

$c_{p_v} - c_g$ is an order of magnitude weaker than $c_{p_v} - c_l$; however, to neglect the variation of L_s with temperature, it would be necessary to write: $c_g = c_{p_v}$.

8.3 Melting

$$L_f = L_s - L_v$$

9 Consequences on saturation

With $v_l = 0$, Clapeyron's equation becomes:

$$\frac{d\ln(e_s)}{dT} = \frac{L_v}{R_v T^2}$$

Using the expression of L_v, and integrating from:

$$(T_t,\ e_s(T_t) = 611.14\ Pa\,)$$

yields:

$$\ln(e_s) = \alpha_l - \frac{\beta_l}{T} - \gamma_l \ln T$$

with:

$$\begin{aligned}
\alpha_l &= \ln(e_s(T_t)) + \frac{\beta_l}{T_t} + \gamma_l \ln T_t \\
\beta_l &= L_v(T_t)/R_v + \gamma_l T_t \\
\gamma_l &= \frac{c_l - c_{pv}}{R_v}
\end{aligned}$$

In the presence of ice, the formula remains valid if the $_l$ are replaced by $_g$.

10 Thermodynamic functions

The thermodynamic functions are gathered in the block of declarations FCT-TRM. They are divided into two groups: the first corresponds to the absolute functions and to the second to the approximate functions whose approximations are consistent with the above statements. This module is inserted in all the subroutines which require thermodynamic calculations. Thus coherence between the various parts of the code is ensured.

Notations:

- T_t temperature of water triple point
- $\gamma_l = (c_l - c_{p_v})/R_v$
- $\gamma_i = (c_i - c_{p_v})/R_v$
- $\beta_l = L_v(T_t)/R_v + \gamma_l T_t$
- $\beta_i = L_s(T_t)/R_v + \gamma_i T_t$
- $\alpha_l = \ln e_s(T_t) + \beta_l/T_t + \gamma_l \ln T_t$
- $\alpha_i = \ln e_s(T_t) + \beta_i/T_t + \gamma_i \ln T_t$
- δ index for liquid/solid calculation: $\delta = \begin{cases} 1 & \text{if liquid whatever T} \\ 0 & \text{if solid whatever T} \end{cases}$
- δ_T index of temperature positivity: $\delta_T = \begin{cases} 1 & \text{if } \mathrm{T} \geq \mathrm{T}_t \\ 0 & \text{otherwise} \end{cases}$

10.1 Absolute Functions

Latent heat of vaporization:

$$L_v(T) = \mathrm{RLV}(T) = L_v(T_t) + (c_{p_v} - c_l)(T - T_t)$$

Latent heat of sublimation:

$$L_s(T) = \mathrm{RLS}(T) = L_s(T_t) + (c_{p_v} - c_i)(T - T_t)$$

Latent heat of fusion:

$$L_f(T) = \mathrm{RLF}(T) = L_s(T) - L_v(T)$$

Saturation pressure above liquid water:

$$e_{sl}(T) = \mathrm{ESW}(T) = \exp\left[\alpha_l - \frac{\beta_l}{T} - \gamma_l \ln T\right]$$

Saturation pressure above solid water:

$$e_{si}(T) = \mathrm{ESS}(T) = \exp\left[\alpha_i - \frac{\beta_i}{T} - \gamma_i \ln T\right]$$

Saturation pressure above liquid/solid water:

$$\begin{aligned} e_s(T) &= \mathrm{ES}(T) \\ &= \exp\left[\alpha_l + (\alpha_i - \alpha_l)\delta_T - \frac{\beta_l + (\beta_i - \beta_l)\delta_T}{T} - (\gamma_l + (\gamma_i - \gamma_l)\delta_T)\ln T\right] \end{aligned}$$

10.2 Functions in the model parametrizations

Saturation pressure:

$$\begin{aligned} e_s(T,\delta) &= \mathrm{FOEW}(T,\delta) \\ &= \exp\left[\alpha_l + (\alpha_i - \alpha_l)\delta - \frac{\beta_l + (\beta_i - \beta_l)\delta}{T} - (\gamma_l + (\gamma_i - \gamma_l)\delta)\ln T\right] \end{aligned}$$

Derivative of the logarithm of the saturation pressure:

$$\frac{\partial \ln e_s}{\partial T}(T,\delta) = \mathrm{FODLEW}(T,\delta) = \frac{\beta_l + (\beta_i - \beta_l)\delta - (\gamma_l + (\gamma_i - \gamma_l)\delta)T}{T^2}$$

Saturation specific moisture:

$$q_s = \mathrm{FOQS}(\frac{e_s}{p}) = \frac{e_s/p}{1 + (R_v/R_a - 1)\max(0,\, 1 - e_s/p)}$$

This formulation makes it possible to have:

$$q_s = \begin{cases} \dfrac{e_s/R_v}{(p - e_s)/R_a + e_s/R_v} & \text{if } e_s(T) \le p \\ \dfrac{e_s}{p} & \text{if } e_s(T) \ge p \end{cases}$$

Derivative saturation of specific moisture:

$$\frac{\partial q_s}{\partial T} = \mathrm{FODQS}(q_s,\, \frac{e_s}{p},\, \frac{\partial \ln e_s}{\partial T}) = \frac{q_s - q_s^2}{1 - e_s/p} \frac{\partial \ln e_s}{\partial T}$$

Latent heat:

$$\begin{aligned} L(T,\delta) &= \mathrm{FOLH}(T,\delta) \\ &= R_v \left[\beta_l + (\beta_i - \beta_l)\delta - (\gamma_l + (\gamma_i - \gamma_l)\delta)T\right] \\ &= L_v(T_t) + \left[L_s(T_t) - L_v(T_t)\right]\delta + \left[c_{p_v} - c_l + (c_l - c_i)\delta\right](T - T_t) \end{aligned}$$

2

Dynamics equations

1 Introduction

Each equation of the model can generally write as:

$$\frac{dX}{dt} = \mathcal{A} + \mathcal{F}$$

where X is a prognostic variable, the evolution of which one wants to know. $\mathcal{A}$ represents all the effects which can be explicitly represented for the current resolution (often named "adiabatic effects"). They are:

- Coriolis force (momentum equation)
- pressure-gradient force term (momentum equation)
- conversion term (temperature equation)
- divergence term (continuity equation)

$\mathcal{F}$ represents all the sub-scale effects (often named "diabatic effects") which are calculated by physical parametrization routines. They are:

- radiation
- clouds and turbulence
- large-scale precipitations
- vertical diffusion

- convection
- orographic gravity wave drag
- soil, snow and vegetation

The time derivative of X means the total temporal derivative, including advection, also known as Lagrangian derivative.

2 Primitive equations in Eulerian form

Making the hydrostatic assumption, we use for vertical coordinate a hybrid coordinate $\eta(p, p_s)$ derived from the pressure coordinate p and terrain following. It must satisfy:

$$\begin{cases} \eta(0, p_s) &= 0 \\ \eta(p_s, p_s) &= 1 \\ \dfrac{\partial \eta}{\partial p}(p, p_s) &> 0 \end{cases}$$

This vertical coordinate η is defined by two functions $A(\eta)$ and $B(\eta)$, in such a way that the pressure at a given point is:

$$p = A(\eta) + B(\eta) p_s$$

where p_s is surface pressure. We have:

$$A(0) = 0 \quad A(1) = 0$$
$$B(0) = 0 \quad B(1) = 1$$

ensuring for η-surfaces to follow orography at the bottom and to be pressure surfaces at the top. The model does not need to explicitly know the functional form of A and B, only their values at the interface of the layers are necessary.

The hydrostatic assumption leads to the equation:

$$\frac{\partial \Phi}{\partial \eta} = -\frac{RT}{p} \frac{\partial p}{\partial \eta}$$

which is used as a diagnostic equation to calculate geopotential Φ on level p by an integral starting at the lower boundary condition $\Phi(p_s) = \Phi_s$.

The evolution of the parameters which define the state of the atmosphere, horizontal wind $\vec{v}$, temperature T and mass moisture ratio q_v is controlled by the following equations, where the total temporal derivative is written as:

$$\frac{d\,X}{d\,t} = \frac{\partial X}{\partial t} + \vec{v}\,\nabla X + \dot{\eta}\frac{\partial X}{\partial \eta} \tag{1}$$

Momentum equation

$$\frac{d\,\overrightarrow{v}}{d\,t} + \underbrace{2\Omega \times \vec{v}}_{\text{Coriolis}} + \underbrace{RT\nabla \ln p + \nabla\Phi}_{\text{pressure force}} = -g\frac{\partial \eta}{\partial p}\frac{\partial \overrightarrow{F_{\vec{v}}}}{\partial \eta} + \overrightarrow{S_{\vec{v}}} + \overrightarrow{K_{\vec{v}}} \tag{2}$$

To conserve momentum in the vertical discretization, the acceleration term due to the pressure force is transformed into:

$$\frac{\partial \eta}{\partial p}\left(\Phi\nabla\frac{\partial p}{\partial \eta} - \frac{\partial \Phi \nabla p}{\partial \eta}\right) + \nabla\Phi$$

Thermodynamics equation

$$\frac{d\,T}{d\,t} - \underbrace{\kappa\,T\,\frac{\omega}{p}}_{\text{conversion}} = -\frac{g}{c_p}\frac{\partial \eta}{\partial p}\frac{\partial F_h}{\partial \eta} + S_h + K_h \tag{3}$$

Moisture equation

$$\frac{d\,q_v}{d\,t} = -g\frac{\partial \eta}{\partial p}\frac{\partial F_{q_v}}{\partial \eta} + S_{q_v} + K_{q_v} \tag{4}$$

In the above equations one takes:

$$\begin{aligned} R &= q_a R_a + q_v R_v \\ c_p &= q_a c_{p_a} + q_v c_{p_v} \\ \kappa &= \frac{R}{c_p} \end{aligned}$$

The terms in the right-hand members of Equations (2), (3) and (4) respectively represent vertical fluxes (noted F), sources (noted S) and horizontal diffusion (noted K) of momentum, enthalpy, and specific moisture.

The continuity equation is written as:

$$\frac{\partial}{\partial \eta}\left(\frac{\partial p}{\partial t}\right) + \nabla\cdot\left(\vec{v}\frac{\partial p}{\partial \eta}\right) + \frac{\partial}{\partial \eta}\left(\dot{\eta}\frac{\partial p}{\partial \eta}\right) = -g\frac{\partial F_p}{\partial \eta} \tag{5}$$

F_p is the mass flux, no source term being considered.

By integrating, one obtains the evolution equation of surface pressure:

$$\frac{\partial p_s}{\partial t} = -\int_0^1 \nabla \cdot \left(\vec{v} \frac{\partial p}{\partial \eta} \right) d\eta - g F_p(1)$$

vertical velocity in pressure coordinate:

$$\omega = -\int_0^\eta \nabla \cdot \left(\vec{v} \frac{\partial p}{\partial \eta} \right) d\eta + \vec{v} \cdot \nabla p - g F_p(\eta)$$

and vertical velocity:

$$\dot{\eta} \frac{\partial p}{\partial \eta} = -\frac{\partial p}{\partial t} - \int_0^\eta \nabla \cdot \left(\vec{v} \frac{\partial p}{\partial \eta} \right) d\eta - g F_p(\eta)$$

The momentum equations are integrated divergence and rotational form:

$$\begin{aligned} \frac{\partial \zeta}{\partial t} &= \nabla \times \left(\overrightarrow{H_{\vec{v}}} - g \frac{\partial \eta}{\partial p} \frac{\partial \overrightarrow{F_{\vec{v}}}}{\partial \eta} + \overrightarrow{S_{\vec{v}}} \right) + K_\zeta \\ \frac{\partial D}{\partial t} &= \nabla \cdot \left(\overrightarrow{H_{\vec{v}}} - g \frac{\partial \eta}{\partial p} \frac{\partial \overrightarrow{F_{\vec{v}}}}{\partial \eta} + \overrightarrow{S_{\vec{v}}} \right) - \Delta(\Phi + E_c) + K_D \end{aligned}$$

with:

$$\begin{aligned} H_u &= (\zeta + f) v - \dot{\eta} \frac{\partial u}{\partial \eta} + \frac{\partial \eta}{\partial p} \frac{\partial \Phi}{\partial \eta} \frac{1}{a} \frac{\partial p}{\partial \lambda} \\ H_v &= -(\zeta + f) u - \dot{\eta} \frac{\partial v}{\partial \eta} + \frac{\partial \eta}{\partial p} \frac{\partial \Phi}{\partial \eta} \frac{(1 - \mu^2)}{a} \frac{\partial p}{\partial \mu} \\ E_c &= \frac{1}{2} \left(u^2 + v^2 \right) \end{aligned}$$

The wind is calculated from velocity potential χ and stream function ψ by:

$$\vec{v} = \nabla \chi + \nabla \times \psi$$

Velocity potential and stream function are obtained from divergence and vorticity by solving Poisson equations:

$$\begin{aligned}\chi &= \Delta^{-1} D \\ \psi &= \Delta^{-1} \zeta\end{aligned}$$

It is in these last three relations, the kernel of the Laplacian Δ is implicitly supposed to reduce to constant functions. It is then equivalent to know the wind or divergence and vorticity pair. This property is true on the sphere as well as on the torus.

3 Variable mesh

3.1 Stretched and tilted grid

ARPEGE makes it possible to increase the horizontal resolution on part of the sphere, while preserving locally the isotropy (Courtier and Geleyn, 1988). For that one uses a new set of coordinates (λ', μ'). First, North Pole is shifted at the point of coordinates (λ_0, μ_0) which becomes the new pole (or tilted pole). One defines new coordinates (λ_b, μ_b) by:

$$\begin{aligned}\mu_b &= \mu_0\mu + \sqrt{1-\mu_0^2}\sqrt{1-\mu^2}\cos(\lambda-\lambda_0) \\ \cos\lambda_b &= (1-\mu_b^2)^{-\frac{1}{2}}(\mu\sqrt{1-\mu_0^2} - \mu_0\sqrt{1-\mu^2}\cos(\lambda-\lambda_0)) \\ \sin\lambda_b &= (1-\mu_b^2)^{-\frac{1}{2}}\sqrt{1-\mu^2}\sin(\lambda_0-\lambda)\end{aligned}$$

The origin longitude is the one which contains the geographical North Pole. Reciprocally:

$$\begin{aligned}\mu &= \mu_0\mu_b + \sqrt{1-\mu_0^2}\sqrt{1-\mu_b^2}\cos\lambda_b \\ \cos(\lambda-\lambda_0) &= (1-\mu^2)^{-\frac{1}{2}}(\mu_b\sqrt{1-\mu_0^2} - \mu_0\sqrt{1-\mu_b^2}\cos\lambda_b) \\ \sin(\lambda_0-\lambda) &= (1-\mu^2)^{-\frac{1}{2}}\sqrt{1-\mu_b^2}\sin\lambda_b\end{aligned}$$

Then, one carries out a stretching of the latitudes (without modifying longitudes, $\lambda' = \lambda_b$) obtained by homothety of a factor c on stereographic projection at the pole of stretching. It comes:

$$\mu' = \frac{(1-c^2)+(1+c^2)\mu_b}{(1+c^2)+(1-c^2)\mu_b}$$

and reciprocally:

$$\mu_b = \frac{(c^2-1)+(c^2+1)\mu'}{(c^2+1)+(c^2-1)\mu'}$$

3.2 Impact on the equations

The conformal transform of η-surfaces described above changes the model equations. The fields are represented by a base of functions defined on transformed surfaces. The equations are integrated on original surfaces. However modifications are necessary in the calculation of the horizontal derivative. It consists of multiplying them by a scale factor m. In the case of the present transform, this factor is:

$$m = \frac{c^2+1}{2c} + \frac{c^2-1}{2c}\mu'$$

At the pole of dilation ($\mu' = 1$) this factor is c. At the pole of contraction ($\mu' = -1$) it is $1/c$. The horizontal wind thus becomes:

$$\vec{v} = m\,\vec{v}\,'$$

and the horizontal gradient:

$$\nabla = m\,\nabla'$$

In going from the real sphere to the transformed sphere, the velocity potential χ and the stream function ψ, which are scalars, are invariant. The main modification consists of solving Poisson equation in a more complicated form:

$$\begin{aligned} \chi &= \Delta'^{-1}\frac{D}{m^2} \\ \psi &= \Delta'^{-1}\frac{\zeta}{m^2} \end{aligned}$$

where Δ'^{-1} is the same formal operator as Δ^{-1} but on the transformed sphere. As a consequence, the state variable of the model is: $\zeta' = \zeta/m^2$ and $D' = D/m^2$ (or equivalently ψ and χ).

The equations become then:

$$\begin{aligned} \frac{\partial \zeta'}{\partial t} &= \nabla' \times \left[\frac{1}{m}\left(\overrightarrow{H_{\vec{v}}} - g\frac{\partial \eta}{\partial p}\frac{\partial \overrightarrow{F_{\vec{v}}}}{\partial \eta} + \overrightarrow{S_{\vec{v}}}\right)\right] + K_{\zeta'} \\ \frac{\partial D'}{\partial t} &= \nabla' \cdot \left[\frac{1}{m}\left(\overrightarrow{H_{\vec{v}}} - g\frac{\partial \eta}{\partial p}\frac{\partial \overrightarrow{F_{\vec{v}}}}{\partial \eta} + \overrightarrow{S_{\vec{v}}}\right)\right] - \Delta'(\Phi + E_c) + K_{D'} \end{aligned}$$

3.3 Impact on post-processing

The files produced by ARPEGE-CLIMAT for restarting as well as for post-processing contain the model prognostic variables, even though, in the case of post-processing, ψ and χ are transformed into $\vec{v}'$. This is also true for momentum fluxes. As a consequence, both components of wind velocity or surface stress have to be multiplied by m before any comparison with observations or other model outputs. This operation can be done, for example, at the same time as the conversion from ARPEGE format to another format.

4 Lagrangian form of the primitive equations

The Lagrangian form of the equations of momentum, thermodynamics and moisture are respectively (2), (3) and (4). The continuity equation (5) has as a Lagrangian form:

$$\frac{d}{dt}\left(\frac{\partial p}{\partial \eta}\right) = -\frac{\partial p}{\partial \eta}\left(D + \frac{\partial \dot{\eta}}{\partial \eta}\right) - g\frac{\partial F_p}{\partial \eta} \tag{6}$$

It can take another form, more adapted to the semi-Lagrangian advection method :

$$\frac{d}{dt}\left[\left(\frac{\partial p}{\partial \eta}\right) J\right] = -g\frac{\partial F_p}{\partial \eta} \tag{7}$$

where J indicates the Jacobian of the transform which associates the position of a point at time t with its position at a reference time t_o.

On the stretched and tilted sphere, the continuity equation (6) becomes:

$$\frac{d}{dt}\left(\frac{\partial p}{\partial \eta}\right) = -\frac{\partial p}{\partial \eta}\left(m^2 D' + \frac{\partial \dot{\eta}}{\partial \eta}\right) - g\frac{\partial F_p}{\partial \eta}$$

and its Lagrangian form (7):

$$\frac{d}{dt}\left[\left(\frac{\partial p}{\partial \eta}\right)\frac{J'}{m^2}\right] = -g\frac{\partial F_p}{\partial \eta}$$

The momentum equation (2) becomes:

$$\frac{d\, m\vec{v}'}{d\, t} + m\left[2\Omega \times \vec{v}' + RT\nabla' \ln p + \nabla'\Phi\right] = -g\frac{\partial \eta}{\partial p}\frac{\partial \overrightarrow{F_{\vec{v}}}}{\partial \eta} + \overrightarrow{S_{\vec{v}}} + \overrightarrow{K_{\vec{v}}}$$

The equations for thermodynamics (3) and moisture (4) are formally unchanged.

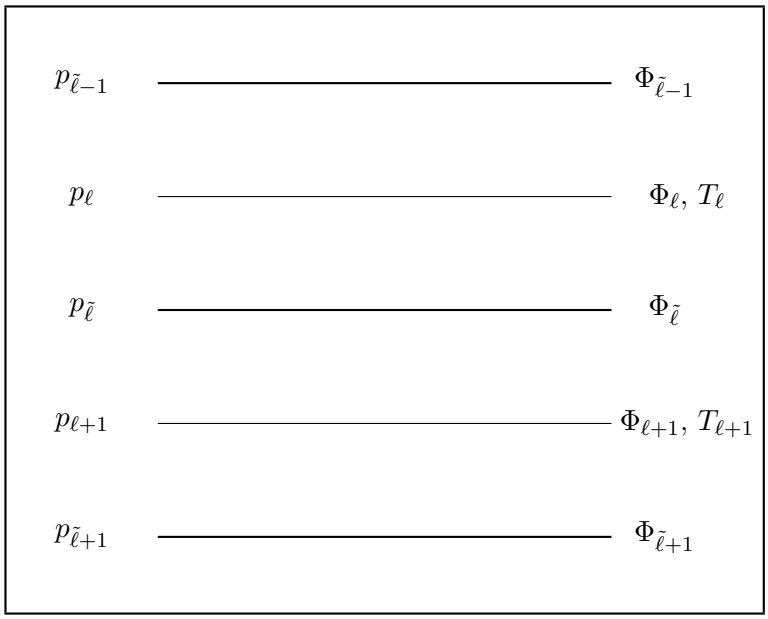

Figure 1: Position of variables on the vertical.

5 Vertical discretization

5.1 Model vertical levels

The atmosphere is vertically split into L layers, defined by the pressures at their interfaces, which are calculated by:

$$p_{\tilde{\ell}} = A_{\tilde{\ell}} + B_{\tilde{\ell}} p_s \qquad \tilde{\ell} = 0, \ldots, L \tag{8}$$

$A_{\tilde{\ell}}$ and $B_{\tilde{\ell}}$ are constants which define the vertical coordinate. The vertical distribution of the variables is presented in Figure 1, indices $_\ell$ relating to the mid-layers (also named full levels) and indices $_{\tilde{\ell}}$ to the inter-layers (also named half levels).

The values of $A_{\tilde{\ell}}$ and $B_{\tilde{\ell}}$ are imposed to the model. In earlier versions of ARPEGE-CLIMAT they were calculated from analytical functions. In recent cycles, one uses the same vertical discretization as in forecast models (Météo-France or ECMWF).

5.2 Vertical discretization of the equations

The vertical discretization scheme is defined according to Simmons and Burridge (1981). One introduces the operator δ which represents the variation

of a variable between the two ends of a layer:

$$\delta p_\ell = p_{\tilde{\ell}} - p_{\tilde{\ell}-1}$$

Index ℓ will be omitted when there is no ambiguity.

Continuity equation

The continuity equation is written as (F_m being the mass flux due to water cycle):

$$\frac{\partial}{\partial \eta}\left(\frac{\partial p}{\partial t}\right) + \nabla \cdot \left(\vec{v}\frac{\partial p}{\partial \eta}\right) + \frac{\partial}{\partial \eta}\left(\dot{\eta}\frac{\partial p}{\partial \eta}\right) = F_m$$

For a given layer, one writes it as:

$$\frac{\partial(\delta p)}{\partial t} = -\nabla \cdot (\vec{v}\,\delta p) - \delta\left(\dot{\eta}\frac{\partial p}{\partial \eta}\right) + F_m$$

One will note, in the following, the physical term of the discretized equation in the same way as the corresponding term of the continuous equation.

Summing on the vertical, one obtains the evolution equation of surface pressure:

$$\frac{\partial p_s}{\partial t} = -\sum_{\ell=1}^{L} [\delta p\, D + \delta B\, \vec{v} \cdot \nabla p_s] - g(P + E)$$

since:

$$\nabla \delta p = \delta B\, \nabla p_s$$

The vertical speed is obtained by summing the continuity equation from the top to the current level:

$$w_{\tilde{\ell}} = \left(\dot{\eta}\frac{\partial p}{\partial \eta}\right)_{\tilde{\ell}} = \sum_{k=1}^{\ell} [-\delta B_k\, \vec{v}_k \cdot \nabla p_s - \delta p_k D_k + F_{mk}] - B_{\tilde{\ell}}\frac{\partial p_s}{\partial t}$$

Eulerian advection

The vertical advections in momentum, thermodynamics and moisture equations are calculated using the scheme:

$$\left(w\frac{\partial X}{\partial p}\right)_\ell = \frac{1}{2\delta p}\left[w_{\tilde{\ell}}(X_{\ell+1} - X_\ell) + w_{\tilde{\ell}-1}(X_\ell - X_{\ell-1})\right]$$

This scheme ensures conservation of X and X^2. It results from the following form of the vertical advection:

$$w\frac{\partial X}{\partial p} = \frac{\partial wX}{\partial p} - X\frac{\partial w}{\partial p}$$

with the interpolation:

$$X_{\tilde{\ell}} = \frac{1}{2}(X_\ell + X_{\ell+1})$$

In the case of the semi-Lagrangian scheme, see Chapter 4.

Hydrostatic equation

The equation of hydrostatic balance is integrated by using the centered scheme:

$$\Phi_{\tilde{\ell}-1} = \Phi_{\tilde{\ell}} - R_\ell T_\ell \ln\frac{p_{\tilde{\ell}-1}}{p_{\tilde{\ell}}}$$

Which gives, summing from the surface:

$$\Phi_{\tilde{\ell}} = \Phi_s + \sum_{k=L}^{\ell+1} R_k T_k \ln\frac{p_{\tilde{k}}}{p_{\tilde{k}-1}}$$

where Φ_s indicates surface geopotential.

To calculate the geopotential in the mid-layers one writes:

$$\Phi_\ell = \Phi_{\tilde{\ell}} + \alpha_\ell R_\ell T_\ell$$

where:

$$\begin{cases} \alpha_1 & = 1 \\ \alpha_\ell & = 1 - \dfrac{p_{\tilde{\ell}-1}}{\delta p_\ell}\ln\dfrac{p_{\tilde{\ell}}}{p_{\tilde{\ell}-1}} \end{cases} \tag{9}$$

The expression of Φ_ℓ is consistent with the discretization of the form:

$$\Phi = \frac{\partial p\Phi}{\partial p} + RT \tag{10}$$

Discretization of the pressure force

For conserving angular momentum, one writes the acceleration term due to the pressure force as:

$$\begin{aligned}\nabla\Phi + RT\,\nabla \ln p &= \left[\nabla\left(\Phi\frac{\partial p}{\partial \eta}\right) - \frac{\partial(\Phi\,\nabla p)}{\partial \eta}\right]\left(\frac{\partial p}{\partial \eta}\right)^{-1} \\ &= \nabla\Phi + \left[\Phi\nabla\left(\frac{\partial p}{\partial \eta}\right) - \frac{\partial(\Phi\,\nabla p)}{\partial \eta}\right]\left(\frac{\partial p}{\partial \eta}\right)^{-1}\end{aligned}$$

The discretization of this term yields:

$$(RT\nabla \ln p)_\ell = R_\ell T_\ell \underbrace{\frac{1}{\delta p_\ell}\left[\delta B_\ell + \frac{C_\ell}{\delta p_\ell}\ln\frac{p_{\tilde{\ell}}}{p_{\tilde{\ell}-1}}\right]}_{\text{ZRTGR}} \cdot\nabla p_s$$

with:

$$C_\ell = A_{\tilde{\ell}}B_{\tilde{\ell}-1} - A_{\tilde{\ell}-1}B_{\tilde{\ell}}$$

Term ZRTGR is also used in the calculation of the energy transformation term. It can be written in the simpler form:

$$\frac{1}{\delta p}\left[\alpha_\ell \delta B_\ell + B_{\tilde{\ell}-1}\ln\frac{p_{\tilde{\ell}}}{p_{\tilde{\ell}-1}}\right]$$

Energy transformation term

The energy transformation term is written as:

$$\frac{RT}{c_p}\frac{\omega}{p}$$

One writes:

$$\frac{\omega}{p} = \vec{v}\cdot\nabla \ln p - \frac{1}{p}\int_0^\eta \left[\vec{v}\cdot\nabla\left(\frac{\partial p}{\partial \eta}\right) + D\frac{\partial p}{\partial \eta} + F_m\right] d\eta$$

The first term of the right-hand member is evaluated in the same way as the corresponding term of the momentum equation:

$$(\vec{v}\cdot\nabla\ln p)_\ell = \underbrace{\frac{1}{\delta p_\ell}\left[\delta B_\ell + \frac{C_\ell}{\delta p_\ell}\ln\frac{p_{\tilde{\ell}}}{p_{\tilde{\ell}-1}}\right]}_{\text{ZRTGR}}\vec{v}_\ell\cdot\nabla p_s$$

and the second term:

$$-\frac{1}{\delta p_\ell}\left[\alpha_\ell\left(\nabla\cdot(\vec{v}_\ell\delta p_\ell)+F_{m\ell}\right)+\left(\ln\frac{p_{\tilde{\ell}}}{p_{\tilde{\ell}-1}}\right)\sum_{k=1}^{\ell-1}\left(\nabla\cdot(\vec{v}_k\delta p_k)+F_{mk}\right)\right]$$

where:

$$\nabla\cdot(\vec{v}_\ell\,\delta p_\ell) = \vec{v}_\ell\cdot\nabla\delta p_\ell + \delta p_\ell\, D_\ell$$

This discretization results from writing the last term in the form:

$$\frac{1}{p}\int X d\eta = \left(\frac{\partial p}{\partial\eta}\right)^{-1}\frac{\partial\ln p}{\partial\eta}\int X d\eta = \left[\frac{\partial}{\partial\eta}\left(\ln p\int X d\eta\right) - X\ln p\right]\left(\frac{\partial p}{\partial\eta}\right)^{-1}$$

in which one calculates the last logarithm of the pressure by:

$$\ln p = \frac{d}{d\,p}\left(p\ln p\right) - 1$$

3

Spectral transforms

1 Introduction

ARPEGE-IFS is a spectral global model. One part of computations is made in spectral space (semi-implicit scheme, horizontal diffusion scheme), the other part in grid-point space on a grid defined by a Gaussian quadrature. It is therefore necessary to perform spectral transforms from spectral space to grid-point space or vice-versa. The present chapter aims at giving a brief summary of the spectral method. For more algorithmic details on can report to Rochas and Courtier (1992) or to Temperton (1991). Computation aspects are described in details in Yessad (2007a). Most subroutines are located in an independent library named TFL.

For a global spectral model, spectral transforms are a combination of a Legendre transform and a Fourier transform. A spectral limited-area model like ALADIN uses a double Fourier representation for spectral fields.

2 Spectral representation

2.1 Spherical harmonics

The spherical Laplacian operator Δ on a sphere Σ of radius a admits as eigenvalues family $-n(n+1)/a^2$ with an order of $2n+1$. The eigenvectors are the surface spherical harmonics. An orthogonal base of an eigenspace is given by:

$$Y_n^m = P_n^m(\mu) e^{im\lambda}$$

where μ is the sine of the latitude and λ longitude. The $P_n^m(\mu)$ are the first-type Legendre polynomials. The standardization of the $P_n^m(\mu)$ is such as:

$$\iint_\sigma Y_n^m(\lambda,\mu)Y_{n'}^{m'}(\lambda,\mu)d\sigma = \delta_{n=n'}\delta_{m=m'}\iint_\sigma d\sigma$$

One has then, for $m \geq 0$:

$$P_n^m(\mu) = \sqrt{(2n+1)\frac{(n-m)!}{(n+m)!}}\ \frac{1}{2^n n!}(1-\mu^2)^{m/2}\frac{d^{n+m}}{d\mu^{n+m}}(\mu^2-1)^n \qquad (1)$$

And for $m \leq 0$:

$$P_n^{-m}(\mu) = P_n^m(\mu)$$

As mentioned above, the spherical harmonics satisfy:

$$\Delta Y_n^m = -\frac{n(n+1)}{a^2}Y_n^m$$

The Laplacian operator is invariant by rotation, his eigenspaces are thus also invariant by rotation. We deduce from it that under the effect of a rotation *i.e.* a change of pole, the coefficients of the decomposition of a field in spherical harmonics are exchanged at fixed n. For each n, there is a linear transformation (thus a matrix) which makes it possible to make the basic change. This property is preserved by the discretization if truncation is triangular. This is why triangular truncation is said to be isotropic.

2.2 Collocation grid

A collocation grid is selected for non-linear calculations which cannot be carried out directly on the coefficients of the spherical harmonics. At each time step, one passes from the spectral coefficients to the grid-point values and reciprocally. From the expression of the Y_n^m, the E-W transforms are Fourier transforms. To use fast Fourier transforms (FFT), one thus needs a regular grid in longitude. In the N-S direction, one uses a Gauss quadrature for the direct transform, therefore the latitudes are not equidistant.

At high latitudes, one takes less points on a latitude circle than Fourier modes, in order to maintain the grid almost isotropic. The collocation grid is said to be reduced (Hortal and Simmons, 1991). The grid is said to be Gaussian quadratic (or simply Gaussian) when the number of latitude

circles is large enough (for a given truncation) so that the Gauss quadrature is exact for any product of two Legendre polynomials in the truncation. This is useful in the case of the Eulerian advection (product of velocity by gradient). When the approximate calculation of the integral is exact only for the Legendre polynomials of the truncation, the grid is said to be linear (Hortal, 1996).

2.3 Spectral transforms

To pass from the spectral coefficients to the grid points values, one uses the two formulas of direct evaluation:

$$A_m(\mu) = \sum_{n=|m|}^{\infty} A_n^m P_n^m(\mu)$$

and:

$$A(\lambda, \mu) = \sum_{m=-\infty}^{+\infty} A_m(\mu) e^{im\lambda}$$

where the A_m are called the Fourier coefficients.

The horizontal derivatives are calculated exactly by using the derivatives of the Legendre functions for the N-S direction and by multiplying by im for the E-W direction.

From the grid point fields, the Fourier coefficients are determined by:

$$A_m(\mu) = \frac{1}{2\pi} \int_0^{2\pi} A(\lambda, \mu)\, e^{-im\lambda}\, d\lambda$$

a formula which ensures that $A_0(\mu)$ is the average of field A along parallel μ. Integration is carried out numerically by using a fast Fourier transform (FFT). The integral in latitude is:

$$A_n^m = \frac{1}{2} \int_{-1}^{1} A_m(\mu) P_n^m(\mu)\, d\mu$$

As mentioned above, we use a Gauss quadrature, discrete version of the preceding integral:

$$A_n^m = \sum_{k=1}^{K} \omega(\mu_k) A_m(\mu_k) P_n^m(\mu_k)$$

where the μ_k are the K roots of the Legendre polynomial of degree K and the Gauss weights $\omega(\mu_k)$ are given by:

$$\omega(\mu_k) = \frac{1-\mu_k^2}{(NP_{N-1})^2}$$

Here, the Legendre polynomial is the one of the mathematicians, the squared norm of which is $1/(2n+1)$.

3 Horizontal discretization

3.1 Spectral truncation

In practical the expression of A is limited to a finite set of harmonics corresponding to $0 \leq n \leq N$ and $-n \leq m \leq n$. That defines a triangular truncation N. The truncated expansion of field A reads:

$$A(\lambda,\mu) = \sum_{m=-N}^{m=N} \sum_{n=|m|}^{n=N} A_n^m P_n^m(\mu) e^{im\lambda}$$

Due to the properties of $P_n^m(\mu)$, expression of A becomes for a real scalar field:

$$A(\lambda,\mu) = \sum_{m=0}^{m=N} \sum_{n=|m|}^{n=N} A_n^m P_n^m(\mu) e^{im\lambda}$$

3.2 Horizontal derivatives

Meridional derivative relative to latitude θ

For a variable A, meridional derivative is discretized in spectral space by the following formula:

$$\left(\cos\theta \frac{\partial A}{\partial \theta}\right)_n^m = -(n-1)e_n^m A_{n-1}^m + (n+2)e_{n+1}^m A_{n+1}^m$$

where $e_0^0 = 0$ and:

$$e_n^m = \sqrt{\frac{n^2-m^2}{4n^2-1}}$$

Zonal derivative relative to longitude λ

For a variable A, zonal derivative is discretized in spectral space by the following formula:

$$\left(\frac{\partial A}{\partial \lambda}\right)_n^m = i\, m A_n^m$$

Such a derivation can be made on Fourier coefficients by a multiplication by $i\, m$.

3.3 Spectral relationships for wind representation

The reduced components of the velocity are obtained by dividing the physical components by the mapping factor M. Divergence and vorticity are divided by M^2. As reduced divergence $D^{'}$ is obtained from velocity potential χ by a laplacian operator, and as reduced vorticity $\zeta^{'}$ is obtained similarly from stream function ψ, we have in spectral space:

$$D'^m_n = -\frac{n(n+1)}{a^2}\chi_n^m$$

$$\zeta'^m_n = -\frac{n(n+1)}{a^2}\psi_n^m$$

Relationship between $U^{'}$, ψ and χ:

$$(U^{'} a \cos\theta) = \frac{\partial \chi}{\partial \lambda} - \cos\theta \frac{\partial \psi}{\partial \theta}$$

the spectral discretization of which is:

$$(U^{'} a \cos\theta)_n^m = i\, m \chi_n^m + (n-1) e_n^m \psi_{n-1}^m - (n+2) e_{n+1}^m \psi_{n+1}^m$$

Relationship between $V^{'}$, ψ and χ:

$$(V^{'} a \cos\theta) = \frac{\partial \psi}{\partial \lambda} + \cos\theta \frac{\partial \chi}{\partial \theta}$$

the spectral discretization of which is:

$$(V^{'} a \cos\theta)_n^m = i\, m \psi_n^m - (n-1) e_n^m \chi_{n-1}^m + (n+2) e_{n+1}^m \chi_{n+1}^m$$

Relationship between $D^{'}$, $U^{'}$ and $V^{'}$:

$$D^{'} = \frac{1}{a\cos\theta}\left(\frac{\partial U^{'}}{\partial\lambda} + \frac{\partial(V^{'}\cos\theta)}{\partial\theta}\right)$$

which can be rewritten:

$$D^{'} = \frac{1}{a^2\cos^2\theta}\left(\frac{\partial(U^{'}a\cos\theta)}{\partial\lambda} + \cos\theta\frac{\partial(V^{'}a\cos\theta)}{\partial\theta}\right)$$

Relationship between $\zeta^{'}$, $U^{'}$ and $V^{'}$:

$$\zeta^{'} = \frac{1}{a\cos\theta}\left(\frac{\partial V^{'}}{\partial\lambda} - \frac{\partial(U^{'}\cos\theta)}{\partial\theta}\right)$$

which can be rewritten:

$$\zeta^{'} = \frac{1}{a^2\cos^2\theta}\left(\frac{\partial(V^{'}a\cos\theta)}{\partial\lambda} - \cos\theta\frac{\partial(U^{'}a\cos\theta)}{\partial\theta}\right)$$

Spectral discretizations allow to retrieve easily spectral components of fields $D^{'}a^2\cos^2\theta$ and $\zeta^{'}a^2\cos^2\theta$, but not directly spectral components of $D^{'}$ and $\zeta^{'}$ (requiring inversion of a penta-diagonal matrix). In fact, the algorithm involved to retrieve spectral coefficients of $D^{'}$ and $\zeta^{'}$ once known values of wind components is slightly different (requiring a division by $a\cos\theta$ in Fourier space), and is described in detail in Temperton (1991).

3.4 Relationship between dimension in spectral space and in grid point space

Quadratic grid, linear grid

Spectral space is defined by a triangular truncation N. Grid point space has *ndgl* latitudes and a maximum number of longitudes equal to *ndlon*. *ndlon* and *ndgl* are always even integers: if *ndlon* is a multiple of 4, $ndgl = ndlon/2$; if *ndlon* is not a multiple of 4, $ndgl = ndlon/2+1$. For a quadratic Gaussian grid, there is a relationship between these parameters to avoid aliasing on quadratic terms.

- If the stretching coefficient c is equal to 1 (no stretching), N is the maximum integer verifying the relationship $3 * N \leq (ndlon - 1)$.

- If the stretching coefficient c is greater than 1 (stretching), N is the maximum integer verifying the relationship $3 * N \leq \min(2 * ndgl - 3, ndlon - 1)$.

In a semi-Lagrangian scheme the advective quadratic terms disappear, so it is possible to use a smaller grid-point space: a linear grid. It is characterized by:

- If the stretching coefficient c is equal to 1 (no stretching), N is the maximum integer verifying the relationship $2 * N \leq (ndlon - 1)$.
- If the stretching coefficient c is greater than 1 (stretching), N is the maximum integer verifying the relationship $2 * N \leq \min(2 * ndgl - 3, ndlon - 1)$.

In ARPEGE-CLIMAT with $c > 1$, some aliasing is allowed, and the same N is taken as in the case $c = 1$.

Admissible dimensions for longitude

The current algorithm for FFT allows integers *ndlon* which can factorize as $2^{1+p_2} * 3^{p_3} * 5^{p_5}$. That limits the possibility of choosing the dimensions in a discontinuous subset of truncations and dimensions for Gaussian grid. In the range compatible with climate multi-year integrations, the admissible sizes (with even number of latitudes) are:

64 72 80 90 96 100 108 120 128 144 150 160 162 180 192 200 216 240 250 256 270 288 300 320 324 360 384 400 432 450 480 486 500 512 540 576 600 640 648 720

Reduced grid

To save memory and computation time (in particular in the physical parametrizations), the number of longitudes per latitude circle is reduced outside the tropics, in order to maintain a quasi-isotropic grid (note that the spectral triangular truncation allows an isotropic representation of the fields, despite the accumulation of grid points near the poles). This optimization is done at the expense of an aliasing error (Williamson and Rosinski, 2000). An algorithm is proposed to compute for a given truncation, the number of longitudes per latitude circle which is the best compromise between accuracy in the spectral transform an isotropy in the physical parametrizations.

4

Semi-lagrangian discretization

1 Introduction

1.1 Purpose

This chapter describes the semi-Lagrangian scheme used in ARPEGE-CLIMAT. The ARPEGE-IFS code contains many other options. See Yessad (2007b) for a comprehensive description of all available features. Equations will be written without horizontal diffusion scheme (which is treated in spectral computations, see Chapter **??**), in order to give a clearer presentation of the discretized equations.

1.2 Eulerian scheme

In Eulerian form of equations, the time dependency equation of a variable X writes as:

$$\frac{\partial X}{\partial t} = -\vec{U}.\overrightarrow{\nabla_3} X + \dot{X} \tag{1}$$

where $\vec{U}$ is the 3D wind, $\overrightarrow{\nabla_3}$ is the 3D gradient operator, $\dot{X}$ is the sum of the dynamical and physical contributions. $X(t+\Delta t)$ is computed knowing $X(t-\Delta t)$ at the same grid-point. Eulerian technique obliges to use a time-step that satisfies to the CFL (Courant Friedrich Levy) condition everywhere. For the variable-mesh spectral global model ARPEGE, the horizontal CFL condition writes as:

$$m \mid U \mid \Delta t \sqrt{\frac{N(N+1)}{a^2}} < 1 \tag{2}$$

where m is the mapping factor, $\mid U \mid$ is the 3D wind module, N is the truncation, a is the Earth radius. The vertical CFL condition writes as:

$$\mid \dot{\eta} \mid \Delta t \Delta \eta < 1 \tag{3}$$

For a T359L31 (triangular truncation 359, 31 levels) model with stretching coefficient c=2.5 (maximum horizontal resolution about 20 km), that gives $\Delta t \simeq 2\, min$.

1.3 Semi-Lagrangian scheme

In semi-Lagrangian form of equations, the time dependency equation of a variable X writes as:

$$\frac{dX}{dt} = \dot{X} \tag{4}$$

In a three-time level semi-Lagrangian scheme $X(t + \Delta t)$ is computed at a grid-point F knowing $X(t - \Delta t)$ at the point O (not necessary a grid-point) where the same particle is at the instant $t - \Delta t$. In a two-time level semi-Lagrangian scheme $X(t + \Delta t)$ is computed at a grid-point F knowing $X(t)$ at the point O (not necessary a grid-point) where the same particle is at the instant t. The semi-Lagrangian technique is more expensive for one time-step than the Eulerian technique because it is necessary to compute the positions of the origin point O and the medium point M along the trajectory and to interpolate some quantities at these points (1.5 times the cost of the Eulerian scheme in the T199L31 model with physics). But it allows to use larger time-steps: the stability condition is now the Lipschitz criterion (trajectories do not cross each other) and is less severe than the CFL condition.

D is the divergence of the horizontal wind on the η-coordinates, $\dot{\eta} = \dfrac{d\eta}{dt}$. Lipschitz criterion writes for a two-time level semi-Lagrangian scheme:

$$\mid D + \frac{\partial \dot{\eta}}{\partial \eta} \mid \frac{\Delta t}{2} < 1 \tag{5}$$

ARPEGE-CLIMAT using a two-time level scheme (2TL), the three-time level scheme (3TL) is not described in this chapter.

2 Equations

2.1 Notations

- $\vec{V}$ is the horizontal wind. Its zonal component (on the Gaussian grid) is denoted by U

- D is the horizontal wind divergence
- w is the z-coordinate vertical velocity: $w = \dfrac{dz}{dt}$
- T is the temperature. T^* is a vertically-constant reference temperature which is used in the semi-implicit scheme. Default value is 300 K or 350 K according to configuration (for more details see documentation about semi-implicit scheme). T_s^{ST} is the reference standard atmosphere surface temperature (288.15 K). $\left[\dfrac{dT}{dz}\right]_{ST}$ is the standard atmosphere tropospheric gradient of temperature ($-0.0065\ K\,m^{-1}$)
- q is the humidity
- p is pressure, p_s is surface pressure. p^* is a reference pressure and p_s^* is a reference surface pressure, which are used in the semi-implicit scheme. These reference quantities are vertically dependent and "horizontally" (*i.e.* on η-surfaces) constant. Default value of p_s^* is $1000\,hPa$ for a 2TL SL scheme. Δp^* are layer depths corresponding to a surface pressure equal to p_s^*. p_s^{ST} is a reference pressure equal to the surface pressure of the standard atmosphere (101325 Pa, variable VP00). p^{ST} is a reference pressure defined on layers and inter-layers corresponding to the surface reference pressure p_s^{ST} (stored in array STPRE).
- $\omega = \dfrac{dp}{dt}$ is the total temporal derivative of pressure
- Φ is the geopotential, Φ_s is the surface geopotential (i.e. the orography)
- $\vec{\Omega}$ is the Earth rotation angular velocity
- $\vec{r}$ is the vector directed upwards, the length of which is the Earth radius
- $\vec{\imath}$ is the unit zonal vector on the Gaussian grid
- g is the gravity acceleration constant
- R is the gas constant for air, R_d the gas constant for dry air and R_v the gas constant for water vapor
- c_p is the specific heat at constant pressure for air and c_{p_a} is the specific heat at constant pressure for dry air
- c_v is the specific heat at constant volume for air and c_{v_a} is the specific heat at constant volume for dry air
- $\overrightarrow{\nabla}$ is the first order horizontal gradient on η-surfaces

- B is the quantity which defines the vertical hybrid coordinate (see chapter 2): B varies from 1 to 0 from bottom to top. Layer value of B is defined as the average of the adjacent inter-layer value of B.
- α_T is a vertical-dependent coefficient used to define a thermodynamic variable $T + \delta_{TR}\frac{\alpha_T \Phi_s}{R_d T^{ST}}$ less sensitive to orography than temperature T. Expression of α_T is:

$$\alpha_T = B\left(-\frac{R_d}{g}\left[\frac{dT}{dz}\right]_{ST}\right)T^{ST}\left(\frac{p^{ST}}{p_s^{ST}}\right)^{\left(-\frac{R_d}{g}\left[\frac{dT}{dz}\right]_{ST}-1\right)} \tag{6}$$

  δ_{TR} being the switch to come back to temperature.

2.2 3D primitive equations hydrostatic model

Momentum equation:

Vector form of momentum equation is used. Coriolis force can be treated explicitly ($\delta_{\vec{V}} = 0$) or implicitly ($\delta_{\vec{V}} = 1$).

$$\frac{d\left(\vec{V} + \delta_{\vec{V}}(2\vec{\Omega} \wedge \vec{r})\right)}{dt} = \left[-2(1-\delta_{\vec{V}})(\vec{\Omega} \wedge \vec{V})\right] - \vec{\nabla}\Phi - RT\vec{\nabla}\ln p + \vec{F}_{\vec{V}} \tag{7}$$

$F_{\vec{V}}$ is the physical contribution on horizontal wind.

Temperature equation:

$$\frac{dT}{dt} = \frac{RT}{c_p}\frac{\omega}{p} + F_T \tag{8}$$

F_T is the physical contribution on temperature. This equation can be modified by replacing temperature T by $T + \delta_{TR}\frac{\alpha_T \Phi_s}{R_d T^{ST}}$ which is less sensitive to orography, as it is made for continuity equation (see next paragraph relative to continuity equation). This modification has been proposed by Ritchie and Tanguay (1996).

$$\frac{d}{dt}\left(T + \delta_{TR}\frac{\alpha_T \Phi_s}{R_d T^{ST}}\right) = \frac{d}{dt}\left(\delta_{TR}\frac{\alpha_T \Phi_s}{R_d T^{ST}}\right) + \frac{RT}{c_p}\frac{\omega}{p} + F_T \tag{9}$$

See Equation (6) for definition of α_T. Term $\frac{d}{dt}\left(\delta_{TR}\frac{\alpha_T \Phi_s}{R_d T^{ST}}\right)$ only contains advection terms linked to horizontal variations of orography and vertical variations of coefficient α_T.

Humidity equation:

$$\frac{dq}{dt} = F_q \tag{10}$$

F_q is the physical contribution on specific humidity, This equation is also valid for other advective variables (GFL).

For non-advectable GFL variables (for example rain in the optional physics q_r), the equation is identical to the Eulerian equation:

$$\frac{\partial q_r}{\partial t} = F_{q_r} \tag{11}$$

F_q is the liquid precipitation flux

Continuity equation:

The impact of water phase changes on atmosphere mass balance is no longer taken into account in ARPEGE-CLIMAT because of the increasing complexity of the code and the unsafety of an option which is not supported by ECMWF. The conservation of dry air mass, also known as continuity equation, is written as:

$$\int_0^1 \frac{\partial B}{\partial \eta} \frac{d\left[\ln p_s + \delta_{TR}\frac{\Phi_s}{R_d T^{ST}}\right]}{dt} d\eta \quad =$$

$$\int_0^1 \frac{\partial B}{\partial \eta}\left(-\frac{1}{p_s}\int_0^1 \vec{\nabla}\left(\vec{V}\frac{\partial p}{\partial \eta}\right)d\eta + \vec{V}\vec{\nabla}\left[\ln p + \delta_{TR}\frac{\Phi_s}{R_d T^{ST}}\right]\right) d\eta \tag{12}$$

Variable δ_{TR} is 0 or 1; when $\delta_{TR} = 1$ the new variable is less sensitive to the orography (see temperature equation about orographic resonance).

3 Generic discretization of the equations

3.1 Notations

Upper index:

- δt is half time-step
- First integration step: $+$ (resp. m, o, $-$) for $t + \Delta t$ (resp. $t + \delta t$, t, t) quantity.

- Following integration steps: $+$ (resp. m, o, $-$) for $t+\Delta t$ (resp. $t+\delta t$, t, $t-\Delta t$) quantity.

Lower index: F (resp. M and O) for final (resp. medium and origin) point.

The different classes of prognostic variables: Prognostic variables can be split into different classes:

- 3D variables, the equation RHS of which has a non-zero adiabatic contribution and a non-zero semi-implicit correction contribution. They are called "GMV" in the code ("GMV" means "grid-point model variables"). This class of variables includes wind components and temperature.
- 3D advectable "conservative" variables. The equation RHS of these variables has a zero adiabatic contribution, only the diabatic contribution (and the horizontal diffusion contribution) can be non-zero. They are called "GFL" in the code ("GFL" means "grid-point fields"). This class of variables may include liquid/ice cloud water, ozone and TKE.
- 3D non advectable pseudo-historic variables. The equation RHS of these variables looks like the one of the 3D advectable "conservative" variables, but there is no advection. They are included in the GFL variables. This class of variables may include rain, snow, graupels, convective precipitation flux, stratiform precipitation flux, moisture convergence, total humidity variation or convective vertical velocity.
- 2D variables, the equation RHS of which mixes 3D and 2D terms, has a non-zero adiabatic contribution and a non-zero semi-implicit correction contribution. They are called "GMVS" in the code ("GMVS" means "grid-point model variables for surface"). This class of variables includes the logarithm of surface pressure (continuity equation).

3.2 Discretization for a 3D variable: general case where the RHS has non-zero linear and non-linear terms (GMV variables).

List of equations:

- Momentum equation
- Temperature equation

Generic notations: Generic notation N(X)LAG stands for:

- NWLAG for momentum equation.
- NTLAG for temperature equation.

Generic notation P(X)L0, P(X)L9, P(X)T1 stands for:

- PUL0, PUL9, PUT1 for U-momentum equation.
- PVL0, PVL9, PVT1 for V-momentum equation.
- PTL0, PTL9, PTT1 for temperature equation.

Generic notation P(X)NLT9 stands for:

- PUNLT9 for U-momentum equation.
- PVNLT9 for V-momentum equation.
- PTNLT9 for temperature equation.

Generic notation for total term, linear term, non linear term, physics:

- $\mathcal{A}$ is the total term (sum of dynamical contributions)
- $\mathcal{B}$ is the linear term (treated in the semi-implicit scheme)
- $\mathcal{A} - \beta\mathcal{B}$ is the non-linear term
- $\mathcal{F}$ is the sum of contributions computed in the physical parametrizations

Other points:

- High-order interpolations: in the following discretizations, "high-order interpolations" means 32-point interpolation for 3D terms (vertical interpolations are cubic), 12-points interpolations for 2D terms
- Uncentering: ϵ is a first-order "uncentering factor"; it allows to remove the noise due to gravity waves (orographic resonance)
- Vectors: for vectors like horizontal wind, a rotation operator $\mathcal{R}$ has to be applied from interpolation point to final point:
  - expression interpolated at O has to be replaced by $\mathcal{R}^{OF}\{this\ expression\}_O$
  - expression interpolated at M has to be replaced by $\mathcal{R}^{MF}\{this\ expression\}_M$

2TL vertical interpolating SL scheme: stable discretization (LSETTLS=.T.) and first-order uncentering The basic equation can be written as:

$$\frac{dX}{dt} = \mathcal{A} + \mathcal{F} \tag{13}$$

When N(X)LAG=3, Equation (13) is discretized by averaging the non-linear term along the trajectory in the RHS.

The $t + \delta t$ non-linear term $\mathcal{A}^m - \beta\mathcal{B}^m$ is calculated by a linear space and time extrapolation.

$$\frac{1}{2}(1+\epsilon)[\mathcal{A}^o - \beta\mathcal{B}^o]_F + \frac{1}{2}(2-\epsilon)[\mathcal{A}^o - \beta\mathcal{B}^o]_O - \frac{1}{2}[\mathcal{A}^- - \beta\mathcal{B}^-]_O$$

This type of extrapolation is available only for N(X)LAG=3. At the first time integration step, values at $t+\delta t$ are set equal to initial values. Quantity $\mathcal{A}^o - \beta\mathcal{B}^o$ has to be saved in a buffer P(X)NLT9 to be available as $\mathcal{A}^- - \beta\mathcal{B}^-$ for the following time-step.

Equation (13) is discretized as follows:

$$\begin{aligned}(X - (1+\epsilon)\delta t\, \beta\mathcal{B})_F^+ \;=\; & \{X^o + [(2-\epsilon)\delta t\, \mathcal{A} - (2-\epsilon)\delta t\, \beta\mathcal{B}]^o \\ & -\delta t[\mathcal{A} - \beta\mathcal{B}]^- + [(1-\epsilon)\delta t\, \beta\mathcal{B} + \Delta t\mathcal{F}]^o\}_O \\ & +\{[(1+\epsilon)\delta t\, \mathcal{A} - (1+\epsilon)\delta t\, \beta\mathcal{B}]^o\}_F\end{aligned}$$

Buffers content before interpolations for N(X)LAG=3:

- P(X)L0: $[(2-\epsilon)\delta t\mathcal{A} - (2-\epsilon)\delta t\, \beta\mathcal{B}]^o - \delta t[\mathcal{A} - \beta\mathcal{B}]^- + [(1-\epsilon)\delta t\, \beta\mathcal{B}]^o$ for tri-linear interpolation at the origin point O.
- P(X)L9: $X^o + [\Delta t\mathcal{F}]^o$ for high-order interpolation at the origin point O.
- P(X)T1: $[(1+\epsilon)\delta t\mathcal{A} - (1+\epsilon)\delta t\, \beta\mathcal{B}]^o$ then provisional add of quantity $[(1+\epsilon)\delta t\, \beta\mathcal{B}]^o$ before $t + \Delta t$ physics; evaluated at the final point F.

3.3 Discretization for a 3D variable: particular case where the RHS has zero linear and non-linear terms (advectable GFL variables)

List of equations:

Humidity equation, and for example:

- Specific humidity equation
- Ozone equation
- Liquid water equation
- Ice equation
- TKE equation
- Extra GFL variables equations

Generic notations

Generic notation P(X)L9, P(X)T1 stands for:

- PGFLL9, PGFLT1 for GFL variables

In the present case $\mathcal{A}$ and $\mathcal{B}$ are equal to zero.

Other points:

- High-order interpolations: in the following discretizations, "high-order interpolations" means 32-point interpolations for 3D terms (vertical interpolations are cubic), 12-point interpolations for 2D terms. For ozone, vertical cubic interpolations can be replaced by vertical Hermite cubic interpolations (switch YO3_NL%LHV in NAMGFL), or vertical spline cubic interpolations (switch YO3_NL%LVSPLIP in NAMGFL).
- Uncentering: ϵ is a first-order "uncentering factor"; It allows to remove the noise due to gravity waves (orographic resonance)

2TL vertical interpolating SL scheme

At the first time integration step, values at $t + \delta t$ are set equal to initial values. This discretization of the 2TL SL scheme follows (Mc Donald and Haugen, 1992).

Equation (13) is discretized as follows:

$$X_F^+ = \{X^o + [\Delta t \mathcal{F}]^o\}_O \tag{14}$$

Buffers content before interpolations:

- P(X)L9: $X^o + [\Delta t \mathcal{F}]^o$ for high-order interpolation at the origin point O
- P(X)T1 contains zero; evaluated at the final point F

3.4 Non advectable pseudo-historic GFL variables

For these variables the discretization always writes:

$$X_F^+ = \{X^o + [\Delta t \mathcal{F}]^o\}_F \tag{15}$$

and there are never interpolations.

3.5 Discretization for a 2D variable in a 3D model (GMVS variables, for example continuity equation)

The equation which is now discretized is:

$$\begin{aligned}[\mathcal{R}_{inte}]_{(top,surf)} \left\langle \frac{\mathcal{W}_{\rm vei}}{\Delta\eta} \frac{dX}{dt} \right\rangle &= [\mathcal{R}_{inte}]_{(top,surf)} \left\langle \frac{\mathcal{W}_{\rm vei}}{\Delta\eta} \mathcal{A} \right\rangle \\ &\quad + [\mathcal{R}_{inte}]_{(top,surf)} \left\langle \frac{\mathcal{W}_{\rm vei}}{\Delta\eta} \mathcal{F} \right\rangle\end{aligned}$$

where:

$$[\mathcal{R}_{inte}]_{(top,surf)} \left\langle \frac{\mathcal{W}_{\rm vei}}{\Delta\eta} \right\rangle = 1 \tag{16}$$

and $[\mathcal{R}_{inte}]_{(top,surf)}$ is the vertical integral matrix operator (the scalar product $[\mathcal{R}_{inte}]_{(top,surf)}\langle X\rangle$ is the discretization of $\int_0^1 X d\eta$, $\langle X\rangle$ is the vector containing the layer values of X: $(X_1; X_2; ...; X_l; ...; X_L)$).

In the thin layer equations, expression of $\mathcal{W}_{\rm vei}$ at full levels is:

$$[\mathcal{W}_{\rm vei}]_l = \Delta B_l \tag{17}$$

List of equations:

- Continuity equation

Generic notations: Generic notation N(X)LAG stands for

- NVLAG for continuity equation

Generic notations P(X2D)9 (2D term), P(X)T1 (2D term), P(X3D)L9 (3D term), stand for

- PX9, PSPT1, PCL9 for continuity equation.

Generic notation P(X)NLT9 (3D term) stands for:

- PSPNLT9 for continuity equation.

Generic notation for total term, linear term, non linear term, physics:

- $\mathcal{A}$ is the total term (sum of dynamical contributions): it is assumed to be a 3D term (sum of 3D and 2D contributions).
- $\mathcal{B}$ is the linear term (treated in the semi-implicit scheme): it is assumed to be a 2D term (vertical integral of a 3D term).
- the difference $\mathcal{A}-\beta\mathcal{B}$ is the non-linear term, considered as a 3D term.

Other points

Horizontal interpolation of 2D terms: since the horizontal position of the interpolation point is vertical dependent, horizontal interpolations of 2D quantities have to be done for each layer. For example, when interpolating a 2D surface variable SV at the origin point, $[\mathcal{R}_{inte}]_{(top,surf)}\left\langle\left[\frac{\mathcal{W}_{\rm vei}}{\Delta\eta}\right]_F[SV]_O\right\rangle$ has no reason to be equal to $[SV]_{O(\eta=1)}$, these quantities are generally different: this is $[\mathcal{R}_{inte}]_{(top,surf)}\left\langle\left[\frac{\mathcal{W}_{\rm vei}}{\Delta\eta}\right]_F[SV]_O\right\rangle$ which has to be computed. $\left\langle\left[\frac{\mathcal{W}_{\rm vei}}{\Delta\eta}\right]_F[SV]_O\right\rangle$ is the vector containing $\left[\frac{[\mathcal{W}_{\rm vei}]_l}{[\Delta\eta]_l}\right]_F[SV]_{O(l)}$, for $l=1$ to L.

2TL vertical interpolating SL scheme: stable discretization (LSETTLS=.T.) and first-order uncentering

The $t+\delta t$ non-linear term $\mathcal{A}^m-\beta\mathcal{B}^m$ is calculated by a linear space and time extrapolation:

$$\frac{1}{2}(1+\epsilon)[\mathcal{A}^o-\beta\mathcal{B}^o]_F+\frac{1}{2}(2-\epsilon)[\mathcal{A}^o-\beta\mathcal{B}^o]_{O(l)}-\frac{1}{2}[\mathcal{A}^--\beta\mathcal{B}^-]_{O(l)}$$

This type of extrapolation is available only for N(X)LAG=3. At the first time integration step, values at $t+\delta t$ are set equal to initial values. Quantity $\mathcal{A}^o-\beta\mathcal{B}^o$ has to be saved in a buffer P(X)NLT9 to be available as $\mathcal{A}^--\beta\mathcal{B}^-$ for the following time-step.

Equation (13) is discretized as follows:

$$
\begin{aligned}
(X-(1+\epsilon)\delta t\beta\mathcal{B})_F^+ \;=\; & [\mathcal{R}_{inte}]_{(top,surf)} \left\langle \left[\frac{\mathcal{W}_{\rm vei}}{\Delta\eta}\right]_F \{X^o \right. \\
& +[(2-\epsilon)\delta t\mathcal{A}-(2-\epsilon)\delta t\beta\mathcal{B}]^o-\delta t[\mathcal{A}-\beta\mathcal{B}]^- \\
& \left. +\,[(1-\epsilon)\delta t\beta\mathcal{B}+\Delta t\mathcal{F}]^o\}_O \right\rangle \\
& +\{[(1+\epsilon)\delta t\mathcal{A}-(1+\epsilon)\delta t\beta\mathcal{B}]^o\}_F
\end{aligned}
$$

Buffers content before interpolations for N(X)LAG=3:

- P(X3D)L0 is not used.
- P(X3D)L9: $[(2-\epsilon)\delta t\mathcal{A}-(2-\epsilon)\delta t\beta\mathcal{B}]^o-[\delta t\mathcal{A}-\delta t\beta\mathcal{B}]^-+[(1-\epsilon)\delta t\beta\mathcal{B}]^o$ for tri-linear interpolation at the origin point $O(l)$
- P(X2D)0 is not used
- P(X2D)9: $X^o+[\Delta t\mathcal{F}]^o$ for horizontal high-order interpolation at the origin point $O(l)$
- P(X)T1: $[(1+\epsilon)\delta t\mathcal{A}-(1+\epsilon)\delta t\beta\mathcal{B}]^o$ then provisional add of quantity $[(1+\epsilon)\delta t\beta\mathcal{B}]^o$ before lagged physics; evaluated at the final point F

3.6 Additional vertical derivatives

If δ_{TR} is non-zero, discretization of temperature equation needs to compute the vertical advection $\left(\dot{\eta}\dfrac{d\alpha_T}{d\eta}\right)$ (at full levels) of α_T. Layers values of α_T (array RCORDIF) are used to define $T+\delta_{TR}\dfrac{\alpha_T\Phi_s}{R_dT^{ST}}$, but inter-layer values of α_T (array RCORDIH) are used to compute vertical advection.

3.7 Remarks for spline cubic vertical interpolations

In this case the vertical interpolation uses all model levels and can be written as the product of two vertical interpolations: the first one uses all model levels and can be done at F in the unlagged grid-point calculations (the intermediate quantity obtained is stored in the array P(X)SPL9), the second one is a 4 points interpolation, done in the lagged grid-point calculations in the interpolation routine. Interpolation routine uses both P(X)SPL9 (for interpolations) and P(X)L9 to apply a monotonicity constraint.

4 Computation of medium and origin points

4.1 Medium point M

The medium point is calculated in subroutines LARMES and LARMES2.

Trajectories are great circles on the geographical sphere. The computation of the medium point M location of the Lagrangian trajectory is performed by an iterative method described by Robert (1981) and adapted to the sphere by Rochas. In a 3TL SL scheme, the particle is at the point M at time t ($t + \delta t$ for the first integration step). In a 2TL SL scheme, the particle is at the point M at $t + \delta t$. M is at the middle position of the origin point O and the final point F.

Notations:

- $\mathcal{R}^{MF}$ is the rotation operator from medium point to final point (see section 6)
- $\mathcal{R}^{OF}$ is the rotation operator from origin point to final point (see section 6)
- $\vec{r}^{F} = C\vec{F}$ (C Earth center, F final point)
- $\vec{r}^{M} = C\vec{M}$ (M medium point)
- ϕ^{MF}: angle $(\widehat{C\vec{M}, C\vec{F}})$
- θ^{F},λ^{F}: latitude, longitude on the geographical sphere of F
- θ^{M},λ^{M}: latitude, longitude on the geographical sphere of M
- $\vec{V}^{M}$: interpolated horizontal wind at M (at $t + \delta t$)
- $\vec{V}^{O}$: interpolated horizontal wind at O (at $t + \delta t$)
- a is the average Earth radius near the surface
- $\vec{r} = a\vec{k}$
- Δt: time-step
- δt: half time-step
- L: number of layers of the model

Definition of the vertical coordinate η:

Research of medium point needs an exact definition of the vertical coordinate η. For the inter-layer number $\bar{l}$ ($\bar{l}$ between 0 and L), $\eta_{\bar{l}}$ is defined by:

$$\eta_{\bar{l}} = \frac{\bar{l}}{L} \tag{18}$$

For the layer number l (l between 1 and L), η_l is defined by:

$$\eta_l = \frac{1}{2}(\eta_{\bar{l}} + \eta_{\bar{l}-1}) \tag{19}$$

Stable algorithm for 2TL SL scheme (LSETTLS=.T.)

Extrapolation of the wind:

This algorithm has been developed by Hortal (2002). The basic idea is to replace the purely temporal extrapolation by a space and time extrapolation:

$$\mathcal{R}^{MF}[\vec{V}]^M(t+\delta t) = \frac{3}{2}\mathcal{R}^{NF}[\vec{V}]^N(t) - \frac{1}{2}\mathcal{R}^{OF}[\vec{V}]^O(t-\Delta t) \tag{20}$$

where N is the position of the particle at time t for a particle which goes from the origin point O at time $t-\Delta t$ to M at time $t+\delta t$. Assuming that the wind is constant along the trajectory one can write:

$$ON = 2NM = 0.5NF \tag{21}$$

and evaluate the angular velocity $\mathcal{R}^{NF}[\vec{V}]^N(t)$ by
$2/3\mathcal{R}^{MF}[\vec{V}]^M(t) + 1/3\mathcal{R}^{OF}[\vec{V}]^O(t)$ or $1/3[\vec{V}]^F(t) + 2/3\mathcal{R}^{OF}[\vec{V}]^O(t)$.
Expression of $[\vec{V}]^M(t+\delta t)$ becomes:

$$\mathcal{R}^{MF}[\vec{V}]^M(t+\delta t) = \frac{1}{2}[\vec{V}]^F(t) + \frac{1}{2}\mathcal{R}^{OF}(2[\vec{V}]^O(t) - [\vec{V}]^O(t-\Delta t)) \tag{22}$$

The same type of extrapolation is done for the η-coordinate vertical velocity. The algorithm of research of trajectory uses directly the RHS of this equation, and for all iterations the origin point O is computed instead of the medium point M.

Algorithm

The origin point is defined by the following iterative scheme: for the iteration $k+1$:

$$[\vec{r}]^O_{k+1} = [\vec{r}]^F \cos\phi_k - \frac{[\vec{V}]^F(t) + \mathcal{R}^{OF}(2[\vec{V}]^O_k(t) - [\vec{V}]^O_k(t-\Delta t))}{\mid [\vec{V}]^F(t) + \mathcal{R}^{OF}(2[\vec{V}]^O_k(t) - [\vec{V}]^O_k(t-\Delta t)) \mid} \sin\phi_k \tag{23}$$

where:

$$\phi_k = \delta t \mid [\vec{V}]^F(t) + \mathcal{R}^{OF}(2[\vec{V}]^O_k(t) - [\vec{V}]^O_k(t - \Delta t)) \mid \tag{24}$$

Some geometrical approximations (small angles on the sphere) yield:

$$[\vec{r}]^O_{k+1} = [\vec{r}]^F \left(1 - \frac{\phi_k^2}{2}\right) - \left([\vec{V}]^F(t) + \mathcal{R}^{OF}(2[\vec{V}]^O_k(t) - [\vec{V}]^O_k(t - \Delta t))\right) \delta t \left(1 - \frac{\phi_k^2}{6}\right) \tag{25}$$

On the vertical:

$$\eta^O_{k+1} = \eta^F - 2\delta t(0.5\dot{\eta}^F(t) + 0.5(2\dot{\eta}^O_k(t) - \dot{\eta}^O_k(t - \Delta t))) \tag{26}$$

First iteration

One starts with $M_0 = F$, $[\vec{V}]^F(t)$ as a first guess for the space and time extrapolated horizontal angular velocity, $\phi_0 = \Delta t \mid [\vec{V}]^F(t) \mid$, $\dot{\eta}^F(t)$ as a first guess for the space and time extrapolated η-coordinate vertical wind. Quantities at t are taken as a first guess and not quantities at $(t + \delta t)$, contrary to the case LSETTLS=.F. . The coordinates of O_1 are $(2[\vec{V}](t) - [\vec{V}](t - \Delta t))$. $(2\dot{\eta}(t) - \dot{\eta}(t - \Delta t))$ is interpolated at this point, which allows to compute the wind components which will be used for the next iteration.

Following iterations

$[\vec{V'}]$ (of coordinates $([u'], [v'])$) is a generic notation for
$1/2([\vec{V}]^F(t) + \mathcal{R}^{OF}(2[\vec{V}]^O_k(t) - [\vec{V}]^O_k(t - \Delta t)))$.

For horizontal displacement use equations:

$$\sin\theta^O_{k+1} = \sin\theta^F \cos\phi_k - \frac{[v']}{\mid [\vec{V'}] \mid} \cos\theta^F \sin\phi_k \tag{27}$$

$$\cos\theta^O_{k+1} \cos(\lambda^O_{k+1} - \lambda^F) = \cos\theta^F \cos\phi_k + \frac{[v']}{\mid [\vec{V'}] \mid} \sin\theta^F \sin\phi_k \tag{28}$$

$$\cos\theta^O_{k+1} \sin(\lambda^O_{k+1} - \lambda^F) = -\frac{[u']}{\mid [\vec{V'}] \mid} \sin\phi_k \tag{29}$$

For vertical displacement use equation:

$$\eta^O_{k+1} = \eta^F - \delta t(\dot{\eta}^F(t) + (2\dot{\eta}^O_k(t) - \dot{\eta}^O_k(t - \Delta t))) \tag{30}$$

4.2 Origin point O

The origin point is calculated in subroutines LARMES and LAINOR2.

In a 2TL SL scheme, the particle is at the point O at time t.

O is on the same great circle arc (on the geographical sphere) as M and F and the length of OF is twice the length of MF. If angle $(\widehat{[\vec{r}]^O, [\vec{r}]^F})$ is small (less than 10^o, what is generally satisfied), on can write for horizontal displacement:

$$[\vec{r}]^O - [\vec{r}]^F \simeq 2([\vec{r}]^M - [\vec{r}]^F) \tag{31}$$

For vertical displacement on can always write:

$$\eta^O - \eta^F = 2(\eta^M - \eta^F) \tag{32}$$

One denotes by:

- $\phi = (\widehat{[\vec{r}]^M, [\vec{r}]^F})$
- $[\vec{V}']$ (of coordinates $([u'], [v'])$) the last interpolated horizontal velocity.

Using the following identities:

$$\cos 2\phi = 2\cos^2\phi - 1 \tag{33}$$

$$\sin 2\phi = 2\sin\phi\cos\phi \tag{34}$$

the origin point horizontal coordinates can be computed by:

$$\sin\theta^O = \sin\theta^F \cos 2\phi - 2\cos\phi \left[\frac{[v']}{\mid [\vec{V}'] \mid} \cos\theta^F \sin\phi \right] \tag{35}$$

$$\cos\theta^O \cos(\lambda^O - \lambda^F) = \cos\theta^F \cos 2\phi + 2\cos\phi \left[\frac{[v']}{\mid [\vec{V}'] \mid} \sin\theta^F \sin\phi \right] \tag{36}$$

$$\cos\theta^O \sin(\lambda^O - \lambda^F) = -2\cos\phi \left[\frac{[u']}{\mid [\vec{V}'] \mid} \sin\phi \right] \tag{37}$$

Terms in brackets are already computed to determine M.

4.3 Refined re-computation of point O

Option L2TLFF controls re-computation of the origin point using the average between the angular velocity at the origin point and the provisional $t + \Delta t$ angular velocity, according to the algorithm previously described. Only term $(2\vec{\Omega} \wedge a\vec{k})$ is computed (always analytically) at this improved position of O (so L2TLFF is active only if LADVF=.T. or LADVFW=.T.). Refined re-computation of point O is available only in a limited set of options. Equations system is integrated to find a first guess of $\vec{V}^F(t + \Delta t)$ and also a first guess of $p_s(t + \Delta t)$ which provides $1/2([\vec{V}]^F + \mathcal{R}^{OF}[\vec{V}]^O)$ is used to recompute O. A correction $(2\vec{\Omega} \wedge a\vec{k})(O \text{ improved}) - (2\vec{\Omega} \wedge \vec{k})(O)$ is analytically computed and added to wind equation to find the "improved" value of $\vec{V}^F(t + \Delta t)$. Computations are currently made in routine LAPINEB and LADINE.

5 The SL discretization of the 3D primitive equation model

5.1 Momentum equation

Definition of X, $\mathcal{A}$, $\mathcal{B}$ and $\mathcal{F}$, top and bottom values

$$X = \vec{V} + \delta_{\vec{V}}(2\vec{\Omega} \wedge \vec{r}) \tag{38}$$

$$\mathcal{A} = [-2(1 - \delta_{\vec{V}})(\vec{\Omega} \wedge \vec{V})] - \vec{\nabla}\Phi - RT\vec{\nabla}(\log(p)) \tag{39}$$

$$\mathcal{B} = -\vec{\nabla}\left[\gamma T + \frac{R_d T^*}{{p_s}^*} p_s\right] + \beta_{Co}[-2(1 - \delta_{\vec{V}})(\vec{\Omega} \wedge \vec{V})] \tag{40}$$

$$\mathcal{F} = \vec{F}_{\vec{V}} \tag{41}$$

Top:

$$\vec{V}_{\eta=0} = \vec{V}_{l=1} \tag{42}$$

Bottom:

$$\vec{V}_{\eta=1} = \vec{V}_{l=L} \tag{43}$$

Remarks

- Coriolis term is treated implicitly ($\delta_{\vec{V}} = 1$, LADVF=.T.) This means that $(2\vec{\Omega} \wedge \vec{r})$ is analytically computed
- With option L2TLFF, term $(2\vec{\Omega} \wedge \vec{r})$ is recomputed at an improved position of the origin point

5.2 Thermodynamic equation

Definition of X, $\mathcal{A}$, $\mathcal{B}$ and $\mathcal{F}$, top and bottom values

$$X = T + \delta_{TR}\frac{\alpha_T \Phi_s}{R_d T_{ST}} \tag{44}$$

$$\mathcal{A} = \frac{RT}{c_p}\frac{\omega}{p} + \delta_{TR}\frac{\alpha_T}{R_d T_{ST}}\vec{V}\vec{\nabla}(\Phi_s) + \delta_{TR}\frac{\Phi_s}{R_d T_{ST}}\left(\dot{\eta}\frac{d\alpha_T}{d\eta}\right) \tag{45}$$

$$\mathcal{B} = -\overline{M}^2 \tau D' \tag{46}$$

$$\mathcal{F} = F_T \tag{47}$$

Top:

$$T_{\eta=0} = T_{l=1} \tag{48}$$

Bottom:

$$T_{\eta=1} = T_{l=L} \tag{49}$$

5.3 Continuity equation

Definition of X, $\mathcal{A}$, $\mathcal{B}$, and $\mathcal{F}$

$$X = \log p_s + \delta_{TR}\frac{\Phi_s}{R_d T_{st}} \tag{50}$$

$$\mathcal{A} = -\frac{1}{p_s}\int_{\eta=0}^{\eta=1}\vec{\nabla}\left(\vec{V}\frac{\partial p}{\partial \eta}\right)d\eta + \vec{V}\vec{\nabla}\left[\log p_s + \delta_{TR}\frac{\Phi_s}{R_d T_{st}}\right] \tag{51}$$

$$\mathcal{B} = -\frac{\overline{M}^2}{M^2}\nu D \tag{52}$$

$$\mathcal{B}' = 0 \tag{53}$$

$$\mathcal{F} = 0 \tag{54}$$

5.4 GFL variables

We detail here the case of specific moisture.

Definition of X, $\mathcal{A}$, $\mathcal{B}$ and $\mathcal{F}$, top and bottom values

$$X = q \tag{55}$$

$$\mathcal{A} = 0 \tag{56}$$

$$\mathcal{B} = 0 \tag{57}$$

$$\mathcal{F} = F_q \tag{58}$$

Top:

$$q_{\eta=0} = q_{l=1} \tag{59}$$

Bottom:

$$q_{\eta=1} = q_{l=L} \tag{60}$$

The other GFL are treated similarly. Quantities are assumed constant above the middle of the upper layer and below the middle of the lower layer.

5.5 Quantities to be interpolated

The computation is performed in subroutine LACDYN.

Research of trajectory

When researching the medium point by an iterative algorithm, the interpolation at the origin point of $([U], [V], \dot{\eta})$ is needed: a tri-linear interpolation is performed. For more details about interpolations, see section 8.

RHS of equations

The list of quantities to be interpolated has been described in subsections 3.2, 3.3 and 3.5 for each type of equation.

Additional quantities to be interpolated at the origin point if L2TLFF
The two components of the $[\vec{V}]$ at time t

6 $\mathcal{R}$ operator

6.1 No tilting

To transport a vector along a trajectory (part of a great circle) from an origin point O to a final point F the following operator $\mathcal{R}^{OF}$ is defined:

$$\vec{V}' = \mathcal{R}^{OF}(\vec{V}) \tag{61}$$

where $\vec{V}'$ has coordinates (u', v'), $\vec{V}$ has coordinates (u, v), and the relationship between (u, v) and (u', v') is:

$$\begin{pmatrix} u' \\ v' \end{pmatrix} = \begin{pmatrix} p & q \\ -q & p \end{pmatrix} \begin{pmatrix} u \\ v \end{pmatrix} \tag{62}$$

where:

$$p = \frac{\vec{i}^F\vec{i}^O + \vec{j}^F\vec{j}^O}{1 + \vec{k}^F\vec{k}^O} = \frac{\cos\theta^F \cos\theta^O + (1 + \sin\theta^F \sin\theta^O)\cos(\lambda^F - \lambda^O)}{1 + \cos\phi} \tag{63}$$

$$q = \frac{\vec{i}^F\vec{j}^O + \vec{j}^F\vec{i}^O}{1 + \vec{k}^F\vec{k}^O} = \frac{(\sin\theta^F + \sin\theta^O)\sin(\lambda^F - \lambda^O)}{1 + \cos\phi} \tag{64}$$

(Notations θ^O,θ^F,λ^O,λ^F,ϕ: see section 4).

p and q verify the following identity:

$$p^2 + q^2 = 1 \tag{65}$$

Computation of p and q is made in subroutine LARCHE.

6.2 Tilting

The coordinates of $\vec{V}'$ and $\vec{V}$ are linked by the following relationship:

$$\begin{pmatrix} u' \\ v' \end{pmatrix} = \begin{pmatrix} GNORDM & GNORDL \\ -GNORDL & GNORDM \end{pmatrix} \begin{pmatrix} p & q \\ -q & p \end{pmatrix} \times \begin{pmatrix} \cos\alpha & -\sin\alpha \\ \sin\alpha & \cos\alpha \end{pmatrix} \begin{pmatrix} u \\ v \end{pmatrix} \tag{66}$$

where:

$$\cos\alpha = \frac{2c}{A\cos\Theta^O}[\sin\theta_p\cos\theta^O - \sin\theta^O\cos\theta_p\cos(\lambda^O - \lambda_p)] \tag{67}$$

$$\sin\alpha = \frac{2c}{A\cos\Theta^O}[\cos\theta_p\sin(\lambda^O - \lambda_p)] \tag{68}$$

$$A = (1+c^2) + (1-c^2)(\sin\theta_p\sin\theta^O + \cos\theta_p\cos\theta^O\cos(\lambda^O - \lambda_p)) \tag{69}$$

and where:

- c is the stretching coefficient
- Θ^O is the latitude on the computational sphere of the origin point O
- (θ_p, λ_p) are the latitude and longitude on the geographical sphere of the stretching pole
- p and q are computed like in the not tilted case (in subroutine LARCHE)
- $\cos\alpha$ and $\sin\alpha$ are also computed in subroutine LARCHE
- $(GNORDL, GNORDM)$ are the coordinates in the computational sphere of the unit vector directed towards the true north, computed in subroutine SUGEM2

7 Longitudes and latitudes on the computational sphere

For interpolations it is necessary to compute (Θ^O, Λ^O), latitude and longitude of the interpolation point O in the computational sphere. The iterative algorithm allowing to find O gives (θ^O, λ^O), latitude and longitude in the geographical sphere (more exactly $\sin\theta^O$, $\cos\theta^O\cos\lambda^O - \lambda^F$ and $\cos\theta^O\sin\lambda^O - \lambda^F$ where (θ^F, λ^F) are the coordinates of the final point on the geographical sphere). Transform formulas giving (Θ, Λ) on the computational sphere once knowing (θ, λ) on the geographical sphere are given by:

$$\sin\Theta = \frac{(1-c^2) + (1+c^2)(\sin\theta_p\sin\theta + \cos\theta_p\cos\theta\cos(\lambda - \lambda_p))}{A} \tag{70}$$

$$\cos\Theta\cos\Lambda = \frac{2c(\cos\theta_p\sin\theta - \sin\theta_p\cos\theta\cos(\lambda - \lambda_p))}{A} \tag{71}$$

$$\cos\Theta\sin\Lambda = \frac{2c\cos\theta\sin(\lambda - \lambda_p)}{A} \tag{72}$$

where:

- $A = (1 + c^2) + (1 - c^2)(\sin\theta_p \sin\theta + \cos\theta_p \cos\theta \cos(\lambda - \lambda_p))$
- c is the stretching coefficient
- (θ_p, λ_p) are the latitude and longitude on the geographical sphere of the stretching pole
- Computation of Θ, Λ is made in subroutine LARCHE

8 Interpolations and weights computations

8.1 Interpolation grid and weights

Computation is done in subroutine LASCAW.

Horizontal interpolation grid and weights for bi-linear interpolations

A 16 points horizontal grid is defined as it is shown in figure **??**. The interpolation point O (medium or origin point) is between B_1, C_1, B_2 and C_2. Λ and Θ are the longitudes and latitudes on the computational sphere. The weights are defined as follows:

- zonal weight number 1:

$$ZDLO1 = \frac{\Lambda_O - \Lambda_{B_1}}{\Lambda_{C_1} - \Lambda_{B_1}}$$

- zonal weight number 2:

$$ZDLO2 = \frac{\Lambda_O - \Lambda_{B_2}}{\Lambda_{C_2} - \Lambda_{B_2}}$$

- meridional weight:

$$ZDLAT = \frac{\Theta_O - \Theta_{B_1}}{\Theta_{B_2} - \Theta_{B_1}}$$

Vertical interpolation grid and weights for vertical linear interpolations

A 4 points vertical grid is defined as it is shown in figure **??**. The interpolation point O (medium or origin point) is between T_{l+1} and T_{l+2}. The vertical weight is defined by:

$$ZDVER = \frac{\eta_O - \eta_{T_{l+1}}}{\eta_{T_{l+2}} - \eta_{T_{l+1}}}$$

Horizontal interpolation grid and weights for 12-point cubic interpolations

A 16 points horizontal grid is defined as it is shown in figure **??**. The interpolation point O (medium or origin point) is between B_1, C_1, B_2 and C_2. The weights are defined as follows:

- zonal weight number 0:

$$ZDLO0 = \frac{\Lambda_O - \Lambda_{B_0}}{\Lambda_{C_0} - \Lambda_{B_0}}$$

- zonal weight number 1:

$$ZDLO1 = \frac{\Lambda_O - \Lambda_{B_1}}{\Lambda_{C_1} - \Lambda_{B_1}}$$

- zonal weight number 2:

$$ZDLO2 = \frac{\Lambda_O - \Lambda_{B_2}}{\Lambda_{C_2} - \Lambda_{B_2}}$$

- zonal weight number 3:

$$ZDLO3 = \frac{\Lambda_O - \Lambda_{B_3}}{\Lambda_{C_3} - \Lambda_{B_3}}$$

- meridional weights:

$$ZCLA2 = \frac{(\Theta_O - \Theta_{B_0})(\Theta_O - \Theta_{B_2})(\Theta_O - \Theta_{B_3})}{(\Theta_{B_1} - \Theta_{B_0})(\Theta_{B_1} - \Theta_{B_2})(\Theta_{B_1} - \Theta_{B_3})}$$

$$ZCLA3 = \frac{(\Theta_O - \Theta_{B_0})(\Theta_O - \Theta_{B_1})(\Theta_O - \Theta_{B_3})}{(\Theta_{B_2} - \Theta_{B_0})(\Theta_{B_2} - \Theta_{B_1})(\Theta_{B_2} - \Theta_{B_3})}$$

$$ZCLA4 = \frac{(\Theta_O - \Theta_{B_0})(\Theta_O - \Theta_{B_1})(\Theta_O - \Theta_{B_2})}{(\Theta_{B_3} - \Theta_{B_0})(\Theta_{B_3} - \Theta_{B_1})(\Theta_{B_3} - \Theta_{B_2})}$$

Vertical interpolation grid and weights for vertical cubic 4-point interpolations

A 4-point vertical grid is defined as it is shown in figure **??**. The interpolation point O (medium or origin point) is between T_{l+1} and T_{l+2}. The vertical weights are defined by:

$$ZCVE2 = \frac{(\eta_O - \eta_{T_l})(\eta_O - \eta_{T_{l+2}})(\eta_O - \eta_{T_{l+3}})}{(\eta_{T_{l+1}} - \eta_{T_l})(\eta_{T_{l+1}} - \eta_{T_{l+2}})(\eta_{T_{l+1}} - \eta_{T_{l+3}})}$$

$$ZCVE3 = \frac{(\eta_O - \eta_{T_l})(\eta_O - \eta_{T_{l+1}})(\eta_O - \eta_{T_{l+3}})}{(\eta_{T_{l+2}} - \eta_{T_l})(\eta_{T_{l+2}} - \eta_{T_{l+1}})(\eta_{T_{l+2}} - \eta_{T_{l+3}})}$$

$$ZCVE4 = \frac{(\eta_O - \eta_{T_l})(\eta_O - \eta_{T_{l+1}})(\eta_O - \eta_{T_{l+2}})}{(\eta_{T_{l+3}} - \eta_{T_l})(\eta_{T_{l+3}} - \eta_{T_{l+1}})(\eta_{T_{l+3}} - \eta_{T_{l+2}})}$$

Vertical interpolation grid and weights for vertical cubic Hermite interpolations

A 4-point vertical grid is defined as it is shown in figure **??**. The interpolation point O (medium or origin point) is between T_{l+1} and T_{l+2}.

First weights to compute vertical derivatives at layers $l+1$ and $l+2$ are computed. For a variable X, $\frac{\partial X}{\partial \eta}$ is computed as close as possible as $\left(\dot{\eta}\frac{\partial X}{\partial \eta}\right)/\dot{\eta}$, but with additional approximations allowing to avoid horizontal interpolations for term $\left(\dot{\eta}\frac{\partial p}{\partial \eta}\right)$.

- For layers other than the first or the last layer, discretization follows:

$$\left(\frac{\partial X}{\partial \eta}\right)_{l+1} = \frac{1}{2}\frac{X_{l+2} - X_l}{\eta_{\bar{l}+1} - \eta_{\bar{l}}} \tag{73}$$

- For layer $l = 1$, discretization assumes that $\left(\dot{\eta}\frac{\partial p}{\partial \eta}\right)_{\bar{l}=0} = 0$; discretization follows:

$$\left(\frac{\partial X}{\partial \eta}\right)_{l=1} = \frac{X_{l=2} - X_{l=1}}{\eta_{\bar{l}=1} - \eta_{\bar{l}=0}} \tag{74}$$

- For layer $l = L$, discretization assumes that $\left(\dot{\eta}\frac{\partial p}{\partial \eta}\right)_{\bar{l}=L} = 0$; discretization follows:

$$\left(\frac{\partial X}{\partial \eta}\right)_{l=L} = \frac{X_{l=L} - X_{l=L-1}}{\eta_{\bar{l}=L} - \eta_{\bar{l}=L-1}} \tag{75}$$

The following weights are computed:

- For an interpolation point included between layers 2 and $L-1$ ($l \geq 1$ and $l \leq L-3$) :

$$VDERW11 = \frac{1}{2}\frac{\eta_{l+2} - \eta_{l+1}}{\eta_{\bar{l}+1} - \eta_{\bar{l}}}$$

$$VDERW21 = \frac{1}{2}\frac{\eta_{l+2} - \eta_{l+1}}{\eta_{\bar{l}+1} - \eta_{\bar{l}}}$$

$$VDERW12 = \frac{1}{2}\frac{\eta_{l+2} - \eta_{l+1}}{\eta_{\bar{l}+2} - \eta_{\bar{l}+1}}$$

$$VDERW22 = \frac{1}{2}\frac{\eta_{l+2} - \eta_{l+1}}{\eta_{\bar{l}+2} - \eta_{\bar{l}+1}}$$

- For an interpolation point included between layers 1 and 2:

$$VDERW11 = 0$$

$$VDERW21 = \frac{\eta_{l=2} - \eta_{l=1}}{\eta_{\bar{l}=1} - \eta_{\bar{l}=0}}$$

$$VDERW12 = \frac{1}{2}\frac{\eta_{l=2} - \eta_{l=1}}{\eta_{\bar{l}=2} - \eta_{\bar{l}=1}}$$

$$VDERW22 = \frac{1}{2}\frac{\eta_{l=2} - \eta_{l=1}}{\eta_{\bar{l}=2} - \eta_{\bar{l}=1}}$$

  such a case is extended to the case where the interpolation point is between the top and the first layer; in this case the interpolation becomes an extrapolation.

- For an interpolation point included between layers $L-1$ and L:

$$VDERW11 = \frac{1}{2}\frac{\eta_{l=L} - \eta_{l=L-1}}{\eta_{\bar{l}=L-1} - \eta_{\bar{l}=L-2}}$$

$$VDERW21 = \frac{1}{2}\frac{\eta_{l=L} - \eta_{l=L-1}}{\eta_{\bar{l}=L-1} - \eta_{\bar{l}=L-2}}$$

$$VDERW12 = \frac{\eta_{l=L} - \eta_{l=L-1}}{\eta_{\bar{l}=L} - \eta_{\bar{l}=L-1}}$$

$$VDERW22 = 0$$

  such a case is extended to the case where the interpolation point is between the last layer and the ground; in this case the interpolation becomes an extrapolation.

Functions $f_{H1}(ZDVER)$ to $f_{H4}(ZDVER)$ (involved in any Hermite cubic interpolation) are:

- $f_{H1}(\alpha) = (1-\alpha)^2(1+2\alpha)$
- $f_{H2}(\alpha) = \alpha^2(3-2\alpha)$
- $f_{H3}(\alpha) = \alpha(1-\alpha)^2$
- $f_{H4}(\alpha) = -\alpha^2(1-\alpha)$

Interpolation grid and weights for tri-linear interpolations

A 64-point grid is defined as it is shown in figure **??**. The interpolation point O (medium or origin point) is between $B_{1,l+1}$, $C_{1,l+1}$, $B_{2,l+1}$, $C_{2,l+1}$, $B_{1,l+2}$, $C_{1,l+2}$, $B_{2,l+2}$ and $C_{2,l+2}$. For the two levels $l+1$ and $l+2$ see section 8.1 corresponding to bi-linear horizontal interpolations for weights computations. For weights needed for vertical interpolations ($ZDVER$) see section 8.1 corresponding to linear vertical interpolations.

Interpolation grid and weights for 32-point interpolations

A 64-point grid is defined as it is shown in figure **??**. The interpolation point O (medium or origin point) is between $B_{1,l+1}$, $C_{1,l+1}$, $B_{2,l+1}$, $C_{2,l+1}$, $B_{1,l+2}$, $C_{1,l+2}$, $B_{2,l+2}$ and $C_{2,l+2}$. For the two levels l and $l+3$ see section 8.1 corresponding to bi-linear horizontal interpolations for weights computations. For the two levels $l+1$ and $l+2$ see section 8.1 corresponding to 12-point horizontal interpolations for weights computations. For weights needed for vertical interpolations ($ZDVER$) see section 8.1 corresponding to linear vertical interpolations.

Other grids and weights

The following interpolation systems are available but not described here:

- vertical cubic splines
- horizontal 16-point linear least-square fit
- horizontal 32-point linear least-square fit
- horizontal 12-point spline cubic
- 32-point spline cubic

8.2 Interpolations

Bilinear interpolation

It is done in subroutine LAIDLI. See figure **??** and section 8.1 for definition of $ZDLO1$, $ZDLO2$, $ZDLAT$ and points B_1, C_1, B_2 and C_2.

For a quantity X, are computed successively:

- a linear interpolation on the longitude number 1:
  $X_1 = X_{B_1} + ZDLO1(X_{C_1} - X_{B_1})$
- a linear interpolation on the longitude number 2:
  $X_2 = X_{B_2} + ZDLO2(X_{C_2} - X_{B_2})$
- a meridional linear interpolation:
  $X_{interpo} = X_1 + ZDLAT(X_2 - X_1)$

Tri-linear interpolation

It is done in subroutine LAITLI. For layers $l+1$ and $l+2$ (see figure **??**) bilinear horizontal interpolations give two interpolated values X_{l+1} and X_{l+2} (see section 8.2). Then the final interpolated value is given by the following expression:

$$X_{interpo} = X_{l+1} + ZDVER(X_{l+2} - X_{l+1})$$

Horizontal 12-point interpolation

It is done in subroutine LAIDDI or its shape-preserving version LAIDQM. See figure **??** and section 8.1 for definition of $ZDLO0$, $ZDLO1$, $ZDLO2$, $ZDLO3$, $ZCLA2$, $ZCLA3$ and $ZCLA4$ and points B_0, C_0, A_1, B_1, C_1, D_1, A_2, B_2, C_2, D_2, B_3 and C_3. Let us define:

- $f_2(\alpha) = (\alpha+1)(\alpha-2)(\alpha-1)/2$
- $f_3(\alpha) = -(\alpha+1)(\alpha-2)\alpha/2$
- $f_4(\alpha) = \alpha(\alpha-1)(\alpha+1)/6$

For a quantity X, are computed successively:

- a linear interpolation on the longitude number 0:
  $X_0 = X_{B_0} + ZDLO0(X_{C_0} - X_{B_0})$

- a cubic 4-point interpolation on the longitude number 1:
  $X_1 = X_{A_1} + f_2(ZDLO1)(X_{B_1} - X_{A_1}) + f_3(ZDLO1)(X_{C_1} - X_{A_1}) + f_4(ZDLO1)(X_{D_1} - X_{A_1})$
- a cubic 4-point interpolation on the longitude number 2:
  $X_2 = X_{A_2} + f_2(ZDLO2)(X_{B_2} - X_{A_2}) + f_3(ZDLO2)(X_{C_2} - X_{A_2}) + f_4(ZDLO2)(X_{D_2} - X_{A_2})$
- a linear interpolation on the longitude number 3:
  $X_3 = X_{B_3} + ZDLO3(X_{C_3} - X_{B_3})$
- a meridional cubic 4-point interpolation:
  $X_{interpo} = X_0 + ZCLA2(X_1 - X_0) + ZCLA3(X_2 - X_0) + ZCLA4(X_3 - X_0)$

There is a shape-preserving version LAIDQM of routine LAIDDI: after cubic 4-point interpolations on longitudes number 1 and 2, X_1 is bounded between X_{B_1}, and X_{C_1} and X_2 is bounded between X_{B_2} and X_{C_2}; after meridian cubic 4-point interpolation $X_{interpo}$ is bounded between X_1 and X_2. Use of switches LQMW (momentum equation), LQMT (temperature equation), LQMQ (humidity equation), LQMV (passive scalar equations), LQMP (continuity equation), allow to use shape-preserving interpolation routine LAIDQM instead of LAIDDI.

Cubic 4-point vertical interpolation

See figure **??** and section 8.1 for definition of $ZCVE2$, $ZCVE3$ and $ZCVE4$. The cubic 4-point vertical interpolation gives the final interpolated value:

$$X_{interpo} = X_l + ZCVE2(X_{l+1} - X_l) + ZCVE3(X_{l+2} - X_l) + ZCVE4(X_{l+3} - X_l)$$

Cubic Hermite vertical interpolation

See figure **??** and section 8.1 for definition of $VDERW11$, $VDERW21$, $VDERW12$ and $VDERW22$. See section 8.1 for definition of $ZDVER$. See section 8.1 for definition of functions f_{H1} to f_{H4}. The cubic Hermite vertical interpolation gives the final interpolated value:

$$X_{interpo} = f_{H1}(ZDVER)X_{l+1} + f_{H2}(ZDVER)X_{l+2} +$$
$$f_{H3}(ZDVER)(VDERW11(X_{l+1} - X_l) + VDERW21(X_{l+2} - X_{l+1})) +$$
$$f_{H4}(ZDVER)(VDERW12(X_{l+2} - X_{l+1}) + VDERW22(X_{l+3} - X_{l+2}))$$

32-point 3D interpolation with vertical cubic 4-point interpolation

It is done in subroutine LAITRI or its shape-preserving version LAITQM. For layers l and $l+3$ (see figure **??**) bilinear horizontal interpolations give two interpolated values X_l and X_{l+3} (see section 8.2). For layers $l+1$ and $l+2$ (see figure **??**) 12-point horizontal interpolations give two interpolated values X_{l+1} and X_{l+2} (see section 8.2). The final interpolated value $X_{interpo}$ is a cubic 4 points vertical interpolation of X_l, X_{l+1}, X_{l+2} and X_{l+3} (see section 8.2).

There is a shape-preserving version LAITQM of routine LAITRI. In LAITQM 12 points horizontal interpolations for layers $l+1$ and $l+2$ are shape-preserving interpolations (see description of routine LAIDQM in section 8.2) and vertical cubic 4-point interpolation is shape-preserving: $X_{interpo}$ is bounded by X_{l+1} and X_{l+2}. Use of switches LQMW (momentum equation), LQMT (temperature equation), LQMQ (humidity equation), LQMV (passive scalar equations), LQMP (continuity equation), allows to use shape-preserving interpolation routine LAITQM instead of LAITRI.

32-point 3D interpolation with vertical cubic Hermite interpolation

It is done in subroutine LAIHVT or its shape-preserving version LAIHVTQM. For layers l and $l+3$ (see figure **??**) bilinear horizontal interpolations give two interpolated values X_l and X_{l+3} (see section 8.2). For layers $l+1$ and $l+2$ (see figure **??**) 12-point horizontal interpolations give two interpolated values X_{l+1} and X_{l+2} (see section 8.2). The final interpolated value $X_{interpo}$ is a cubic Hermite vertical interpolation of X_l, X_{l+1}, X_{l+2} and X_{l+3} (see section 8.2).

There is a shape-preserving version LAIHVTQM of routine LAIHVT. In LAIHVTQM 12-point horizontal interpolations for layers $l+1$ and $l+2$ are shape-preserving interpolations (see description of routine LAIDQM in section 8.2) and vertical cubic Hermite interpolation is shape-preserving: $X_{interpo}$ is bounded by X_{l+1} and X_{l+2}. Use of switch LQMV (passive scalar equations), allows to use shape-preserving interpolation routine LAIHVTQM instead of LAIHVT.

Other algorithms

The following interpolation methods are also available but are not described here:

- diffusive bilinear interpolation (subroutine LAIDLIHD)
- diffusive tri-linear interpolation (subroutine LAITLIHD)

- 48-point 3D interpolation with vertical cubic spline interpolation (subroutine LAITVSPCQM)
- semi-lagrangian horizontal diffusion (subroutine LAITSLD)
- horizontal 16-point linear least-square fit interpolation
- 32-point with linear least-square fit horizontal and linear vertical interpolation (subroutine LAISMOO)
- horizontal 12-point spline interpolation (subroutine LAIDSP)
- 32-point 3D cubic spline interpolation
- semi-lagrangian horizontal diffusion with cubic splines (subroutine LAITSLDSP)

inputfigslag

9 Computation of $\dot{\eta}$ on layers

This quantity is needed to find the height of the medium and origin points. $\dot{\eta}_{\bar{l}}$ (resp. $\dot{\eta}_l$) is the η-coordinate vertical velocity $\dot{\eta}$ at the inter-layer $\bar{l}$ (resp. layer l), Δp_l is the pressure depth of layer l.

$\dot{\eta}$ can be written:

$$\dot{\eta} = \left(\dot{\eta}\frac{\partial p}{\partial \eta}\right)\frac{\partial \eta}{\partial p} \tag{76}$$

where $\left(\dot{\eta}\frac{\partial p}{\partial \eta}\right)$ is computed at inter-layers (and stored in the array PEVEL) using a vertical integration of continuity equation, and $\left(\frac{\partial \eta}{\partial p}\right)$ is computed at layers.

Discretization of Equation (76) is:

$$\dot{\eta}_l = \frac{1}{2}\left[\left(\dot{\eta}\frac{\partial p}{\partial \eta}\right)_{\bar{l}} + \left(\dot{\eta}\frac{\partial p}{\partial \eta}\right)_{\bar{l}-1}\right]\frac{\eta_{\bar{l}} - \eta_{\bar{l}-1}}{\Delta p_l} \tag{77}$$

10 Lateral boundary conditions

10.1 Extra longitudes

Let us denote by LX the number of longitudes (in the array NLOENG for each latitude in the code). For a quantity X, let us define:

- X(longitude number 0)=X(longitude number LX).
- X(longitude number LX+1)=X(longitude number 1).
- X(longitude number LX+2)=X(longitude number 2).

These extra computations are necessary for all interpolated fields. For distributed memory computations are done when making the halo (routine SLCOMM or SLCOMM1+SLCOMM2A which exchange data with other processors).

10.2 Extra latitudes

Let us denote by lx the number of latitudes (NDGLG in the code): latitudes number -1,0,$lx+1$,$lx+2$ are respectively the symmetric of latitudes number 2,1,lx,$lx-1$. These extra computations are necessary for all interpolated fields. For distributed memory computations are done in SLEXTPOL or SLEXTPOL1A+SLEXTPOL2.

10.3 Vertical boundary conditions

Vertical linear interpolations for layer variables at the medium point: The medium point has a vertical coordinate always included between $\eta_{\bar{l}=0}$ and $\eta_{\bar{l}=L}$ in case of vertical interpolating scheme. Therefore no extrapolated values are needed.

Vertical cubic 4-point interpolations for layer variables at the origin point: When the origin point is above the layer number 2 (resp. below the layer number $L-1$), the vertical cubic 4-point interpolations using data of the layers number 1, 2, 3 (resp. $L-2$, $L-1$, L) and the extra-layer number 0 (resp. $L+1$) are degenerated into linear interpolations between the layers number 1 and 2 (resp. $L-1$ and L). The extrapolated values at the extra-layer number 0 (resp. $L+1$) are always multiplied by a weight equal to 0 and are set to 0 in subroutine LAVABO. This algorithm extends itself to the case where the origin point is between the top (resp. surface) and the layer number 1 (resp. L), but in this case the interpolation using data of the layers number 1 and 2 (resp. $L-1$ and L) becomes an extrapolation.

Vertical cubic 4-point interpolations for inter-layer variables at the origin point: When the origin point is above the inter-layer number 1 (resp. $L-1$), the vertical cubic 4-point interpolations using data of the inter-layers number -1, 0, 1, 2 (resp. $L-2$, $L-1$, L and $L+1$) are degenerated into linear interpolations between the inter-layers numbers 0 and 1 (resp. $L-1$ and L).

Vertical cubic Hermite interpolations for layer variables at the origin point: When the origin point is above the layer number 2 (resp. $L-1$), interpolation is still a vertical cubic Hermite one, computation of vertical derivatives is modified for layer number 1 (resp. L). This algorithm extends to the case where the origin point is between the top (resp. ground) and the layer number 1 (resp. L), but in this case the interpolation using data of the layers number 1 and 2 (resp. $L-1$ and L) becomes an extrapolation.

Vertical cubic spline interpolations for layer variables at the origin point: Some top and bottom values are computed and the vertical interpolation always uses 4 points.

5

Semi-Implicit spectral computations

1 General considerations

1.1 Purpose

This chapter describes the semi-implicit scheme used in ARPEGE-CLIMAT. The ARPEGE-IFS code contains many other options. See Yessad (2007c) for a comprehensive description of all available features.

It is necessary to treat implicitly the linear terms source of (fast moving) gravity waves to ensure a good numerical stability at reasonable time steps; hence the solution of the equations involves the inversion of a linear system leading to a Helmholtz equation: inversion of such a system is more convenient to do in spectral space.

1.2 Advection scheme

In semi-Lagrangian form of equations, the time dependency equation of a variable X writes as:

$$\frac{dX}{dt} = \mathcal{A} + \mathcal{F} \tag{1}$$

where $\mathcal{A}$ is the dynamical contribution and $\mathcal{F}$ the contribution of the physical parametrizations. In a two-time level semi-Lagrangian scheme (abbreviated into 2TL SL scheme) $X(t+\Delta t)$ is computed at a grid point F knowing $X(t)$ at the point O (not necessary a grid point) where the same particle is at t.

1.3 Semi-implicit treatment of linear terms

Adding of a semi-implicit correction: The linear terms source of gravity waves must be treated implicitly, in order to allow time-steps compatible with an efficient use of the model. Expression of the semi-implicit linear terms is obtained assuming a definition of a reference state. Reference state is defined by a dry resting isotherm atmosphere in hydrostatic balance, reference orography is zero. Equation (1) becomes, in 2TL SL scheme without uncentering factor:

$$\frac{dX}{dt} = \mathcal{A} + \mathcal{F} + \left(-\beta \mathcal{B}^{t+0.5\Delta t} + \frac{\beta}{2}\mathcal{B}^{t} + \frac{\beta}{2}\mathcal{B}^{t+\Delta t} \right) \tag{2}$$

where $\mathcal{B}$ is the linear term source of gravity waves, β is a tunable parameter. $\beta = 0$ corresponds to an explicit formulation, $\beta = 1$ to an implicit formulation.

Discretization of Equation (2):

Equation (2) gives the following discretized equation, where Δt is the time step (without uncentering factor):

$$X^{t+\Delta t} - 0.5\beta\Delta t\mathcal{B}^{t+\Delta t} = X^{t} + \Delta t(\mathcal{A}+\mathcal{F}) - \beta\Delta t\mathcal{B}^{t+0.5\Delta t} + 0.5\beta\Delta t\mathcal{B}^{t} \tag{3}$$

where $X^{t+\Delta t} - 0.5\beta\Delta t\mathcal{B}^{t+\Delta t}$ is computed at the final grid point of the semi-Lagrangian trajectory, X^t and $0.5\beta\Delta t\mathcal{B}^t$ are computed at the origin point of the semi-Lagrangian trajectory, $-\beta\Delta t\mathcal{B}^{t+0.5\Delta t}$ and $\dot{X}$ are computed either at the medium point or as an average between the origin and final points of the trajectory.

If there is a first-order uncentering factor ϵ, averages along the semi-Lagrangian trajectory will be weighted by $(1-\epsilon)$ at the origin point and $(1+\epsilon)$ at the final point. In this case, Δt is replaced by $(1-\epsilon)\Delta t$ for terms at the origin point, and Δt is replaced by $(1+\epsilon)\Delta t$ for terms at the final point. For more details see Chapter 4.

$\mathcal{B}^{t+0.5\Delta t}$, $\mathcal{B}^t$ and $\mathcal{B}^{t-\Delta t}$ are computed in grid point space. The right-hand side member of Equation (3) is computed in grid point space, then transformed into spectral space. Once in spectral space, a system of equations of the following type must be solved:

$$X^{t+\Delta t} - 0.5\beta\Delta t\mathcal{B}^{t+\Delta t} = \mathcal{X}^{*} \tag{4}$$

where $\mathcal{X}^*$ is known and $X^{t+\Delta t}$ is unknown. Now the spectral computations to solve this system of equations are described for a primitive equations 3D model.

2 Prognostic variables and quantities involved in the semi-implicit scheme

2.1 Prognostic variables

Prognostic variables are components of the horizontal wind $\vec{V}$, temperature T, humidity q and logarithm of surface pressure $\ln p_s$ (for continuity equation).

2.2 Notations

- M is the mapping factor. $\overline{M}$ is a reference mapping factor for semi-implicit computations. $\overline{M} = c$ (stretching factor) if semi-implicit scheme with reduced divergence (LSIDG=.F.). $\overline{M} = M$ (mapping factor) if semi-implicit scheme with unreduced divergence (LSIDG=.T.). The latter option is used when horizontal resolution is not uniform
- a is the Earth mean radius
- $\vec{V}$ is the horizontal geographical wind. Its zonal component is U. Its meridional component is V
- D is the unreduced divergence of horizontal wind, $D^{'}$ is the reduced divergence. D and $D^{'}$ are linked by the relationship $D = M^2 * D^{'}$
- ζ is the unreduced vorticity of horizontal wind, $\zeta^{'}$ is the reduced vorticity. ζ and $\zeta^{'}$ are linked by the relationship $\zeta = M^2 * \zeta^{'}$
- T is the temperature. T^* is a vertically-constant reference temperature which is used in the semi-implicit scheme. Default value is $300\,K$ or $350\,K$ according to configuration
- q is the humidity
- p is pressure, p_s is surface pressure. p^* is a reference pressure and p_s^* is a reference surface pressure, which are used in the semi-implicit scheme and in some non-hydrostatic equations. These reference quantities are vertically dependent and horizontally (i.e. on η surfaces) constant. Default value of p_s^* is $1000\,hPa$ for a 2TL SL scheme. Δp^* are layer depths corresponding to a surface pressure equal to p_s^*
- p_s^{ST} is a reference pressure equal to the surface pressure of the standard atmosphere (variable VP00). Default value is $101325\,Pa$
- $\omega = \dfrac{dp}{dt}$ is the total temporal derivative of (vertical velocity in pressure coordinate)

- Φ is geopotential, Φ_s is the surface geopotential (i.e. the orography)
- $\vec{\Omega}$ is the Earth rotation angular velocity
- $\vec{r}$ is the vector directed upwards, the length of which is the Earth radius a
- g is the gravity acceleration constant
- R is the gas constant for air, R_d the gas constant for dry air and R_v the gas constant for water vapor
- c_p is the specific heat at constant pressure for air and c_{p_a} is the specific heat at constant pressure for dry air
- c_v is the specific heat at constant volume for air and c_{v_a} is the specific heat at constant volume for dry air
- $\overrightarrow{\nabla}$ is the unreduced first order horizontal gradient on η-surfaces. $\overrightarrow{\nabla}'$ is the reduced first order horizontal gradient. These two operators are linked by the relationship $\overrightarrow{\nabla} = M * \overrightarrow{\nabla}'$
- L: number of layers of the model
- A, B define pressure on the η levels ($p = A + Bp_s$, where p_s is the hydrostatic surface pressure)
- β coefficient for the semi-implicit scheme (between 0 and 1)
- γ, τ, ν, μ are generic notations for semi-implicit linear operators (see section 2.3)

2.3 Quantities used for vertical discretizations and linear operators

Operators α^* and δ^*: these operators are used for discretizations of some vertical integrals.

$$\alpha_l^* = 1 - \frac{p_{l-1}^*}{\Delta p_l^*} \ln\left(\frac{p_l^*}{p_{l-1}^*}\right)$$

$$\delta_l^* = \ln\left(\frac{p_l^*}{p_{l-1}^*}\right)$$

$$\alpha_{l=1}^* = 1 \quad , \; \delta_{l=1}^* = \ln\frac{p_1^*}{0.1}$$

Linear operator γ: this operator is applied to temperature for semi-implicit term in momentum equation.

$$(\gamma Z)_l = \alpha_l^* R_d Z_l + \sum_{k=l+1}^{L} R_d Z_k \delta_k^*$$

Linear operator τ : this operator is applied to divergence for semi-implicit term in temperature equation.

$$(\tau Z)_l = \frac{R_d T^*}{c_{p_d}} \left[\alpha_l^* Z_l + \frac{\delta_l^*}{\Delta p_l^*} \sum_{k=1}^{l-1} \Delta p_k^* Z_k \right]$$

Linear operator ν: this operator is applied to divergence for semi-implicit term in continuity equation.

$$(\nu Z) = \frac{1}{{p_s}^*} \sum_{l=1}^{L} \Delta p_l^* Z_l$$

Linear operator μ: this operator is applied to $\ln p_s$ for semi-implicit term in momentum equation. If $\ln p_s$ is the prognostic variable in continuity equation, definition of (μZ) is:

$$(\mu Z) = R_d T^* Z \tag{5}$$

(μZ) is applied to $\ln p_s$.

3 Semi-implicit scheme with reduced divergence

3.1 3D hydrostatic primitive equations model

Expression of the semi-implicit term $\mathcal{B}$:

- Continuity equation $(X = \ln p_s)$:

$$\mathcal{B} = -\overline{M}^2 \nu D' \tag{6}$$

- Divergence equation $(X = D')$:

$$\mathcal{B} = -\vec{\nabla}'^2 (\gamma T + \mu \ln p_s) \tag{7}$$

- Vorticity equation ($X = \zeta^{'}$):

$$\mathcal{B} = 0 \tag{8}$$

- Temperature equation ($X = T$):

$$\mathcal{B} = -\overline{M}^2 \tau D^{'} \tag{9}$$

- Humidity equation ($X = q$) and more generally GFL variables:

$$\mathcal{B} = 0 \tag{10}$$

System to be solved:

$$\ln p_{s\ t+\Delta t} + \beta \frac{\Delta t}{2} \overline{M}^2 \nu D^{'}_{t+\Delta t} = \mathcal{P}^* \tag{11}$$

$$D^{'}_{t+\Delta t} + \beta \frac{\Delta t}{2} \vec{\nabla}^{'2} (\gamma T_{t+\Delta t} + \mu \ln p_{s\ t+\Delta t}) = \mathcal{D}^{'*} \tag{12}$$

$$T_{t+\Delta t} + \beta \frac{\Delta t}{2} \overline{M}^2 \tau D^{'}_{t+\Delta t} = \mathcal{T}^* \tag{13}$$

$\mathcal{P}^*$, $\mathcal{D}^{'*}$, $\mathcal{T}^*$ correspond to $\mathcal{X}^*$ defined in Equation (4) and are available in spectral arrays (SPSP, SPDIV, SPT) at the beginning of the spectral computations. Equations (11) to (13) yield (Helmholtz equation):

$$(1 - \beta^2 \frac{\Delta t^2}{4} \overline{M}^2 B \vec{\nabla}^{'2}) D^{'}_{t+\Delta t} = \mathcal{D}^{'*} - \beta \frac{\Delta t}{2} \vec{\nabla}^{'2} (\gamma \mathcal{T}^* + \mu \mathcal{P}^*) \tag{14}$$

where $B = \gamma\tau + \mu\nu$ is a matrix operator $L * L$ (precomputed in routines SUDYN, SUBMAT and stored in the array SIB).

Spectral computations to solve system of equations (11) to (13)

Algorithm works zonal wave number by zonal wave number m ($\mid m \mid$ varies between 0 and the truncation N_s) and performed in the routine SPCSI before all horizontal diffusion schemes. For a given zonal wave number m:

- After a preliminary memory transfer the right-hand side member of Equation (14) is computed for all total wave numbers n between m and N_s.
- Inversion of Helmholtz equation: method via a diagonalization in the eigenmodes space (LSITRIC=.F. in NAMCT0).

- First the diagonalization of B is used: $B = Q^{-1}AQ$, where A is a diagonal $L * L$ matrix, the diagonal coefficients a_l of which are stored in the array SIVP. Q is a $L * L$ matrix stored in the array SIMI, Q^{-1} is stored in the array SIMO. Note that vertical operators ν, μ, τ, γ, $\mathcal{B}$, Q commute with the horizontal operator $\vec{\nabla}'^2$.
- Helmholtz equation (14) becomes, for each eigenmode l:

$$(1 - \beta^2 \frac{\Delta t}{4}^2 a_l \overline{M}^2 \vec{\nabla}'^2) Q D'_{t+\Delta t} = Q(\mathcal{D}'^* - \beta \frac{\Delta t}{2} \vec{\nabla}'^2 (\gamma \mathcal{T}^* + \mu \mathcal{P}^*)) \qquad (15)$$

- For each eigenmode l and each zonal wave number m: $(1 - \beta^2 \frac{\Delta t}{4}^2 a_l \overline{M}^2 \vec{\nabla}'^2)$ is a diagonal matrix operator $(N_s + 1 - \mid m \mid) \times (N_s + 1 - \mid m \mid)$: spectral coefficients of the right-hand side member of (15) are simply divided by the diagonal coefficients of this matrix. Then the result is multiplied by Q^{-1}.

- Once known $D'_{t+\Delta t}$ Equation (11) provides $p_{s\ t+\Delta t}$ and Equation (13) provides $T_{t+\Delta t}$.
- Semi-implicit scheme ends by a final memory transfer.

4 Semi-implicit scheme with unreduced divergence

4.1 Shortcomings of this formulation of the semi-implicit scheme in case of stretching

In the grid points computations for some equations (for example temperature and continuity equation), the semi-implicit term $\mathcal{B}$ contains the reduced quantity $(\overline{M}^2 D')$. This quantity is added to geographical quantities. That is no problem near the high resolution pole. This reduced quantity becomes very large near the low resolution pole: if the stretching coefficient is c, $(\overline{M}/M)^2 = c^4$ at the low resolution pole, which is equal to 81 if $c = 3$. Thus the order of magnitude of the semi-implicit correction tendency becomes too high and physically absurd in the low resolution zone (gravity waves are no longer treated implicitly). That leads to instabilities in regions of the low resolution zone with high orography, in adiabatic Eulerian runs, or in semi-lagrangian runs with time-steps over the limit imposed by the Courant-Friedrich-Levy condition. In Eulerian runs with physics, the combination of physics and small time-steps inhibits this instability. In order to avoid this instability, another formulation of the semi-implicit scheme can be used (controlled by LSIDG) which provides an implicit treatment of the gravity waves everywhere on the sphere and not only near the high resolution pole. This

formulation is a formulation with unreduced divergence (simply by replacing the quantity $\overline{M}$ by the mapping factor M).

4.2 3D hydrostatic primitive equations model

Expression of the semi-implicit term $\mathcal{B}$:

As in section 3. Just replace $\overline{M}$ by M in Equations (6) to (10).

System to be solved:

As in section 3. Just replace $\overline{M}$ by M in Equations (11) to (14).

Spectral computations to solve system of equations (11) to (13).

Algorithm works zonal wave number by zonal wave number m ($\mid m \mid$ varies between 0 and the truncation N_s). Algorithm is performed in the routine SPCSI. For a given zonal wave number m:

- After a preliminary memory transfer the right-hand side member of equation (14) is computed for all total wave numbers n between m and N_s.
- Inversion of Helmholtz equation is more complicated than in the case of semi-implicit scheme with reduced divergence because the left-hand side member of Helmholtz equation contain values of the divergence for all levels and five total wave numbers ($n-2$ to $n+2$). Of course M^2 is a symmetric penta-diagonal matrix, for a given zonal wave number m. Pay attention to the fact that M^2 does not commute with the diagonal operator $\vec{\nabla}'^2$.
  - First the diagonalization of B is used: $B = Q^{-1}AQ$, where A is a diagonal $L * L$ matrix, the diagonal coefficients a_l of which are stored in the array SIVP. Q is a $L * L$ matrix stored in the array SIMI, Q^{-1} is stored in the array SIMO. Note that vertical operators ν, μ, τ, γ, $\mathcal{B}$, Q commute with the horizontal operators $\vec{\nabla}'^2$ and M^2.
  - Helmholtz Equation (14) becomes, for each eigenmode l:

$$(1 - \beta^2 \frac{\Delta t}{4}^2 a_l \vec{\nabla}'^2 M^2) Q D'_{t+\Delta t} = Q(\mathcal{D}'^* - \beta \frac{\Delta t}{2} \vec{\nabla}'^2 (\gamma \mathcal{T}^* + \mu \mathcal{P}^*)) \qquad (16)$$

  - For each eigenmode l and each zonal wave number m: $(\vec{\nabla}'^{-2} - \beta^2 \frac{\Delta t}{4}^2 a_l M^2)$ is a symmetric penta-diagonal matrix operator of size:
    $(N_s + 1 - \mid m \mid) \times (N_s + 1 - \mid m \mid)$.
    The factorization LU of this matrix is computed, where L is a

lower triangular tri-diagonal matrix, U is a upper triangular tri-diagonal matrix with coefficients equal to 1 on the main diagonal. All useful coefficients of L, U are computed in the set-up routine SUHEG and stored in the array SIHEG.

– For the zonal wave number $m = 0$ Equation (16) is not multiplied by $\vec{\nabla}'^{-2}$ because, for the total wave number $n = 0$, $\vec{\nabla}'^{2}$ is equivalent to a multiplication by 0 and $\vec{\nabla}'^{-2}$ is equivalent to a division by 0. The only difference is that the penta-diagonal but non-symmetric operator $(1-\beta^2\frac{\Delta t^2}{4}\, a_l\vec{\nabla}'^{2}M^2)$ is factorized and inverted. All useful coefficients of L, U are computed in the set-up routine SUHEG and stored in the arrays SIHEG and SIHEG2.

- Once known $D'_{t+\Delta t}$ equation (11) provides $\ln p_{st+\Delta t}$ and Equation (13) provides $T_{t+\Delta t}$. Spectral multiplications by M^2 are performed by the product of a symmetric penta-diagonal matrix of size:
$(N_s + 1 - \mid m \mid) \times (N_s + 1 - \mid m \mid)$
(useful coefficients computed in routine SUSMAP and stored in the array SCGMAP) by a vector containing spectral coefficients (m, n) for n varying from $\mid m \mid$ to N_s

- Semi-implicit scheme ends by a final memory transfer.

5 Spectral multiplications by polynomial expressions of the mapping factor

Expression of mapping factor M in spectral space.

Let us denote by:

$$a_c = \frac{1}{2}(c + \frac{1}{c})$$

$$b_c = \frac{1}{2}(c - \frac{1}{c})$$

$$e_{(0,0)} = 0$$

$$e_{(m,n)} = \sqrt{\frac{n^2 - m^2}{4n^2 - 1}}$$

Expression of M is:

$$M = a_c + b_c\xi \tag{17}$$

where ξ is the sine of computational sphere latitude. Expression of $[MX]_{(m,n)}$ is:

$$[MX]_{(m,n)} = b_c e_{(m,n)} X_{(m,n-1)} + a_c X_{(m,n)} + b_c e_{(m,n+1)} X_{(m,n+1)} \quad (18)$$

It is easy from (18) to retrieve the coefficients of spectral multiplication by any first degree polynomial of M. This is equivalent to a multiplication by a tri-diagonal symmetric matrix in spectral space.

Expression of M^2 in spectral space

$$\begin{aligned}[M^2X]_{(m,n)} &= b_c^2 e_{(m,n)} e_{(m,n-1)} X_{(m,n-2)} + 2a_c b_c e_{(m,n)} X_{(m,n-1)} + \\ &\quad (a_c^2 + b_c^2(e_{(m,n)}^2 + e_{(m,n+1)}^2))X_{(m,n)} + \\ &\quad 2a_c b_c e_{(m,n+1)} X_{(m,n+1)} + \\ &\quad b_c^2 e_{(m,n+1)} e_{(m,n+2)} X_{(m,n+2)} \end{aligned} \quad (19)$$

This is equivalent to a multiplication by a penta-diagonal symmetric matrix in spectral space.

6

Horizontal diffusion and nudging

1 Introduction

In the code of ARPEGE-IFS horizontal diffusion computations are spectral computations. The main horizontal diffusion scheme acts in spectral space. It is implicit in order to remain stable even with high diffusion coefficients and is called after the semi-implicit scheme.

Details on options of this scheme not used in ARPEGE-CLIMAT, on the other horizontal schemes (enhanced horizontal diffusion scheme, semi-lagrangian horizontal diffusion) may be found in Yessad (2007d).

2 Formulation of the horizontal diffusion

2.1 General considerations

In the spectral space the horizontal diffusion formulation is close to:

$$\frac{\partial X}{\partial t} = -K_X M \vec{\nabla}'^r X \tag{1}$$

where K_X is a vertically dependent and horizontally constant coefficient. K_X is generally complex: $\exp(i\frac{\pi}{2}r)$ multiplied by a real positive coefficient. The power of the scheme is r. M is the mapping factor.

$$K_X = \exp(-i\frac{\pi}{2}r) \left[\sqrt{\frac{N_s(N_s+1)}{a^2}} \right]^{-r} \Omega h_X \, g \tag{2}$$

a is the mean Earth radius, N_s is the truncation (maximum total wavenumber), g is a vertical profile, Ω is the angular velocity of the Earth rotation ($7.29\ 10^{-5} s^{-1}$). h_X is a constant coefficient for each prognostic variable. There are seven constants, one for vorticity (h_ζ), one for divergence (h_D), one for temperature (h_T), one for humidity (h_q), one for ozone ($h_{\mathcal{O}3}$), one for the extra GFL variables (h_{SV}), and one for surface pressure (h_{SP}). For divergence, expression of h_D matches:

$$\frac{1}{\Omega h_D} = r_{dampD} \frac{2\pi a}{NLO} \frac{(1 + 0.5RLG)^{2.5}}{DIF} \tag{3}$$

RLG is the increment from linear to quadratic grid (RNLGINC), $RLG = 0$ for a linear grid, 1 for a quadratic grid); DIF is a tuning parameter; NLO is the maximum number of longitudes of the computational sphere (NDLON), $2\pi a/NLO$ is the grid size before stretching.

For the other 3D upper air fields:

$$h_X = \frac{r_{dampD}}{r_{dampX}} h_D \tag{4}$$

The basic control of horizontal diffusion in the namelist is done by RRDXTAU (DIF), the different RDAMPx (r_{dampX}), and REXPDH (r).

3 Discretization of the horizontal diffusion

3.1 Unstretched model

The discretized equation which is coded is:

$$X^+_{(m,n)} - X^-_{(m,n)} = -\Omega h_X g(l) f(n, N, n_0(X), x_0, r) \Delta t\, X^+_{(m,n)} \tag{5}$$

where the superscripts + and − indicate respectively variables after horizontal diffusion and variables before horizontal diffusion, Δt is the time step, n is the total wave number (between 0 and the truncation N_s), m is the zonal wave number (between $-n$ and n in a triangular truncation), r is the order of the horizontal diffusion operator, N is a reference wave number, $n_0(X)$ is a threshold depending on variable X (generally zero except for vorticity where it is 2), x_0 is a threshold between 0 and 1. $\vec{\nabla}'$ is the first order horizontal reduced derivative operator (i.e in the grid point space, $\vec{\nabla} = M\vec{\nabla}'$, where M is the mapping factor). h_X is a coefficient depending on the variable X. The vertical dependency is expressed by $g(l)$.

This horizontal diffusion scheme is an implicit horizontal diffusion scheme (in the right-hand side member of the equation there is $X^{+}_{(m,n)}$ and not $X^{-}_{(m,n)}$). Equation (5) becomes (6):

$$X^{+}_{(m,n)} = \frac{1}{1 + \Omega h_X g(l) f(n, N_s, n_0(X), x_0, r) \Delta t} X^{-}_{(m,n)} \tag{6}$$

Expression of $f(n, N, n_0(X), x_0, r)$ is currently:

$$f(n, N, n_0(X), x_0, r) = \max\left(0, \min\left(1, \left(\frac{x - x_0}{1 - x_0}\right)^r\right)\right) \tag{7}$$

with:

$$x = \left(\frac{\max(0, n(n+1) - n_0)}{\max(0, N(N+1) - n_0)}\right)^{\frac{1}{2}}$$

An exact discretization of equation (1) would give:

$$f(n, N, n_0(X), x_0, r) = f(n, N_s, 0, 0, r) \tag{8}$$

For layer number l, expression of $g(l)$ is:

$$g(l) = \frac{y_0}{\min(y_0, \max(y_3, p_l^{ST}/p_s^{ST}))} \tag{9}$$

where p_l^{ST} is the standard atmosphere pressure for the layer number l, p_s^{ST} is a reference pressure (sea level pressure for the standard atmosphere: $1013.25\, hPa$). The dimensionless parameter y_0 is between 0 and 1: $g(l) = 1$ if p_l^{ST}/p_s^{ST} is above y_0 and $g(l) > 1$ if p_l^{ST}/p_s^{ST} is below y_0. The dimensionless parameter y_3 is between 0 and y_0. In practical it is much less than y_0 and is used to avoid too high diffusion in the upper stratosphere.

3.2 Stretched model

Approximation of the mapping factor

Expression of mapping factor in spectral space

Let us denote by:

- $a = \frac{1}{2}\left(c + \frac{1}{c}\right)$

- $b = \frac{1}{2}\left(c - \frac{1}{c}\right)$
- $\epsilon_{(0,0)} = 0$
- $\epsilon_{(m,n)} = \sqrt{\frac{n^2 - m^2}{4n^2 - 1}}$

Expression of M is:

$$M = a + b\mu \tag{10}$$

where μ is the sine of computational sphere latitude. Expression of $[MX]_{(m,n)}$ is:

$$[MX]_{(m,n)} = b\epsilon_{(m,n)}X_{(m,n-1)} + aX_{(m,n)} + b\epsilon_{(m,n+1)}X_{(m,n+1)} \tag{11}$$

A multiplication by M in spectral space is equivalent to a multiplication by a symmetrical tri-diagonal matrix.

Discretization

$$\begin{aligned} X^{-}_{(m,n)} &= X^{+}_{(m,n)} + \Omega h_X g(l)\Delta t \Big[\\ &\quad b\epsilon_{(m,n)} f(n-1, N, n_0(X), x_0, r) X^{+}_{(m,n-1)} \\ &\quad + a f(n, N, n_0(X), x_0, u) X^{+}_{(m,n)} \\ &\quad + b\epsilon_{(m,n+1)} f(n+1, N, n_0(X), x_0, r) X^{+}_{(m,n+1)} \Big] \end{aligned}$$

Solving this equation is equivalent to invert a tri-diagonal matrix for each zonal wave number m. The computation of this matrix and a decomposition into a product of two triangular bi-diagonal matrices are performed in the set-up routine SUHDU. At each time step these two triangular bi-diagonal matrices are inverted in order to compute $X^{+}_{(m,n)}$.

3.3 Second reference truncation N_2 in the stratosphere

It is possible in the code to modify $g(l)$ in order to simulate a replacement of $f(n, N_s, n_0(X), x_0, r)$ by $f(n, N_2, n_0(X), x_0, r)$, where $N_2 < N_s$, for standard pressure $p_l^{ST} < y_1 * p_s^{ST}$, where $y_1 < y_0$. In this case $g(l)$ (and K'_X) also depends on n for standard pressures below $y_0 * p_s^{ST}$. If p_l^{ST}/p_s^{ST} is below y_1:

$$g(l,n) = \frac{y_0}{\min(y_0, (\max(y_3, p_l^{ST}/p_s^{ST}))} \frac{f(n, N_2, n_0(X), x_0, r)}{f(n, N_s, n_0(X), x_0, r)} \tag{12}$$

If p_l^{ST}/p_s^{ST} is over y_1 and below y_0:

$$g(l,n) = \frac{y_0 * p_s^{ST} - b(n)}{p_l^{ST} - b(n)} \tag{13}$$

where:

$$b(n) = \frac{(y_0 * p_s^{ST})(y_1 * p_s^{ST})(f(n, N_2, n_0(X), x_0, r) - f(n, N_s, n_0(X), x_0, r))}{(y_0 * p_s^{ST}) f(n, N_2, n_0(X), x_0, r) - (y_1 * p_s^{ST}) f(n, N_s, n_0(X), x_0, r)}$$

One can check that (13) yields $g(l,n) = 1$ for $p_l^{ST} = y_0 * p_s^{ST}$ and that (12) and (13) are continuous for $p_l^{ST} = y_1 * p_s^{ST}$. When taking $N_2 = N_s$, one retrieves formula (9). Choice of $N_2 < N_s$ is useful in simulations with high vertical resolution in the stratosphere.

3.4 Discretized equations

GMV and GFL variables

- reduced vorticity $\zeta^{'}$ $(n_0(\zeta) = 2)$
- reduced divergence $D^{'}$ $(n_0(D) = 0)$
- specific humidity q $(n_0(q) = 0)$
- other spectral GFL variables (e.g. ozone) $(n_0 = 0)$

For grid point GFL variables (e.g. liquid water) and non-advectable GFL variables, no horizontal diffusion is applied

Temperature

The role of horizontal diffusion for temperature is not to reduce the horizontal gradient between mountains and valleys. With a terrain-following vertical coordinate like η, we cannot apply the scheme directly to T. For this reason, $T - \alpha \ln p_s$ is diffused instead of T, where α is a coefficient depending on the altitude and using parameters related to standard atmosphere. Let us denote by T_s^{ST} the surface temperature in a standard atmosphere $(288.15\,K)$, R the air constant, g the acceleration due to gravity, $\left[\frac{dT}{dz}\right]_{ST}$ the tropospheric temperature vertical gradient in a standard atmosphere $(-0.0065\,K\,m^{-1})$, T_{tro}^{ST} the tropopause temperature in a standard atmosphere $(217.15\,K)$.

If:

$$T_s^{ST}\left(\frac{p^{ST}}{p_s^{ST}}\right)^{\left(\frac{R}{g}\left[\frac{dT}{dz}\right]_{ST}\right)} \quad > \quad T_{tro}^{ST}$$

the expression of α_l for layer number l is:

$$\alpha_l = -B_l \frac{R}{g}\left[\frac{dT}{dz}\right]_{ST} T_s^{ST}\left(\frac{p^{ST}}{p_s^{ST}}\right)^{-\left(\frac{R}{g}\left[\frac{dT}{dz}\right]_{ST}+1\right)} \tag{14}$$

where B_l is used in the definition of pressure on layers and inter-layers (hybrid vertical coordinate).

In the other cases:

$$\alpha_l = 0 \tag{15}$$

Thus temperature horizontal diffusion reads:

$$T^+_{(m,n)} - \alpha\,(\ln p_s)^-_{(m,n)} = \frac{(T^-_{(m,n)} - \alpha\,(\ln p_s)^-_{(m,n)})}{1 + \Omega h_T g(l) f(n, N, n_0(T), x_0, r)\Delta t} \tag{16}$$

which yields:

$$T^+_{(m,n)} = \frac{(T^-_{(m,n)} + \alpha\Omega h_T g(l) f(n, N, n_0(T), x_0, r)\Delta t\,(\ln p_s)^-_{(m,n)})}{1 + \Omega h_T g(l) f(n, N, n_0(T), x_0, r)\Delta t} \tag{17}$$

This scheme is fully implicit only when $h_{SP} = 0$, which is the default. For temperature $n_0(T) = 0$.

4 Nudging

This scheme called just after horizontal diffusion (for spectral variables) is a linear relaxation of prognostic variables towards pre-defined fields and is not properly saying a diffusion scheme. The generic equation is:

$$\frac{\partial X}{\partial t} = -\frac{1}{\tau_X}(X - X_{ref})$$

Pre-defined fields X_{ref} (for example reanalyzed fields) can be read on a file every NFRHIS time steps (typically at 6 h frequency) and interpolated at

each time step linearly. A cubic spline for time interpolation is also possible, but it requires more IO and more memory for a tiny impact. Nudging coefficients $1/\tau_X$ can be different for each variable. A vertical profile (common to each variable) can be applied to the coefficients.

Nudging can be applied to most prognostic variables in spectral space or in grid point space. When applied to spectral variables, it can be restricted to wave numbers less than a critical value. This allows to drive the large-scale features and let the model adjust the small scales freely. When applied to grid-point variables (the same as spectral ones, except that velocity potential and stream function are replaced by u- and v- components) there is a possibility of applying a 2D mask which modulates horizontally the strength of the relaxation. One can thus mimic the behavior of a limited area model or impose the atmosphere variables in a particular region of the globe. As for the vertical or the spectral modulation, this horizontal modulation is the same for all variables.

There is also nudging for some grid-point variables in grid-point space, such as surface temperature, surface moisture, deep moisture and snow depth. In the case of surface temperature, when the nudging coefficient is not zero, it is considered as infinite over sea (i.e. model values are prescribed by the driving field). This allows to replace an obsolete feature of ARPEGE-CLIMAT which updated some fields at daily frequency from two monthly boundary condition files (subroutine UPDCLIDM, switch LMCC01). See Chapter 7 for information about boundary conditions. The grid-point nudging is not called in the spectral subroutine SPCHOR, but in the grid-point subroutine MFPHYS.

Another interesting feature of nudging (spectral or grid-point variables) is the behavior in case of negative nudging coefficient. In this case, the model is no longer relaxed toward the driving field, but the driving field is just added to the time derivative:

$$\frac{\partial X}{\partial t} = X_{ref} + \cdots$$

This allows to introduce flux correction for some variables. Nudging and correction can be easily combined:

$$\frac{\partial X}{\partial t} = -\frac{1}{\tau_X}(X - X_{ref}) + C$$

can be rewritten

$$\frac{\partial X}{\partial t} = -\frac{1}{\tau_X}(X - (X_{ref} - C\tau_X))$$

Each variable can be treated in nudging or correction mode separately, since each variable has its own relaxation coefficient (one for spectral and one for grid point in the case of atmospheric fields).

In any case, the time discretization is implicit for numerical stability. The control is made in NAMNUD; each coefficient is expressed as an inverse of the time step, e.g. a value of one means that the time relaxation is one time step and a value of zero (the default value) means that no relaxation is applied to the variable. The driving data are found in ARPEGE files with name RX$DATE with DATE expressed as YYYYMMDDHH.

7

Boundary conditions

1 Introduction

To carry out an integration of the atmosphere equations, the model needs to know the values of a certain number of variables (named historical or prognostic) at time $t = 0$ (initial conditions), but also of a certain number of variables for which the evolution is not calculated (boundary conditions). At the end of an integration, the model provides the values of the historical variables at time $t = T$, which are used as initial conditions for the next integration.

In the current version of ARPEGE-CLIMAT, the initial conditions are now split into 2 files : one file for the atmosphere variables and one file for the surface variables. The boundary conditions are read on the same file as the initial conditions. For the atmosphere variables, this work is carried out by subroutines SUSPECA (fields in spherical harmonics like orography) and SUGRIDADM (fields on the collocation grid) at the beginning of any integration. These variables come from monthly climatological files. For the surface variables, the subroutine AROINI_SURF (fields on the collocation grid) is called at the beginning of any integration. These variables (physiography and orography fields) come from the ECOCLIMAP, orography, sand and clay fractions files.

Those climatological files as well as the physiographic fields need to be calculated for any geometry (truncation, rotation and stretching, vertical discretization).

The files of boundary conditions are obtained first by external scripts, followed by run of specific binaries in charge of aerosols and ozone. In the model script, the binaries UPDCLI and UPDOZO updates the atmospheric

restart file with monthly (and possibly yearly varying) fields taken from the climatological files.

The fields of sea surface temperature, sea-ice extent and sea-ice albedo are read in the course of integration (in principle once per day) from the data produced by the ocean model and prepared by the coupler OASIS in subroutine UPDCPL .

2 Surface boundary conditions

The surface physiographic fields The data come from :

- the ECOCLIMAP-II data base (see SURFEX - Scientific Documentation - II LAND USE: ECOCLIMAP) which is a global database of land surface parameters (land covers) at 1-km resolution. It is intented to be used to initialize the soil-vegetation-atmosphere transfer schemes (SVATs) in meteorological and climate models.

- the orography file GTOPO30 (source : U.S Geological Survey) : resolution of 30 " XXX A REVOIRXXXX

- the HSWD database for the clay fraction and the sand fraction of the near-surface soil : resolution of 5'

The physiographic fields are averaged or interpolated on the specified grid by the program PGD provided in the ARPEGE-CLIMATsource code. The fields are stored in a file, called PGD file, but only with the physiographic 2D fields, the geographic and grid data written in it. Therefore, the PGD file contains the spatial characteristics of the surface and all the physiographic data necessary to run the interactive surface schemes for vegetation and town.

Output data

1. land cover
2. orography parameters (averaged, silhouette, maximum, mininum)[1]
3. subgrid-scale orography parameters (slope , anisotropy, standard deviation, direction of sso ...)
4. sub-grid surface runoff slope
5. continuous drainage
6. topographic index statistics

[1]During ARPEGE-CLIMATrun, the model is forced to use the orography coming from the atmospheric boundary conditions and not from the surface boundary conditions.

7. bathymetry
8. clay fraction
9. sand fraction
10. percentage of sand
11. percentage of clay

The surface prognostic fields. The surface init file will contain the prognostic fields. The PREP binary (source code provided within ARPEGE-CLIMAT) performs the initialization of the surface scheme prognostic variables, as temperature profiles, water and ice soil contents, interception reservoirs, snow reservoirs.

Output data

1. surface temperature
2. deep soil temperature
3. third layer temperature
4. sea surface temperature
5. water temperature
6. surface liquid volumetric water content
7. root liquid volumetric water content
8. deep liquid volumetric water content
9. surface frozen volumetric water content
10. root frozen volumetric water content
11. third layer frozen volumetric water content
12. liquid water retained by the foliage
13. 1st layer snow water equivalent
14. 1st layer snow water density
15. glacier ice storage reservoir
16. snow albedo
17. aerodynamical resistance

18. leaf area index
19. vegetation fraction
20. surface roughness length witout snow
21. fraction of each patch (12 ISBA vegetation types/patches)
22. soil layer thicknesses
23. sea/nature/water/town fractions (the 4 SURFEX tiles)
24. orography roughness length
25. roughness length over the ocean
26. water surface roughness length
27. rainfall rate
28. snowfall rate

3 Additional boundary forcings

3.1 Ozone

In former versions, ARPEGE-CLIMAT could use the variable ozone as a passive tracer. To parametrize the photochemical sources and sinks, Cariolle and Déqué (1986) introduced a linear parametrization of the form:

$$\frac{\partial r_{O3}}{\partial t} = A_2 + (A_3 + A_6 R_{Cl}^2)(r_{O3} - A_1) + A_5(T - A_4) + A_7(\Sigma r_{O3} - \Sigma A_1)$$

where r_{O3} is the ozone mass mixing ratio, Σr_{O3} the vertically integrated ozone between the current level and the top of the atmosphere, T the temperature, R_{Cl} a chlorine index, and A_i coefficients which depend on latitude, pressure and month.

3.2 Aerosols

There are 6 types of aerosols: continental (organic), maritime (salt), urban (soot), desert (dust), sulfate and stratospheric. The default horizontal distribution of the first 5 is proposed by Tegen et al. (1997). The horizontal resolution is very coarse, but the data are used on a grid of 72 longitude by 46 latitudes. The horizontal interpolation is performed by basic barycentric interpolation (no masking) in prepaero.sh script. The stratospheric aerosols

are uniformly distributed on the sphere and does not need interpolation. The global effect of volcanic eruption can be taken into account by changing each year the solar constant.

The horizontal distribution of the anthropogenic sulfate aerosols may also be obtained from Boucher and Pham (2002) on a grid of 96 longitudes by 73 latitudes with decadal variation and anthropogenic scenarios. A fraction of the sulfate of each decade divided by the sulfate of decade 1990 is interpolated on the target grid. This ratio is multiplied by the Tegen sulfate distribution already interpolated on the target grid.

For future use, an additional field with volcano aerosols containing uniformly 10.5 10^{-3} is written.

4 Coupling with an ocean model

Arpege-climat can be used in coupled mode with an ocean model. In this case sea surface temperature, sea-ice mask and the attached variables (surface albedo ...) are no longer provided externally at the beginning of each month, but at a proper frequency (NFRCPL) during the course of a monthly integration. Because of the coupling, there is a feedback between the surface fluxes calculated by Arpege-climat and the sea surface temperature imposed to it.

In the present version Arpege-climat is coupled with NemoV2-3 (from CNRS/IPSL) as the ocean model through OasisV3 (from Cerfacs) as the coupler with the switch LMCC03.

At each coupling time step, the atmosphere and ocean models exchange fields with the help of the coupler in charge of the communication between the models and the interpolation between the two different grids. The exchanged fields are averaged over the coupling time period preceding each coupling time step. The atmospheric model sends wind stress fluxes, surface total energy flux, surface net solar flux, surface net hydrological flux and run-off flux; while the ocean model sends the sea surface temperature, the ice cover, the sea surface albedo and the surface currents (to be used in the wind stress computation). In the present version, no sea-ice model is taken into account and a monthly climatology is used by Oasis to mimic the presence of a sea-ice model. Through the switch LMCC02, Arpege-climat treats sea-ice as land and balances the surface temperature with the surface heat flux (see Chapter 14)

4.1 Ocean model

The NEMO ocean model web site is
`http://www.locean-ipsl.upmc.fr/NEMO/`
and its reference publication is Madec (2008).

The ocean model NEMO is a primitive equation model adapted to regional and global ocean circulation problems. Prognostic variables are the three-dimensional velocity field, a linear or nonlinear sea surface height, the temperature and the salinity. In the horizontal direction, the model uses a curvilinear orthogonal grid and in the vertical direction, a full or partial step z-coordinate, or s-coordinate, or a mixture of the two. The distribution of variables is a three-dimensional Arakawa C-type grid. Various physical choices are available to describe ocean physics, including TKE and KPP vertical physics.

In more details, NEMO presents the following characteristics:

The model is discretized on a staggered grid (Arakawa C grid) with masking of land areas and uses a leap-frog environment for time-stepping. Vertical discretization used depends on both how the bottom topography is represented and whether the free surface is linear or not. Full step or partial step z-coordinate or s- (terrain-following) coordinate is used with linear free surface (level position are then fixed in time). In nonlinear free surface, the corresponding rescaled height coordinate formulation (z* or s*) is used (the level position then vary in time as a function of the sea surface height). Explicit, split-explicit and implicit free surface formulations are implemented as well as rigid-lid case. A number of numerical schemes are available for momentum advection, for the computation of the pressure gradients, as well as for the advection of tracers (second or higher order advection schemes, including positive ones).

The model allows penetration of solar radiation There is an optional geothermal heating at the ocean bottom.

Global configurations of the model make use of the ORCA tripolar grid, with special north fold boundary condition. Free-slip or no-slip boundary conditions are allowed at land boundaries.

The model includes an implicit treatment of vertical viscosity and diffusivity. The lateral laplacian and bi-harmonic viscosity and diffusion can be rotated following a geopotential or neutral direction. There is an optional eddy induced velocity (Gent and Mc Williams 1990) with a space and time variable coefficient Tréguier et al. (1997). The model has vertical harmonic viscosity and diffusion with a space and time variable coefficient, with options to compute the coefficients with Blanke and Delecluse (1993), Large et al. (1994), or Pacanowski and Philander (1981) mixing schemes

Specific on-line diagnostics are available in the model : output of all the tendencies of the momentum and tracers equations, output of tracers tendencies averaged over the time evolving mixed layer.

The model is implemented in Fortran 90, with preprocessing (C preprocessor). It is optimized for vector computers and parallelized by domain decomposition with MPI. All input and output is done in NetCDF with a optional direct access format for output.

4.2 Coupler

The Oasis coupler web site is
`http://www.cerfacs.fr/globc/software/oasis/`
and reference publication is Valcke (2006).

Oasis 3 is the direct evolution of the Oasis coupler developed since more than 10 years at Cerfacs. Oasis 3 is a portable set of Fortran 77, Fortran 90 and C routines. At run-time, Oasis 3 acts as a separate mono process executable, which main function is to interpolate the coupling fields exchanged between the component models, and as a library linked to the component models, the Oasis 3 PRISM Model Interface Library (Oasis 3 PSMILe). Oasis 3 supports 2D coupling fields only. To communicate with Oasis 3, directly with another model, or to perform I/O actions, a component model needs to include few specific PSMILe calls. Oasis 3 PSMILe supports in particular parallel communication between a parallel component model and Oasis 3 main process based on Message Passing Interface (MPI) and file I/O using the mpp-io library from GFDL.

Different transformations and 2D interpolations are available in Oasis 3 to adapt the coupling fields from a source model grid to a target model grid. They are divided into five general classes that have precedence one over the other in the following order: time transformation (with PSMILe only), preprocessing, interpolation, adjustments, and postprocessing. This order of precedence is conceptually logical, but is also constrained by the Oasis 3 software internal structure.

Oasis 3 notably includes the interpolation techniques offered by Los Alamos National Laboratory SCRIP 1.4 library. These interpolation techniques are the following: distance weighted nearest neighbor interpolation, nearest neighbor interpolation weighted by their distance and a Gaussian function, bilinear and bi-cubic interpolation, 1st or 2nd order conservative remapping, which means that the weight of a source cell is proportional to area intersected by target cell.

8

Radiation

1 Radiative fluxes

This chapter describes the salient features concerning the radiation scheme, used in NWP as well as in ARPEGE-CLIMAT. The present chapter is based on the IFS Documentation-Cy31r1 and on the Meso-NH documentation:

`http://mesonh.aero.obs-mip.fr/mesonh/`

The detailed original ECMWF scientific documentation is available online at

`http://www.ecmwf.int/research/ifsdoc/CY31r1/`

The package calculates the radiative fluxes taking into account absorption-emission of longwave radiation and reflection, scattering and absorption of solar radiation by the earth's atmosphere and surfaces. The longwave radiation scheme is based on that of the ECMWF model, the Rapid Radiation Transfer Model (RRTM). The shortwave part of the scheme, originally developed by Fouquart and Bonnel (1980) solves the radiation transfer equation and integrates the fluxes over the whole shortwave spectrum between 0.2 and 4 mm.

The radiative heating rate is computed as the divergence of net radiation fluxes F so that

$$(\frac{\partial T}{\partial t})_{rad} = -\frac{g}{c_p}\frac{\partial F}{\partial p} \tag{1}$$

where F is a net flux: i.e. $F = F^{\uparrow} + F^{\downarrow}$ sum of the upward $F^{\uparrow}$ and downward $F^{\downarrow}$ fluxes, and a total flux: i.e. $F = F_{LW} + F_{SW}$ sum of the solar or shortwave

F_{SW} and atmospheric or longwave F_{LW} fluxes and c_p is the specific heat at constant pressure of moist air.

Sections 2 and 3 describe the computation of the shortwave and longwave radiative fluxes respectively. The solution of the radiative transfer equation to obtain the fluxes is unfortunately very expensive, and we cannot afford to do it more than every 3 hours. A description of the inputs, in particular the climatologically defined quantities of radiative importance is given in Section 4.

2 Shortwave radiation

2.1 First glance

The rate of atmospheric warming by absorption and scattering of shortwave radiation is:

$$\frac{\partial T}{\partial t} = \frac{g}{c_p}\frac{\partial F}{\partial p} \tag{2}$$

where $F = F_{SW}$ is the net total shortwave flux, expressed in W m^{-2} and positive when downward.

$$F = \int_0^\infty d\nu \int_0^{2\pi} d\phi \int_{-1}^{+1} \mu\, L_\nu(\delta, \mu, \phi)\, d\mu\, d\phi \tag{3}$$

L_ν is the diffuse radiance at wavenumber ν, in a direction given by ϕ, the azimuth angle and ϑ the zenith angle such as $\mu = \cos\vartheta$. In (3), we assume a plane parallel atmosphere with the optical depth δ, as a convenient vertical coordinate when the energy source is outside the medium

$$\delta(p) = \int_p^0 \beta_\nu(p)\, dp \tag{4}$$

where $\beta_\nu^{ext}(p)$ is the extinction coefficient equal to the sum of the scattering coefficient β_ν^{sca} of the aerosol and cloud particle absorption coefficient β_ν^{abs} and of the purely molecular absorption coefficient k_ν. The diffuse radiance L_ν is governed by the radiation transfer equation

$$\mu \frac{dL_\nu(\delta,\mu,\phi)}{d\delta} = L_\nu(\delta,\mu,\phi) - \frac{\overline{\omega}_\nu(\delta)}{4} P_\nu(\delta,\mu,\phi,\mu_0,\phi_0)\, E^0_\nu e^{-\frac{\delta}{\mu_0}} \quad (5)$$

$$- \frac{\overline{\omega}_\nu(\delta)}{4} \int_0^{2\pi}\int_{-1}^{+1} P_\nu(\delta,\mu,\phi,\mu',\phi')\, L_\nu(\delta,\mu',\phi')\, d\mu'\, d\phi' \quad (6)$$

E^0_ν is the incident solar irradiance in the direction $\mu_0 = cos\vartheta_0$, $\overline{\omega}_\nu$ is the single scattering albedo ($= \beta^{sca}_\nu / k_\nu$) and $P_\nu(\delta,\mu,\phi,\mu',\phi')$ is the scattering phase function which defines the probability that radiation coming from direction (μ',ϕ') is scattered in direction (μ,ϕ). The shortwave part of the scheme, originally developed by Fouquart and Bonnel (1980) , solves the radiation transfer equation and integrates the fluxes over the whole shortwave spectrum between 0.2 and 4 μm. Upward and downward fluxes are obtained from the reflectances and transmittances of the layers, and the photon-path-distribution method allows to separate the parametrization of the scattering processes from that of the molecular absorption.

2.2 Spectral integration

Solar radiation is attenuated by absorbing gases, mainly water vapor, uniformly mixed gases (oxygen, carbon dioxide, methane, nitrous oxide) and ozone, and scattered by molecules (Rayleigh scattering), aerosols and cloud particles. Since scattering and molecular absorption occur simultaneously, the exact amount of absorber along the photon path length is unknown, and band models of the transmission function cannot be used directly as in the longwave radiation transfer. The approach of the photon path distribution method is to calculate the probability $p(U)\, dU$ that a photon contributing to the flux F_c in the conservative case (i.e. no absorption, $\overline{\omega}_\nu = 1, k_\nu = 0$) has encountered an absorber amount between U and $U + dU$. With this distribution, the radiative flux at wavenumber ν is related to F_c by

$$F_\nu = F_c \int_0^\infty p(U)\, \exp(-k_\nu U)\, dU \quad (7)$$

and the flux averaged over the spectral interval $\Delta\nu$ can then be calculated with the help of any band model of the transmission function $t_{\Delta\nu}$

$$F = \frac{1}{\Delta\nu} \int_{\Delta\nu} F_\nu\, d\nu = F_c \int_0^\infty p(U)\, t_{\Delta\nu}(U)\, d\nu. \quad (8)$$

To find the distribution function $p(U)$, the scattering problem is solved first, by any method, for a set of arbitrarily fixed absorption coefficients k_l, thus

giving a set of simulated fluxes F_{k_l}. An inverse Laplace transform is then performed on (7) to get $p(U)$ (Fouquart 1974). The main advantage of the method is that the actual distribution $p(U)$ is smooth enough that (7) gives accurate results even if $p(U)$ itself is not known accurately. In fact, $p(U)$ needs not be calculated explicitly as the spectrally integrated fluxes are, in the two limiting cases of weak and strong absorption:

$$F = F_c\, t_{\Delta\nu}(< U >) \qquad \text{where} \qquad < U >= \int_0^\infty p(U)\, U\, dU \quad (9)$$

$$F = F_c\, t_{\Delta\nu}(< U^{\frac{1}{2}} >) \qquad \text{where} \qquad < U^{\frac{1}{2}} >= \int_0^\infty p(U)\, U^{\frac{1}{2}}\, dU \quad (10)$$

respectively. The atmospheric absorption in the water vapor bands is generally strong and the scheme determines an effective absorber amount U_e between $< U >$ and $< U^{\frac{1}{2}} >$ derived from

$$U_e = \frac{1}{k_e}\, \ln(\frac{F_{k_e}}{F_c}) \quad (11)$$

where k_e is an absorption coefficient chosen to approximate the spectrally averaged transmission of the clear-sky atmosphere:

$$k_e = (\frac{U_{tot}}{\mu_0})^{-1}\, \ln(t_{\Delta\nu}\frac{U_{tot}}{\mu_0}) \quad (12)$$

with U_{tot} the total amount of absorber in a vertical column and $\mu_0 = \cos\vartheta_0$. Once the effective absorber amounts of H_2O and uniformly mixed gases are found, the transmission functions are computed using Padé approximants:

$$t_{\Delta\nu}(U) = \frac{\sum_{i=0}^{N} a_i U^{i-1}}{\sum_{j=0}^{N} b_j U^{j-1}}. \quad (13)$$

Absorption by ozone is also taken into account, but since ozone is located at low pressure levels for which molecular scattering is small and Mie scattering is negligible, interactions between scattering processes and ozone absorption

are neglected. Transmission through ozone is computed using (13) where the amount of ozone U_{O_3} is:

$$U^d_{O_3} = M \int_p^0 dU_{O_3}$$

for the downward transmission of the direct solar beam, and:

$$U^u_{O_3} = r \int_{p_s}^p dU_{O_3} + U^d_{O_3}(p_s)$$

for the upward transmission of the diffuse radiation with $r = 1.66$ the diffusivity factor and M, the magnification factor (Rodgers 1967) used instead of μ_0 to account for the sphericity of the atmosphere at very small solar elevations:

$$M = \frac{35}{\sqrt{\mu_0^2 + 1}}. \tag{14}$$

To perform the spectral integration, it is convenient to discretize the solar spectrum into subintervals in which the surface reflectance, molecular absorption characteristics, and cloud optical properties can be considered as constants. One of the main causes for such a spectral variation is the sharp increase in the reflectivity of the vegetation in the near-infrared. Also, water vapour does not absorb below 0.69 μm nor do liquid water clouds. Till June 2000, the ECMWF shortwave scheme considered only two spectral intervals, one for the visible (0.2/0.69 μm), one for the near-infrared (0.69/4.00 μm) parts of the solar spectrum. From June 2000 to April 2002, the near-infrared interval was sub-divided into three intervals (0.69/1.19/2.38/4.00 μm) to account better for the spectral variations of the cloud optical properties. Till April 2002, all the molecular absorption coefficients (for O3, H2O, uniformly mixed gases) were derived from statistical models of the transmission function using spectroscopic parameters derived from various versions of the HITRAN database (Rothman et al., 1987, 1992). In April 2002, following the recomputation of all the molecular absorption coefficients from an updated version of the shortwave lineby- line model of Dubuisson et al. (1996) using spectroscopic data from HAWKS (2000):

`http://www.hitran.com`

the ultraviolet and visible part of the spectrum are now considered in three spectral intervals (0.20/0.25/0.69 μm) making the scheme having a total of six spectral intervals over which the aerosol and cloud optical properties are also defined. The cut-off at 0.69 μm allows the scheme to be more computational efficient, in as much as the interactions between gaseous absorption (by water vapour and uniformly mixed gases) and scattering processes are accounted for only in the near-infrared interval(s).

2.3 Vertical integration

Considering an atmosphere where a fraction C_{tot} (as seen from the surface or the top of the atmosphere) is covered by clouds (the fraction C_{tot} depends on which cloud overlap assumption is assumed for the calculations), the final fluxes are given as

$$F^{\downarrow} = C_{tot}\, F^{\downarrow}_{cloudy} + (1 - C_{tot})\, F^{\downarrow}_{clear} \tag{15}$$

with a similar expression holding for the upward flux. Contrarily to the scheme of Geleyn and Hollingsworth (1979) , the fluxes are not obtained through the solution of a system of linear equations in a matrix form. Rather, assuming an atmosphere divided into N homogeneous layers, the upward and downward fluxes at a given interface j are given by:

$$F^{\downarrow}(j) = F_0 \prod_{k=j}^{N} T_b(k), \tag{16}$$

$$F^{\uparrow}(j) = F^{\downarrow}(j)\, R_t(j-1), \tag{17}$$

where $R_t(j)$ and $T_b(j)$ are the reflectance at the top and the transmittance at the bottom of the j^{th} layer. Computations of R_t's start at the surface and work upward, whereas those of T_b's start at the top of the atmosphere and work downward. R_t and T_b account for the presence of cloud in the layer:

$$R_t = C_j\, R_{cdy} + (1 - C_j)\, R_{clr}, \tag{18}$$

$$T_b = C_j\, T_{cdy} + (1 - C_j)\, T_{clr}. \tag{19}$$

The subscripts $_{clr}$ and $_{cdy}$ respectively refer to the clear-sky and cloudy fractions of the layer with C_j the cloud fraction of the layer j.

Cloudy fraction of the layers

$R_{t_{cdy}}$ and $T_{b_{cdy}}$ are the reflectance at the top and transmittance at the bottom of the cloudy fraction of the layer calculated with the Delta-Eddington approximation. Given δ_c, δ_a and δ_g, the optical thicknesses for the cloud and the aerosol, and the molecular absorption of the gases, g_c and g_a the cloud and aerosol asymmetry factors, $R_{t_{cdy}}$ and $T_{b_{cdy}}$ are calculated as functions of:

- the total optical thickness of the layer δ^*:

$$\delta^* = \delta_c + \delta_a + \delta_g$$

- the total single scattering albedo:

$$\omega^* = \frac{\delta_c + \delta_a}{\delta_c + \delta_a + \delta_g} \tag{20}$$

- the total asymmetry factor:

$$g^* = \frac{\delta_c}{\delta_c + \delta_a} g_c + \frac{\delta_a}{\delta_c + \delta_a} g_a \tag{21}$$

of the reflectance $R\_$ of the underlying medium (surface or layers below the j^{th} interface) and of the effective solar zenith angle $\mu_e(j)$ which accounts for the decrease of the direct solar beam and the corresponding increase of the diffuse part of the downward radiation by the upper scattering layers.

The effective solar zenith angle $\mu_e(j)$ is equal to:

$$\mu_e(j) = \left[\frac{(1 - C_{cld}^{eff}(j))}{\mu} + r\, C_{cld}^{eff}(j) \right]^{-1}, \tag{22}$$

with $C_{cld}^{eff}(j)$ the effective total cloudiness over level j and r the diffusivity factor.

$$C_{cld}^{eff}(j) = 1 - \prod_{i=j+1}^{N} (1 - C_{cld}(i)E(i))$$

and

$$E(i) = 1 - \exp\left[-\frac{(1 - \omega_c(i)g_c(i)^2)\delta_c(i)}{\mu}\right] \tag{23}$$

where $\delta_c(i)$, $\omega_c(i)$ and $g_c(i)$ are the optical thickness, single scattering albedo and asymmetry factor of the cloud in the ith layer.

The scheme follows the Eddington approximation, first proposed by Shettle and Weiman (1970), then modified by Joseph et al. (1976) to account more accurately for the large fraction of radiation directly transmitted in the forward scattering peak in case of highly asymmetric phase functions. Eddington's approximation assumes that, in a scattering medium of optical thickness δ^*, of single scattering albedo ω, and of asymmetry factor g, the radiance L entering (5) can be written as:

$$L(\delta, \mu) = L_0(\delta) + \mu\, L_1(\delta). \tag{24}$$

In that case, when the phase function is expanded as a series of associated Legendre functions, all terms of order greater than one vanish when (5) is integrated over μ and ϕ. The phase function is therefore given by

$$P(\theta) = 1 + \beta_1(\theta)\, \cos\theta,$$

where θ is the angle between incident and scattered radiances. The integral in (5) thus becomes

$$\int_0^{2\pi}\int_{-1}^{+1} P(\mu, \phi, \mu', \phi')\, L(\mu', \phi')\, d\mu'\, d\phi' = 4\pi\, (L_0 + \pi L_1) \tag{25}$$

where g, the asymmetry factor identifies as

$$g = \frac{\beta_1}{3} = \frac{1}{2}\int_{-1}^{+1} P(\theta)\, \cos\theta\, d(\cos\theta).$$

Using (25) in (5) after integrating over μ and dividing by 2π, we get

$$\mu \frac{d(L_0 + \mu L_1)}{d\delta} = -(L_0+\mu L_1)+\omega\,(L_0+g\mu L_1)+\frac{1}{4}\omega\,F_0\,\exp(\frac{-\delta}{\mu_0})\,(1+3g\mu_0\,\mu). \quad (26)$$

where ω is the single scattering albedo.

We obtain a pair of equations for L_0 and L_1 by integrating (26) over μ:

$$\frac{d(L_0)}{d\delta} = -3(1-\omega)\,L_0 + \frac{3}{4}\omega\,F_0\,\exp(\frac{-\delta}{\mu_0}), \quad (27)$$

$$\frac{d(L_1)}{d\delta} = -(1-\omega g)\,L_1 + \frac{3}{4}\omega\,g\,\mu_0\,F_0\,\exp(\frac{-\delta}{\mu_0}). \quad (28)$$

For the cloudy layer assumed non-conservative ($\omega < 1$), the solutions to (27) and (28) are, in the range $0 \le \delta \le \delta^*$:

$$L_0(\delta) = C_1\,\exp(-k\delta) + C_2\,\exp(+k\delta) - \alpha\,\exp(\frac{-\delta}{\mu_0}), \quad (29)$$

$$L_1(\delta) = p(C_1\,\exp(-k\delta) - C_2\,\exp(+k\delta)) - \beta\,\exp(\frac{-\delta}{\mu_0}), \quad (30)$$

where

$$\begin{aligned} k &= [3\,(1-\omega)\,(1-\omega g)]^{\frac{1}{2}} \\ p &= [3\,(1-\omega)/(1-\omega g)]^{\frac{1}{2}} \\ \alpha &= 3\,\omega\,F_0\,\mu_0\,\frac{[1+3g\,(1-\omega)]}{4\,(1-k^2\mu_0^2)} \\ \beta &= 3\,\omega\,F_0\,\mu_0\,\frac{[1+3\,g\,(1-\omega)\,\mu_0^2]}{4\,(1-k^2\mu_0^2)}. \end{aligned}$$

The two boundary conditions allow to solve the system for C_1 and C_2. First, the downward directed diffuse flux at the top of the layer is zero

$$F^{\downarrow}(0) = [L_0(0) + \frac{2}{3}L_1(0)] = 0,$$

which translates into

$$(1+\frac{2p}{3})\,C_1 + (1-\frac{2p}{3})\,C_2 = \alpha + \frac{2\beta}{3}. \quad (31)$$

For the second condition, one assumes that the upward directed flux at the bottom of the layer is equal to the product of the downward directed diffuse and direct fluxes by the corresponding diffuse and direct reflectances (R_d and $R\_$, respectively) of the underlying medium

$$F^{\uparrow}(\delta^*) = [L_0(\delta^*) - \frac{2}{3} L_1(\delta^*)] = R\_ \, [L_0(\delta^*) + \frac{2}{3} L_1(\delta^*)] + R_d \, \mu_0 \, F_0 \, \exp(\frac{-\delta^*}{\mu_0}),$$

which translates into

$$(1 - R\_ - \frac{2p}{3}(1 + R\_)) \, C_1 \, \exp(-k \, \delta^*) + (1 - R\_ + \frac{2p}{3}(1 + R\_)) \, C_2 \quad \exp(+k \, \delta^*) \quad (32)$$

$$= ((1 - R\_)\alpha - \frac{2}{3}(1 + R\_)\beta + R_d \, \mu_0 \, F_0) \quad \exp(\frac{-\delta^*}{\mu_0}) \quad (33)$$

In the Delta-Eddington approximation, the phase function is approximated by a Dirac delta function (forward scatter peak) and a two-term expansion of the phase function

$$P(\theta) = 2f \, (1 - \cos\theta) + (1 - f) \, (1 + 3g' \, \cos\theta),$$

where f is the fractional scattering into the forward peak and g' the asymmetry factor of the truncated phase function. As shown by Joseph et al. (1976), these parameters are:

$$f = g^2 \quad (34)$$

$$g' = \frac{g}{1 + g}. \quad (35)$$

The solution of the Eddington's equations remains the same provided that the total optical thickness, single scattering albedo and asymmetry factor entering (26)-(32) take their transformed values:

$$\delta' = (1 + \omega f) \, \delta^*, \quad (36)$$

$$\omega' = \frac{(1 - f) \, \omega}{1 - \omega f}. \quad (37)$$

Practically, the optical thickness, single scattering albedo, asymmetry factor, and solar zenith angle entering (26)-(31) are δ^*, ω^*, g^* and u_e defined in (21) and (22).

Clear-sky fraction of the layers

In the clear-sky fraction of the layers, the shortwave scheme accounts for scattering and absorption by molecules and aerosols. The following calculations are practically done twice, once for the clear-sky fraction $(1 - C_{cld}^{tot})$ of the atmospheric column μ with equal to μ_0, simply modified for the effect of Rayleigh and aerosol scattering, the second time for the clear-sky fraction of each individual layer within the fraction C_{cld}^{tot} of the atmospheric column containing clouds, with μ equal to μ_e.

As the optical thickness for both Rayleigh and aerosol scattering is small, $R_{clr}(j-1)$ and $T_{clr}(j)$ the reflectance at the top and transmittance at the bottom of the j^{th} layer can be calculated using respectively a first and a second-order expansion of the analytical solutions of the two-stream equations similar to that of Coakley and Chylek (1975). For Rayleigh scattering, the optical thickness, single scattering albedo and asymmetry factor are respectively δ_R, $\omega_R = 1$ and $g_R = 0$, so that

$$R_R = \frac{\delta_R}{2\,\mu + \delta_R}, \tag{38}$$

$$T_R = \frac{2\mu}{2\,\mu + \delta_R}. \tag{39}$$

The optical thickness δ_R of an atmospheric layer is simply:

$$\delta_R = \delta_R^* \frac{(p(j) - p(j-1))}{p_{surf}},$$

where δ_R^* is the Rayleigh optical thickness of the whole atmosphere parameterized as a function of solar zenith angle (Deschamps et al. 1983):

$$\delta_R^* = \sum_{i=0}^{5} a_i\,\mu_0^{i-1}.$$

For aerosol scattering and absorption, the optical thickness, single scattering albedo and asymmetry factor are respectively δ_a, ω_a (with $1 - \omega_a \ll 1$) and g_a so that:

$$den = 1 + (1 - \omega_a + back(\mu_e)\,\omega_a)\,\frac{\delta_a}{\mu_e} + (1 - \omega_a)\,(1 - \omega_a + 2\,back(\mu_e)\,\omega_a)\,\frac{{\delta_a}^2}{{\mu_e}^2}$$

$$R(\mu_e) = \frac{back(\mu_e)\,\omega_a\,\delta_a/\mu_e}{den} \tag{40}$$

$$T(\mu_e) = \frac{1}{den}$$

where $back(\mu_e) = (2 - 3\mu_e g_a)/4$ is the backscattering factor.

Practically, R_{clr} and T_{clr} are computed using (40) and the combined effect of aerosol and Rayleigh scattering comes from using modified parameters corresponding to the addition of the two scatters with provision for the highly asymmetric aerosol phase function through a Delta-Eddington approximation of the forward scattering peak (as in (34)-(36)):

$$\delta^+ = \delta_R + \delta_a(1 - \omega_a g_a^2)$$

$$g^+ = \frac{g_a}{1 + g_a}\frac{\delta_a}{(\delta_R + \delta_a)}$$

$$\omega^+ = \frac{\delta_R}{\delta_R + \delta_a}\omega_R + \frac{\delta_a}{\delta_R + \delta_a}\frac{\omega_a(1 - g_a^2)}{1 - \omega_a g_a^2}$$

As for their cloudy counterparts, R_{clr} and T_{clr} must account for the multiple reflections due to the layers underneath:

$$R_{clr} = R(\mu_e) + \frac{T(\mu_e)}{1 - R^*\,R\_}\,R\_, \tag{41}$$

$$T_{clr} = \frac{T(\mu_e)}{(1 - R^*\,R\_)}, \tag{42}$$

with $R^* = R(1/r)$, $T^* = T(1/r)$, $R\_ = R_t(j-1)$ is the reflectance of the underlying medium and r is the diffusivity factor.

Since interactions between molecular absorption and Rayleigh and aerosol scattering are negligible, the radiative fluxes in a clear-sky atmosphere are simply those calculated from (16) and (41) attenuated by the gaseous transmissions (13).

2.4 Multiple reflections between layers

To deal properly with the multiple reflections between the surface and the cloud layers, it should be necessary to separate the contribution of each individual reflecting surface to the layer reflectances and transmittances in as much as each such surface gives rise to a particular distribution of absorber amount. In case of an atmosphere including N cloud layers, the reflected light above the highest cloud consists of photons directly reflected by the highest cloud without interaction with the underlying atmosphere and of photons that have passed through this cloud layer and undergone at least one reflection on the underlying atmosphere. In fact, (8) should be written

$$F = \sum_{l=0}^{N} F_{cl} \int_0^{\infty} p_l(U)\, t_{\Delta\nu}(U)\, d\nu, \tag{43}$$

where F_{cl} and $p_l(U)$ are the conservative fluxes and the distributions of absorber amount corresponding to the different reflecting surfaces.

Fouquart and Bonnel (1980) have shown that a very good approximation to this problem is obtained by evaluating the reflectance and transmittance of each layer (using (32) and (41)), assuming successively a non-reflecting underlying medium ($R\_ = 0$), then a reflecting underlying medium ($R\_ \neq 0$). First calculations provide the contribution to reflectance and transmittance of those photons interacting only with the layer into consideration, whereas the second ones give the contribution of the photons with interactions also outside the layer itself.

From these two sets of layer reflectances and transmittances (R_{t_0}, T_{t_0}) and $(R_{t_{\neq}}, T_{t_{\neq}})$ respectively, effective absorber amounts to be applied to computing the transmission functions for upward and downward fluxes are then derived using (11) and starting from the surface and working the formulas upward:

$$U^{\downarrow}_{e_0} = \frac{1}{k_e} \ln\left(\frac{T_{b_0}}{T_{b_c}}\right),$$

$$U^{\downarrow}_{e_{\neq}} = \frac{1}{k_e} \ln\left(\frac{T_{b_{\neq}}}{T_{b_c}}\right),$$

$$U^{\uparrow}_{e_0} = \frac{1}{k_e} \ln\left(\frac{R_{t_0}}{R_{t_c}}\right),$$

$$U^{\uparrow}_{e_{\neq}} = \frac{1}{k_e} \ln(\frac{R_{t_{\neq}}}{R_{t_c}}),$$

where R_{t_c} and T_{b_c} are the layer reflectance and transmittance corresponding to a conservative scattering medium. Finally the upward and downward fluxes are obtained as:

$$F^{\uparrow}(j) = F_0 \left[R_{t_0}\, t_{\Delta\nu}(U^{\uparrow}_{e_0}) + (R_{t_{\neq}} - R_{t_0})\, t_{\Delta\nu} U^{\uparrow}_{e_{\neq}}) \right] \tag{44}$$

$$F^{\downarrow}(j) = F_0 \left[T_{b_0}\, t_{\Delta\nu}(U^{\downarrow}_{e_0}) + (T_{b_{\neq}} - T_{b_0})\, t_{\Delta\nu} U^{\downarrow}_{e_{\neq}}) \right] \tag{45}$$

3 Longwave radiation: the RRTM scheme

The main characteristics of RRTM are:

- Solution of radiative transfer equation: Two-stream method
- Number of spectral intervals: 16
- Absorbers : H_2O, CO_2, $O3$, CH_4, N_2O, $CFC11$, $CFC12$, aerosols
- Spectroscopic data base: HITRAN 1996
- Absorption coefficient: From LBLRTM line-by-line model
- Cloud handling: True cloud fraction
- Cloud optical properties: 16-band spectral emissivity
- Cloud overlap assumption: Maximum random
- References : Mlawer et al. (1997)

As stated in Mlawer et al. (1997), the objective in the development of RRTM has been to obtain an accuracy in the calculation of fluxes and heating rates consistent with the best line-by-line models. It utilizes the correlated-k methode and shows its filiation to the Atmospheric and Environmental Research, Inc. (AER) line-by-line model (LBLRTM; Clough et al. 1989, 1992; Clough and Iacono 1995) through its use of absorption coefficients for the relevant k-distributions derived from LBLRTM. Therefore the k-coefficients in RRTM

include the effect of the CKD2.2 water vapour continuum (Clough et al. 1989).

The main point in the correlated-k method (Lacis and Oinas 1991; Fu and Liou 1992) is the mapping of the absorption coefficient $k(\nu)$ from the spectral space (where it varies irregularly with wavenumber ν) to the g-space (where $g(k)$ is the probability distribution function, i.e. the fraction of the absorption coefficients in the set smaller than k). The effect of this reordering is a rearrangement of the sequence of terms in the integral over wavenumber in the radiative transfer equation (RTE), which makes it equivalent to what would be done for monochromatic radiation.

In the ECMWF (hence, ARPEGE-CLIMAT) model, no provision is presently taken for scattering in the longwave. Therefore, in order to get the downward radiance, the integration over the vertical dimension is simply done starting from the top of the atmosphere, going downward layer by layer. At the surface, the boundary condition (in terms of spectral emissivity, and potential reflection of downward radiance) is computed, then, in order to get the upward radiance, the integration over the vertical dimension is repeated, this time from the surface upward.

The spectrally averaged radiance (between ν_1 and ν_2) emerging from an atmospheric layer is

$$\overline{R} = \frac{1}{(\nu_1 - \nu_2)} \int_{\nu_2}^{\nu_1} d\nu \left\{ R_0(\nu) + \int_{t_\nu}^{1} \left[B(\nu, T(t'_\nu)) \; - R_0(\nu) \right] dt' \right\} \qquad (46)$$

where R_0 is the incoming radiance to the layer, $B(\nu, T)$ is the Planck function at wavenumber ν and temperature T, t_ν is the transmittance for the layer optical path, and t'_ν is the transmittance at a point along the optical path in the layer. Under the mapping $\nu \rightarrow g$, this becomes

$$\overline{R} = \int_0^1 dg \left\{ B_{\text{eff}}(g, T_g) + \left[R_0(g) - B_{\text{eff}}(g, T_g) \right] \exp \left[-k(g, P, T) \frac{\rho \delta z}{\cos \phi} \right] \right\} \qquad (47)$$

where $B_{\text{eff}}(g, T)$ is an effective Planck function for the layer that varies with the layer's transmittance such as to ensure continuity of flux across layer boundaries for opaque conditions. The dependence of the transmittance is now written in terms of the absorption coefficient $k(g, P, T)$ at layer pressure P and temperature T, the absorber density ρ, the vertical thickness of the layer δz, and the angle ϕ of the optical path.

For a given spectral interval, the domain of the variable g is partitioned into subintervals (see Table 8.1, number of g-points), each corresponding to a limited range of $k(g)$ values and for which a characteristic value κ_j of the

absorption coefficient is chosen. These κ_j are then used to compute the outgoing radiance

$$\overline{R} = \Sigma_j W_j \left[B_{\text{eff}_j} + (R_0(g) - B_{\text{eff}_j}) \exp\left(-\kappa_j \frac{\rho \delta z}{\cos \phi} \right) \right] \tag{48}$$

where W_j is the size of the sub-intervals ($\Sigma W_j = 1$).

The accuracy of these absorption coefficients has been established by numerous and continuing high-resolution validations of LBLRTM with spectroscopic measurements, in particular those from the Atmospheric Radiation Measurement program (ARM). Compared to the original RRTM (Mlawer et al. 1997), the version used at ECMWF (hence ARPEGE-CLIMAT) has been slightly modified to account for cloud optical properties and surface emissivity defined for each of the 16 bands over which spectral fluxes are computed. For efficiency reason, the original number of g-points ($256 = 16 \times 16$) has been reduced to 140 (see Table 8.1). Other changes are the use of a diffusivity approximation (instead of the three-angle integration over the zenith angle used in the original scheme) to derive upward and downward fluxes from the radiances, and the modification of the original cloud random overlapping assumption to include (to the same degree of approximation as used in the operational SW scheme) a maximum-random overlapping of cloud layers. Given the monochromatic form of the RTE, the vertical integration is simply carried out one layer at a time from the top-of-the-atmosphere to the surface to get the downward fluxes. The downward fluxes at the surface are then used with the spectral surface emissivities and the surface temperature to get the upward longwave fluxes in each of the 140 subintervals. Then the upward fluxes are obtained in a similar fashion from the surface to the top of the atmosphere.

For the relevant spectral intervals of the RRTM schemes, ice cloud optical properties are derived from Ebert-Curry (1992), and water cloud optical properties from Smith and Shi (1992) . Whereas in the previous operational scheme the cloud emissivity used to compute the effective cloud cover is defined over the whole LW spectrum from spectrally averaged mass absorption coefficients and the relevant cloud water and/or ice paths, in RRTM, the cloud optical thickness is defined as a function of spectrally varying mass absorption coefficients and relevant cloud water and ice paths, and is used within the true cloudy fraction of the layer. Alternate sets of cloud optical properties are also available for RRTM (Section 4).

Table 8.1: Spectral distribution of the absorption by atmospheric gases in RRTM

Spectral intervals cm^{-1}	Number of g-points	Gases included	
		Troposphere	Stratosphere
10-250	8	H2O	H2O
250-500	14	H2O	H2O
500-630	16	H2O, CO2	H2O, CO2
630-700	14	H2O, CO2	O3, CO2
700-820	16	H2O, CO2, CCl4	O3, CO2, CCl4
820-980	8	H2O, CFC11, CFC12	CFC11, CFC12
980-1080	12	H2O, O3	O3
1080-1180	8	H2O, CFC12, CFC22	O3, CFC12, CFC22
1180-1390	12	H2O, CH4	CH4
1390-1480	6	H2O	H2O
1480-1800	8	H2O	H2O
1800-2080	8	H2O	
2080-2250	4	H2O, N2O	
2250-2380	2	CO2	CO2
2380-2600	2	N2O, CO2,	
2600-3000	2	H2O , CH4	

4 Input to the radiation scheme

4.1 Solar irradiance data

Depending on the experiment, the solar constant can be specified on a yearly basis in the model. For instance, for XXth century simulations, the historic reconstruction recommended by CMIP5 is used:

`http://www.geo.fu-berlin.de/en/met/ag/strat/forschung/SOLARIS/Input_data/CMIP5_solar_irra`

4.2 Clouds

Cloud fraction, and liquid/ice water content are provided in all layers by the cloud scheme.

4.3 Ground albedo and emissivity

Ground albedo and emissivities are calculated in the SURFEX module (see chapter “Surfex processes schemes”). The main features are the following ones:

1. one emissivity by type of vegetation (coming from the Ecoclimap 1 km resolution data base) and for ocean and sea-ice.

2. Albedo:

- over continental areas. It is deduced from the Ecoclimap data base, one by type of vegetation.
- over ocean: the diffuse albedo is taken as a constant (0.061); the direct albedo is computed as a function of the zenithal angle, the function is chosen to obtain similar results than with the value 0.061 on a whole annual cycle.
- over snow: albedo varies with the age of snow following Douville et al. (1995)

4.4 Aerosols

The aerosol distributions are given by outputs of simulations run with the LMDZ-INCA chemical model (Balkanski, personnal communication; Schulz (2007)), forced with observed emissions. The vertically integrated monthly averaged optical thicknesses are then available from 1850 to 2000, and from 2000 to 2100 for each RCP scenario. To smooth interannual variability, a running average on 11 years is calculated. Five aerosol types are used: maritime, sulfate, continental, soot and desert. An option for volcanic class is available. The 2D optical thicknesses are vertically distributed in the RADAER subroutine according to the aerosol type. In the same subroutine aerosols are also redistributed in 6 types:

- Continental (Organic) + Sulfate + Background tropospheric.
- Maritime (seasalt aerosols)
- Desert (soil dust type aerosols)
- Urban (mainly black-carbon type aerosols)
- Volcanic class (background)
- Stratospheric (background) + volcanic eruptions

	Diffusion RPIZA		Asymmetry factor RCGA		Normalized optical depth	

Spectral bands	0.25-0.68 μm	0.68-4.0 μm	0.25-0.68 μm	0.68-4.0 μm	0.25-0.68 μm	0.68-4.0 μm
Organic + Sulfate + Tropospheric	0.9148907	0.8814597	0.729019	0.663224	1.69446	0.40174
Maritime	0.9956173	0.9920407	0.803129	0.793746	1.11855	0.89383
Desert	0.7504584	0.9239428	0.784592	0.696315	1.09212	0.89546
Carbonic	0.8131335	0.7546879	0.712208	0.652612	1.72145	0.40741
Volcanic	0.9401905	0.9515548	0.7008249	0.6608509	1.03858	0.51143
Stratospheric	0.9999999	0.9938563	0.7270548	0.6318786	1.12044	0.32646

Coefficients for the solar radiation and for the two spectral intervals case. For the other cases, see routine SUAERSN for short-wave coefficients and SUAERL for long-wave coefficients.

Spectral bands	>2.85 μm	1.25-2.0 μm	1.25-2.0 μm	0.9-1.0 μm	2.0-2.85 μm	
Organic + sulfate + tropospheric	0.036271	0.030153	0.017343	0.015002	0.008806	0.006865
Maritime	0.026561	0.032657	0.017977	0.014210	0.016775	0.022123
Desert	0.014897	0.016359	0.019789	0.030777	0.013341	0.014321
Carbonic	0.001863	0.002816	0.002355	0.002557	0.001774	0.001780
Volcanic	0.011890	0.016142	0.021105	0.028908	0.011890	0.011890
Stratospheric	0.013792	0.026810	0.052203	0.066338	0.013792	0.013792

Absorption coefficients for long-wave radiation (SUAERL).

Indirect forcing of the sulfate aerosols

The aerosols can act as cloud condensation nuclei. At constant cloud liquid water, increasing aerosol concentration leads to a larger concentration of cloud droplets of small radius and increases cloud reflectivity. A simple parametrization from Quaas and Boucher (2005) simulates this effect in the case of sulfate aerosols. The cloud droplet concentration CDN (in cm^{-3}) is given by:

$ln\text{CDN} = 1.7 + 0.2 \ln \text{m}_{SO_4^{2-}}$

with $m_{SO_4^{2-}}$expressed in $\mu g m^{-3}$. The mean cloud droplet radius is then calculated from the cloud liquid water content q_l by:

$r_v = \sqrt[3]{\frac{3q_l}{4\pi\rho_l CDN}}$

and the effective radius r_e =1.1 r_v.

The sulfate aerosols are available as output of the routine RADAER in the 3D array ZAERINDS.

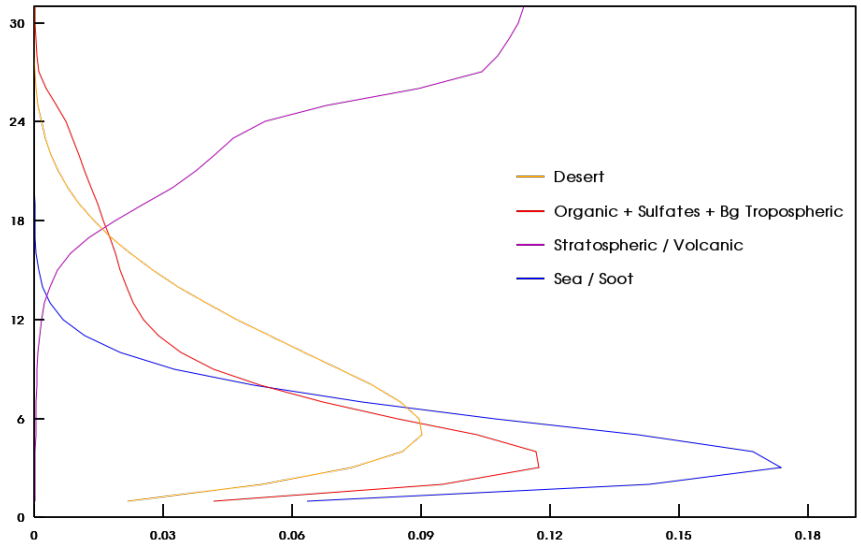

Figure 1: Mean global profiles of types of aerosols as input of the RRTM scheme: optical thickness by level (sum of all the levels gives the vertically integrated optical thickness, normalized to 1 for each aerosol type).

4.5 Radiatively active compounds

Concentrations of carbon dioxide, methane, nitrous oxide, CFC-11, CFC-12 and chlorine are given in namelist NAERAD. During the simulation, values are evolving yearly following the IPCC data. The CFC-12 compound also includes the CFC-12 equivalent of halocarbon species. Outputs from the CNRM REPROBUS chemical model, simulating coefficients which describe 3D ozone distributions, are used as input of a linear interactive scheme (Cariolle and Teyssèdre, 2007). The value NVCLIS = 7 (in NAMDPHY) means that seven of the climatological coefficients of the REPROBUS outputs are used. Evolution of ozone chemistry is due to chlorine and meteorological parameters (temperature, humidity) evolutions.

4.6 Cloud optical properties

For the SW radiation, the cloud radiative properties depend on three different parameters: the optical thickness, the asymmetry factor and the single scattering albedo of particles. For LW the cloud properties are linked with emissivity and spectral optical thickness. All these properties are defined for water and ice particles in the RADLSW routine. They depend on liquid (or ice) water path or on the effective radius of the particles. These characteristic parameters can be calculated by different ways according to NRADLP, NRADIP, NLIQOPT, NICEOPT:

Cloud liquid particles

- NRADLP = 0; cloud water effective radius is calculated as a function of pressure (old parameterisation).
- NRADLP = 1; the cloud effective radius is equal to 10 μm over land and equal to 13 μm over the ocean.
- NRADLP = 2; parameterisation based on Martin et al. (1994).
- NRADLP =3: the effective radius of cloud particle is calculated taking into account the indirect effects of sulfate aerosols.

Cloud ice particles

- NRADIP = 0; the ice particle effective radius is fixed at 40 μm.
- NRADIP = 1; ice particle effective radius calculated as f(T) from Ou and Liou (1995).

- NRADIP = 2; ice particle effective radius calculated as f(T) from Ou and Liou (1995) and fixed between 30 and 60 microns .
- NRADIP = 3; Ice effective radius calculated as a function of temperature and ice water content from Sun and Rikus (1999) and revised by Fu and Sun (2001).

SW radiation
Cloud water optical properties depend on NLIQOPT:

- NLIQOPT different from zero, refers to Slingo (1989).
- NLIQOPT = 0, refers to Parol et al. (1991).

Ice water optical properties depend on NICEOPT:

- NICEOPT lower than or equal to 1 , refers to Ebert and Cury (1992).
- NICEOPT = 2, refers to Fu and Liou (1993).
- NICEOPT = 3, refers to Fu (1996).

LW radiation

Cloud water emissivity depends on NLIQOPT:

- NLIQOPT = 0 or greater than or equal to 3, refers to Smith and Shi (1992).
- NLIQOPT = 1 , refers to Savijarvi and Raisanen (1997).
- NLIQOPT = 2 , refers to Lindner and Li (2000).

Ice cloud emissivity depends on NICEOPT:

- NICEOPT = 0, refers to Smith and Shi (1992).
- NICEOPT = 1, refers to Ebert-Curry (1992).
- NICEOPT = 2, refers to Fu and Liou (1993).
- NICEOPT = 3, refers to Fu et al. (1998) including parametrisation for LW scattering effect .

The current values are NRADLP = 3, NRADIP = 2, NLIQOPT = 0 and NICEOPT = 1.

4.7 Cloud overlap assumption

The cloud overlap assumption is used for the determination of C_{tot} (see Section 2). It is determined by the NOVLP variable: NOVLP = 1 means "maximum-random overlap", NOVLP = 2 means "maximum overlap " and NOVLP = 3 means "random overlap" (NOVLP = 1 in the present code).

4.8 Interactions with the SURFEX module

To obtain consistent radiative fluxes in ARPEGE and in SURFEX, downward fluxes calculated by ARPEGE and provided to the SURFEX scheme have to be cut into spectral bands. Moreover, for the long-wave radiative fluxes, additional corrections have to be made in the APLPAR subroutine to ensure equal radiative net budgets in ARPEGE as well as in SURFEX.

5 Simplified radiation scheme

Given the computation cost of the radiation scheme, it seems interesting to call it only at some time steps, named radiative time steps. Nevertheless, it is necessary to produce radiative flows at each time step. One thus needs a way to calculate these fluxes at low cost. This is carried out in Arpege-climat by calling subroutine RADHEAT.

The idea of this routine is to save between two radiative time steps the solar transmissivity and long-wave emissivity. Let F_{SW} (PFRSO in APLPAR) and F_{LW} (PFRTH) be total net fluxes of solar and infrared radiation calculated at the last radiative time step. The approximation consists in maintaining constant the values of transmissivities t_0 (PTRSOL) and emissivities (PEMTD) ϵ_0 calculated at this time:

$$t_0 = \frac{F_{SW0}}{\mu_0 E^0} \tag{49}$$

$$\epsilon_0 = \frac{F_{LW0}}{\sigma T_0^4} \tag{50}$$

Then, in the next time steps, one recomposes solar and infrared fluxes by modifying only the solar incidence μ and temperature T:

$$F_{SW} = t_0 \mu_0 E^0 \tag{51}$$

$$F_{LW} = \epsilon_0 \sigma T^4 \tag{52}$$

9

Clouds and turbulence

1 General description of the scheme

This scheme was developed by Ricard and Royer (1993) and has been used in the former versions of ARPEGE-CLIMAT. It calculates the stratiform cloud fraction, the stratiform liquid water content and the coefficients of turbulent vertical mixing as well as the Brunt-Vaïsala frequency.

1.1 Condensate assumptions

The scheme of sub-grid condensation is based on Deardorff (1977) and Mellor (1977), resumed and adapted by Bougeault (1981, 1982). These studies use the conservative variables of Betts (1973), namely the potential temperature of liquid water θ_l and the specific moisture of total water q_w (vapor + condensed).

ARPEGE-CLIMAT does not have a prognostic equation for condensate, where, by definition, all condensate precipitates. Ricard and Royer considered that the original variables of the model T and q_v were to play the role of the conservative variables in the equations. Calculations will thus be made with the variables of Betts (θ_l, q_w), by replacing them by (θ, q_v) in the code.

1.2 Turbulent kinetic energy assumptions

(B) For the turbulence part , the problem of closure is solved by the sub-grid scheme of order 2 described in Mellor and Yamada (1974, 1975, 1982) and Galperin et al. (1988), in which the effects of liquid water and the water vapor are taken into account.

These order 2 schemes use a diagnostic turbulent kinetic energy $e_T = (\overline{u'^2} + \overline{v'^2} + \overline{w'^2})/2$ which comes from a stationary equation $d(e_T)/dt = 0$. The moments of order 2 such as the correlations and the variances (for example $\overline{w'u'}$, $\overline{w'\theta'_l}$, $\overline{\theta'^2_l}$ or $\overline{q'^2_w}$) are calculated using a parametrization according to e_T and of the wet conservative variables (θ_l, q_w).

The exchange coefficients are in the form $K_X = l\sqrt{2\,e_T}\,S_X$, for $X = (u, v, T, q)$. Even if the mixing length l has a known and imposed analytical formulation, the functions of stability S_X do not have a fully determined analytical formulation. One difficulty of the scheme comes from that functions S_X depend on the Richardson number Ri and the condensate q_l which must be determined according to the deficit to standardized saturation $Q_1 = a\,(q - q_{sat})/(2\sigma_s)$ and of the functions introduced by Bougeault (1981, 1982) F_0, F_1 and F_2 . One obtains $R = F_0(Q_1)$, $q_l = (2\sigma_s)\,F_1(Q_1)$ and $\overline{s'q'_l} = (2\sigma_s^2)\,F_2(Q_1)$.

It is necessary to solve implicit equations of type $Q_1[q_l(Q_1)]$, admitting one or more solutions. After the study of the various cases which can arise, a method of resolution by successive iterations was developed by Ricard (1992) or Ricard and Royer (1993).

1.3 Sub-grid condensation scheme

This scheme was developed by Sommeria and Deardorff (1977) and Mellor (1977). It accounts for sub-grid condensation in the case of non-precipitating clouds. It makes it possible to evaluate the cloudy fraction and the liquid quantity of water from the small scale turbulence. In this chapter, the term "stratiform" is understated when the terms "cloudy fraction" and "liquid water" are mentioned.

In order to describe the thermodynamical properties of the planetary boundary layer, one uses the "conservative variables" θ_l (potential temperature of liquid water) and q_w (total water content), in the place of potential temperature θ, of specific moisture of vapor q and of liquid water content q_l. These variables are defined as:

$$\begin{cases} \theta_l & = \theta - \dfrac{L}{c_p}\dfrac{\overline{\theta}}{\overline{T}} q_l \\ q_w & = q + q_l \end{cases} \tag{1}$$

Resumed and adapted by Bougeault (1981, 1982), this scheme relies on three assumptions:

- a systematic condensation.
- fluctuations of θ_l and q_w are weak.
- a knowledge of the joint distribution function of θ_l and q_w.

Systematic condensation

At the scale of the particle, one supposes that there is immediate condensation as soon as the specific moisture of the water vapor, q, reaches the specific moisture at saturation for the ambient temperature, q_s. Liquid total water content formed locally is expressed then using the equation:

$$q_l = (q_w - q_s)\, H(q_w - q_s) \tag{2}$$

where H is Heavyside function: $H : x \longrightarrow \begin{cases} 1 & \text{si } x > 0 \\ 0 & \text{si } x \leq 0 \end{cases}$

Fluctuations of θ_l and q_w are weak

The formulation of q_l being defined, cloud fraction R and liquid water content $\overline{q_l}$ are expressed using these two double integrals:

$$\begin{cases} R &= \iint_{I\!R^2} H(q_w - q_s)\, \widetilde{G}(\theta_l, q_w)\, d\theta_l\, dq_w \\ \overline{q_l} &= \iint_{I\!R^2} (q_w - q_s)\, H(q_w - q_s)\, \widetilde{G}(\theta_l, q_w)\, d\theta_l\, dq_w \end{cases} \tag{3}$$

where $\widetilde{G}$ indicates the joint distribution of θ_l and q_w.

The difficulty in resolving these two integrals comes from the fact that q_s depends on T, which depends in turn on q_w and θ_l. The way of solving this problem is to find an expression of q_s as a function of T_l, temperature of liquid water.

In a volume around a given grid point, it is supposed that fluctuations of the potential temperature of liquid water (θ_l) and of the total water content (q_w) remain weak. In this way, one can carry out a Taylor development of q_s around $\overline{T_l}$ to the first order, with the help of the approximation which consists in neglecting the influence of the fluctuations in pressure on q_s compared to those of temperature on it:

$$q_s(T) = q_s(\overline{T_l}) + (T - \overline{T_l}) \frac{\partial q_s}{\partial T}(\overline{T_l}) \tag{4}$$

This approximation is justified by an analysis in order of magnitude which relies on these two formulas:

- the formula giving saturated specific moisture as a function of pressure p and temperature T:

$$q_s(T,p) = 0.622\frac{e_s(T)}{p - 0.378\,e_s(T)}\text{ , hence }\frac{\partial q_s}{\partial p} = -\frac{q_s(T,p)}{p - 0.378\,e_s(T)}$$

- Clapeyron equation:

$$\frac{\partial q_s}{\partial T} = \frac{q_s L}{R_v T^2}$$

It is shown that $\frac{\partial q_s}{\partial T}\Delta T \sim 10^4 \frac{\partial q_s}{\partial p}\Delta p$, which justifies the last approximation Assuming that $\frac{T}{\theta} \sim \frac{\overline{T_l}}{\overline{\theta_l}} \sim \frac{\overline{T}}{\overline{\theta}}$, one can rewrite Equation (4) in the following way:

$$q_s(T) = q_s(\overline{T_l}) + \left(\frac{\overline{T}}{\overline{\theta}}\theta'_l + \frac{L}{c_p}q'_l\right)\frac{L\,q_s(\overline{T_l})}{R_v\overline{T_l}^2} \tag{5}$$

When $q_w > q_s$, q_l can then be put in the form:

$$q_l = a\Delta\overline{q} + a(q'_w - \alpha_1\theta'_l) \tag{6}$$

in which:

$$a = \left[1 + \frac{L}{c_p}\frac{\partial q_s}{\partial T}(\overline{T_l})\right]^{-1} \qquad \alpha_1 = \frac{\overline{T}}{\overline{\theta}}\frac{\partial q_s}{\partial T}(\overline{T_l}) \quad \Delta\overline{q} = \overline{q_w} - q_s(\overline{T_l}) \tag{7}$$

Introduction of variable s

At this stage, one introduces a linear combination of q'_w and θ'_l which allows an integration with respect to single variable s, defined as:

$$s = \frac{a}{2}(q'_w - \alpha_1\theta'_l) \tag{8}$$

In a diagram (θ_l, q_w), curves $q_l = cste$ are parallel to the curve of saturation $q_s(\theta_l)$; s represents the local algebraic variation to saturation. The liquid water q_l depends only on variable s which is measured on a perpendicular axis. The algebraic deviation to saturation averaged on the mesh is given by $a\Delta\overline{q}$.

Under these conditions, q_l is written:

$$\begin{cases} q_l = 0 & \text{if } s < s_{min} \\ q_l = a\Delta\overline{q} + 2s & \text{if } s > s_{min} \end{cases} \qquad \text{with } s_{min} = -\frac{a\Delta\overline{q}}{2} \tag{9}$$

Using variables s and r, r being defined by $r = \frac{a}{2}(q'_w + \alpha_1 \theta'_l)$, one carries out a transformation which aims at replacing the conservative variables (θ'_l, q'_w) by (r, s). Posing $G(s) = |J| \int_{-\infty}^{+\infty} \widetilde{G}(\frac{r-s}{a\,\alpha_1}, \frac{r+s}{a\,\alpha_1})\, dr$, where J is the Jacobian of the transformation ($J = -\frac{2}{a^2 \alpha_1}$), one obtains:

$$\left\{ \begin{array}{lll} R & = \int_{s_{min}}^{+\infty} G(s)\, ds \\ \overline{q_l} & = \int_{s_{min}}^{+\infty} q_l(s)\, G(s)\, ds \\ \overline{s' q'_l} & = \int_{s_{min}}^{+\infty} s\;\; q_l(s)\, G(s)\, ds \end{array} \right. \tag{10}$$

Introduction of variable t

One carries out a last transformation by introducing the standardized variable defined by $t = s/\sigma_s$ where σ_s is the standard deviation of s. One obtains:

$$\sigma_s = \sqrt{\overline{s'^2}} = \frac{a}{2} \sqrt{\left[\overline{q'_w}^{\,2} - \,(2\,\alpha_1)\,\overline{\theta'_l q'_w} + \,(\alpha_1)^2\,\overline{\theta'^2_l}\right]}. \tag{11}$$

Let Q_1 be an algebraic measurement of the distance to the curve of saturation:

$$Q_1 = \frac{a\,\Delta\overline{q}}{2\,\sigma_s} = -\frac{s_{min}}{\sigma_s}. \tag{12}$$

Under these conditions, the local value of q_l is given by the following relation:

$$\frac{q_l}{2\,\sigma s} \;=\; (Q_1 + t)\; H(Q_1 + t)\,. \tag{13}$$

Posing $\mathbf{G} = \sigma_s\; G(\sigma_s t)$, System (10) becomes:

$$\left\{ \begin{array}{lll} R & = F_0(Q_1) = \int_{-Q_1}^{+\infty} \mathbf{G}(t)\, dt \\ \dfrac{\overline{q_l}}{2\,\sigma_s} & = F_1(Q_1) = \int_{-Q_1}^{+\infty} (Q_1 + t)\; \mathbf{G}(t)\, dt \\ \dfrac{\overline{s' q'_l}}{2\,{\sigma_s}^2} & = F_2(Q_1) = \int_{-Q_1}^{+\infty} t\;\; (Q_1 + t)\; \mathbf{G}(t)\, dt \end{array} \right. \tag{14}$$

where F_0, F_1, F_2, functions of Q_1, depend only on the of distribution function $\mathbf{G}$.

From System (14), in order to calculate cloud fraction R and mean liquid water content $\overline{q}_l$ on the mesh, it is sufficient to know the distribution function of t and the standard deviation of s.

Distribution function G(t)

Sommeria and Deardorff (1977) and Mellor (1977) supposed that the joint distribution of θ_l and q_w is Gaussian or bi-normal.

Three functions F_0, F_1, F_2 were proposed by Bougeault (1981, 1982) who stated that the form of the distribution of s (or t) was not very significant for calculations of cloud fraction R and $\overline{q_l}/(2\sigma_s)$. However, he showed that an asymmetric distribution seemed more effective than a Gaussian distribution to parametrize the cumuliform trade wind layer: in such a layer, strong ascents in the clouds balance weak subsidences out of the clouds. This phenomenon cannot be represented by a Gaussian distribution.

For this scheme, an asymmetric distribution was thus selected:

$$G(t) \;=\; e^{-(t+1)}\; H(t+1) \tag{15}$$

System (14) can then be written:

$$Q_1 < 1 \begin{cases} F_0(Q_1) &= e^{Q_1-1} \\ F_1(Q_1) &= e^{Q_1-1} \\ F_2(Q_1) &= (2-Q_1)\; e^{Q_1-1} \end{cases} \qquad Q_1 \geq 1 \begin{cases} F_0(Q_1) &= 1 \\ F_1(Q_1) &= Q_1 \\ F_2(Q_1) &= 1 \end{cases} \tag{16}$$

The evaluation of σ_s requires an estimate of correlation $\overline{\theta_l' q_w'}$ and variances of temperature $\overline{\theta_l'^2}$ and moisture $\overline{q_w'^2}$, which justifies the use of the sub-grid turbulence scheme which is described hereafter.

1.4 Sub-grid turbulence scheme

For reasons of simplicity of setting up, reliability and robustness, the model used is a level 2 Mellor and Yamada (1974, 1975, 1982) model.

This model relies on the following assumptions:

- Boussinesq hypotheses.
- horizontal homogeneity for turbulent motion: cloudy regions are produced by turbulent fluctuations only. This hypothesis is valid outside regions with strong advection.

- in the prognostic equation for turbulent kinetic energy $e_T = (\overline{u'^2} + \overline{v'^2} + \overline{w'^2})/2$, the divergence of mean turbulent kinetic energy flux, i.e. the diffusion term:

$$-\frac{\partial}{\partial z}(\overline{w' e'_T} + \frac{\overline{p'w'}}{\rho} - \nu \frac{\partial \overline{e_T}}{\partial z})$$

  is neglected

- the turbulent kinetic energy equation is stationary.

Under these assumptions, the equations are:

$$\left\{ \begin{array}{ll} \dfrac{\partial \overline{u}}{\partial t} & = -\dfrac{\partial \overline{w'u'}}{\partial z} - \dfrac{1}{\rho}\dfrac{\partial p}{\partial x} + \nu \dfrac{\partial^2 \overline{u}}{\partial z^2} + f\overline{v} \\ \dfrac{\partial \overline{v}}{\partial t} & = -\dfrac{\partial \overline{w'v'}}{\partial z} - \dfrac{1}{\rho}\dfrac{\partial p}{\partial x} + \nu \dfrac{\partial^2 \overline{v}}{\partial z^2} - f\overline{u} \\ \dfrac{\partial \overline{\theta}}{\partial t} & = -\dfrac{\partial \overline{w'\theta'}}{\partial z} + \nu_\theta \dfrac{\partial^2 \overline{\theta}}{\partial z^2} \\ \dfrac{\partial \overline{p}}{\partial z} & = -\rho g \\ \dfrac{\partial \overline{e_T}}{\partial t} & = 0 = -\left(\overline{w'u'}\dfrac{\partial \overline{u}}{\partial z} + \overline{w'v'}\dfrac{\partial \overline{v}}{\partial z}\right) + \beta\,\overline{w'\theta'_v} - C_\epsilon \dfrac{\overline{e_T}^{3/2}}{l_\epsilon} \end{array} \right. \tag{17}$$

where $\beta = g/T$ and where θ_v is the virtual temperature defined by Lilly (1968), Deardorff (1976), Sommeria and Deardorff (1977), see Equation (26).

N.B: a level 2.5 Mellor and Yamada model (with a prognostic equation for the turbulent kinetic energy) could have been used but it has the disadvantage of being less robust. Indeed, Helfand and Labraga (1988) showed that the model can explode when the two following conditions are met: the Richardson number is negative and the turbulent kinetic energy is lower than the equilibrium turbulent kinetic energy given by the level 2 model.

In order that the sub-grid condensation scheme is compatible with the sub-grid turbulence scheme, it is necessary to introduce the effects of the water vapor and liquid water into it. To go from the dry air system (in θ and q) to the moist air system (in θ_l and q_w), the steps are:

- replace θ by θ_l,
- add prognostic equations for q_w and correlations between q_w and (u, v, w, θ_l),
- modify the expression of virtual temperature, taking θ_v defined by Equation (26).

Mean motion equations

The realization of the first two points makes it possible to lead to the following system:

$$\left\{\begin{array}{ll} \dfrac{\partial \overline{u}}{\partial t} & = -\dfrac{\partial \overline{w'u'}}{\partial z} - \dfrac{1}{\rho}\dfrac{\partial p}{\partial x} + \nu \dfrac{\partial^2 \overline{u}}{\partial z^2} + f\overline{v} \\ \dfrac{\partial \overline{v}}{\partial t} & = -\dfrac{\partial \overline{w'v'}}{\partial z} - \dfrac{1}{\rho}\dfrac{\partial p}{\partial x} + \nu \dfrac{\partial^2 \overline{v}}{\partial z^2} - f\overline{u} \\ \dfrac{\partial \overline{\theta_l}}{\partial t} & = -\dfrac{\partial \overline{w'\theta'_l}}{\partial z} + \nu_\theta \dfrac{\partial^2 \overline{\theta_l}}{\partial z^2} \\ \dfrac{\partial \overline{q_w}}{\partial t} & = -\dfrac{\partial \overline{w'q'_w}}{\partial z} + \nu_q \dfrac{\partial^2 \overline{q_w}}{\partial z^2} \\ \overline{E_T} & = P_d + P_\theta \end{array}\right. \tag{18}$$

$$\text{where} \left\|\begin{array}{ll} P_\theta & = \beta\, \overline{w'\theta'_v} \\ P_d & = -(\overline{w'u'}\,\dfrac{\partial \overline{u}}{\partial z} + \overline{w'v'}\,\dfrac{\partial \overline{v}}{\partial z}) \\ \overline{E_T} & = C_\epsilon \dfrac{\overline{e_T}^{3/2}}{l_\epsilon} \;=\; \dfrac{\overline{e_T}^{3/2}}{\Lambda_1} \end{array}\right.$$

P_θ is the term of production by buoyancy of the turbulent kinetic energy, P_d is the dynamic production term and $\overline{E_T}$ is the dissipation of turbulent kinetic energy term. As previously, $\beta = g/T$.

Second order moments

It is necessary to introduce the effects of liquid water and of water vapor into the second order moments of the level 2 Mellor and Yamada (1974) scheme, as redefined in Yamada and Mellor (1975) and in Mellor and Yamada (1982). One should pay attention that, in these papers, the quadratic speed average $q = \sqrt{2\, e_T}$ is used, with $l_1 = A_1\, l$, $l_2 = A_2\, l$, $\Lambda_1 = B_1\, l = l_\epsilon / C_\epsilon$ and $\Lambda_2 = B_2\, l$. But in this documentation, one will use directly kinetic turbulent energy $e_T = q^2/2$, with the mixing length l and the 5 coefficients (A_1, A_2, B_1, B_2, C_1).

Under these conditions, one has:

$$\begin{cases} \overline{u'^2} &= \dfrac{2\,e_T}{3} + \dfrac{A_1\,l}{\sqrt{2\,e_T}}\left[-4\overline{w'u'}\dfrac{\partial\overline{u}}{\partial z} + 2\overline{w'v'}\dfrac{\partial\overline{v}}{\partial z} - 2P_\theta\right] \\ \overline{v'^2} &= \dfrac{2\,e_T}{3} + \dfrac{A_1\,l}{\sqrt{2\,e_T}}\left[2\overline{w'u'}\dfrac{\partial\overline{u}}{\partial z} - 4\overline{w'v'}\dfrac{\partial\overline{v}}{\partial z} - 2P_\theta\right] \\ \overline{w'^2} &= \dfrac{2\,e_T}{3} + \dfrac{A_1\,l}{\sqrt{2\,e_T}}\left[2\overline{w'u'}\dfrac{\partial\overline{u}}{\partial z} + 2\overline{w'v'}\dfrac{\partial\overline{v}}{\partial z} + 4P_\theta\right] \end{cases} \tag{19}$$

$$\begin{cases} \overline{u'\theta'_l} &= -\dfrac{3\,A_2\,l}{\sqrt{2\,e_T}}\left[\overline{w'u'}\dfrac{\partial\overline{\theta_l}}{\partial z} + \overline{w'\theta'_l}\dfrac{\partial\overline{u}}{\partial z}\right] \\ \overline{v'\theta'_l} &= -\dfrac{3\,A_2\,l}{\sqrt{2\,e_T}}\left[\overline{w'v'}\dfrac{\partial\overline{\theta_l}}{\partial z} + \overline{w'\theta'_l}\dfrac{\partial\overline{v}}{\partial z}\right] \\ \overline{w'\theta'_l} &= -\dfrac{3\,A_2\,l}{\sqrt{2\,e_T}}\left[\overline{w'^2}\dfrac{\partial\overline{\theta_l}}{\partial z} - \beta\,\overline{\theta'_l\theta'_v}\right] \end{cases} \tag{20}$$

$$\begin{cases} \overline{u'v'} &= -\dfrac{3\,A_1\,l}{\sqrt{2\,e_T}}\left[\overline{w'u'}\dfrac{\partial\overline{v}}{\partial z} + \overline{w'v'}\dfrac{\partial\overline{u}}{\partial z}\right] \\ \overline{u'w'} &= -\dfrac{3\,A_1\,l}{\sqrt{2\,e_T}}\left[(\overline{w'^2} - 2\,e_T\,C_1)\dfrac{\partial\overline{u}}{\partial z} - \beta\overline{u'\theta'_v}\right] \\ \overline{v'w'} &= -\dfrac{3\,A_1\,l}{\sqrt{2\,e_T}}\left[(\overline{w'^2} - 2\,e_T\,C_1)\dfrac{\partial\overline{v}}{\partial z} - \beta\overline{v'\theta'_v}\right] \end{cases} \tag{21}$$

$$\begin{cases} \overline{u'q'_w} &= -\dfrac{3\,A_2\,l}{\sqrt{2\,e_T}}\left[\overline{w'u'}\dfrac{\partial\overline{q_w}}{\partial z} + \overline{w'q'_w}\dfrac{\partial\overline{u}}{\partial z}\right] \\ \overline{v'q'_w} &= -\dfrac{3\,A_2\,l}{\sqrt{2\,e_T}}\left[\overline{w'v'}\dfrac{\partial\overline{q_w}}{\partial z} + \overline{w'q'_w}\dfrac{\partial\overline{v}}{\partial z}\right] \\ \overline{w'q'_w} &= -\dfrac{3\,A_2\,l}{\sqrt{2\,e_T}}\left[\overline{w'^2}\dfrac{\partial\overline{q_w}}{\partial z} - \beta\,\overline{q'_w\theta'_v}\right] \end{cases} \tag{22}$$

$$\begin{cases} \overline{\theta_l'^2} & = -\dfrac{B_2\, l}{\sqrt{2\, e_T}}\, \overline{w'\theta_l'}\, \dfrac{\partial \overline{\theta_l}}{\partial z} \\ \overline{{q_w'}^2} & = -\dfrac{B_2\, l}{\sqrt{2\, e_T}}\, \overline{w' q_w'}\, \dfrac{\partial \overline{q_w}}{\partial z} \\ \overline{\theta_l' q_w'} & = -\dfrac{B_2\, l}{2\sqrt{2\, e_T}} \left[\overline{w' q_w'} \dfrac{\partial \overline{\theta_l}}{\partial z} + \overline{w'\theta_l'} \dfrac{\partial \overline{q_w}}{\partial z} \right] \end{cases} \tag{23}$$

The exchange coefficients are defined by:

$$\begin{cases} \overline{w'u'} & = -K_m \dfrac{\partial \overline{u}}{\partial z} \\ \overline{w'v'} & = -K_m \dfrac{\partial \overline{v}}{\partial z} \\ \overline{w'\theta_l'} & = -K_h \dfrac{\partial \theta_l}{\partial z} \\ \overline{w' q_w'} & = -K_c \dfrac{\partial \overline{q_w}}{\partial z} \end{cases} \qquad \begin{cases} K_m & = l\, \sqrt{2\, e_T}\, \widetilde{S_m} \\ K_h & = l\, \sqrt{2\, e_T}\, \widetilde{S_h} \\ K_c & = l\, \sqrt{2\, e_T}\, \widetilde{S_c} \end{cases} \tag{24}$$

$$\begin{cases} G_m & = \dfrac{l^2}{2\, e_T} \left[\left(\dfrac{\partial \overline{u}}{\partial z} \right)^2 + \left(\dfrac{\partial \overline{v}}{\partial z} \right)^2 \right] \\ G_h & = -\dfrac{l^2}{2\, e_T} \beta \dfrac{\partial \overline{\theta_l}}{\partial z} \\ G_c & = -\dfrac{l^2}{2\, e_T} \beta \dfrac{\partial \overline{q_w}}{\partial z} \end{cases} \tag{25}$$

Expression of the virtual potential temperature

The third point is dealt by introducing the expression of the virtual potential temperature defined in Lilly (1968), Deardorff (1977) and Sommeria and Deardorff (1977):

$$\theta_v = \theta\, [1 + (RETV)\, q - q_l] \tag{26}$$

where, in the code, $RETV = R_v/R_d - 1 \approx 0.601$.

Using conservative variables $\theta_l = \theta - \dfrac{L}{c_p} \left(\dfrac{p_0}{p} \right)^{\kappa} q_l$ and $q_w = q + q_l$, the preceding equation can be rewritten as:

$$\theta_v = \theta_l + C_{T_0}\, q_w + D(z)\, q_l \tag{27}$$

where:

- $C_{T_0} = (RETV)\,\theta$
- $D(z) = \left(\frac{p_0}{p}\right)^{\kappa} \frac{L}{c_p} - (1 + RETV)\,\theta = \left(\frac{L}{c_p\,T} - \frac{R_v}{R_d}\right)\theta$

In system (18), the order two moments using virtual temperature are expressed as a function of variables θ'_l, q'_w and of q'_l:

$$\begin{aligned} \overline{m'\theta'_v} &= \overline{m'\theta'_l} + C_{T_0}\,\overline{m'q'_w} + D(z)\,\overline{m'q'_l} \\ & m \in \{u, v, w, \theta_l, q_w\} \end{aligned} \tag{28}$$

The correlations involving liquid water potential temperature ($\overline{m'\theta'_l}$) and total water content ($\overline{m'q'_w}$) do not generate calculation problems. However, correlations involving liquid water content ($\overline{m'q'_l}$) are difficult to estimate. To solve this problem, Bougeault (1982) proposed the following assumption:

$$\begin{cases} \overline{m'q'_l} &= \overline{m's'}\left(\dfrac{\overline{s'q'_l}}{{\sigma_s}^2}\right) \\ \text{where} \quad \overline{m's'} &= \dfrac{a}{2}\left(\overline{m'q'_w} - \alpha_1\,\overline{m'\theta'_l}\right) \end{cases} \tag{29}$$

The calculations carried out by Mellor (1977) show that this assumption is valid if the joint distribution for the pair of variables (s, m) is Gaussian. However, Bougeault (1982) assumes that System (29) can be applied to the non-Gaussian cases

Like $F_2(Q_1) = \dfrac{\overline{s'q'_l}}{2\,\sigma_s^2}$, the order two moments using liquid water content are written in the form:

$$\overline{m'q'_l} = a\,F_2(Q_1)\,\left(\overline{m'q'_w} - \alpha_1\,\overline{m'\theta'_l}\right) \tag{30}$$

Reformulation of the Richardson number

The flux Richardson number, ratio of the production by buoyancy P_θ and the dynamic production P_d of turbulent kinetic energy, is defined as follows, with $\beta = g/T$:

$$Rf = -\frac{P_\theta}{P_d} = \frac{\beta\overline{w'\theta'_v}}{\overline{w'u'}\,\dfrac{\partial\overline{u}}{\partial z} + \overline{w'v'}\,\dfrac{\partial\overline{v}}{\partial z}} \tag{31}$$

In Equation (28), replacing $\overline{w'q'_l}$ by the second member of Equation (30) ($m = w$) yields a reformulation of the flux Richardson number:

$$Rf = \beta \left[\frac{\overline{w'\theta'_l} + C_{T_0}\overline{w'q'_w}}{\overline{w'u'}\,\dfrac{\partial\overline{u}}{\partial z} + \overline{w'v'}\,\dfrac{\partial\overline{v}}{\partial z}} \right] \; + \; F_2(Q_1)\,\beta\,a\,D(z) \left[\frac{\overline{w'q'_w} - \alpha_1\overline{w'\theta'_l}}{\overline{w'u'}\,\dfrac{\partial\overline{u}}{\partial z} + \overline{w'v'}\,\dfrac{\partial\overline{v}}{\partial z}} \right]$$

or:

$$Rf = (Rf)_h + F_2(Q_1)\,(Rf)_c \tag{32}$$

R_f is therefore the sum of two terms using:

- a flux Richardson number $(Rf)_h$ taking into account water vapor effect:

$$(Rf)_h = \beta \left[\frac{\overline{w'\theta'_l} + C_{T_0}\overline{w'q'_w}}{\overline{w'u'}\,\dfrac{\partial\overline{u}}{\partial z} + \overline{w'v'}\,\dfrac{\partial\overline{v}}{\partial z}} \right]$$

- a complementary flux Richardson number $(Rf)_c$ taking account of the effects of liquid water:

$$(Rf)_c = \beta\,a\,D(z) \left[\frac{\overline{w'q'_w} - \alpha_1\overline{w'\theta'_l}}{\overline{w'u'}\,\dfrac{\partial\overline{u}}{\partial z} + \overline{w'v'}\,\dfrac{\partial\overline{v}}{\partial z}} \right]$$

In a similar way, the gradient Richardson number is split into two terms:

$$R_i = (Ri)_h + F_2(Q_1)\,(Ri)_c \tag{33}$$

where $(Ri)_h = \dfrac{\widetilde{S_m}}{\widetilde{S_h}}\,(Rf)_h$ and $(Ri)_c = \dfrac{\widetilde{S_m}}{\widetilde{S_h}}\,(Rf)_c$, $\widetilde{S_m}$ and $\widetilde{S_h}$ being terms involved in fluxes and second order moments: see System (24) and consequences on Systems (19) to (22).

A property arises from this last equation: as function F_2 is a bijection of $\mathbb{R}$ onto $]0,1[$, the Richardson number function, defined as follows, is a bijection:

$$\begin{cases} \mathbb{R} \longrightarrow \,] \,(Ri)_{min}, (Ri)_{max}\, [\\ R_i : \quad Q_1 \hookrightarrow \; (Ri)_h + F_2(Q_1)\,(Ri)_c \end{cases} \tag{34}$$

$$\text{where} \left\| \begin{array}{ll} (Ri)_{min} & = \min[\,(Ri)_h, (Ri)_h + (Ri)_c\,] \\ (Ri)_{max} & = \max[\,(Ri)_h, (Ri)_h + (Ri)_c\,] \end{array} \right.$$

This last property shows that the knowledge of the Richardson number Ri in interval $]\,(Ri)_{min}, (Ri)_{max}\,[$ leads to the knowledge of the position of Q_1 in $I\!R$, therefore leads to evaluation of σ_s since $\sigma_s = \dfrac{a\,\Delta\overline{q}}{2\,Q_1}$.

1.5 Solving an implicit equation

Mixing length

In old versions of ARPEGE-CLIMAT, the mixing length was the same as in routine ACCOEFK, with a profile which depended on ALMAV, BEDIFV and UHDIFV.

Further work allowed, as an option, a boundary layer depth variable in time and space. If the profile of mixing length $l(z)$ was supposed to be constant above the planetary boundary layer, the boundary layer depth H (ZHCPLV) either was imposed and equal to AHCLPV, or was calculated in subroutine ACPBLH at previous time step (see Chapter 11) when AHCLPV= 0. The value of this mixing length in the free atmosphere is λ =ALMAV, the asymptotic length used in ACCOEFK. The need to limit the number of adjustable parameters in the scheme was dictated by the constraint to have a parametrization which is robust in simulations of climate change. To this goal, a cubic profile according to $z + z_0$ was used for the mixing length between the ground and the top of the boundary layer.

In order to better mimic the quadratic feature of the mixing length $l(z)$ usually observed within the boundary layer (i.e. the PBL located between $z = 0$ and $z = Z_i$ =ZHCLPV), the cubic profile decribed above is replaced in by a new formulation, adapted from the general formulas from Lenderink and Holtslag (2004).

This new quadratic profile is computed for $l(z)$ if LMLH is set to TRUE. in the namelist. If LMLH is set to .FALSE., $l(z)$ is equal to the old cubic profile.

From the study of Lenderink and Holtslag (2004), the mixing length is deduced from a general function $F(R_i)$, a prescribed function of the local Richarson number $R_i(z)$. For the simple case of a constant value $F(R_i)$ = RLMLH1 (with RLMLH1 available in the namelist), the master "integral" mixing length at the height $z > 0$ is defined in terms of "$(z + z_0)$" (if z_0 is the roughtness length), by

$$L_{int}(z) \;\equiv\; \text{Max}\left(\;0\;;\;\text{RLMLH1}\,\frac{(z+z_0)\,[Z_i-(z+z_0)]}{Z_i}\;\right). \qquad (35)$$

Z_i is the top PBL height and it is denoted by ZHCLPV in the code, depending on the choice for AHCLPV. As for $g\,L_{int}$, it is denoted by ZGLINT in the code.

The method described in Lenderink and Holtslag (2004) for computing this "integral" mixing length $L_{int}(z)$ - and then the corresponding mixing length $l(z)$ - is considered as a "poor man's parcel method", obtaining rather similar results to those of the non-local method of Bougeault and Lacarrere (1989) for convective situations, though at a much lower computational cost.

For a constant value $F(R_i) =$ RLMLH1, the maximum of $L_{int}(z)$ is reached for the height $Z_i\,/\,2 - z_0$, located very close to the middle of the PBL, since z_0 is much smaller than Z_i. This maximum is equal to RLMLH1 $* Z_i\,/4$ and it depends linearly of the local top PBL height. For RLMLH1 = 0.4 and Z_i = 1500 m, this maximum is equal to 150 m. The quadratic profile of $L_{int}(z)$ is ensured from the second order formulation (35), with $L_{int}(0) \approx 0$ and $L_{int}(Z_i) \approx 0$, assuming small values for z_0.

Close to the surface $L_{int}(z) \approx$ RLMLH1 $* (z + z_0)$. Thus, RLMLH1 can be chosen close to the Von Karman constant, equal to $\kappa = 0.4$. But possible higher or lower values for RLMLH1 can be set in the namelist (for instance between 0.2 and 0.8).

Still close to the surface, the length scale is also limited to half the neutral length scale $l_n/2 = 0.5\,c_n\,\kappa\,(z+z_0)$, with $c_n = (c_0)^{-1/2}$ and $c_0 = 3.75$ (leading to $c_n \approx 0.5164$). In the code $0.5\,c_n$ is denoted by ZLMCS.

Above the Planetary Boundary Layer, the too small value of $L_{int}(z)$, for $z > 0.9\,Z_i$ or so, are avoided by a relaxation toward the asymptotic value $\lambda =$ ALMAV, with ALMAV available in the namelist. Above the top PBL height Z_i, $L_{int}(z)$ is presently set to the value $\lambda =$ ALMAV.

The two limitations $l(z) > 0.5\,c_n\,\kappa\,(z+z_0)$ close to the surface and $l(z) \approx \lambda =$ ALMAV close to the top of the PBL are realized via a common minimum value $L_{min}(z)$, defined by the Blackadar formulae (B.3) of the Appendix B in Lenderink and Holtslag (2004)

$$\frac{1}{L_{min}(z)} \;\equiv\; \frac{1}{\lambda} \;+\; \frac{1}{0.5\;c_n\;\kappa\;(z\,+\,z_0)}\;. \tag{36}$$

In the code $g\,L_{min}$ is denoted by ZGLMIN.

Another similar limiting value L^*_{min} is defined by

$$L^*_{min}(z) \;\equiv\; \mathrm{Min}\;(\;\lambda\;\;;\;\;0.5\;c_n\;\kappa\;(z\,+\,z_0)\;)\;. \tag{37}$$

In the code $g\,L^*_{min}$ is denoted by ZGLMIN2.

The final formulation for the quadratic mixing length $l(z)$ is given by Eq.(B.4) in the Appendix B of Lenderink and Holtslag (2004), where the stable mixing length l_s is dropped and with the special choice $p = 1$ and $q = 2$ for the two free exponents

$$l(z) \equiv \text{Max} \left(\sqrt{(L_{int})^2 + (L_{min})^2} \;\; ; \;\; L^*_{min}(z) \right) . \tag{38}$$

In the code $g\,l(z)$ is denoted by ZGLUZ.

Presentation of the implicit equation

A new formulation of σ_s is seeked, avoiding calculations of correlation between the fluctuations of temperature and those of moisture, and calculations of variances of fluctuations of temperature and moisture. For that, one uses the three equations of System (22), namely:

$$\begin{cases} \overline{\theta_l'^2} & = -\dfrac{B_2\, l}{\sqrt{2\, e_T}}\, \overline{w'\theta_l'} \dfrac{\partial \overline{\theta_l}}{\partial z} \\ \overline{{q_w'}^2} & = -\dfrac{B_2\, l}{\sqrt{2\, e_T}}\, \overline{w' q_w'} \dfrac{\partial \overline{q_w}}{\partial z} \\ \overline{\theta_l' q_w'} & = -\dfrac{1}{2}\, \dfrac{B_2\, l}{\sqrt{2\, e_T}} \left(\overline{w'\theta_l'} \dfrac{\partial \overline{q_w}}{\partial z} + \overline{w' q_w'} \dfrac{\partial \overline{\theta_l}}{\partial z} \right) \end{cases} \tag{39}$$

Here, B_2 is one of the constants specified in the Mellor and Yamada (1982) scheme and defined as follows:

$$(A_1, A_2, B_1, B_2, C_1) = (0.92, 0.74, 16.6, 10.1, 0.08)$$

In addition, l is the mixing length introduced above. One should pay attention that another set of values was defined and used in Mellor and Yamada (1974) and Yamada and Mellor (1975). It is necessary to take that of the 1982 paper.

One rewrites Equation (11) by carrying out substitutions of the variables using System (39). The coefficients of vertical exchange K_h and K_c are introduced into the equation obtained:

$$\begin{cases} \overline{w'\theta_l'} & = -K_h \dfrac{\partial \overline{\theta_l}}{\partial z} \quad \text{and } K_h \quad = l\, \sqrt{2\, e_T}\, \widetilde{S_h} \\ \overline{w' q_w'} & = -K_c \dfrac{\partial \overline{q_w}}{\partial z} \quad \text{and } K_c \quad = l\, \sqrt{2\, e_T}\, \widetilde{S_c} \end{cases} \tag{40}$$

As $\widetilde{S_h} = \widetilde{S_c}$, we have $K_h = K_c$ and we obtain for σ_s defined by Equation (11):

$$\sigma_s = \frac{al}{2}\sqrt{B_2\widetilde{S_h}}\left|\frac{\partial\overline{q_w}}{\partial z} - \alpha_1\frac{\partial\overline{\theta_l}}{\partial z}\right|. \tag{41}$$

Replacing in this last equation σ_s by $\frac{a\Delta\overline{q}}{2Q_1}$, the following equation is obtained:

$$Q_1\sqrt{\widetilde{S_h}(Q_1)} = \frac{\Delta\overline{q}}{l\sqrt{B_2}\left|\frac{\partial\overline{q_w}}{\partial z} - \alpha_1\frac{\partial\overline{\theta_l}}{\partial z}\right|} = TTB\,. \tag{42}$$

The second member of Equation (42) – TTB – being known, Q_1 is the solution to the implicit equation:

$$Q_1\sqrt{\widetilde{S_h}(Q_1)} = TTB \tag{43}$$

Whereas in the level 2.5 model, $\widetilde{S_h}$ depends on two variables (G_h, G_m), the level 2 model has the advantage of expressing $\widetilde{S_h}$ as a function of a single variable, namely the flux Richardson number. Indeed:

$$\widetilde{S_h} = 3\,A_2\left(\gamma_1 - \gamma_2\frac{Rf}{1-Rf}\right)$$

where γ_1 and γ_2 are calculated starting from Mellor and Yamada constants (see hereafter for definitions of γ_1 and γ_2). Ultimately, $\widetilde{S_h}$ is a function of single variable Q_1, which facilitates the solution of the implicit Equation (43).

Studying the curves

Ricard (1992) studied of curves $Q_1 \hookrightarrow Q_1\sqrt{\widetilde{S_h}(Q_1)}$ according to the sign of $(Ri)_c$ and the relative position of $(Ri)_{min}$, $(Ri)_{moy} = (Ri)_h + (Ri)_c/2$, $(Ri)_{max}$ and $(Ri)_{crit}$. His study thus considered eight cases reported in Table 9.1 from which one can draw some information about monotony of the curve representing $Q_1 \hookrightarrow Q_1\sqrt{\widetilde{S_h}(Q_1)}$.

We need to know how many solutions Equation $Q_1\sqrt{\widetilde{S_h}(Q_1)} = TTB$ has, when function $Q_1 \hookrightarrow Q_1\sqrt{\widetilde{S_h}(Q_1)}$ is not monotonous. The solution of such a problem involves the localization of the pairs $[(Ri)_h, (Ri)_c]$ for which curves $Q_1 \hookrightarrow Q_1\sqrt{\widetilde{S_h}(Q_1)}$ are not monotonous. Refer to Ricard (1992) for a graphical discussion of the three zones (no extremum, one extremum, two extrema).

$(Ri)_c < 0$	$(Ri)_c > 0$
$(Ri)_{crit} < (Ri)_{min}$	$(Ri)_{crit} < (Ri)_{min}$
$(Ri)_{min} < (Ri)_{crit} < (Ri)_{moy}$	$(Ri)_{min} < (Ri)_{crit} < (Ri)_{moy}$
$(Ri)_{moy} < (Ri)_{crit} < (Ri)_{max}$	$(Ri)_{moy} < (Ri)_{crit} < (Ri)_{max}$
$(Ri)_{max} < (Ri)_{crit}$	$(Ri)_{max} < (Ri)_{crit}$

Table 9.1: Positions of minimum, mean, maximum and critical Richardson numbers according to the sign of $(Ri)_c$.

Successive iterations method and convergence accelerator

The method of successive substitutions is adopted to solve Equation (42). To improve the speed of convergence of this method, one uses Wegstein convergence accelerator.

Sufficient convergence criterion

This method consists in rewriting Equation (42) in the following way:

$$Q_1 = F(Q_1)\ ,\ \text{where}\ F(Q_1) = \frac{TTB}{\sqrt{\widetilde{S_h}}}\ .$$

A sufficient criterion so that successive substitutions method converges is:

$$\mid F'(Q_1) \mid < 1 \quad \forall\, Q_1 \in I\!R$$

In other words, if in a given point Q_1,

$$0 < \left(Q_1\sqrt{\widetilde{S_h}(Q_1)}\right)' < 2\sqrt{\widetilde{S_h}}\ ,\ \text{then}\ \mid F'(Q_1) \mid < 1\ .$$

Thus, the method of resolution by successive substitutions converges locally.

On the other hand, if in Q_1 the curve meets $\left(Q_1\sqrt{\widetilde{S_h}(Q_1)}\right)' < 0$, then $\mid F'(Q_1) \mid > 1$ and this method diverges locally.

Application of this criterion

One considers a curve $Q_1 \hookrightarrow Q_1\sqrt{\widetilde{S_h}(Q_1)}$ admitting two extrema. For certain values of TTB, Equation $Q_1\sqrt{\widetilde{S_h}(Q_1)} = TTB$ admits three solutions, noted S_1, S_2 and S_3.

Between the two extrema, the part of curve has a negative slope –local divergence of the method–, while the other two parts have a positive slope – local convergence of the method–. Consequently, the successive substitutions method discards solution S_2.

From a physical point of view, one rejects solution S_2 located on the decreasing part of the curve for the following reason: in the vicinity of S_2, the response to an increase in $\Delta\overline{q}$ is at the same time an increase in TTB (cf Equations (42) and (43)) and a reduction in Q_1; this is not compatible with Equation (12) which shows that Q_1 and $\Delta\overline{q}$ vary in the same direction (a and σ_s are positive).

The two physically acceptable solutions S_1 and S_3 correspond to the same large-scale environment, but the cloud cover and sub-grid turbulence differ.

Wegstein convergence accelerator

The Wegstein convergence accelerator method consists in modifying the successive substitutions method in order to increase its convergence speed and systematically impose it. Details on this method are given in Gourdin and Boumahrat (1983). In order to maintain the divergent solutions generated by the successive substitutions method, it is necessary to apply Wegstein method only in the case of convergence:

- One calculates α, coefficient which optimizes convergence of the iterative process, in the following way:

$$\begin{cases} x_n &= F(x_{n-1}) \\ \Delta &= \dfrac{F(x_n) - x_n}{x_n - x_{n-1}} \\ \alpha &= \dfrac{1}{1-\Delta} \end{cases} \tag{44}$$

- If $\alpha < \frac{1}{2}$, one applies the method of successive substitutions.
- If $\alpha > \frac{1}{2}$, one calculates x_{n+1} by the formula of Wegstein method :

$$x_{n+1} = x_n + \alpha\,[F(x_n) - x_n]$$

Number of iterations

A study by Ricard (1992) highlighted two significant remarks:

- the transition from the stable to the unstable state is perfectly reached after two steps

- the transition from the unstable to the stable state is slower: after 10 iterations a perfect accuracy is not yet reached

From this study, it proved to be necessary to choose an iteration number allowing the best compromise between precision of the results and speed of calculation. This number was fixed to 2.

Initialization of Q_1

The best initialization of Q_1 would consist of starting from the value of Q_1 at the previous time step for each grid point. Indeed, this method would be of two interests:

- a better accuracy with respect to an arbitrary initialization of Q_1
- a tendency to remain in the same state as at the previous time step, namely stable or turbulent: this introduces a hysteresis effect

In ARPEGE, saving the value of Q_1 at the previous time step is heavy to set up because it requires the introduction of a 3-d array (latitude, longitude, level). This kind of process is usually done for 2-d variables like Halstead coefficient, planetary boundary layer depth or roughness length. Recently, convective precipitation of the previous time step, necessary to the calculation of convective cloud cover, was fully saved in memory (pseudo-historical variables).

In the current code, the initial value of Q_1 is zero, and no pseudo-historical variable is used.

1.6 Summing up

The use of both a sub-grid scale condensation scheme and sub-grid scale level 2 turbulence scheme gives all the ingredients for the calculation of the cloud fraction and the liquid water content.

As far as the coefficients of turbulent vertical exchange are concerned, their calculation involves 2.5 level formulas (Galperin et al., 1988) in order to avoid the feedback, in further calculations, of the inaccuracy from the solution of implicit Equation (42). Indeed, it is not unlikely that numerical solution Q_1^* is somewhat far from real solution. In some cases, $\widetilde{S_h}(Q_1^*)$ does not satisfy Equation $Q_1\sqrt{\widetilde{S_h}(Q_1)} = TTB$.

In the current code, some constants derived from Mellor and Yamada (1974, 1975, 1982) and Galperin et al. (1988) are defined in modules (for GALP, TURB, TYM[1-5]) or locally at the beginning of the subroutine:

$$\text{ZGAMMA1} = \gamma_1 = \frac{1}{3} - \frac{2\,A_1}{B_1}\,;\ \text{ZGAMMA2} = \gamma_2 = \frac{(B_2 + 6\,A_1)}{B_1}$$

$$\text{ZBETA0} = \beta_0 = \gamma_1 + \gamma_2 - 3\,\frac{A_1}{B_1}$$

$$\text{ZBETA1} = \beta_1 = \left(\frac{A_2}{2\,A_1}\right)\left(\frac{\beta_0}{\gamma_1 - C_1 + (6\,A_1 + 3\,A_2/B_1)}\right)$$

$$\text{ZBETA2} = \beta_2 = \left(\frac{A_1}{A_2}\right)\left(\frac{\gamma_1 - C_1}{\beta_0}\right)\ ;\ \text{ZBETA3} = \beta_3 = \frac{\gamma_1}{\beta_0}$$

$$\text{ZGAX1} = g_1 = A_2\left(1 - 6\,\frac{A_1}{B_1}\right)$$

$$\text{ZGAX2} = g_2 = (-3A_2)\,(6A_1 + B_2)\,;\ \text{ZGAX3} = g_3 = A_1\,(1 - 3C_1 - 6A_1/B_1)$$

$$ZGAX4 = g_4 = (-3A_1A_2)\ [(B_2 - 3A_1)(1 - 6A_1/B_1) - 3C_1(B_2 + 6A_1)]$$

$$\text{ZGAX5} = g_5 = -9A_1A_2\,;\ \text{ZGALP2} = (\text{GALP})^2/\text{TURB}$$

These constants being available, one deduces from them the limit values for the Richardson numbers and Mellor and Yamada functions:

$$\text{ZRFCRIT} = (R_f)_{crit} = \frac{\gamma_1}{\gamma_1 + \gamma_2}$$

$$\text{ZRICRIT} = (R_i)_{crit} = \left[\frac{(R_f)_{crit}}{\beta_3 - (R_f)_{crit}}\right]\ \left[\frac{\beta_2 - (R_f)_{crit}}{2\,\beta_1}\right]$$

$$\text{ZSHCRIT} = (\widetilde{S_h})_{crit} = \frac{g_1}{1 - g_2\text{ZGALP2}}\,;\ \text{ZSHMAX} = (\widetilde{S_h})_{max} = 3A_2(\gamma_1 + \gamma_2)$$

$$\text{ZSMCRIT} = (\widetilde{S_m})_{crit} = \frac{g_3 - (\text{ZGALP2})\,g_4}{[1 - (\text{ZGALP2})\,g_2]\ [1 - (\text{ZGALP2})\,g_5]}$$

Here is a summary of the steps which must be followed:

1. Calculation of vertical gradients between layer (JLEV − 1) and (JLEV + 1), for the variables ZDPHI = $\Delta(q_v)$, ZDTL = $\Delta(T + \phi/c_p)$ and
ZDVENT = $\Delta(u^2 + v^2)$.

2. Calculation of gradient Richardson number ZRIH = $(Ri)_h$.

3. Calculation of complementary gradient Richardson number ZRIC = $(Ri)_c$.

4. Calculation of mixing length ZLE.

5. Calculation of ZTTB = TTB for implicit Equation (43)

$$TTB = \Delta\overline{q}\left[l\sqrt{B_2}\left|\frac{\partial\overline{q_w}}{\partial z} - \alpha_1\frac{\partial\overline{\theta_l}}{\partial z}\right|\right]^{-1}$$

6. Calculation of ZQ11 = Q_1 from $(Ri)_h$, $(Ri)_c$ and TTB at mesh scale: solution of implicit Equation (43) using the successive substitutions method and Wegstein convergence accelerator for $Q_1\sqrt{\widetilde{S_h}(Q_1)} = TTB$. One iterates ITER = 2 times the following actions:

   (a) calculation of ZRI = $Ri = (Ri)_h + F_2(\text{ZQ11})\,(Ri)_c$

   (b) calculation of ZRF = $FORF$(ZRI),
   with $FORF(\text{ZRI}) = \beta_1\left[\text{ZRI} + \beta_2 - \sqrt{FODD(\text{ZRI})}\right]$
   and $FODD(\text{ZRI}) = (\text{ZRI})^2 + 2\,\text{ZRI}\,(\beta_2 - \beta_3)/\beta_1 + (\beta_2)^2$

   (c) calculation of ZQ12 = $TTB/\sqrt{FOSH(\text{ZRF})}$,
   with $FOSH(\text{ZRF}) = A_2\,[\gamma_1 - \gamma_2\,FOGAMMA(\text{ZRF})]$,
   where $FOGAMMA(\text{ZRF}) = ZRF/(1 - \text{ZRF})$

   (d) calculation of ZRI = $Ri = (Ri)_h + F_2(\text{ZQ12})\,(Ri)_c$,
   then of ZRF = $FORF$(ZRI)

   (e) calculation of the new ZQ13 = $TTB/\sqrt{FOSH(\text{ZRF})}$

   (f) calculation of the new ZQ11 = ZQ12 + ZALPHA(ZQ13 − ZQ12), where
   ZALPHA = α is the parameter for convergence acceleration used and defined in Equation (44). It depends on
   ZDELTA = Δ = (ZQ13 − ZQ12) / (ZQ12 − ZQ11).

7. Use of the last Q_1 = ZQ11 to calculate ZIGMAS = σ_s by solving Equation (12), i.e.: $\sigma_s = (a\,\Delta\overline{q})/(2\,Q_1)$

8. Calculation of $F_2(Q_1)$, assuming that the distribution function of t is asymmetrical (System (16))

9. Calculation of the gradient Richardson number
ZRI $= Ri = (Ri)_h + F_2(Q_1)\,(Ri)_c$

10. Calculation of ZSH $= \widetilde{S_h}$ by solving implicit Equation (42). One obtains:
$\widetilde{S_h} = (TTB/Q_1)^2$

11. Calculation of ZGH $= G_h$ using the level 2.5 formula of Galperin et al. (1988):

$$\widetilde{S_h} = \frac{g_1}{1 + g_2\, G_h} \quad ; \text{ then : } G_h = \frac{g_1 - \widetilde{S_h}}{g_2\ \widetilde{S_h}}$$

12. Calculation of $ZGM = G_m$ defined by: $G_m = - G_h/Ri$

13. Calculation of $\widetilde{S_m}$ by the level 2.5 formula of Galperin et al. (1988):

$$\text{ZSM} = S_m = \frac{(\, g_3 + g_4\, G_h\,)}{(\, 1 + g_2\, G_h\,)\,(\, 1 + g_5\, G_h\,)}$$

14. The calculation of the turbulent kinetic energy (e_T) can be made by solving Equation (24) for G_h , in order to deduce the "mean quadratic speed":

$$\text{ZKE} = \sqrt{2\, e_T} = \frac{l}{\sqrt{G_m}} \sqrt{\left(\frac{\partial \overline{u}}{\partial z}\right)^2 + \left(\frac{\partial \overline{v}}{\partial z}\right)^2}$$

15. One deduces turbulent vertical exchange coefficients:

$$\begin{cases} \text{ZKM} = K_m = l\,\sqrt{2\, e_T}\ \widetilde{S_m} & \text{coefficient of vertical exchange for } u \text{ and } v \\ \\ \text{ZKH} = K_h = l\,\sqrt{2\, e_T}\ \widetilde{S_h} & \text{coefficient of vertical exchange for } T \text{ and } q \end{cases}$$

16. Calculation of $F_0(Q_1)$ and $F_1(Q_1)$, assuming that the distribution function of t is asymmetrical (System (16))

17. Calculation of stratiform cloud fraction R and stratiform liquid water q_l by System (14). One obtains PNEBS $= R = F_0(Q_1)$ and PQLIS $= q_l = (2\,\sigma_s)\, F_1(Q_1)$

18. Calculation of the Brunt-Vaïsala frequency used in ACDRAG:
PNBVNO $= N^2/(\rho\, g)^2$, where $N^2 = \beta\,(\partial \theta_v/\partial z)$ is a symbolic squared value which can be negative. Concretely, in the code of ACNEBR, with $\rho = p/(R\,T)$, one obtains:

$$\text{PNBVNO} = N^2/(\rho\, g)^2 = \frac{R^2}{p^2}\ \frac{T}{\Delta \phi}\ \Delta(T + \phi/c_p)$$

1.7 Tuning the scheme

At the time of the set up of the parametrization, numerical problems appeared:

- mixing length reaches too high values in stable zones
- cloud liquid water becomes unrealistic when mixing length is too large

These two problems are solved by limitating G_h, l and TTB.

Lower limitation of G_h in stable zones

It is necessary to limit l in the stable layers, i.e. where the Richardson number is higher than the critical Richardson number. The restriction used by André et al. (1978) and Galperin et al. (1988) is defined as:

$$l \leq \frac{0.53\sqrt{2\,e_T}}{N} \tag{45}$$

where $N = (\beta \frac{\partial \theta_v}{\partial z})^{1/2}$ is Brunt-Vaïsala frequency.

As for $G_h = -\frac{l^2 N^2}{2\,e_T}$, the limitation on l is equivalent to the following limitation on G_h:

$$G_h \geq -(0.53)^2 = -0.28 = (G_h)_{crit} \tag{46}$$

Ricard (1992) noted that taking this critical value produced unrealistic downward heat fluxes in the polar areas (up to $-22.6\ W/m^2$ in zonal mean). This remark resulted in introducing coefficient $TURB$ such as:

$$G_{hcrit} = -\frac{(0.53)^2}{TURB} = -\frac{0.28}{TURB} \tag{47}$$

During the first adjustments of this coefficient, a value 0.2 had been retained, for which the downward heat fluxes showed more realistic values in these areas, namely lower than $-10.6\ W/m^2$. But currently the neutral value $TURB = 1$ is used.

Negative moisture

A study of the mixing length showed that unrealistic results can appear when the probability of negative moistures is not negligible. Indeed, it is shown thereafter that for very high mixing lengths the cloud liquid water obtained takes too large values. This phenomenon can easily be highlighted. Relation $\sigma_s = \frac{al}{2}\sqrt{B_2\widetilde{S_h}}\left|\frac{\partial\overline{q_w}}{\partial z} - \alpha_1\frac{\partial\overline{\theta_l}}{\partial z}\right|$ shows that $\sigma_s \sim (\,K\;l\,)$ when $l \longrightarrow +\infty$ (K being a positive constant), therefore that $\lim_{l\to+\infty}(Q_1) = 0$ since $Q_1 = \frac{a\,\Delta\overline{q}}{2\,\sigma_s}$. Thus, $\overline{q_l} = 2\,\sigma_s\,F_1(Q_1)$ drives to:

$$\lim_{l\to+\infty}(\overline{q_l}) = 2\sigma_s F_1(0) \quad \text{i.e.} \quad q_l \sim Cl \text{ as } l \longrightarrow +\infty \tag{48}$$

It was thus shown that when the mixing length tends towards infinity, the cloud liquid water grows towards infinity so that it reaches values higher than q_w.

To solve this problem, it appears essential to limit the occurrence of negative moistures. However, a direct limitation on q_w (to impose $q_w \geq 0$ i.e. $q'_w \leq \overline{q_w}$) is not easy to implement due to the use of variable s, linear combination of the fluctuations of moisture and temperature.

Hence, a condition is imposed not on q_w but on its standard deviation σ_{qw}. It is supposed that specific moisture follows a Gaussian law of the type:

$$G(q_w) = \frac{1}{\sqrt{2\pi}\sigma_{q_w}}\exp\left[-\frac{(q_w - \overline{q_w})^2}{2{\sigma_{q_w}}^2}\right] \tag{49}$$

Thus the limitation of the occurrence of negative specific moistures is carried out by the following inequality:

$$\int_{-\infty}^{0} G(q_w)\,dq_w < \epsilon \quad \text{where } \epsilon \text{ is an arbitrary constant} \tag{50}$$

This inequality is equivalent to:

$$\frac{\overline{q_w}}{\sigma_{q_w}} > A\,, \text{ where } A \text{ is such that } \frac{1}{\sqrt{2\pi}}\int_0^A e^{-t^2/2}\,dt \;=\; \frac{1}{2} - \epsilon \tag{51}$$

It appears that $\epsilon = 0$ and $\epsilon = 1/2$ correspond to $A = +\infty$ and $A = 0$, respectively. To impose the preceding condition on q_w comes to eliminating

the values from Q_1 in the vicinity of 0. Indeed, it is sufficient that the following inequality is met:

$$|Q_1| \; > \; \frac{A \;|\Delta\overline{q}| \; \left|\dfrac{\partial\overline{q_w}}{\partial z}\right|}{\overline{q_w}\left|\dfrac{\partial\overline{q_w}}{\partial z} - \alpha_1\dfrac{\partial\overline{\theta_l}}{\partial z}\right|} \; \equiv \; (Q_1)_{min} \tag{52}$$

Using equation $Q_1\sqrt{\widetilde{S_h}(Q_1)} = TTB$, one can obtain a value $(TTB)_{min}$ from TTB satisfying inequality $\mid TTB \mid > (TTB)_{min}$. Consequently, the equation:

$$TTB = \frac{\Delta\overline{q}}{l\sqrt{B_2}\left|\dfrac{\partial\overline{q_w}}{\partial z} - \alpha_1\dfrac{\partial\overline{\theta_l}}{\partial z}\right|} \Longrightarrow l_{max} = \frac{1}{(TTB)_{min}\sqrt{B_2}} \frac{\Delta\overline{q}}{\left|\dfrac{\partial\overline{q_w}}{\partial z} - \alpha_1\dfrac{\partial\overline{\theta_l}}{\partial z}\right|}$$

allows to determine the maximum value for mixing length, that is to say l_{max}, by taking for TTB its minimal value $(TTB)_{min}$.

The above mentioned algorithm, which aims at limiting the probability of negative moistures, resulted in introducing into the scheme a new adjustable parameter (ϵ or A). A study by Ricard showed that any value of A ranging between 1 and 2 appeared reasonable. In practice, this value is set to STTBMIN ($\sqrt{3}$).

2 Turbulent coefficients in stratosphere

On the model levels where cloudiness is calculated, one uses the above described turbulence scheme to calculate the exchange coefficients for the vertical diffusion (starting from level KTDIAN). At the higher levels, one uses Louis scheme (ACCOEFK). For more details on this parametrization of atmospheric turbulence, see Louis (1979), Louis *et al.* (1982) and Geleyn (1986).

We have:

$$\frac{\partial\psi}{\partial t} = \frac{1}{\rho}\frac{\partial}{\partial z}\left(\rho\, K\, \frac{\partial\psi}{\partial z}\right)$$

where K is the exchange coefficient (m^2/s). One seeks flux F_ψ such as

$$\frac{\partial\psi}{\partial t} = -\,g\,\frac{\partial F_\psi}{\partial p}$$

but as:

$$F_\psi = \frac{\rho\, K\, g\, \Delta\psi}{\Delta\phi}$$

one stores:

$$-KUROV = -\frac{\rho\, K\, g}{\Delta\phi}$$

and one expresses:

$$K = g\, l^2 \mid \frac{\partial \vec{u}}{\partial \phi} \mid f(R_i)$$

The mixing length l takes the value λ_U (ALMAV) for momentum and $\lambda_T = \lambda_U \sqrt{3d/2}$ for energy.

2.1 Stability

Let Ri be the Richardson number:

$$Ri = \frac{g}{c_{pT}} \frac{\frac{\partial s}{\partial z}}{\left\| \frac{\partial \vec{v}}{\partial z} \right\|^2}$$

This number is calculated by taking into account, under the approximation to the first order (with a 15% accuracy):

$$\frac{c_{p_a}}{c_{p_v}} \approx \frac{R_a}{R_v}$$

of the influence of moisture on buoyancy. Thus one "moves" the particles, to compare their level of buoyancy, in the middle (in geopotential) of the layer (see ACHMT in chapter 11). One thus replaces $\Delta s / C_p T$ by:

$$\frac{R_j T_j - R_{j+1} T_{j+1} + \Delta\phi R_a / c_{p_a}}{(R_j T_j + R_{j+1} T_{j+1})/2}$$

As in ACHMT, one can impose an upper limit $(Ri)_{cr}$ on Ri by taking a non-zero value for USURIC $(= 1/(Ri)_{cr})$:

$$\text{if } Ri > 0 \text{ then } Ri \leftarrow \frac{Ri}{1 + Ri/(Ri)_{cr}}$$

One represents atmospheric stability by value ZIS. The atmosphere is stable if $Ri > 0$ and unstable if $Ri < 0$. One calculates the sign of Ri starting from ZSTA$=Ri \cdot \|\Delta\vec{v}\|^2$.

2.2 Calculations for the wind components

One calculates the coefficient of vertical diffusion for wind (PKUROV).

In the stable case:

$$f(R_i) = \frac{1}{1 + 2bR_i/\sqrt{1 + dR_i}}$$

and in the unstable case:

$$f(R_i) = 1 - \frac{2bR_i}{1 + 3bc\left(\frac{1}{\sqrt{27}}\right)\left(\frac{\lambda_T}{z + z_0}\right)^2 \sqrt{\mid R_i \mid}}$$

2.3 Calculations fore temperature and moisture

One calculates the coefficient of vertical diffusion for energy (PKTROV).

In the stable case:

$$f(R_i) = \frac{1}{1 + 3bR_i\sqrt{1 + dR_i}}$$

and in the unstable case:

$$f(R_i) = 1 - \frac{3bR_i}{1 + 3bc\left(\frac{1}{\sqrt{27}}\right)\left(\frac{\lambda_T}{z + z_0}\right)^2 \sqrt{\mid R_i \mid}}$$

2.4 Brunt-Vaïsala frequency

One calculates here the squared Brunt-Vaïsala frequency N divided by g and by density:

$$\left(\frac{N}{\rho g}\right)^2 = \frac{\mathrm{ZSTA}}{(\rho\Delta\phi)^2} = \frac{\mathrm{ZSTA}(\overline{RT})^2}{(p'\Delta\phi)^2}$$

p' is the pressure at half-levels. $\overline{RT}$ is calculated there by simple averaging. The symbolic square of the above formula can be negative in the case of unstable atmosphere.

3 Convective cloudiness

The convective clouds are poorly represented by the above scheme as they correspond to a small fraction of the mesh, but to a large quantity of liquid water. The cloud condensate and corresponding cloud cover are described by diagnostic relations. These relations involve convective fluxes which must thus be saved at the previous time step, since calculations of the convection are carried out after the vertical diffusion, which uses the results of the radiation scheme to perform an implicit temporal discretization. However the calculation of cloudiness must precede the radiation scheme. If LNEBCO is activated, the following calculations are carried out.

Let q_{cc} be the specific cloud moisture (in liquid and solid form); it is written as:

$$q_{cc} = q_{cx} \left[1 - \exp \left(- \frac{\alpha_c \, g \, \dfrac{\partial F_{pc}}{\partial p} \Delta t}{q_{cx}} \right) \right]$$

with

- F_{pc} convective precipitation flux
- Δt time step
- α_c tunable coefficient (QSSUSC).
- q_{cx} maximum specific humidity of the condensate in a model mesh (QSUSX).

One deduces convective cloudiness:

$$n_c = \alpha_{n_c} q_{cc}$$

where n_c convective cloudiness and α_{n_c} adjustable coefficient (QSNEBC).

4 Total cloudiness

If LRNUMX is activated (option LRAY), or if NOVLP$<$ 3 (option LRAYFM), or if NOVLP15$<$ 3 (option LRAYFM15), the two types of condensate and cloudiness (stratiform and convective) are combined by maximum overlap:

$$\begin{aligned} q_c &= \max(q_{cs}, q_{cc}) \\ n &= \max(n_s, n_c) \end{aligned}$$

Otherwise, random overlap is used:

$$\begin{aligned} q_c &= q_{cs} + q_{cc} \\ n &= n_s + (1 - n_s)\, n_c \end{aligned}$$

Then one divides the condensate by cloudiness (limited to XNBMAX), to obtain condensate in the cloud. One obtains a proportion of condensate per unit of cloud mesh (q_c/n_s). Then one makes the partition of q_c/n_s in a liquid part (PQLI) and a solid part (PQICE). One introduces a function of temperature giving the proportion of ice into a cloud cell. The experimental measurements carried out by Matveev (1984) and resumed by Rockel *et al.* (1991) recommend a curve having a complement-Gaussian shape, null for $T = T_t$ and having for width 15 K at e^{-1}.

This function is modeled by postulating that the proportion of ice, at temperature $T < T_t$, is related to the integral of the difference between the saturation functions of liquid and solid water. One thus writes:

$$f(T) = \begin{cases} \dfrac{\displaystyle\int_T^{T_t} e_w(t) - e_i(t)\, dt}{\displaystyle\int_0^{T_t} e_w(t) - e_i(t)\, dt} & \text{if } T < T_t \\ \\ 0 & \text{otherwise} \end{cases}$$

The usable form of this expression is obtained by a Gaussian adjustment:

$$f(T) = \delta_{T_t} \left[1 - \exp \left\{ \frac{-1}{2\Delta T^2} (T - T_t)^2 \right\} \right]$$

where T_t is the temperature the triple point and δ_{T_t} the Heavyside function, being 1 if $T < T_t$, 0 otherwise

One uses for ΔT the the difference between the temperature of triple point and the abscissa of the maximum of $e_w(T) - e_i(T)$, that is to say 11.82 K, which provides a good approximation of the integral. The variable used in the code is RDT (in YOMCST).

The value of $f(T)$ being known, one calculates the liquid/ice partition in the cloud by:

- $q_l = [1 - f(T)]\; q_c$
- $q_i = f(T)\; q_c$

10

Large-scale precipitation

1 Description of the scheme

This scheme results from the statistical precipitation scheme of Smith (1990). It must be associated with the statistical cloud scheme (ACNEBR, see Chapter 9). This scheme has been used in the former versions of ARPEGE-CLIMAT.

Ricard (1992) explained why the first tests of the Kessler-type precipitation scheme (1969), did not give satisfaction when the old cloud scheme ACNEBT were replaced by ACNEBR. The cloud amount was too weak, reaching 30% in global average. The Kessler-type scheme type eliminated any supersaturation at the mesh scale. Coarse tests to allow supersaturation up to 110% showed positive impacts and it was decided to connect the rate of precipitation to the liquid water amount which is calculated by statistical scheme ACNEBR, thanks to Smith (1990) scheme, which itself results from a simplification of the Sundqvist (1978) scheme.

Thus, in ACPLUIS, one takes into account the quantity of condensate (PQLI-S=liquid+solid) and of stratiform cloudiness (PNEBS) in each mesh, both already calculated by statistical scheme ACNEBR. ACPLUIS thus fits in same approach as the statistical cloud generation scheme, in the sense that it includes the concept of sub-grid variance.

The atmosphere is scanned from top to bottom, in the direction of precipitation. These calculations led in a layer cannot be independent of calculations of the directly upper layer, because there is a mass transport. Therefore, there is a necessarily transmission of the information from layer to layer (precipitation flux and proportion of snow).

The random overlap assumption is made here, which supposes that the precipitation flux coming from the upper layer is the same in term of unit of

mesh area as in term of unit saturated (or unsaturated) mesh area. This assumption makes it possible to treat independently the saturated part and the unsaturated part of the mesh, since each one receives the same precipitation flux at the top of the mesh.

It should be noted that in ARPEGE-CLIMAT, the maximum-random overlap assumption is used in ACNEBR to calculate "radiative cloudiness", (for transmission to the radiation scheme).

The parametrization used is mainly that of Smith (1990), however the Kessler (1969) formulation concerning the evaporation of precipitations has been used.

Three processes are involved: precipitation, evaporation and melting or freezing. They are dealt in the next three sections.

2 Precipitation in a cloud layer (Smith)

The Smith (1990) model requires a parametrization of the reduction in cloud water due to precipitations. The conversion rate of cloud water into precipitation depends on the phase of water. One supposes here an abrupt transition between the liquid state and the solid state at the temperature of triple point T_t.

One uses a partition of condensate q_c (PQLIS) in liquid water q_l and solid water q_i

$$f(T) = \delta_{T_t}$$

where T_t is the temperature of triple point and δ_{T_t} Heavyside function , yielding 1 if $T < T_t$, 0 if not.

It should be noted that in the other parts of the code of ARPEGE-CLIMAT one uses a Gaussian and continuous function in the transition from the liquid form to the solid form (with a characteristic width $\Delta T = 11.82\ K$ (RDT) and with a coexistence of the two phases between $T_t - \Delta T$ and T_t).

The value of $f(T)$ being known, one calculates the partition liquid/ice q_c by:

- $q_l = [1 - f(T)]\ q_c$
- $q_i = f(T)\ q_c$

2.1 Liquid phase

The parametrization of the tendency of liquid cloud water due to precipitation is defined as (Smith, 1990):

$$\frac{\partial q_l}{\partial t} = -\left[C_t\left\{1-\exp\left[-\left(\frac{q_l/n_s}{C_w}\right)^2\right]\right\}+C_a F_{P_h}\right] q_l \;=\; -[\,A\,]\,q_l \qquad (1)$$

where

- C_a, C_t and C_w are constants, respectively TCA, TCT and TCW in `namelist`
- n_s is stratiform cloud fraction (PQLIS) and q_l stratiform liquid water
- F_{P_h} is precipitation flux per unit area coming from the upper layer

The exponential factor inhibits the liquid water conversion per unit of cloud mesh q_l/n_s into precipitations, if this one is weak compared to C_w.

2.2 Solid phase

The tendency of cloud solid water (per unit of mesh) due to precipitation is expressed in the following way (Smith, 1990):

$$\frac{\partial q_i}{\partial t} = \left(\frac{F_{P_h}}{\rho\,\Delta z}\right) - \left(\frac{v_f}{\Delta z}\right)\; q_i \;=\; B \;-\; D\,q_i \qquad (2)$$

where

- Δz is layer depth
- v_f = TVF is falling speed for ice/snow. One supposes here that TVF = $1\ m/s$

.

2.3 Precipitation flux at the base of the saturated part of the mesh

In the cloud part, the principle consists in calculating the tendencies of moisture due to the process of condensation in the sub-grid cloud, then to

convert these tendencies into precipitation flux. One can write the formulas (1) and (2) in the form:

$$\begin{cases} \dfrac{\partial q_l}{\partial t} = -A\, q_l & \text{liquid case} \\ \dfrac{\partial q_i}{\partial t} = B - D\, q_i & \text{solid case} \end{cases} \tag{3}$$

where A, B and D are defined in Equations (1) and (2).

In the current version of ACPLUIS, the total value $q_c = q_l + q_i$ intervenes everywhere in Equation (3). One obtains tendencies $(\partial q_c/\partial t)_{(l)} = -A\, q_c$ and $(\partial q_c/\partial t)_{(i)} = B - D\, q_c$ which undergo the later recombination:

$\partial q_c/\partial t = [1 - f(T)]\,(\partial q_c/\partial t)_{(l)} \;+\; [f(T)]\,(\partial q_c/\partial t)_{(i)}$

(see the following sub-section). One should use separately q_l and then q_i in System (3), to obtain directly

$\partial q_l/\partial t = -A\, q_l$ and $\partial q_i/\partial t = B - D\, q_i$

as envisaged in Smith (1990). There would be more simply

$\partial q_c/\partial t = \partial q_l/\partial t + \partial q_i/\partial t.$

The scheme remains consistent as long as it does not make coexist the solid and liquid phases, as it is currently the case in this part of the code which uses Heavyside function $f(T) = \delta_{T_t}$.

For numerical stability reasons, one uses an implicit scheme where the second member of each one of these two equations is taken at time $t + \Delta t$. For example, the first equation of System (3) is written as:

$$\left(\frac{\partial q_l}{\partial t}\right)^{(t)} = -A\,(q_l)^{t+1} = -A\left[(q_l)^t + \Delta t \left(\frac{\partial q_l}{\partial t}\right)^{(t)}\right] \tag{4}$$

One then obtains classically the Smith (1990) equations of moisture tendency in their implicit form:

$$\begin{cases} \dfrac{\partial q_l}{\partial t} = \dfrac{-A\, q_l^t}{1 + A\,\Delta t} \equiv \left(\dfrac{\partial q_c}{\partial t}\right)_{(l)} & \text{liquid case} \\ \dfrac{\partial q_i}{\partial t} = \dfrac{B - D\, q_i^t}{1 + D\,\Delta t} \equiv \left(\dfrac{\partial q_c}{\partial t}\right)_{(i)} & \text{solid case} \end{cases} \tag{5}$$

2.4 Recombination of the total condensation flux

With the above values for function $f(T)$, the total tendencies (solid and liquid) due to the condensation of the Smith (1990) scheme are obtained starting from the combination of the partial tendencies given by System (5):

$$\frac{\partial q_c}{\partial t} = [1 - f(T)] \left(\frac{\partial q_c}{\partial t} \right)_{(l)} + [f(T)] \left(\frac{\partial q_c}{\partial t} \right)_{(i)}$$

The conversion of the moisture tendencies into precipitation flux is given by:

$$\left[\frac{\partial q_n}{\partial t} \right]_{precip} = \frac{g}{\Delta p} \left(F_{P_s} - F_{P_h} \right) \tag{6}$$

where Δp is the layer thickness in pressure (positive).

In the code, the moisture tendencies are positively counted if they contribute to precipitations.

One keeps the total precipitations flux of Smith for the values of q_v which are greater than QSMIN $= 10^{-4}$. For values less than QSMIN, a Kessler (1969) scheme is coded and replaces that of Smith (1990). Consistently, the same threshold QSMIN is used in ACNEBR to put cloudiness at a residual value (10^{-12}) if $q_v <$ QSMIN. The motivation of this threshold is to avoid having too strong cloudiness and precipitation in higher troposphere and polar stratosphere. Elsewhere, for high altitudes, safety relies on a limitation along the vertical which is ensured through maximum levels given in NAMTOPH (where ETNEBU=100 hPa is the highest level for both ACNEBR and ACPLUIS).

3 Evaporation in the unsaturated parts (Kessler)

A precipitation flux falling into an unsaturated zone in the lower layer is reduced at the base of this sub-mesh by evaporation phenomena for which Kessler (1969) proposes the following parametrization:

$$\frac{\partial \sqrt{F_P}}{\partial (1/p)} = E_{vap} (q_w - q) \tag{7}$$

$$\text{where} \qquad E_{vap} = C_{Evap} \cdot [1 - r_{me} (1 - RV)]$$

Here, $C_{Evap} =$ EVAP $= 0.48\, 10^7$ is an empirical coefficient, $RV =$ REVGSL $=$ 80 is the ratio of evaporation speed between snow and liquid water, and r_{me} are the fictitious proportion of snow in precipitations.

By integrating Equation (7) between the top and the base of each layer, one obtains F_{P_c}, precipitation flux, at the base of the layer per unit of area of unsaturated mesh:

$$F_{P_c} = \left[\sqrt{F_{P_h}} - E_{vap}\,(q_w - q)\frac{\Delta p}{p^2}\right]^2 \tag{8}$$

Applying these two processes, namely condensation and evaporation, leads to the knowledge of the precipitation flux at the base of the layer per unit of area of unsaturated mesh (F_{P_c}) and of saturated mesh (F_{P_s}). Obtaining the precipitation flux at the base of the layer per unit of area of mesh (F_{P_b}) is done by:

$$F_{P_b} = n_s F_{P_s} + (1 - n_s) F_{P_c} \tag{9}$$

4 Melting or freezing (Kessler)

In the configuration which consists in taking into account the cryoscopic cycle, the equation governing the phenomenon of snow melt or freezing of liquid water is:

$$\frac{\partial r_f}{\partial\,(1/p)} = F_{melt}\,\frac{T - T_t}{\sqrt{F_P}}, \tag{10}$$

where F_{melt} represents the melting of precipitation:

$$F_{melt} = C_{Fonte} \cdot \left[1 - r_{me}\,(1 - RV)\right]. \tag{11}$$

Here, $C_{Fonte} = \text{FONT} = 0.24\,10^5$, with the same definitions as previously for $RV = \text{REVGSL} = 80$ and for r_{me}.

The component of the snow proportion (r_f) due to melting or freezing of new precipitation results from the integration of Equation (10) between the top and the base of the layer, whose result is:

$$r_f = F_{melt}\frac{T_t - T}{0.5(\sqrt{F_{P_h}} + \sqrt{F_{P_b}})}\,\frac{\Delta p}{p^2} \tag{12}$$

To obtain the actual snow proportion (r_n), one adds to r_f the snow proportion in the precipitation flux (r_g).

The term r_g is calculated from the snow proportion r_n of the upper layer and precipitation flux. It depends on the part of the mesh in which it is calculated: saturated part or unsaturated part.

4.1 Saturated part of the mesh

Two cases arise according to whether one is above or below the triple point:

- If $T > T_t$

There cannot be condensation in solid phase. If vapor condensates, liquid water is formed. Noting r_n the snow fraction in the upper layer and $F_{P_{bc}}$ the precipitation flux at layer base, due only to condensation in the cloudy sub-mesh, the snow fraction produced by precipitation (r_g) is:

$$r_g = r_n \frac{F_{P_h}}{F_{P_{bc}}} \tag{13}$$

- If $T < T_t$

  If there is condensation, snow is formed; r_g is expressed using the equation:

$$r_g = 1 - (1 - r_n) \frac{F_{P_h}}{F_{P_{bc}}} \tag{14}$$

4.2 Unsaturated part of the mesh

The snow proportion due to precipitation does not change in the non-cloudy zone: the evaporation and the sublimation of precipitation are done in the same proportions.

The process of melting or freezing intervenes in the determination of the nature of the precipitation. One obtains stratiform precipitation fluxes in liquid form and solid form by multiplying the precipitation flux at the base of each layer by (1-r_n) and r_n respectively.

One uses here a partition of condensate in rain and/or snow according to a Gaussian and continuous formulation:

$f(T) = \delta_{T_t} \left\{ 1 - \exp \left[-(T - T_t)^2 / (2\,\Delta T^2) \right] \right\}$

One uses for ΔT the difference between the temperature of triple point and the abscissa of the maximum of $e_w(T) - e_i(T)$, *i.e.* $\Delta T = 11.82\ K$, which provides a good approximation of the integral. The variable used in the code for ΔT is noted RDT in YOMCST.

11

Vertical diffusion

1 General comment the scheme

This scheme is associated with the cloud scheme ACNEBR and has been used in the former versions of ARPEGE-CLIMAT. The coupling with SURFEX implies that surface fluxes, radiative properties and surface diagnostics variables are computed inside the SURFEX routines. The parametrization of turbulent fluxes in the surface boundary layer, *i.e.* between the surface and the last level of the model is described in details by Louis (1979), Louis *et al.* (1982), and Geleyn (1988).

2 Equation of the vertical diffusion for a conservative quantity ψ

Variable ψ is used here in the place of the horizontal components of wind (u and v), of specific moisture vapor (q_v) or of dry static energy (s).

$$\text{with :} \quad \left\{ \begin{array}{l} s = c_p T + \phi \quad (\phi : \text{ geopotential}) \\ c_p = c_{p_a} + (c_{p_v} - c_{p_a})\, q_v \end{array} \right.$$

One has:

$$\frac{\partial \psi}{\partial t} = \frac{1}{\rho} \frac{\partial F_\psi}{\partial z} \qquad \text{with} \qquad \left\{ \begin{array}{l} F_\psi = -\overline{\rho \psi' w'} \ : \text{ flux oriented downwards} \\ w \ : \text{ vertical velocity} \end{array} \right.$$

Taking into account the hydrostatic relation ($\partial w / \partial z = 0$), the vertical balance of the atmosphere is written as:

$$dp = -\rho g dz = -\rho d\phi$$

One thus obtains:

$$\frac{\partial \psi}{\partial t} = -g \frac{\partial F_\psi}{\partial p}$$

3 Parametrization

3.1 Parametrization in the free atmosphere

Let:

$$F_\psi = \rho g K \frac{\Delta \psi}{\Delta \phi} = \acute{K} \Delta \psi$$

$$\text{with} \quad \begin{cases} K \ : \ \text{turbulent exchange coefficient (in } m^2 s^{-1}) \\ \acute{K} \ : \ \text{computed coefficient (see ACNEBR)} \end{cases}$$

3.2 Parametrization at ground level

All details are given in the SURFEX Scientific Documentation.

4 Algorithm of flux calculation

The implicit coupling of the atmosphere model with SURFEX implies the computation, by the atmosphere model, of the coefficients for vertical turbulent diffusion from the top to the last but one layer for : momentum, dry static enrgy, potential temperature, specific humidity (including a negative humidity correction), liquid and solid water (ACDIFV1).
The atmosphere calls the surface model (ARO_GROUND_PARAM). SURFEX will use atmospheric variables from the lowest atmospheric layer :

- air temperature
- specfic humidity
- wind components
- pressure
- surface pressure
- CO2 concentration

- dry air density
- height of model interlayers
- orography of atmospheric model
- cosine of zenithal angle at t
- cosine of zenithal angle at t+1
- liquid precipitation surface flux
- snow precipitation surface flux
- graupel precipitation surface flux

to compute the surface fluxes and variables.

The surface model send back to the atmosphere :

- surface flux of potential temperature
- surface flux of water vapor
- surface flux of scalar or flux of chemical variables
- surface flux of CO2
- surface fluxes of horizontal momentum
- direct albedo for each spectral band
- diffuse albedo for each spectral band
- surface emissivity
- surface radiative temperature

Then, the atmosphere model procedes with the computation of the vertical turbulent diffusion by back substitution, vertical turbulent fluxes, and thermal radiation fluxes correction (ACDIFV2).

4.1 Flux of momentum:F_u and F_v

Let ψ_i be u_i or v_i. One has then:

$$\psi_i^+ - \psi_i^- = \psi_i^{t+\Delta t} - \psi_i^{t-\Delta t} = -g\frac{\Delta t}{\delta p_i}[F_{\psi_i} - F_{\psi_{i-1}}]$$

$$\Longleftrightarrow \psi_i^+ - \psi_i^- = -g\frac{\Delta t}{\delta p_i}[\acute{K}_i(\psi_i^+ - \psi_{i+1}^+) - \acute{K}_{i-1}(\psi_{i-1}^+ - \psi_i^+)]$$

This equation is written in matrix form ($w_{i,j} = g\acute{K}_i\Delta t/\delta p_j$) and ($x_N = g\acute{C}_d\Delta t/\delta p_N$):

$$\mathcal{M} \quad \begin{pmatrix} \psi_1^+ \\ \psi_2^+ \\ . \\ \psi_{N-1}^+ \\ \psi_N^+ \end{pmatrix} = \begin{pmatrix} \psi_1^- \\ \psi_2^- \\ . \\ \psi_{N-1}^- \\ \psi_N^- + \psi_s x_s \end{pmatrix}$$

where $\mathcal{M}$ is the matrix:

$$\begin{pmatrix} 1+w_{1,1} & -w_{1,1} & & & (0) \\ -w_{1,2} & 1+w_{1,2}+w_{2,2} & -w_{2,2} & & \\ & . & . & . & \\ & & . & . & -w_{N-1,N-1} \\ (0) & & & -w_{N-1,N} & 1+w_{N-1,N}+x_N \end{pmatrix}$$

The surface conditions impose that $\vec{v}_s = (u_s, v_s) = \vec{0}$ thus $\psi_s x_s = 0$ One uses the method of Gauss to solve this system. The variables then are considered: ZELIM to indicate the element sub-diagonal by which it is necessary to multiply the preceding line in order to eliminate it by subtraction, ZMUL to indicate the multiplicative factor intended to put the diagonal at 1. A system is then obtained of the type:

$$\begin{pmatrix} 1 & a_{1,2} & & & (0) \\ & 1 & a_{2,3} & & \\ & & . & . & \\ & & & 1 & a_{N-1,N} \\ (0) & & & & 1 \end{pmatrix}$$

By going up the values of ψ_N^+ with ψ_1^+, one deduces from this system atmospheric fluxes in the form: $w_{k,l}\Delta\psi_{i,i+1}^+$ and surface flux: $\rho C_d \|\vec{v}\| \vec{v}_N^+$.

4.2 Flux of heat F_{q_v} and F_s

Let ψ_i be s_i or q_{vi}. One has in the same way:

$$\psi_i^+ - \psi_i^- = -g\frac{\Delta t}{\delta p_i}[\acute{K}_i(\psi_i^+ - \psi_{i+1}^+) - \acute{K}_{i-1}(\psi_{i-1}^+ - \psi_i^+)]$$

But the equation of evolution of T_s is written as:

$$\frac{\partial T_s}{\partial t} = C_s(\sum F_{energy}) + \frac{2\pi}{\tau_1}(T_p - T_s)$$

It couples through the latent heat flux the evolutions of s_N, T_s and q_{vN}. One thus will simultaneously solve the 2 implicit systems by adding to them a linearized equation for T_s:

$$\begin{aligned}\frac{\partial T_s}{\partial t} &= \frac{2\pi}{\tau_1}(T_p - T_s^+) + C_s\{\varepsilon(F^T - \sigma T_s^4) + F^S(1-\alpha) \\ &- \rho C_h \|\vec{v}\| \{[c_{p_a} + (c_{p_v} - c_{p_a})(HUq_{sat}(T_s) + HQq_{vN})]T_s \\ &+ \phi_s - (c_p T + \phi)_N^+ \\ &+ [L_{T=0} + (c_{p_a} - C_w)T_s][HUq_{sat}(T_s) + (HQ-1)q_{vN}^+]\}\}\end{aligned}$$

By considering the following relations of linearization:

$$\begin{cases} \sigma {T_s^+}^4 = \sigma {T_s^-}^4 + 4\sigma {T_s^-}^3(T_s^+ - T_s^-) \\ \\ q_{sat}(T_s^+) = q_{sat}(T_s^-) + \dfrac{\partial q_{sat}}{\partial T_s^-}(T_s^+ - T_s^-) \end{cases}$$

and by removing terms $(T_s^+ - T_s^-)$ of the second order, one obtains:

$$\begin{aligned} {T_s^+}\Big[1 + \frac{2\pi\Delta t}{\tau_1} + C_s\Delta t\{4\varepsilon\sigma {T_s^-}^3 + \rho C_h \|\vec{v}\| ({c_{p_s}}^- \\ + {L_s}^- HU\frac{\partial q_{sat}}{\partial {T_s}^-} + (c_{p_a} - C_w)({q_{vs}}^- - {q_{vN}}^-))\}\Big] \quad = \\ T_s^- + \frac{2\pi\Delta t}{\tau_1}T_p + C_s\Delta t\Big[\varepsilon F^T + F^S(1-\alpha) + 3\varepsilon\sigma(T_s^-)^4 \\ +\rho\, C_h \|\vec{v}\| \left\{(\phi + c_p T)_N^+ - \phi_s + L_s^- HU(T_s^- \frac{\partial q_{sat}}{\partial T_s^-} - q_{sat}T_s^-)\right\} \\ +T_s^- \left\{(c_{p_a} - C_w)(q_{vs}^- - q_{vN}^-) + (c_{p_v} - c_{p_a})q_{vs}^-\right\} \\ + \left\{L_s^-(1-HQ) - (c_{p_v} - c_{p_a})T_s^-\right\} q_{vN}^+\Big] \end{aligned} \tag{1}$$

Remark: in Equation (1), in contradiction with the principle of linearization, one considers first term $HQ\, q_{vN}$ only in index $^-$, in order to obtain a perfectly tri-diagonal matrix (see term 0_* in matrix $\mathcal{A}$ below).

These equations are written in matrix form:

$$\mathcal{N} \begin{pmatrix} s_1^+ \\ s_2^+ \\ . \\ s_N^+ \\ T_s^+ \\ q_{vN}^+ \\ . \\ q_{v2}^+ \\ q_{v1}^+ \end{pmatrix} = \begin{pmatrix} s_1^- \\ s_2^- \\ . \\ \\ \mathcal{B} \\ \\ \\ . \\ q_{v2}^- \\ q_{v1}^- \end{pmatrix}$$

where $\mathcal{N}$ is the matrix:

$$\begin{pmatrix} 1+w_{1,1} & -w_{1,1} & & & & & & (0) \\ -w_{1,2} & 1+w_{1,2}+w_{2,2} & -w_{2,2} & & & & & \\ & . & . & . & & & & \\ & & \lceil & & \rceil & & & \\ & & & \mathcal{A} & & & & \\ & & \lfloor & & \rfloor & & & \\ & & & & . & . & . & \\ & & & & . & . & -w_{1,2} & \\ (0) & & & & & -w_{1,1} & 1+w_{1,1} & \end{pmatrix}$$

where central matrix $\mathcal{A}$ is in the form:

$$\begin{pmatrix} -w_{N-1,N} & \mathcal{A}_1^2 & -w_{N,N}CTVS & 0_* & 0 \\ 0 & -CSVT & 1+CTVT & -CQVT & 0 \\ 0 & 0 & -w_{N,N}CTVQ & \mathcal{A}_3^4 & -w_{N-1,N} \end{pmatrix}$$

with $\mathcal{A}_1^2 = 1 + w_{N-1,N} + w_{N,N}$ and $\mathcal{A}_3^4 = 1 + w_{N-1,N} + w_{N,N}CQVQ$, and central vector $\mathcal{B}$ in the form:

$$\begin{pmatrix} s_N^- + w_{N,N}RHSS \\ T_s^- + RHST \\ q_{vN}^- + w_{N,N}RHSQ \end{pmatrix}$$

Note: one uses the elimination method of the preceding paragraph, but with $2N+1$ lines. Terms $CTVS$ with $RHSQ$ are obtained by formal identification with the complex expression of Equation (1) and the formation of surface fluxes computed by SURFEX.

5 Parametrization of planetary boundary layer depth

Subroutine ACPBLH calculates the height of the planetary mixing layer according to surface fluxes and of the vertical stability of the air column. This pseudo-historical variable is used in the formulation of the vertical profile of mixing length (see Chapter 9). For more details on this parametrization, see Troen and Mahrt (1986).

This parametrization is activated if LNEBCO and LNEBR are `.T.`, and if AHCLPV is equal to zero.

If AHCLPV>0, the parametrization is not taken into account and the mixing layer depth takes exactly the value of AHCLPV. There is thus no variation in time and space of this parameter.

If AHCLPV$=0$, the the mixing layer depth becomes a pseudo-historical variable of the model. This variable is given according to the variation of the Richardson number for mass $\mathcal{R}_i$ (*bulk number*) to a critical value $\mathcal{R}_c$.

$$\mathcal{R}_i(j) = \frac{(\theta_v(j) - \theta_s)}{\theta_{vs}|\vec{v}(j)|^2}\, g\, Z_j$$

with
$$\begin{cases} \theta_v & : \text{potential virtual temperature} \\ |\vec{v}| & : \text{wind modulus} \\ Z_j & : \text{height of level } j \\ s & : \text{index for surface value} \end{cases}$$

$\mathcal{R}_i$ is diagnosed between each level of the model, (sub-scripted j in the equation) and surface.

Let j and $j-1$ be the two levels such as:

$$\mathcal{R}_i(j) < \mathcal{R}_c$$

$$\mathcal{R}_i(j-1) > \mathcal{R}_c$$

h, the top of the mixing layer satisfies:

$$\mathcal{R}_i(h) = \mathcal{R}_c$$

By supposing that $\mathcal{R}_i$ varies linearly between these two levels, one deduces h as the linear interpolation between j and $j-1$.

The recommended value for $\mathcal{R}_c$ generally lies between 0.25 and 0.5. This makes it possible to take into account the inertia and the particle entrainment.

The value of θ_{vN} is preferred to that of T_o used in the simplified theories, in agreement with Holtslag and Boville (1993).

θ_s represents the temperature of the air near surface.

In the stable cases, *i.e.* if the average value of surface turbulent flux $\overline{(w'\theta'_v)}_s < 0$, one gets:

$$\theta_s = \theta_{vs}$$

In the unstable cases, if $\overline{(w'\theta'_v)}_s > 0$, the kinematic heat flux of the low layers is taken into account, θ_s is corrected by θ_T, heat flux resulting from convective thermals.

$$\theta_s = \theta_{vs} + \theta_T$$

$$\theta_T = C\frac{\overline{(w'\theta'_v)_s}}{w_m}$$

$$\text{with} \quad \begin{cases} C & : \text{empirical dimensionless constant (8.5)} \\ \overline{(w'\theta'_v)_s} & : \text{surface virtual heat flux} \\ w_m & : \text{scale of turbulent speed} \end{cases}$$

$$\overline{(w'\theta'_v)_s} = \overline{(w'\theta')_s} + 0.608 \cdot \theta_{vs}\overline{(w'q')_s}$$

$$\overline{(w'\theta'_v)_s} = -(\frac{1}{\rho_s C_p}F_{sens} + \text{RETV} \cdot \theta_{vs}\frac{1}{\rho_s L}F_{lat})$$

F_{sens} and F_{lat} are respectively the surface sensible and latent heat fluxes (calculated by SURFEX and sent back to the atmosphere). w_m is a function of friction speed and of convective speed scale:

$$w_m = ({u*}^3 + c\,{w*}^3)^{\frac{1}{3}}$$

$$\begin{cases} w* & = (\frac{g}{\theta_{vs}}\overline{(w'\theta'_v)}_s h*)^{\frac{1}{3}} \\ u* & = [\overline{(w'u')}_s^2 + \overline{(w'v')}_s^2]^{\frac{1}{4}} \\ u* & = [(\frac{Fu_s}{\rho_s})^2 + (\frac{Fv_s}{\rho_s})^2]^{\frac{1}{4}} \end{cases}$$

c is an empirical dimensionless constant of 0.6 (Dyer, 1974, Troen and Mahrt, 1986). Fu and Fv are turbulent fluxes of momentum calculated by ARO_GROUND_PARAM (interface to call SURFEX) . Instead of an implicit system for the calculation of h in the equation of $w*$, one uses $h*$ as an approximation to h. $h*$ is the value of h calculated at previous time step.

6 Additional surface parameters

Subroutine ACHMTLS, calculated the surface density (PGWDCS) and Brunt-Vaïsala frequency N_s for use in the gravity wave drag parameterization .

$PGWDCS = \frac{p_s}{RT}$

One calculates, as in ACNEBR but for the surface, the Brunt-Vaïsala frequency N_s divided by g and the density:

$$\left(\frac{N_s}{\rho g}\right)^2 = \frac{\text{ZSTA}}{(\rho\Delta\phi)^2} = \frac{\text{ZSTA}(\overline{RT})^2}{(p_s\Delta\phi)^2}$$

$ZSTA = approximation\, of\, \Delta\phi * \Delta \ln\theta$

p_s being pressure of surface (uncentered calculation). The symbolic square of the above formula can be negative in case of unstable atmosphere.

12

Convection

1 Principle of the convection scheme

The scheme used has been described by Bougeault (1985) and further developed in successive cycles of ARPEGE. The version described here corresponds to the parametrization used in the former versions of ARPEGE-CLIMAT.

The deep convection occurs under two conditions: a convergence of humidity at low layers is required and the vertical temperature profile must be unstable. The convection adjusts the unstable profile to a cloudy profile, which is assumed to be moist adiabatic.

The scheme uses the mass-flux concept where the vertical ascent in the cloud ($\omega^* = -M_c$, where M_c is the mass-flux) is compensated by a large-scale subsidence.

A Kuo-type closure is assumed where the available moisture is either precipitated or recycled into the environment by the detrainment term.

The scheme equations are written as :

$$\begin{cases} \left(\frac{\partial u}{\partial t}\right)^{conv} = \omega^* \frac{\partial u}{\partial p} + K\left(u_c - u\right) \\ \left(\frac{\partial v}{\partial t}\right)^{conv} = \omega^* \frac{\partial v}{\partial p} + K\left(v_c - v\right) \\ \left(\frac{\partial s}{\partial t}\right)^{conv} = \omega^* \frac{\partial s}{\partial p} + K\left(s_c - s\right) + g\frac{\partial F_s^{dif}}{\partial p} \\ \left(\frac{\partial q}{\partial t}\right)^{conv} = \omega^* \frac{\partial q}{\partial p} + K\left(q_c - q\right) + g\frac{\partial F_q^{dif}}{\partial p} \end{cases}$$

where K is a relaxation coefficient (to be determined). The index c represents the cloud profile.

As the convection includes vertical diffusion effects of temperature and moisture, the diffusive fluxes F_s^{dif} and F_q^{dif} are subtracted from the equations for dry static energy and moisture to avoid double counting.

The mass-flux $-\omega^*$ is due to buoyancy which causes a conversion between moist static and kinetic energy: ω^* is thus proportional to the square root of the difference between the moist static energy inside and outside the cloud. The proportionality factor α is obtained by the Kuo-type closure assumption: the available humidity is the sum of the large-scale advection and the humidity tendency produced by the vertical diffusion; it must be equal to the sum of convective precipitation and detrainment:

$$\int_{p_t}^{p_b} \left(-\omega \frac{\partial q}{\partial p} - u \nabla q - g \frac{\partial F_q^{dif}}{\partial p} \right) \frac{dp}{g} =$$
$$\int_{p_t}^{p_b} \left(- \left(\frac{\partial q}{\partial t} \right)^{conv} + K \left(q_c - q \right) + g \frac{\partial F_q^{dif}}{\partial p} \right) \frac{dp}{g}$$

where p_b is the pressure at the bottom of the cloud, p_t at the top. Thus, one obtains :

$$\alpha = \frac{\displaystyle\int_{p_t}^{p_b} \left(-\omega \frac{\partial q}{\partial p} - u \nabla q \right) \frac{dp}{g} + F_q^{dif}\left(p_t\right) - F_q^{dif}\left(p_b\right)}{\displaystyle\int_{p_t}^{p_b} -\sqrt{\frac{p}{T}(h_c - h)}\, \frac{\partial q}{\partial p} \frac{dp}{g}}$$

The factor K is then deduced from the moist static energy conservation between the top and the bottom of the cloud. The wind components u_c and v_c in the cloud are calculated considering entrainment effect of surrounding air, horizontal pressure gradient between cloud and surrounding air, and momentum conservation in the convective column.

2 Preliminary calculations

2.1 Initialization of the convergence of moisture

Moisture available for the convection is calculated by subroutine APLPAR in the form of tendency $\left(\frac{\partial q}{\partial t} \right)_{HDC}$ (PCVGQ):

$$\left(\frac{\partial q}{\partial t} \right)_{HDC} = -r \left((\vec{v} \cdot \vec{\nabla}) q + \omega \frac{\partial q}{\partial p} \right) - g \frac{\partial F_q^{dif\_tur}}{\partial p}$$

Term $\left(-g\frac{\partial F_q^{dif\_tur}}{\partial p}\right)$ is provided by the vertical diffusion scheme.

Term $\left((\vec{v}\cdot\vec{\nabla})q+\omega\frac{\partial q}{\partial p}\right)$ is provided to APLPAR by the dynamics of the model; taking into account the fact that the convection scheme provides only the part of precipitation corresponding to the ascents unresolved by the model dynamics, the convective effects should decrease as resolution increases. One tries to represent this effect by a reduction of moisture convergence. Coefficient r reducing convergence has as an expression:

$$r=\frac{1}{1+T_{le}/T_c}$$

with T_{le} equivalent local spectral truncation of the model and critical T_c truncation: T_c corresponds to the truncation beyond which a part of the convective phenomena becomes resolved by dynamics. In APLPAR, the above expression involves the geometry of ARPEGE: $r=1/(1+\chi f_e)$ with χ (TEQK) ratio of a critical mesh size REFLKUO by the unstretched mesh size and f_e (PGM) scale factor.

2.2 Wet-bulb thermometer calculation

Calculation the temperature of the wet-bulb thermometer and corresponding moisture is carried out in subroutine ACTQSAT. One starts from an origin state defined by $(T_0, q_{v\,0})$ and one seeks a final state defined by $(T_f, q_{v\,f})$ with $q_{v\,f}=q_{sat}(T_f,p)$ such as the transformation is done at constant energy and pressure. In the presence of snow (index ZDELTA=1), calculations are modified: it is then necessary to replace the terms in $c_{p_v}-C_w$ by terms in $c_{p_v}-C_i$ which intervene *inter alia* in the calculation of the latent heat, q_s and $\partial q_s/\partial t$.

$$c_p dT+L dq_v=0 \qquad \text{with} \qquad \begin{cases} c_p=c_{p\,0}+(c_{p_v}-C_w)(q_v-q_{v\,0}) \\ L=L_0+(c_{p_v}-C_w)(T-T_0) \end{cases}$$

hence:

$$c_p\frac{dL}{c_{p_v}-C_w}+L\frac{dc_p}{c_{p_v}-C_w}=0 \quad \Rightarrow \quad Lc_p=\text{constant}=L_0\,c_{p\,0}$$

which can take the two following forms:

$$c_{p\,0}(T_f-T_0)+L_f(q_{v\,f}-q_{v\,0})=0$$

$$\text{or} \quad c_{p\,f}(T_f-T_0)+L_0(q_{v\,f}-q_{v\,0})=0 \qquad \text{indifferently}$$

q_s not being linear in T, one uses a Newton algorithm with linearization in the vicinity of the result of the preceding iteration:

$$q_{v\,i+1} = q_{sat}(T_i) + \frac{\partial q_{sat}}{\partial T_i}(T_{i+1} - T_i)$$

which combines with:

$$c_{p\,0}(T_{i+1} - T_0) + L_{i+1}(q_{v\,i+1} - q_{v\,0}) = 0$$

to give:

$$c_{p\,0}[(T_{i+1} - T_i) + (T_i - T_0)] + [L_0 + (c_{p_v} - C_w)((T_{i+1} - T_i) + (T_i - T_0))] \times \left[(q_{sat}(T_i) - q_{v\,0}) + \frac{\partial q_{sat}}{\partial T_i}(T_{i+1} - T_i)\right] = 0$$

One neglects the square terms in $T_{i+1} - T_i$ to have the linearized solution:

$$[c_{p\,0}(T_i - T_0) + L_i(q_{sat}(T_i) - q_{v\,0})] + (T_{i+1} - T_i)\left[c_{p_0} + (c_{p_v} - C_w)(q_{sat}(T_i) - q_{v\,0}) + L_i\frac{\partial q_{sat}}{\partial T_i}\right] = 0 \quad (1)$$

One defines $q_{v\,i}$ by:

$$c_p(T_i - T_0) + L_i(q_{v\,i} - q_{v\,0}) = 0 \quad (2)$$

and thus $q_{v\,i+1}$ by:

$$c_p(T_{i+1} - T_i) + L_{i+1}(q_{v\,i+1} - q_{v\,i}) = 0 \quad (3)$$

or:

$$c_{p\,i+1}(T_{i+1} - T_i) + L_i(q_{v\,i+1} - q_{v\,i}) = 0 \quad (4)$$

The combination of Equations (1), (2) and (3) gives:

$$L_i(q_{sat}(T_i) - q_{v\,i}) \quad +$$

$$(T_{i+1} - T_i)\left[c_{p\,i} + (c_{p_v} - C_w)(q_{sat}(T_i) - q_{v\,i}) + L_i\frac{\partial q_{sat}}{\partial T_i}\right] = 0$$

$$\Rightarrow \qquad L_{i+1}(q_{sat}(T_i) - q_{v\,i}) + (T_{i+1} - T_i)[c_{p\,i} + L_i\frac{\partial q_{sat}}{\partial T_i}] = 0$$

$$\Rightarrow \qquad (q_{sat}(T_i) - q_{v\,i}) = (q_{v\,i+1} - q_{vi})[1 + \frac{L_i}{c_{p\,i}} \frac{\partial q_{sat}}{\partial T_i}] \tag{5}$$

One uses Equations (4) and (5) to build the algorithm:

$$q_{v\,i+1} - q_{v\,i} = (q_{sat}(T_i) - q_{v\,i})/(1 + \frac{L_i}{c_{p\,i}} \frac{\partial q_{sat}}{\partial T_i})$$

$$c_{p\,i+1} = c_{p\,i} + (c_{p_v} - C_w)(q_{v\,i+1} - q_{v\,i})$$

$$T_{i+1} - T_i = -\frac{L_i}{c_{p\,i+1}}(q_{v\,i+1} - q_{vi})$$

$$L_{i+1} = L_i + (c_{p_v} - C_w)(T_{i+1} - T_i)$$

$$(L/c_p) = (L_0/c_{p\,i+1})$$

with as first guess $(T_0, q_{v\,0})$. The algorithm converges towards (T_w, q_w) after NBITER iterations (a number fixed at the beginning). At the time of the first iteration one stores in PQSAT value $q_{sat}(T_0)$.

Relative humidity H_r is calculated by:

$$H_r = \frac{q(1 + (R_v/R_a - 1)q_s)}{q_s(1 + (R_v/R_a - 1)q)}$$

3 Elements of the convection scheme

3.1 Determination of the profile of (s_n, q_n)

(s_n, q_n) is determined: the cloudy ascent is defined as the pseudo-adiabatic resulting from "blue" point T_w of a level, involving environmental air; the calculation of values (T_n, q_n) is carried out by the process:

1. Calculation of "blue" point T_w: full calculation is described below.
2. Construction of the wet pseudo-adiabatic up to the next level, while considering entrainment of environmental air; the taking into account of entrainment of environmental air is done through a relaxation of the cloudy variables towards the environmental ones at a rate λ:

$$\frac{\partial \mu_n}{\partial \phi} = \lambda(\mu - \mu_n)$$

with $\mu = T$, q or ℓ; the omission of entrainment would over-estimate the altitude of the top of the clouds. Rate λ varies with altitude, with two possible formulations: λ is λ_x at the base of the cloud; it tends towards λ_n to the top; the rate of decrease of λ is taken arbitrarily equal to $\lambda_x^{3/4}\lambda_n^{1/4}$ which represents an average value of λ:

$$\lambda = \lambda_n + (\lambda_x - \lambda_n)\, e^{-\lambda_x^{3/4}\lambda_n^{1/4}(\phi-\phi_b)}$$

or:

$$\lambda = \frac{C_\lambda}{\min(z, z_{clp})}$$

with C_λ a constant and z_{clp} the planetary boundary layer depth.

3. Liquid lift in the cloud: in order to take into account the reduction of cloudy instability due to the presence of liquid water, one diagnoses a specific quantity of liquid water ℓ_n intervening later on in the calculation of instability below, then in calculation of cloud mass flux.

   ℓ_n is diagnosed by:

   $$\frac{\partial(q_n + \ell_n)}{\partial\phi} = -\frac{\ell_n}{\phi_0}$$

   This equation yields weak ℓ_n in clouds with low geopotential thickness. ϕ_0 is a constant corresponding to critical thickness of precipitating clouds.

4. Test of convective activity of the level: a level is declared convective if cloudy buoyancy and total moisture available are both positive.

5. Comparison of the temperature of the cloud to that of the environment; if it is lower than that of the environment one takes the blue point of the level to continue the ascent. If not, one continues with the properties of the current cloud.

3.2 Algorithm of the reversible saturated adiabatic

One seeks here to determine the final temperature of a particle rising from a bottom level defined by (T_b, q_b, p_b) to reach a level defined by (T_s, q_h, p_h), with conservation of wet static energy (p_b and p_h are constants of calculation and $q_h = q_s(T_s, p_h)$).

Differential equation

$$c_p dT + Ldq + d\phi = 0 \quad \text{with:} \quad \begin{array}{l} c_p = c_{p_b} + (c_{p_v} - c_{w/i})(q - q_b) \\ L = L_b + (c_{p_v} - c_{w/i})(T - T_b) \end{array}$$

This differential equation is also written:

$$c_p \frac{dL}{c_{pv} - c_{w/i}} + L \frac{dc_p}{c_{pv} - c_{w/i}} + d\phi = 0$$

posing $\phi_b = 0$ arbitrarily (and thus $\phi_h = \Delta\phi$):

$$Lc_p + (c_{p_v} - c_{w/i})\phi = \text{Cte} = L_b c_{pb}$$

One thus has:

$$\frac{L_b c_{pb}}{c_{p_v} - c_{w/i}} + \phi_b = \frac{L_h c_{ph}}{c_{p_v} - c_{w/i}} + \phi_h$$

and the exact integral of b with h take indifferently one of the two following forms:

$$c_{pb}(T_s - T_b) + L_h(q_h - q_b) + \Delta\phi = 0 \tag{6}$$

$$c_{ph}(T_s - T_b) + L_b(q_h - q_b) + \Delta\phi = 0 \tag{7}$$

Geopotential calculation

For $\Delta\phi$, if one knew the $(\Delta \ln p)^b$ and $(\Delta \ln p)^h$ having been used for calculation of the environment:

$$(\Delta \ln p)^b = \ln \frac{p_b}{p_i}$$

$$\Delta \ln p)^h = \ln \frac{p_i}{p_h}$$

one would have then:

$$\Delta\phi = R_b T_b (\Delta \ln p)^b + R_h T_s \Delta \ln p)^h$$

$$= R_b T_b (\Delta \ln p)^b + [R_b + R_v(q_h - q_b)]\, T_s (\Delta \ln p)^h$$

that one writes:

$$= \tilde{R}_b^- T_b + \tilde{R}_b^+ T_s + \tilde{R}_v^+ T_s (q_h - q_b)$$

$\tilde{R}_b^-$, $\tilde{R}_b^+$ and $\tilde{R}_v^+$ being variables independent of later calculation of q_h and T_s.

Linearized equation $h = i + 1$

q_s being nonlinear in T, one will calculate the solution by a Newton algorithm with linearization about the previous iteration:

$$q_{i+1} = q_s(T_i) + \frac{\partial q_s}{\partial T_i}(T_{i+1} - T_i)$$

which one combines with:

$$c_{pb}(T_s - T_b) + L_h(q_h - q_b) + \tilde{R}_b^- T_b + \tilde{R}_b^+ T_s + \tilde{R}_v^+ T_s(q_h - q_b) = 0$$

where subscript h is replaced by $i + 1$ for temperature, to obtain:

$$\tilde{R}_b^- T_b + \tilde{R}_b^+ T_i + \tilde{R}_b^+ (T_{i+1} - T_i) + c_{pb}\left[(T_{i+1} - T_i) - (T_i - T_b)\right]$$

$$+ \left[L_b + \tilde{R}_v^+ T_b + (c_{pv} - c_{w/i} + \tilde{R}_v^+)\left[(T_{i+1} - T_i) - (T_i - T_b)\right]\right]$$

$$\left[q_s(T_i) - q_b + \frac{\partial q_s}{\partial T_i}(T_{i+1} - T_i)\right] \quad = \quad 0$$

One neglects the square terms in $(T_{i+1} - T_i)$ to obtain the linearized equation:

$$\tilde{R}_b^- T_b + \tilde{R}_b^+ T_i + c_{pb}(T_i - T_b) + (L_i + \tilde{R}_v^+ T_i)(q_s(T_i) - q_b)$$

$$+(T_{i+1} - T_i)\left[c_{pb} + (c_{pv} - c_{w/i} + \tilde{R}_v^+)(q_s(T_i) - q_b)\right.$$

$$\left.+(L_i + \tilde{R}_v^+ T_i)\frac{\partial q_s}{\partial T_i} + \tilde{R}_b^+\right] \quad = \quad 0 \tag{8}$$

Equation $h = i$

Starting from:

$$c_{pb}(T_i - T_b) + L_i(q_i - q_b) + \phi_i - \phi_b = 0$$

one gets:

$$c_{pb}(T_i - T_b) + L_i(q_i - q_b) + \tilde{R}_b^- T_b + \tilde{R}_b^+ T_i + \tilde{R}_v^+ T_i(q_i - q_b) = 0$$

and:

$$(\tilde{R}_b^+ + c_{pb})(T_i - T_b) + \left[\tilde{R}_v^+ T_b + L_i + \tilde{R}_v^+(T_i - T_b)\right](q_i - q_b)$$

$$+ \left[\tilde{R}_v^+ T_b + L_i + \tilde{R}_v^+(T_i - T_b)\right](q_i - q_b) + (\tilde{R}_v^+ + \tilde{R}_b^-)T_b \quad = \quad 0$$

One poses:

$$\tilde{c}_p = \tilde{R}_b^+ + c_p + \tilde{R}_v^+(q - q_b) \tag{9}$$

$$\tilde{L} = \tilde{R}_v^+ T_b + L + \tilde{R}_v^+(T - T_b) \tag{10}$$

Note: we have still:

$$\frac{\partial \tilde{c}_p}{\partial q} = \frac{\partial \tilde{L}}{\partial q} \qquad (= c_{pv} - c_{w/i} + \tilde{R}_v^+) \tag{11}$$

It comes:

$$\tilde{c}_{pb}(T_i - T_b) + \tilde{L}_i(q_i - q_b) + (\tilde{R}_b^+ + \tilde{R}_b^-)T_b = 0 \tag{12}$$

and:

$$\tilde{c}_{pb}(T_{i+1} - T_b) + \tilde{L}_{i+1}(q_{i+1} - q_b) + (\tilde{R}_b^+ + \tilde{R}_b^-)T_b = 0 \tag{13}$$

Subtracting (13) − (12) gives:

$$\tilde{c}_{pi}(T_{i+1} - T_i) + L_{i+1}(q_{i+1} - q_i) = 0 \tag{14}$$

which, according to (6) and (7), can be also written as:

$$\tilde{c}_{p(i+1)}(T_{i+1} - T_i) + L_i(q_{i+1} - q_i) = 0 \tag{15}$$

Equation (12) with $b = i$ leads to:

$$\tilde{R}_b^+ + \tilde{R}_b^- = 0 \tag{16}$$

Equation (8) with $b = i$ and Equation (16) leads to:

$$\tilde{L}_i(q_s(T_i) - q_i) + (T_{i+1} - T_i)\left[\tilde{c}_{pi}\right.$$

$$+(c_{pv}-c_{w/i}+\tilde{R}_v^+)(q_s(T_i)-q_i)+\tilde{L}_i\frac{\partial q_s}{\partial T_i}\Big] \quad = \quad 0$$

using Equation (10) with $b=i$ on level $i+1$:

$$\tilde{L}_{i+1}(q_s(T_i)-q_i)+(T_{i+1}-T_i)\left[\tilde{c}_{pi}+\tilde{L}_i\frac{\partial q_s}{\partial T_i}\right]=0$$

and with Equation (14):

$$q_s(T_i)-q_i=(q_{i+1}-q_i)\left[1+\frac{\tilde{L}_i}{\tilde{c}_{pi}}\frac{\partial q_s}{\partial T_i}\right] \tag{17}$$

Newton algorithm

One uses Equations (17), (15) and (11) to build the algorithm:

$$\begin{aligned}
q_{i+1}-q_i &= \frac{q_s(T_i)-q_i}{1+\dfrac{\tilde{L}_i}{\tilde{c}_{pi}}\dfrac{\partial q_s}{\partial T_i}} \\
\tilde{c}_{p(i+1)}-\tilde{c}_{pi} &= (c_{pv}-c_{w/i}+\tilde{R}_v^+)(q_{i+1}-q_i) \\
T_{i+1}-T_i &= -\frac{\tilde{L}_i}{\tilde{c}_{p(i+1)}}(q_{i+1}-q_i) \\
\tilde{L}_{i+1}-\tilde{L}_i &= (c_{pv}-c_{w/i}+\tilde{R}_v^+)(T_{i+1}-T_i)
\end{aligned} \tag{18}$$

the starting point being:

$$\left\{\begin{array}{lcl}
T_0 & = & T_b+\Delta T \quad (e.g.\ \Delta T=T_s-T_b) \\
\tilde{L}_0 & = & \tilde{L}_b+\tilde{R}_v^+T_b=(c_{pv}-c_{w/i}+\tilde{R}_v^+)(T_0-T_b) \\
\tilde{L}_0(q_0-q_b) & = & -(\tilde{R}_b^++\tilde{R}_b^-)T_b-\tilde{c}_{ph}(T_0-T_b) \\
\tilde{c}_{p0} & = & c_{pb}+\tilde{R}_b^++(c_{pv}-c_{w/i}+\tilde{R}_v^+)(q_0-q_b)
\end{array}\right.$$

3.3 Advection of compensatory subsidence

It is obtained by resolving the equation:

$$\left[\frac{\partial\psi}{\partial t}\right]_{conv\_tur}^{impl}=-\frac{\partial}{\partial p}\left[\omega^*\psi\right]$$

with $M_c=-\omega^*$ and $\psi=q$, h, u and v, the discretization of this equation is carried out implicitly for stability reason:

$$\psi_l^+-\psi_l=-c_l\frac{\psi_{l+1}^++\psi_l^+}{2}+c_{l-1}\frac{\psi_l^++\psi_{l-1}^+}{2}$$

where $c_l = \omega_l^* \Delta t / \delta p_l$ is a coefficient of vertical CFL and ψ^+ indicates the value of ψ at time $t + \Delta t$. But the linear tri-diagonal system obtained for ψ^+ may be ill-conditioned (non-dominant diagonal) for non negligible values of c_l. The formulation is thus:

$$\psi_l^+ - \psi_l = -c_l \frac{\psi_{l+1} + 2\psi_l^+ - \psi_l}{2} + c_{l-1} \frac{\psi_l + 2\psi_{l-1}^+ - \psi_{l-1}}{2}$$

which leads to a triangular system which can be written as:

$$(1 + c_l)\psi_l^+ - c_{l-1}\psi_{l-1}^+ = \psi_l + c_{l-1} \frac{2\psi_l^+ - \psi_{l-1} - \psi_{l+1}}{2} + (c_l - c_{l-1}) \frac{\psi_l - \psi_{l+1}}{2}$$

a nonlinear instability can appear if $\dfrac{|c_l - c_{l-1}|}{|1 + c_l|} > 1$. One replaces c_l by c'_l by calculating:

$$c'_l = c'_{l-1} + \frac{(c_l - c'_{l-1})(1 + c'_{l-1})}{1 + |c_l - c'_{l-1}|}$$

One thus modifies to second order the mass flux by ensuring that $\dfrac{|c'_l - c'_{l-1}|}{|1 + c'_l|} < 1$. For more details on this algorithm, to see Geleyn *et al.* (1982). One thus obtains final value ψ^+ of ψ after effect of compensatory subsidence, so that:

$$\left[\frac{\partial \psi}{\partial t}\right]_{conv\_tur}^{expl} = T_\psi^{conv\_tur} = \frac{\psi^+ - \psi}{\Delta t}$$

3.4 Determination of coefficient K

It is carried out by ensuring the integral conservation of wet static energy; indeed, convection involves reorganizations of mass and condensate losses in an atmospheric column, and thus the vertical integral of $h = c_p T + gz + Lq$ must be conserved.

One writes:

$$\int_{p_1}^{p_2} \frac{\partial h}{\partial t} \frac{dp}{g} = 0$$

$$\int_{p_1}^{p_2} \left[T_s^{conv\_tot} + L T_q^{conv\_tot}\right] \frac{dp}{g} = 0$$

$$\int_{p_1}^{p_2} \left[\omega^* \frac{\partial h}{\partial p} + K(h_n - h) - T_h^{dif\_tur}\right] \frac{dp}{g} = 0$$

which leads, by posing $-g\frac{\partial}{\partial p}F_s^{dif-tur} = T_s^{dif-tur}$, to:

$$K = \frac{-\int_{p_1}^{p_2} \omega^* \frac{\partial h}{\partial p}\frac{dp}{g} + F_h^{dif-tur}(p_1) - F_h^{dif-tur}(p_2)}{\int_{p_1}^{p_2}(h_n - h)\frac{dp}{g}}$$

3.5 Effect on horizontal wind

Wind profile

One can first write vertical balance, according to the assumption that convective processes just produce a reorganization on the vertical of heat, moisture and the momentum. This can be written, for the ascending current:

$$\int_{p_t}^{p_b} \left(\frac{\partial \vec{v}}{\partial t}\right)_{conv}^{ud} dp = 0$$

To build the profile, one must consider the effect of entrainment on the surrounding air in the ascending current, and the effect of pressure gradient between the cloud and his environment. One can write:

$$\hat{\omega^*}\frac{\partial \vec{v}_u}{\partial p} = -\left(\nabla\phi\right)^u + \frac{\lambda^u}{\rho}\hat{\omega^*}\left(\vec{v}_u - \vec{v}\right)$$

$$\check{\omega^*}\frac{\partial \vec{v}_d}{\partial p} = -\left(\nabla\phi\right)^d + \frac{\lambda^d}{\rho}\check{\omega^*}\left(\vec{v}_d - \vec{v}\right)$$

The entrainment coefficients λ^u and λ^d are the same as for thermodynamic variables s and q, since the air is driven with all its properties.

Kershaw and Gregory (1997) showed that the horizontal pressure gradient between the air and its environment is proportional to the mass flux and the vertical shearing of large-scale. In their experiments, the proportionality factor was practically the same for the upward and downward currents: $\mathcal{G}^d \simeq \mathcal{G}^u \simeq 0.7$.

$$\frac{\partial \vec{v}_u}{\partial p} = \frac{\lambda^u}{\rho}\left(\vec{v}_u - \vec{v}\right) + \mathcal{G}^u\frac{\partial \vec{v}}{\partial p} \quad \text{or} \quad \frac{\partial \vec{v}_u}{\partial \phi} = -\lambda^u\left(\vec{v}_u - \vec{v}\right) + \mathcal{G}^u\frac{\partial \vec{v}}{\partial \phi} \tag{19}$$

$$\frac{\partial \vec{v}_d}{\partial p} = \frac{\lambda^d}{\rho}\left(\vec{v}_d - \vec{v}\right) + \mathcal{G}^d\frac{\partial \vec{v}}{\partial p} \quad \text{or} \quad \frac{\partial \vec{v}_d}{\partial \phi} = -\lambda^d\left(\vec{v}_d - \vec{v}\right) + \mathcal{G}^d\frac{\partial \vec{v}}{\partial \phi}$$

Calculation for the upward currents is developed here. One will obtain the same thing, except for some changes of sign, for the downward currents. In ARPEGE-CLIMAT the downward currents are not coded.

To discretize Equation (19), one must keep in mind the way in which one discretized the entrainment equation for q and s:

$$\frac{\partial \psi_c}{\partial \phi} = -\lambda(\psi_c - \psi)$$

$$\psi_c^l = \psi_c^{l+1} + \left(\phi^l - \phi^{l+1}\right) \lambda^{l+1} \left(\psi^{l+1} - \psi_c^{l+1}\right)$$

instead of using the values at the intermediate levels:

$$\psi_c^l = \psi_c^{l+1} + \left(\phi^l - \phi^{l+1}\right) \lambda^{\bar{l}} \left(\psi^{\bar{l}} - \psi_c^{\bar{l}}\right)$$

To avoid this approximation, it would be necessary to initially calculate a value for ψ^l which would depend on the value of ψ_c^l in the loop of Newton, which would imply a double iterative calculation. Thus, we will make the same approximation for Equation (19):

$$\vec{v}_c^{\,l} - \vec{v}_c^{\,l+1} - \mathcal{G}^u \left(\vec{v}^{\,l} - \vec{v}^{\,l+1}\right) = -\left(\phi^l - \phi^{l+1}\right)\ \lambda^{l+1}\ \left(\vec{v}_c^{\,l+1} - \vec{v}^{\,l+1}\right)$$

That is to say

$$\xi^l \equiv \left(\phi^l - \phi^{l+1}\right)\ \lambda^{l+1} > 0$$

$$\Longrightarrow \vec{v}_c^{\,l} = \vec{v}_c^{\,l+1} \left(1 - \xi^l\right) + \mathcal{G}^u \vec{v}^{\,l} - \left(\mathcal{G}^u - \xi^l\right) \vec{v}^{\,l+1}$$

We impose the wind at the cloud base: $\vec{v}_c^{\,b} = \vec{v}_{c0}$.

By taking an expression of the form:

$$\vec{v}_c^{\,l} = \beta_l \vec{v}_{c0} + (1 - \beta_l)\, \overline{\vec{v}}^{\,l} \quad \text{or} \quad \vec{v}_c^{\,l+1} = \beta_{l+1} \vec{v}_{c0} + (1 - \beta_{l+1})\, \overline{\vec{v}}^{\,l+1}$$

we obtain

$$\vec{v}_c^{\,l} = \left(1 - \xi^l\right) \left\{\beta_{l+1} \vec{v}_{c0} + (1 - \beta_{l+1})\, \overline{\vec{v}}^{\,l+1}\right\} + \mathcal{G}^u \vec{v}^{\,l} - \left(\mathcal{G}^u - \xi^l\right) \vec{v}^{\,l+1}$$

$$\Longrightarrow \quad \beta_l = \left(1 - \xi^l\right) \beta_{l+1}$$

$$\beta_b = 1$$

$$(1-\beta_l)\,\overline{\vec{v}}^{l} = \left(1-\xi^l\right)(1-\beta_{l+1})\,\overline{\vec{v}}^{l+1} + \mathcal{G}^u\vec{v}^l - \left(\mathcal{G}^u - \xi^l\right)\vec{v}^{l+1}$$

$$\Longrightarrow \quad \overline{\vec{v}}^{l} = \left(1-\xi^l\right)\frac{(1-\beta_{l+1})}{(1-\beta_l)}\overline{\vec{v}}^{l+1} + \frac{\mathcal{G}^u\vec{v}^l - (\mathcal{G}^u-\xi_l)\,\vec{v}^{l+1}}{(1-\beta_l)}$$

$$= \overline{\vec{v}}^{l+1}\frac{\left(1-\xi^l\right)-\beta_l}{(1-\beta_l)} + \frac{\mathcal{G}^u\vec{v}^l - \left(\mathcal{G}^u-\xi^l\right)\vec{v}^{l+1}}{(1-\beta_l)}$$

$$= \overline{\vec{v}}^{l+1} + \frac{\xi^l\left(\vec{v}^{l+1}-\overline{\vec{v}}^{l+1}\right) + \mathcal{G}^u\left(\vec{v}^l-\vec{v}^{l+1}\right)}{(1-\beta_l)}$$

At the cloud base:

$$\beta_b = 1 \quad \Longrightarrow \quad \beta_{b-1} = \left(1-\xi^b\right) \quad \Longleftrightarrow \quad (1-\beta_{b-1}) = \xi^{b-1}$$

$$\overline{\vec{v}}^{b-1} = \vec{v}^b + \frac{\mathcal{G}^u\left(\vec{v}^{b-1}-\vec{v}^b\right)}{\xi^{b-1}}$$

If $\mathcal{G}^u = 0$ we obtain:

$$\overline{\vec{v}}^{b-1} = \vec{v}^b \quad \text{and} \quad \overline{\vec{v}}^{l} = \overline{\vec{v}}^{l+1} + \frac{\xi^l\left(\vec{v}^{l+1}-\overline{\vec{v}}^{l+1}\right)}{(1-\beta_l)}$$

which is exactly the parametrization used before (without the effects of pressure gradient).

Calculation of the wind at the base

One writes the conservation of momentum on the vertical:

$$\int_{p_t}^{p_b}\left(\frac{\partial\vec{v}}{\partial t}\right)^u_{conv} dp = 0 = \int_{p_t}^{p_b}\left[\omega^*\frac{\partial\vec{v}}{\partial p} + K^u\left(\vec{v}_u-\vec{v}\right)\right]dp$$

$$= \int_{p_t}^{p_b}\left(\frac{\partial\vec{v}}{\partial t}\right)^u_{cs} dp + K^u\left[\int_{p_t}^{p_b}\vec{v}_u dp - \int_{p_t}^{p_b}\vec{v}dp\right]$$

$$\Longrightarrow \quad \vec{v}_{c0} = \frac{-\int_{p_t}^{p_b}\left(\frac{\partial\vec{v}}{\partial t}\right)^u_{cs} dp + K^u\int_{p_t}^{p_b}\vec{v}\,dp - K^u\int_{p_t}^{p_b}(1-\beta)\overline{\vec{v}}\,dp}{K^u\int_{p_t}^{p_b}\beta dp}$$

Calculation of flux and tendency

$$\left(\frac{\partial \vec{v}}{\partial t}\right)^{u}_{conv} = -g\frac{\partial F_{\vec{v}_u}}{\partial p} = \left(\frac{\partial \vec{v}}{\partial t}\right)_{cs} + K^u\,(\vec{v}_u - \vec{v})$$

$$= \frac{\vec{v}_{cs} - \vec{v}}{\Delta t} - K^u\,\vec{v} + K^u(1-\beta)\overline{\vec{v}} + \beta\,K^u\,\vec{v}_{c0}$$

$$= \frac{\vec{v}_{cs} - \vec{v}(1+K'^u) + K'^u(1-\beta)\overline{\vec{v}} + \beta\,K'^u\,\vec{v}_{c0}}{\Delta t}$$

posing, for stability reasons :

$$K'^u \equiv ZALFS = \frac{K\Delta t}{1+K\Delta t}$$

The parametrization must return fluxes:

$$F_{\vec{v}_u}{}^{\bar{l}} = F_{\vec{v}_u}{}^{\overline{l-1}} - \delta_{stab}\frac{\Delta p^l}{g\Delta t}\left[(\vec{v}^l_{cs} - \vec{v}^l) + K^u(\vec{v}^l_u - \vec{v}^l)\right]$$

$$= F_{\vec{v}_u}{}^{\overline{l-1}} - \delta_{stab}\frac{\Delta p^l}{g\Delta t}\left[\vec{v}_{cs} - \vec{v}(1+K'^u) + K'^u(1-\beta)\overline{\vec{v}} + \beta K'^u\,\vec{v}_{c0}\right]$$

3.6 Energetics in the scheme

Latent heat of flux

One investigates here the relation between the precipitation flux F_p and the dry static energy flux $(F_s)_{conv\_prec}$, these two fluxes being defined by:

- dry static energy flux:

$$r_\eta\left(\frac{\partial s}{\partial t}\right)_{conv\_prec} = \frac{\partial}{\partial \eta}(F_s)_{conv\_prec} + \delta_m F_p\frac{\partial s}{\partial \eta}$$

with $r_\eta = -\frac{1}{g}\frac{\partial p}{\partial \eta}$ pseudo-density in η coordinate. This form of the tendency of s due to precipitations separates the pseudo-advection part from the remainder by the vacuum left by precipitation which corresponds to a mass flux $r_\eta\dot{\eta} = \delta_m F_p$.

- precipitation flux:

$$r_\eta \left(\frac{\partial q}{\partial t}\right)_{conv\_prec} = \frac{\partial F_p}{\partial \eta}$$

and one seeks L_{flux} such as:

$$(F_s)_{conv\_prec} = -L_{flux} F_p$$

On the basis of:

$$r_\eta c_p \left(\frac{\partial T}{\partial t}\right)_{conv\_prec} = -L(T)\frac{\partial F_p}{\partial \eta} + \delta_m F_p \frac{\partial \phi}{\partial \eta} + F_p \frac{\partial T}{\partial \eta}(c_{w/i} - c_{p_a}(1-\delta_m))$$

and of:

$$\left(\frac{\partial s}{\partial t}\right)_{conv\_prec} = c_p \left(\frac{\partial T}{\partial t}\right)_{conv\_prec} + \left(\frac{\partial c_p}{\partial t}\right)_{conv\_prec} T$$

one expresses c_p in q to obtain:

$$r_\eta \left(\frac{\partial s}{\partial t}\right)_{conv\_prec} = -\frac{\partial}{\partial \eta}(F_p\left[L(T) - (1-\delta_m q_v)(c_{pv} - c_{pa})T\right]) + \delta_m F_p \frac{\partial s}{\partial \eta}$$

One thus has:

$$L_{flux} = L(T) - (1-\delta_m q_v)(c_{pv} - c_{pa})T \tag{20}$$

Effective local latent heat

One tries here to answer the following question: "which energy contribution to the whole column in sensible heat form does produce a local variation in water vapor due to precipitation/evaporation ?" the answer will be provided by L_{eff} such as:

$$-L_{eff}\frac{\partial F_p}{\partial \eta} d\eta = d\left[\int_{\eta_1}^{\eta_2} c_p \left(\frac{\partial T}{\partial t}\right)_{conv\_prec} r_\eta d\eta\right] \tag{21}$$

Taking into account the assumptions carried out on the water cycle, L_{eff} will consist of three terms:

1. Conversion of latent heat into sensible heat: $L(T)$ (true mass latent heat of the water vapor at this temperature).

2. Transformation of potential energy of water vapor going in a time step from the ground to the level considered (or opposite way according to the sign of $\partial F_p/\partial\eta$): $\delta_m(\phi - \phi_s)$

3. Redistribution of sensible heat; indeed, precipitation is adjusted on each level at the local temperature: $(c_{w/i} - c_{p_a}(1-\delta_m))(T - T_s)$

Effective local latent heat:

$$L_{eff} = L(T) + \delta_m(\phi - \phi_s) + (c_{w/i} - c_{pa}(1-\delta_m))(T - T_s)$$

which is also written in the form:

$$L_{eff} = L(T_s) + \delta_m(\phi - \phi_s) + (c_{pv} - c_{pa}(1-\delta_m))(T - T_s)$$

satisfies Equation (21), and thus:

$$\int_{\eta_1}^{\eta_2} \left[L_{eff} \frac{\partial F_p}{\partial \eta} + c_p \left(\frac{\partial T}{\partial t} \right)_{conv\_prec} \right] r_\eta d\eta = 0$$

Latent heat of budget

One takes again the problem of the preceding paragraph, while being interested this time not in sensible heat but in dry static energy $s = c_p T + \phi$: "which energy contribution to the whole column in dry static form does produce a local water vapor variation due to precipitation/evaporation?" The answer will be provided by L_{bil} such as:

$$-L_{bil} \frac{\partial F_p}{\partial \eta} d\eta = d \left[\int_{\eta_1}^{\eta_2} c_p \left(\frac{\partial s}{\partial t} \right)_{conv\_prec} r_\eta d\eta \right]$$

One has:

$$\left(\frac{\partial s}{\partial t} \right)_{conv\_prec} = c_p \left(\frac{\partial T}{\partial t} \right)_{conv\_prec} + \left(\frac{\partial c_p}{\partial t} \right)_{conv\_prec} T + \left(\frac{\partial \phi}{\partial t} \right)_{conv\_prec}$$

One neglects $\left(\frac{\partial \phi}{\partial t} \right)_{conv\_prec}$. The first term of right-hand side is the same as that of the preceding paragraph (related to the effective local latent heat). Let us detail the second:

$$\left(\frac{\partial c_p}{\partial t} \right)_{conv\_prec} T = T(c_{p_v} - c_{p_a}) \left(\frac{\partial q}{\partial t} \right)_{conv\_prec}$$

$$= T(c_{p_v} - c_{p_a})(1 - \delta_m q)\frac{\partial F_p}{\partial \eta}$$

One thus has:

$$L_{bil} = L_{eff} + (c_{pv} - c_{pa})(1 - \delta_m q)T$$

and finally:

$$L_{bil} = L(T_s) - (c_{p_v} - c_{p_a}(1 - \delta_m))T_s + \delta_m(c_p T + \phi - \phi_s) \tag{22}$$

13

Gravity wave drag

1 Parametrization of orographic gravity wave drag

1.1 Calculation at the surface

The momentum flux due to a wave excited by the displacement of a large-scale flow, vertically, on a small scale mountain, is given by:

$$\vec{\tau}_s = \rho_s N_s \vec{v}_s K_g h_s \tag{1}$$

This vector corresponds in the code to PSTRDU and PSTRDV at level KLEV. It represents the drag exerted by the lowest atmospheric layer on surface. In the right-hand side:

- ρ_s is the density at surface (PGWDCS)
- $\vec{v}_s$ is the effective wind at surface (see section 2.1)
- N_s is the effective Brunt-Vaïsala frequency at surface (see section 2.1)
- h_s is the standard deviation of unresolved orography
- K_g is a dimensionless coefficient for the adjustment of the parametrization (GWDSE)

1.2 Calculation at a given level

The momentum flux of a wave of amplitude a and wavelength λ is given by:

$$\tau = \rho N U \frac{a^2}{\lambda}$$

where U is the projection of wind $\vec{v}$ on the effective wind at surface $\vec{v}_s$:

$$U = \frac{\vec{v} \cdot \vec{v}_s}{\|\vec{v}_s\|}$$

As long as the wave remains linear (low amplitude compared to the wavelength), there is no interaction with the large-scale flow (surge or saturation) and τ remains constant on the vertical. It is admitted moreover that:

- the wave breaks at the surface.
- the condition of saturation is: $\lambda = CU/N$ (Lindzen criterion) where C is a constant on the vertical.

Thus, posing:

$$\Gamma = \frac{\rho}{\rho_s} \left(\frac{U}{U_s} \right)^3 \frac{N_s}{N} \qquad \text{(ZRAPP)} \tag{2}$$

there will be saturation if $\tau = \Gamma \tau_s$. One thus has $\tau_l = \min(\Gamma \tau_s, \tau_{l+1})$. In fact, one defines a factor of proportionality to τ_s. One takes at surface $\Gamma_L = 1$, and one goes up while posing $\Gamma_l = \min(\Gamma, \Gamma_{l+1})$. As soon as $\Gamma_l \leq 0$, one poses $\Gamma_l = 0$ and one sets it to zero above (there is no more flux because the wave has been completely absorbed). That occurs as soon as wind $\vec{v}_l$ forms an angle higher than 90° with the surface wind, or, at last, at the top of the atmosphere ($\rho = 0$).

2 Refinements for orographic gravity wave drag

2.1 Effective surface wind

The formulas above utilize the surface wind $\vec{v}_s$. In the model, the surface wind is zero, and using the lowest model level wind would introduce a dependence of the scheme with the vertical discretization. It is supposed that the wave generating orography induces a boundary layer thickness $H = K_h h_s$ where K_h is an empirical dimensionless coefficient (HOBST). One calculates the average parameters in this mountainous boundary layer:

$$\vec{v}_s = <\vec{v}> = \frac{1}{H} \int_0^H \vec{v}\, dz \quad \text{(ZSUMU,ZSUMV)}$$

in the same way for $< N_s^2/(\rho_s g)^2 >$ (ZSUMF). To maintain the continuity of Γ_l, one modifies the vertical profile of wind in the mountainous boundary layer:

$$\vec{v}_l = \vec{v}_s(1 - \Delta p_l / \Delta p_{obst}) + \vec{v}_l \Delta p_l / \Delta p_{obst} \quad \text{(ZU,ZV)}$$

where Δp_l is the thickness in pressure between the surface and level l, and Δp_{obst} the thickness between the surface and the top of the mountainous boundary layer. The same way is applied for the standardized Brunt-Vaïsala frequency (ZNFNO).

2.2 Mountain anisotropy

The theory supporting this parametrization makes the assumption that the flow is two-dimensional. In fact the sub-grid scale orography can be represented by the anisotropic coefficient γ^2 (PVRLAN) which is the ratio of the two eigenvalues of the tensor of variance of unresolved orography, and angle ψ (PVRLDI) which are the direction (null in the direction of increasing pseudo-longitudes) of the first eigenvector of this tensor. The surface stress is not co-linear to the surface wind. One calculates a fictitious surface wind (u_{fs}, v_{fs}), in the code (ZUSUR, ZVSUR), which would give in the isotropic case same flux as the one obtained with (u_s, v_s):

$$u_{fs} = Au_s + D(u_s \cos 2\psi + v_s \sin 2\psi)$$

$$v_{fs} = Av_s + D(u_s \sin 2\psi - v_s \cos 2\psi)$$

$$A = \gamma^2 + \frac{1}{2\pi}(4(1-\gamma)(1+\alpha_1\gamma) - \gamma(1+\alpha_2)\ln\gamma)$$

$$D = \frac{1}{2\pi}(4(1-\gamma)(1+\delta_1\gamma) + 3\gamma(1+\delta_2)\ln\gamma)$$

Coefficients α_1, α_2, δ_1, and δ_2 are calculated from elliptic integrals and are about 1.44, 0.22, 0.67 and 0.44 respectively (more accurate values are used in the code, based on asymptotic approximations). One thus uses $\vec{v}_{fs}$ to calculate the surface flux and the projection of the wind in the free atmosphere in the place of $\vec{v}_s$ in Equations (1) and (2).

2.3 Resonance

This theory assumes the wave does not deposit all its momentum on the saturation level, but is reflected downwards, and can, after a certain number of reflections, produce a resonance. The theory has been developed by Clark and Peltier (1977). They showed from very simplified considerations, and also with results from simulations with a mesoscale model, that resonant amplification takes place when altitude z of the critical level checks:

$$\frac{N}{U}\, z \equiv \frac{3\pi}{2} \qquad [2\pi]$$

One defines a function of resonance f, periodical and of average value 1, as a reference for the parametrization:

$$f(\theta) = |1 - iK_a e^{i\theta} - K_a^2 e^{2i\theta} + \cdots| = (1 + 2K_a \sin\theta + K_a^2)^{-\frac{1}{2}}$$

where K_a is an empirical dimensionless parameter (GWDAMP). This function reaches its maximum $1/(1 - K_a)$ for $\theta = 3\pi/2$ (amplification) and its minimum $1/(1 + K_a)$ for $\theta = \pi/2$ (destruction).

In the parametrization of the friction of the orographic gravity waves, one includes the assumption of resonance as formulated above. One locates p_{crit} the first critical level reached (Γ_l lower than 1, for the first time), where the wave is likely to be reflected in phase with itself; one evaluates amplification by resonance by calculating:

$$\theta = \int_0^{z_{crit}} \frac{N}{U}\, dz$$

One deduces $f(\theta)$ from it. One defines Γ_{crit} as $\min(1, f(\theta))$, and one modifies factor Γ_l:

- between the surface and the critical level, one takes a linear profile with pressure, with $f(\theta)$ at the surface and Γ_{crit} at the critical level.
- above the critical level, one takes $\min(\Gamma_l, \Gamma_{crit})$.

One does not take into account the phenomena of reflection on the levels above the first critical level.

2.4 Trapping

In the case of a neutral or unstable stratification of the atmosphere, the Brunt-Vaïsala frequency goes to zero as well as the drag due to the orographic gravity waves. One seeks the first level starting from bottom where N is zero or changes sign. If this level is below the critical level of resonance, one does not apply the modification of the profile by resonance (by imposing $f(\theta) = 1$). Profile Γ_l is modified:

- above level $N = 0$ by setting it to zero.
- below level $N = 0$, by cutting off a linear function of pressure in order not to modify the surface stress and to set it to zero at level $N = 0$.

2.5 Sub-grid orography

The effect of blocking of flow by the succession of the mountains and the valleys was taken into account in certain models by envelope orography, method which consisted in replacing the average orography by an increase of a fraction of the standard deviation of the unresolved fluctuations. Lott and Miller (1995) using the results of the PYREX experiment, proposed to better define the local impact of the unresolved mountains by means of an increase in friction by gravity waves only in the model levels occupied by the actual orography. The adaptation to ARPEGE consists in multiplying coefficient Γ_l (and consequently tension $\vec{\tau}$) by:

$$1 + a_d \sqrt{\frac{\left(1 - \frac{z}{b_d H}\right)^3}{\left(1 + \frac{z}{H}\right)}}$$

on the levels whose altitude z is lower than $b_d H$, where H is the thickness of boundary layer calculated above. From projection U_s of the effective surface wind $\vec{v}_s$ onto the fictitious wind (which takes into account the anisotropy of orography) $\vec{v}_{fs}$, one introduces a standardized thickness H_N:

$$H_N = H \, \frac{N_s \, \|\vec{v}_{fs}\|}{U_s^2}$$

Two empirical parameters are introduced: a factor of friction at the surface K_d (GWDCD) and a critical value for standardized thickness H_{NC} (1/GWDBC). When standardized thickness H_N is higher than the critical value, coefficients a_d (ZAA) and b_d (ZBB) are given by:

$$a_d = K_d \, \frac{\|\vec{v}_{fs}\|^2}{U_s^2} \, \frac{H_N - H_{NC}}{H_N^2} \qquad \text{and} \qquad b_d = \frac{H_N - H_{NC}}{H_N}$$

In the opposite case, a_d and b_d are zero and the stress is not modified.

2.6 The *lift* effect

Here one takes into account the transverse force exerted on the wind attacking an unresolved mountain due to the effect of terrestrial rotation combined with the deviation of the flow which circumvents the obstacle (in an asymmetrical way). In theory it would be necessary that this force is exerted transversely to a hypothetical flow undisturbed by the obstacle (geostrophic wind for example). But this calculation would be difficult to carry out in

ARPEGE: the force defined by this way would produce a work, a property contrary with the principle of the effect of rising (hereafter called *lift*), and whose conjugation with the effect of *form-drag* of the sub-grid orography (see section 2.5) would be unexpected. One could also have constrained this force to be exactly orthogonal with the forces due to orographic friction previously defined in this chapter, but this would have answered only the second of the two criticisms formulated above. As a simplification here, we just have defined a (positive) complement to Coriolis force, with an intensity proportional to the volume of the sub-grid mountain.

This force of *lift* is exerted on the volume of atmosphere of the model between the ground and H and varies according to $(1-z/H)/(1+z/H)$ to remain in agreement with the choice of the shape of the sub-grid mountain implicitly made in section 2.5. There is a multiplying coefficient Lt whose intensity corresponds to the vertical integral of the effects layer by layer (and thus with the total stress applied): GWDLT. For a value 1 of this coefficient, one obtains on average a doubling of the "Coriolis" effect on depth H. From the phenomenological point of view, this amounts (when GWDLT = 1) to increasing the rotational effects of the mountain solved by what would give an effect of envelope orography with coefficient K_h, without having now the effects of vertical displacement and blocking associated with the modification with the large-scale orography seen by the model.

The effect of *lift* is calculated with gravity waves by convenience and because the effects of the sub-grid orography intervene there in a way close to what is made in the section 2.5. But as this additional force physically does not have anything common with the remainder of calculations previously described, it will be added in an absolutely independent way. In particular it will not undergo to the numerical securities described hereafter. By applying it without caution to a wind which is perhaps not the average of the vector wind over the duration of the time step, this force would consume or produce energy, even marginally, and this could cause problem for very long integrations. A trapezoidal split-implicit calculation is thus carried out so that the wind vector conserves its module, when this effect is the only one taken into account during the time step.

All this leads to the following formulations. For $z < H$:

$$f^* = Lt\ f\ \frac{\dfrac{1-z/H}{1+z/H}}{K_h(2\ln(2)-1)}$$

$$\left(\frac{\partial u}{\partial t}\right)_{lift} = +f^*\frac{v - u\,\Delta t\,f^*/2}{1+(\Delta t\,f^*/2)^2}$$

$$\left(\frac{\partial v}{\partial t}\right)_{lift} = -f^*\frac{u + v\,\Delta t\,f^*/2}{1+(\Delta t\,f^*/2)^2}$$

For $z > H$ there is no *lift* force.

3 Numerical securities in orography waves

3.1 Implicit formulation versus surface wind

All fluxes are proportional to projection U_s of wind $\vec{v}_s$ on $\vec{v}_{fs}$, therefore the tendency of U_s also:

$$\frac{\partial U_s}{\partial t} = -KU_s$$

However, for large time steps the system can become unstable. Consequently the following relations are used (U_s indicating the value with t and U_s^+ with $t + \Delta t$):

$$\frac{U_s^+ - U_s}{\Delta t} = -KU_s^+$$

$$\frac{U_s^+ - U_s}{\Delta t} = -\acute{K}U_s$$

One replaces K by $\acute{K} = \frac{K}{1 + K\Delta t}$ (split-implicit scheme). This is equivalent to multiplying all relations of proportionality between flux at a given level and U_s by:

$$\frac{1}{1 - \frac{\Delta t}{U_s}\frac{\partial U_s}{\partial t}}$$

$\frac{\partial U_s}{\partial t}$ is calculated by integrating the vertical derivative of flux inside the mountainous boundary layer defined in the section 2.1.

3.2 Implicit advective formulation

One has just seen how to implicitly take into account the dependence of the tendency of $\vec{v}$ on $\vec{v}_s$; in fact, one has treated only component of the wind in the direction of $\vec{v}_{fs}$, but the tendency of wind is zero in the direction orthogonal to $\vec{v}_{fs}$. However one does not take into account the dependence

on $\vec{v}$ itself, since it does not appear in a linear way in the equations. One wants to discretize:

$$\frac{\partial U}{\partial t} = -g\frac{\partial \tau}{\partial p}$$

where U is the projection of $\vec{v}$ on $\vec{v}_{fs}$. Here $\tau = \Gamma_l \tau_s$ and Γ_l depends on U (Equation (2) and corrections). One poses:

$$\tau_l = \frac{1}{g} U_l M_l$$

If one regards the phenomenon as a vertical advection of moment, M_l plays the role a vertical velocity (or of a mass flux, by analogy with the convection). One introduces the dimensionless quantity, similar to a vertical CFL criterion:

$$A_l = \frac{M_l \Delta t}{\delta p_l}$$

One discretizes the pseudo-advection with an upstream implicit scheme:

$$U_l^+ - U_l = -(A_l U_l^+ - A_{l-1} U_{l-1}^+)$$

which one can write as:

$$(1 + A_l)(U_l^+ - U_l) = -A_l U_l + A_{l-1} U_{l-1} + A_{l-1}(U_{l-1}^+ - U_{l-1})$$

If one knows the implicit tendency on level $l-1$, $U_{l-1}^+ - U_{l-1}$, and the explicit tendency calculated by parametrization on level l, $-A_l U_l + A_{l-1} U_{l-1}$, one deduces from it the implicit tendency on level l. One starts at level $l = 1$ since the tendency is null at the top and one carries out a downward loop. One will replace stress τ by a stress $\acute{\tau}$ such as:

$$\frac{U^+ - U}{\Delta t} = -g\frac{\partial \acute{\tau}}{\partial p}$$

It comes:

$$\acute{\tau}_0 = 0$$

$$\acute{\tau}_l = \acute{\tau}_{l-1} - \frac{1}{1 + A_l}(\acute{\tau}_{l-1} - \tau_l)$$

In the code, $\dfrac{1}{(1 + A_l)}$ is called ZALPHA.

4 Parametrization of convective gravity wave drag

This parametrization of impact of tropospheric convection on the stratospheric jets was introduced by Bossuet *et al.* (1998).

4.1 Calculations at the top of the cloud

In a way similar to the flow over a mountain, the convective zones produce vertical small-scale velocities which generate gravity waves in the stable atmosphere layers located above. The parametrization described here supposes that the intensity of these waves is a function of the precipitation flux at the base of the cloud (as an index of the intensity of the convection). It is supposed that these waves move vertically in the reference frame related to the base of the cloud, and that, similarly with the waves of orographic origin, the interaction with the large-scale flow occurs only in the direction of the absolute wind at the top of the cloud, level of the source of the gravity waves.

The momentum flux due to a wave excited by convective motions can be empirically represented by:

$$\vec{\tau}_s = K_c P_{con} \frac{\vec{v}_s}{\|\vec{v}_s\|} \tag{3}$$

This vector corresponds in the code to ZSTUS and ZSTVS. It also corresponds to vector PSTRCU and PSTRCV at level KIUPC (stress at the top of the cloud). This vector represents the stress exerted by a layer on the layer below. In the right-hand side:

- K_c is a tuning parameter
- P_{con} is convective precipitation (rain+snow)
- $\vec{v}_s$ is wind at the top of the cloud

4.2 Calculations above the cloud

As long as the wave remains linear (low amplitude compared with the wavelength), there is no interaction with the large-scale flow (surge or saturation) and τ remains constant on the vertical. By using Lindzen criterion for the surge, one introduces, in the same way as for the orographic waves, profile Γ:

$$\Gamma = \frac{\rho}{\rho_s} \left(\frac{U}{U_s} \right)^3 \frac{N_s}{N} \qquad \text{(ZRAPP)} \tag{4}$$

where U is projection on the wind at the top of the cloud of the relative wind in the reference frame related to the base of the cloud:

$$U = \frac{(\vec{v} - \vec{v}_b) \cdot \vec{v}_s}{\|\vec{v}_s\|}$$

There will be saturation if $\tau = \Gamma\tau_s$. One thus has $\tau_l = \min(\Gamma\tau_s, \tau_{l+1})$. In fact, one defines a factor of proportionality to τ_s. One takes at the top of cloud $\Gamma_s = 1$, and one goes up while posing $\Gamma_l = \min(\Gamma, \Gamma_{l+1})$. As soon as $\Gamma_l \leq 0$, one poses $\Gamma_l = 0$ and one sets it to zero above (flux is zero because the wave has been completely absorbed). That occurs as soon as the wind at level l forms an angle greater than 90° with the wind at the top of the cloud (in the mobile reference frame), or, at last, at the top of atmosphere ($\rho = 0$).

4.3 Calculations inside the cloud

In the case of the waves of orographic origin, the momentum borrowed from the atmosphere is yielded to the earth, according to the principle of conservation. In the case here, there is no exchange of momentum with the ground, and the quantity must be yielded to the lower atmospheric layers. It is reasonable to think that the stable layers located under the base of the cloud are not affected either. One thus takes a linear variation of flow between value $\acute{\tau}_s$ at the top and zero at the base.

In the above calculation, one considers that if there are several convective layers disjointed, one takes the bottom of the lowest layer and the top of the highest layer.

5 Numerical securities for convective waves

The temporal evolution of the wind at level l depends, via U_l on the wind itself. As a consequence, an explicit formulation of the temporal advance can lead to numerical instabilities. It would be too complicated to solve the full system with an implicit scheme because it is non-linear (with cubic terms and thresholds) and multidimensional. In fact one wants to discretize:

$$\frac{\partial U}{\partial t} = -g\frac{\partial \tau}{\partial p}$$

where U is the projection of the relative wind. We have $\tau = \Gamma_l\tau_s$, and Γ_l depends on U (Equation (4)). One poses:

$$\tau_l = \frac{1}{g}U_l M_l$$

If one considers the phenomenon as a vertical advection of momentum, M_l plays the role a vertical velocity (or of a mass flux, by analogy with the convection). One introduces the dimensionless quantity:

$$A_l = \frac{M_l \Delta t}{\delta p_l}$$

One discretizes the pseudo-advection with an upstream implicit scheme:

$$U_l^+ - U_l = -(A_l U_l^+ - A_{l-1} U_{l-1}^+)$$

which can be written as:

$$(1 + A_l)(U_l^+ - U_l) = -A_l U_l + A_{l-1} U_{l-1} + A_{l-1}(U_{l-1}^+ - U_{l-1})$$

If one has calculated the implicit tendency on level $l-1$, $U_{l-1}^+ - U_{l-1}$, and the explicit tendency calculated by parametrization on level l, $-A_l U_l + A_{l-1} U_{l-1}$, one deduces from it the implicit tendency at level l. One starts at level $l = 1$ since the tendency is null at the top and one carries out a downward loop. One will replace stress τ by a stress $\acute{\tau}$ such as:

$$\frac{U^+ - U}{\Delta t} = -g \frac{\partial \acute{\tau}}{\partial p}$$

Then:

$$\acute{\tau}_0 = 0$$

$$\acute{\tau}_l = \acute{\tau}_{l-1} - \frac{1}{1 + A_l}(\acute{\tau}_{l-1} - \tau_l)$$

This is the same procedure as in section 3.2.

14

Surface processes scheme

1 Introduction

The ISBA land surface scheme has been used in the former versions of ARPEGE-CLIMAT. A more recent version is now available in SURFEX. SURFEX (stands for SURFace EXternalisée) gathers all developments and improvements made in surface schemes. Not only physical parameterizations have been externalized, but also the preparation of specific surface parameters needed by physical schemes and the initialization of all state variables of the different models. More recently, the modelling of urban areas has began to be of great interest in the research community. TEB (Town Energy Balance) model, specially designed to represent the exchanges between a town and the atmosphere is available in SURFEX . Moreover, the surface representation has been improved and thus SURFEX system has been enhanced with the specific treatment for water surfaces. Indeed, up to now, the exchanges of energy between water surfaces and the atmosphere were treated in a very simple way, while now a physically based model have been introduced to build a more complex but accurate surface model, available for all atmospheric models.

In SURFEX, the exchanges between the surface and the atmosphere are realized by mean of a standardized interface (Polcher et al., 1998; Best et al., 2004) that proposes a generalized coupling between the atmosphere and surface. During a model time step, each surface grid box receives the upper air temperature, specific humidity, horizontal wind components, pressure, total precipitation, long-wave radiation, short-wave direct and diffuse radiations and possibly concentrations of chemical species and dust. In return, SURFEX computes averaged fluxes for momentum, sensible and latent heat and possibly chemical species and dust fluxes and then sends these quanti-

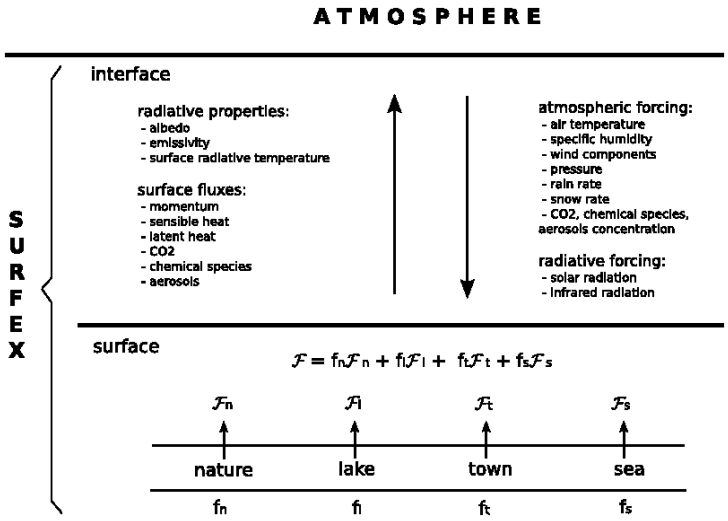

Figure 1: Description of the exchanges between an atmospheric model sending meteorological and radiative fields to the surface and SURFEX composed of a set of physical models that compute tiled variables $\mathcal{F}_*$ covering a fraction f_* of a unitary grid box and an interface where the averaged variables $\mathcal{F}$ are sent back to the atmosphere

ties back to the atmosphere with the addition of radiative terms like surface temperature, surface direct and diffuse albedo and also surface emissivity.

All this information is then used as lower boundary conditions for the atmospheric radiation and turbulent schemes. In SURFEX, each grid box is made of four adjacent surfaces: one for nature, one for urban areas, one for sea or ocean and one for lake. The coverage of each of these surfaces is known through the gobal ECOCLIMAP database (Masson et al., 2003), which combines land cover maps and satellite information. The SURFEX fluxes are the average of the fluxes computed over nature, town, sea/ocean or lake, weighted by their respective fraction.

The complete description of SURFEX is in it's proper scientific documentation.

2 Soil, snow and vegetation : ISBA surface scheme

The ISBA scheme (Noilhan and Planton, 1989; Noilhan and Mahfouf, 1996) computes the exchanges of energy and water between the continuum soil-vegetation-snow and the atmosphere above. In its genuine version, the evapotranspiration of the vegetation is controlled by a resistance like proposed by (Jarvis, 1976). A more recent version of the model named Isba-A-gs accounts

for a simplified photosynthesis model where the evaporation is controlled by the aperture of the stomates, the component of the leaves that regulates the balance between the transpiration and the assimilation of CO2. The current version ARPEGE-CLIMAT will use the ISBA scheme with the Force restore method (Noilhan and Planton, 1989) to treat the transfer of water and heat in the soil (option : 3 layers for tempertaure, liquid water and ice) the snow scheme from Douville (1995a, 1995b ,).

2.1 Force restore approach

Treatment of the soil heat content

The prognostic equations for the surface temperature T_s and its mean value T_2 over one day τ, are obtained from the force-restore method proposed by Bumralkar (1975) and Blackadar (1976):

$$\frac{\partial T_s}{\partial t} = C_T(R_n - H - LE) - \frac{2\pi}{\tau}(T_s - T_2), \quad (1)$$

$$\frac{\partial T_2}{\partial t} = \frac{1}{\tau}(T_s - T_2), \quad (2)$$

where H and LE are the sensible and latent heat fluxes, and R_n is the net radiation at the surface. The surface temperature T_s evolves due to both the diurnal forcing by the heat flux $G = R_n - H - LE$ and a restoring term towards its mean value T_2. In contrast, the mean temperature T_2 only varies according to a slower relaxation towards T_s.

The coefficient C_T is expressed by

$$C_T = 1/\left(\frac{(1-veg)(1-p_{sng})}{C_g} + \frac{veg(1-p_{snv})}{C_v} + \frac{p_{sn}}{C_s}\right) \quad (3)$$

where veg is the fraction of vegetation, C_g is the ground heat capacity, C_s is the snow heat capacity, C_v is the vegetation heat capacity, and

$$p_{sng} = \frac{W_s}{W_s + W_{crn}} \quad (4)$$

$$p_{snv} = \frac{h_s}{h_s + 5000 z_0} \quad (5)$$

$$p_{sn} = (1-veg)p_{sng} + veg\,p_{snv} \quad (6)$$

are respectively the fractions of the bare soil and vegetation covered by snow, and the fraction of the grid covered by snow. Here, $W_{crn} = 10\ mm$, and

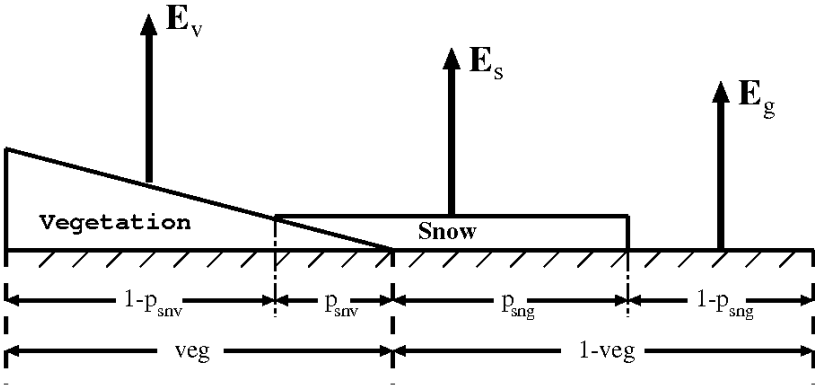

Figure 2: Partitioning of the grid

$h_s = W_s/\rho_s$ is the thickness of the snow pack (ρ_s is the snow density). The partitioning of the grid into bare soil, vegetation, and snow areas, is indicated in Fig.(2) .

Treatment of the soil water

Equations for w_g and w_2 are derived from the force-restore method applied by Deardorff (1977) to the ground soil moisture:

$$\frac{\partial w_g}{\partial t} = \frac{C_1}{\rho_w d_1}(P_g - E_g) - \frac{C_2}{\tau}(w_g - w_{geq}); \quad (7)$$

$$0 \leq w_g \leq w_{sat} \quad (8)$$

$$\frac{\partial w_2}{\partial t} = \frac{1}{\rho_w d_2}(P_g - E_g - E_{tr}) - \frac{C_3}{d_2 \tau}\ max\left[0., (w_2 - w_{fc})\right]; \quad (9)$$

$$0 \leq w_2 \leq w_{sat} \quad (10)$$

where P_g is the flux of liquid water reaching the soil surface (including the melting), E_g is the evaporation at the soil surface, E_{tr} is the transpiration rate, ρ_w is the density of liquid water, and d_1 is an arbitrary normalization depth of 1 centimeter. In the present formulation, all the liquid water from the flux P_g goes into the reservoirs w_g and w_2, even when snow covers fractions of the ground and vegetation. The first term on the right hand side of Eq. (12) represents the influence of surface atmospheric fluxes when the contribution of the water extraction by the roots is neglected. The coefficients C_1 and C_2, and the equilibrium surface volumetric moisture w_{geq}, have been calibrated for different soil textures and moistures.

The expression for C_1 differs depending on the moisture content of the soil.

For wet soils (i.e., $w_g \geq w_{wilt}$), this coefficient is expressed as

$$C_1 = C_{1sat} \left(\frac{w_{sat}}{w_g} \right)^{b/2+1} \tag{11}$$

For very dry soils (i.e., $w_g < w_{wilt}$), the vapor phase transfer needs to be considered in order to reproduce the physics of water exchange. These transfers are parameterized as a function of the wilting point w_{wilt}, the soil water content w_g, and the surface temperature T_s, using the Gaussian expression (Braud et al., 1993; Giordani, 1993).

$$C_1 = C_{1max} \exp \left[-\frac{(w_g - w_{max})^2}{2\sigma^2} \right] \tag{12}$$

where w_{max}, C_{1max}, and σ are respectively the abscissa of the maximum, the mode, and the standard deviation of the Gaussian functions (see 4). The other coefficient, C_2, and the equilibrium water content, w_{geq}, are given by

$$C_2 = C_{2ref} \left(\frac{w_2}{w_{sat} - w_2 + 0.01} \right) \tag{13}$$

$$w_{geq} = w_2 - a w_{sat} \left(\frac{w_2}{w_{sat}} \right)^p \left[1 - \left(\frac{w_2}{w_{sat}} \right)^{8p} \right] \tag{14}$$

For the w_2 evolution, Eq. (13) represents the water budget over the soil layer of depth d_2. The drainage, which is proportional to the water amount exceeding the field capacity (i.e., $w_2 - w_{fc}$), is considered in the second term of the equation (see Mahfouf et al., 1994). The coefficient C_3 does not depend on w_2 but simply on the soil texture (see 4). Similarly, run-off occurs when w_g or w_2 exceeds the saturation value w_{sat} or when a sub-grid runoff scheme is used. Coefficients C_{1sat}, C_{1max}, C_{2ref} and p are made dependant on the soil texture (Noilhan and Mahfouf, 1996)

Root zone soil layer option

In the standard two-soil layer version of ISBA, it is not possible to distinguish the root zone and the total soil water reservoirs. With the three-layer version, the deepest soil layer may provide water to the root zone through capillary rises only, and the available water content for transpiration is defined as $(w_{sat} - w_{sat}) \times d_2$.

The bulk soil layer (referred to as w_2 in the previous sections) is divided into a root-zone layer (with a depth d_2) and base-flow layer (with a thickness

defined as $d_3 - d_2$). The governing equations for the time evolution of soil moisture for the two sub-surface soil layers are written following Boone et al. (1999) as

$$\frac{\partial w_2}{\partial t} = \frac{1}{\rho_w d_2}\left(P_g - E_g - E_{tr}\right) - \frac{C_3}{d_2\tau}\max\left[0,\,(w_2 - w_{fc})\right] \quad (15)$$

$$- \frac{C_4}{\tau}\left(w_2 - w_3\right) \quad (16)$$

$$\frac{\partial w_3}{\partial t} = \frac{d_2}{(d_3 - d_2)}\left\{\frac{C_3}{d_2\tau}\max\left[0,\,(w_2 - w_{fc})\right] + \frac{C_4}{\tau}\left(w_2 - w_3\right)\right\} \quad (17)$$

$$- \frac{C_3}{(d_3 - d_2)\,\tau}\max\left[0,\,(w_3 - w_{fc})\right]\,; \qquad 0 \le w_3 \le w_{sat} \quad (18)$$

where C_4 represents the vertical diffusion coefficient. It is defined as

$$C_4 = C_{4\,ref}\,\overline{w}_{2,3}{}^{C_{4b}} \quad (19)$$

where $\overline{w}_{2,3}$ represents the interpolated volumetric water content representative of the values at the layer interface (d_2). The $C_{4\,ref}$ and C_{4b} coefficients are defined using the soil sand and clay contents, consistent with the other model parameters (see the section on model coefficients). In addition, the $C_{4\,ref}$ coefficient is scaled as a function of grid geometry. The equations are integrated in time using a fully implicit method.

Exponential profile of k_{sat}

In this version, the soil column assumes an exponential profile of the saturated hydraulic conductivity, k_{sat}, with soil depth (Decharme et al., 2006). This parameterization depends only on two parameters, which represent the rate of decline of the k_{sat} profile and the depth where k_{sat} reaches its so-called "compacted" value.

$$k_{sat}(z) = k_{sat,c}e^{-f(z-d_c)} \quad (20)$$

where $z(m)$ is the depth of the soil profile, $f(m^{-1})$ is the exponential profile decay factor and $d_c(m)$ the compacted depth where k_{sat} reaches its compacted value, $k_{sat,c}$ given by Clapp and Hornberger (1978). In the standard approach, f varies with soil properties (texture and/or rooting depth) but can not exceed $2m^{-1}$ and d_c assumes to be equal to rooting depth d_2. Sensitivity tests to these parameters and a detailed discussion about this parameterization can be found in Decharme et al. (2006). The main hypothesis is that roots and organic matter favor the development of macropores and enhance the water movement near the soil surface, and that soil compaction

is an obstacle for vertical water transfer in the deeper soil. This exponential soil profile increases the saturated hydraulic conductivity at the surface by approximately a factor 10, and its mean value increases in the root zone and decreases in the deep layer in comparison with the values given by Clapp and Hornberger (1978). In ISBA, all hydraulic force-restore coefficients ($C1, C2, C3$ and $C4$) are re-formulated to take into account this k_{sat} profile.

Treatment of runoff in the Isba initial version

Run-off occurs when w_2 exceeds the saturation value w_{sat}. In its standard version, ISBA simulates surface runoff through the saturation excess mechanism (also known as Dune mechanism), therefore, runoff is only produced when the soil is saturated (i.e. w_2 exceeds the saturation value w_{sat}). Note that if w_3 exceeds the saturation, the excess water is added to the drainage term.

When the scale of variability of runoff production is smaller than the typical scale of the grid scale (which is common in most applications), the soil almost never saturates and the runoff production is very low, even though, in reality, a fraction of the cell is saturated and does produce surface runoff.

In order to account for subgrid scale runoff, three parametrisations are available

- the variable Infiltration Capacity (VIC) scheme (Dümenil and Todini, 1992)

- the TOPography based MODEL (TOPMODEL) approach

- the Horton runoff approach

Arpege-climat is using the TOPMODEL parametrisation for the subgrid runoff and the Horton runoff. These two parametrisations are described hereafter.

TOPMODEL approach

TOPMODEL (TOPography based MODEL) attempted to combine the important distributed effects of channel network topology and dynamic contributing areas for runoff generation (Beven et al., 1979; Silvapalan et al., 1987). This formalism takes into account topographic heterogeneities explicitly by using the spatial distribution of the topographic indices, $\lambda_i(m)$, in each grid-cell defined as follows:

$$\lambda_i = \ln\left(a_i / \tan\beta_i\right) \tag{21}$$

where $a_i(m)$ is the drainage area per unit of contour of a local pixel, i, and $\tan\beta_i$ approximates the local hydraulic gradient where β_i is the local surface slope. If the pixel has a large drainage area and a low local slope, its topographic index will be large and thus, its ability to be saturated will be high. Then, this topographic index can be related to a local water deficit, and using the spatial distribution of the topographic indices over the grid cell, a saturated fraction, fsat, inversely proportional to the grid cell mean deficit, $D_t(m)$, can be defined. The "coupling" between TOPMODEL and ISBA was proposed by Habets et al. (2001) and generalized by Decharme et al. (2006). The active layer used for the ISBA-TOPMODEL coupling is the rooting layer, and not the total soil column. TOPMODEL describes generally the evolution of a water storage deficit near the soil surface that reacts quasi-instantaneously following rainy events (Beven et al., 1979). In that case, the root zone appears to be a reasonable compromise in ISBA. So, the relation between the grid cell mean deficit and the soil moisture computed by ISBA is simply expressed as:

$$0 \leq D_t = (w_{sat} - w_2) \times d_2 \leq d_0 \tag{22}$$

where $d_2(m)$ is the rooting depth and $d_0(m)$ the maximum deficit computed as the difference between the saturation, w_sat, and the wilting point, w_wilt :

$$d_0 = (w_{sat} - w_{wilt}) \times d_2 \tag{23}$$

So for a given rooting soil moisture, w_2, a mean deficit, D_t, is calculated and it is therefore possible to determine the saturated fraction of the grid-cell. The runoff, Q_{top}, is thus simply given by: $Q_{top} = P_g \times f_{sat}$ where P_g is the throughfall rain rate. For w_2 lower than the wilting point, the mean deficit is a maximum, $D_t = d_0$, $f_{sat} = 0$ and no surface runoff occurs. Note that, the spatial distribution of the topographic index in each grid-cell can be computed with the three- parameter gamma distribution introduced by Silvapalan et al. (1987). The three parameters are derived from the mean, standard deviation, and skewness of the actual distribution that can be done by the HYDRO1K dataset at a 1 km resolution or another database. This TOPMODEL approach has been intensively validated both at the regional and global scale Decharme et al. (2006 , 2007).

Horton runoff approach.

The Horton runoff occurs for a rainfall intensity that exceeds the effective maximum infiltration capacity. This infiltration excess mechanism tends to

dominate the overland flow production in most desert or semiarid regions where short rainfall events can be very intense, but also where the absence of vegetation and other organic matter prevents the development of a porous soil structure through which water can move easily. The development of a thin crust at the soil surface can also inhibit the infiltration (arid or frozen soil). So the Horton runoff, Q_{hort}, is calculated using two infiltration functions following Decharme et al. (2006):

$$\begin{aligned} Q_{hort} &= (1-\delta_f) \times \max(0, S_m + P_g - I_{unf}) && (24) \\ &\quad +\delta_f \max(0, S_m + P_g - I_f) && (25) \end{aligned}$$

where S_m is snowmelt, P_g the throughfall rain rate, I_{unf} and I_f the infiltration functions over unfrozen and frozen soil, and δ_f the fraction of the frozen soil. These functions depend on root zone soil moisture conditions as well as on soil hydraulic properties. When the Horton runoff (being estimated only on the non-saturated fraction of the grid) is activated with the VIC or the TOPMODEL runoff, the surface runoff is given by :

$$Q_s = Q_{top\_or\_vic} + (1 - f_{sat})\, Q_{hort} \quad (26)$$

Treatment of drainage

The gravitational drainage when $w > w_{fc}$ is given by the following equations (Mahfouf and Noilhan, 1996 ; Boone et al ,1999) :

$$\begin{aligned} K_2 &= \frac{C_3}{\tau}\frac{d_3}{d_2}\max[0, (w_2 - w_{fc})] && (27) \\ K_3 &= \frac{C_3}{\tau}\frac{d_3}{d_3 - d_2}\max[0, (w_3 - w_{fc})] && (28) \end{aligned}$$

where τ is a characteristic time (one day).

C_3 is the *force-restore* parameter which account for the velocity at which the humidity profile is restored to the field capacity. This parameter depends on the hydraulic properties of the soil. In ISBA, it can be described by an empirical equation and depends on the proportion of clay in the grid cell.

$$C_3 = 5.327 \cdot X_{clay}^{-1.043} \quad (29)$$

Subgrid drainage

In the original formulation, the drainage stops below the field capacity w_{fc}. Within the framework of the Safran-Isba-Modcou model (Habets et al., 2008) a subgrid drainage was introduced in order to account for unresolved aquifers in the model. A residual drainage was introduced in ISBA. The equations above are slightly modified :

$$K_2 = \frac{C_3}{\tau}\frac{d_3}{d_2}\max[w_{d2}, (w_2 - w_{fc})] \tag{30}$$

$$K_3 = \frac{C_3}{\tau}\frac{d_3}{d_3 - d_2}\max[w_{d3}, (w_3 - w_{fc})] \tag{31}$$

In this formulation, w_{di} (for each layer i) is expressed as :

$$w_{di} = w_{drain} max\left(0, \frac{min(w_{fc}, w_i) - w_{g_{min}}}{w_{fc} - w_{g_{min}}}\right) \tag{32}$$

where w_{drain} is a parameter to be calibrated, and $w_{g_{min}}$ a small parameter to avoid numerical problems.

w_{drain} must be calibrated using discharge measurements during dry periods. See Caballero et al. (2007) and Habets et al. (2008) for calibration with discharge for the Safran-Isba-Modcou model.

Treatment of soil ice

The inclusion of soil freezing necessitates the addition of so-called phase change to the thermal and hydrologic transfer equations. In addition, a freezing/drying wetting/thawing analogy is used to model changes in the force-restore coefficients so that they must also be modified accordingly. Terms which have been added to the baseline ISBA scheme are underlined in this section, while terms which are modified are denoted using an $*$ superscript. Additional details related to soil freezing scheme can be found in Boone et al. (2000, 2001).

2.2 Treatment of the canopy water

Rainfall and dew intercepted by the foliage feed a reservoir of water content W_r. This amount of water evaporates in the air at a potential rate from the fraction δ of the foliage covered with a film of water, as the remaining part $(1 - \delta)$ of the leaves transpires.

$$\delta = \left(\frac{W_r}{W_{rmax}}\right)^{2/3} \tag{33}$$

Following Deardorff (1978), we set

$$\frac{\partial W_r}{\partial t} = vegP - (E_v - E_{tr}) - R_r \ ; \ 0 \leq W_r \leq W_{rmax} \tag{34}$$

where P is the precipitation rate at the top of the vegetation, E_v is the evaporation from the vegetation including the transpiration E_{tr} and the direct evaporation E_r when positive, and the dew flux when negative (in this case $E_{tr} = 0$), and R_r is the runoff of the interception reservoir. This runoff occurs when W_r exceeds a maximum value W_{rmax} depending upon the density of the canopy, i.e., roughly proportional to $vegLAI$. According to Dickinson (1984), we use the simple equation:

$$W_{rmax} = 0.2 vegLAI \qquad [mm] \tag{35}$$

2.3 Spatial variability of precipitation intensities

SURFEX offers 2 options for spatial distribution of rainfall intensity : to activate an homogeneous distribution or an exponential distribution which depends on the fraction of the mesh where it rains. ARPEGE-CLIMAT is set with the second option.

With this option, the main assumption is that, generally, the rainfall intensity is not distributed homogeneously over an entire grid cell. As a first-order approximation, the sub- grid variability in liquid precipitation, P_i, can be given by an exponential probability density distribution, $f(P_i)$:

$$f(P_i) = \frac{\mu}{P} e^{-\mu \frac{P_i}{P}} \tag{36}$$

where P represent the mean rainfall rate over the grid cell and μ a fraction of the grid cell affected by rainfall. μ is calculated using the results of Fan et al. (1996), who showed an exponential relationship between the fractional coverage of precipitation and rainfall rate, based on their analyses of over 2 years radar observations and rain gauge measurements over the Arkansas-Red river basin in the southern plains of the United States. This relationship is:

$$\mu = 1 - e^{-\beta P} \tag{37}$$

where β is a parameter which depends on grid resolution, dx :

$$\beta = 0.2 + 0.5 e^{-0.001 dx} \tag{38}$$

dx represents represents lengths of square grid cells ranging from 40km to 500km. In consequence, the μ parameter is fixed to 1 at high resolution ($\leq 10km$). This Spatial variability of precipitation intensities induces a new expression for the runoff from the interception reservoir, W_r :

$$W_r = P \times e^{\frac{\mu(W_r - W_{r_{max}})}{P\Delta t}} \tag{39}$$

The second consequence is that the Horton runoff, Q_{hort}, is calculated by integrating the difference between the local rainfall and the local maximum infiltration capacity, I_i, as follows:

$$Q_{hort} = \mu \int_{I_i}^{\infty} (P_i - I_i)\, f(P_i) dP_i \tag{40}$$

Another assumption is made on the spatial heterogeneity of the local maximum infiltration capacity. Its spatial distribution can also be approximated by an exponential probability density distribution:

$$g(I_i) = \frac{1}{\overline{I}} e^{-\frac{I_i}{\overline{I}}} \tag{41}$$

where $\overline{I}$ is the mean maximum infiltration rate over the grid cell. As previously said, $\overline{I}$ is calculated for unfrozen and frozen soil conditions. So Eq.40 , without snowmelt, can be noted as :

$$\begin{aligned} Q_{hort} &= \mu(1-\delta_f) \int_0^{\infty} \int_{I_{unf,i}}^{\infty} (P_i - I_{unf,i}) f(P_i) g(I_{unf,i}) dP_i dI_{unf,i} \\ &\quad + \mu\delta_f \int_0^{\infty} \int_{I_{f,i}}^{\infty} (P_i - I_{f,i}) f(P_i) g(I_{f,i}) dP_i dI_{f,i} \end{aligned} \tag{42}$$

After some mathematical developments, the Horton runoff in presence of rainfall and snowmelt, S_m, is given following Decharme et al. (2006):

$$\begin{aligned} Q_{hort} &= (1-\delta_f) \left(\frac{P}{1 + \overline{I_{unf}} \frac{\mu}{P}} + max(0, S_m - \overline{I_{unf}}) \right) \\ &\quad + \delta_f \left(\frac{P}{1 + \overline{I_f} \frac{\mu}{P}} + max(0, S_m - \overline{I_f}) \right) dP_i dI_{f,i} \end{aligned} \tag{43}$$

2.4 Treatment of the snow

One-layer snow scheme option and Multi-layer snow scheme option are available with SURFEX. This section will describe the one-layer snow scheme option used by ARPEGE-CLIMAT.

The evolution of the equivalent water content of the snow reservoir is given by

$$\frac{\partial W_s}{\partial t} = P_s - E_s - melt \tag{44}$$

where P_s is the precipitation of snow, and E_s is the sublimation from the snow surface.

The presence of snow covering the ground and vegetation can greatly influence the energy and mass transfers between the land surface and the atmosphere. Notably, a snow layer modifies the radiative balance at the surface by increasing the albedo. To consider this effect, the albedo of snow α_s is treated as a new prognostic variable. Depending if the snow is melting or not, α_s decreases exponentially or linearly with time.

If there is no melting (i.e., $melt = 0$):

$$\alpha_s(t) = \alpha_s(t - \Delta t) - \tau_a \frac{\Delta t}{\tau} + \frac{P_s \Delta t}{W_{crn}}(\alpha_{smax} - \alpha_{smin}) \tag{45}$$

$$\alpha_{smin} \leq \alpha_s \leq \alpha_{smax} \tag{46}$$

where $\tau_a = 0.008$ is the linear rate of decrease per day, $\alpha_{smin} = 0.50$ and $\alpha_{smax} = 0.85$ are the minimum and maximum values of the snow albedo.

If there is melting (i.e., $melt > 0$):

$$\alpha_s(t) = [\alpha_s(t - \Delta t) - \alpha_{smin}] \exp\left[-\tau_f \frac{\Delta t}{\tau}\right] + \alpha_{smin} + \frac{P_s \Delta t}{W_{crn}}(\alpha_{smax} - \alpha_{smin}) \tag{47}$$

$$\alpha_{smin} \leq \alpha_s \leq \alpha_{smax} \tag{48}$$

where $\tau_f = 0.24$ is the exponential decrease rate per day. Of course, the snow albedo increases as snowfalls occur, as shown by the second terms of Eqs. (21) and (23).

The average albedo of a model grid-area is expressed as

$$\alpha_t = (1 - p_{sn})\alpha + p_{sn}\alpha_s \tag{49}$$

Similarly, the average emissivity ϵ_t is also influenced by the snow coverage:

$$\epsilon_t = (1 - p_{sn})\epsilon + p_{sn}\epsilon_s \tag{50}$$

where $\epsilon_s = 1.0$ is the emissivity of the snow. Thus, the overall albedo and emissivity of the ground for infrared radiation is enhanced by snow.

Because of the significant variability of thermal properties related with the snow compactness, the relative density of snow ρ_s is also considered as a prognostic variable. Based on Verseghy (1991), ρ_s decreases exponentially at a rate of τ_f per day:

$$\rho_s(t) = [\rho_s(t - \Delta t) - \rho_{smax}] \exp\left[-\tau_f \frac{\Delta t}{\tau}\right] + \rho_{smax} + \frac{P_s \Delta t}{W_s} \rho_{smin} \quad (51)$$

$$\rho_{smin} \leq \rho_s \leq \rho_{smax} \quad (52)$$

where $\rho_{smin} = 0.1$ and $\rho_{smax} = 0.3$ are the minimum and maximum relative density of snow.

Finally, the average roughness length z_{0t} is

$$z_{0t} = (1 - p_{snz0}) z_0 + p_{snz0} z_{0s} \quad (53)$$

where

$$p_{snz0} = \frac{W_s}{W_s + W_{crn} + \beta_s g z_0} \quad (54)$$

Here, $\beta_s = 0.408\ s^2 m^{-1}$ and $g = 9.80665\ ms^{-2}$ are physical constants, whereas z_{0s} is the roughness length of the snow.

2.5 The surface fluxes

Only one energy balance is considered for the whole system ground-vegetation-snow (when the 3-layer snow scheme option is not in use). As a result, heat and mass transfers between the surface and the atmosphere are related to the mean values T_s and w_g.

The net radiation at the surface is the sum of the absorbed fractions of the incoming solar radiation R_G and of the atmospheric infrared radiation R_A, reduced by the emitted infrared radiation:

$$R_n = R_G(1 - \alpha_t) + \epsilon_t \left(R_A - \sigma_{SB} {T_s}^4\right) \quad (55)$$

where σ_{SB} is the Stefan-Boltzmann constant.

The turbulent fluxes are calculated by means of the classical aerodynamic formulas. For the sensible heat flux:

$$H = \rho_a c_p C_H V_a (T_s - T_a) \quad (56)$$

where c_p is the specific heat; ρ_a, V_a, and T_a are respectively the air density, the wind speed, and the temperature at the lowest atmospheric level; and C_H, as discussed below, is the drag coefficient depending upon the thermal stability of the atmosphere. The explicit snow scheme sensible heat flux is calculated using the same formulation (but with T_{sn}). The water vapor flux E is the sum of the evaporation of liquid water from the soil surface (i.e., $E_{g\,l}$), from the vegetation (i.e., E_v), and sublimation from the snow and soil ice (i.e, E_s and $E_{g\,f}$):

$$
\begin{aligned}
LE &= LE_{g\,l} + LE_v + L_i\,(E_s + E_{g\,f}) && (57)\\
E_{g\,l} &= (1-veg)(1-p_{sng})\,(1-\delta_i)\;\rho_a C_H V_a\,(h_u q_{sat}(T_s) - q_a) && (58)\\
E_v &= veg(1-p_{snv})\rho_a C_H V_a h_v\,(q_{sat}(T_s) - q_a) && (59)\\
E_s &= p_{sn}\rho_a C_H V_a\,(q_{sat}(T_s) - q_a) && (60)\\
E_{g\,f} &= (1-veg)\,(1-p_{sng})\;\delta_i\,\rho_a C_H V_a\,(h_{ui}\,q_{\rm sat}\,(T_s)\;-\;q_a) && (61)
\end{aligned}
$$

where L and L_i are the specific heat of evaporation and sublimation, $q_{sat}(T_s)$ is the saturated specific humidity at the temperature T_s, and q_a is the atmospheric specific humidity at the lowest atmospheric level. The water vapor flux E from the explicit snow surface is expressed as

$$
\begin{aligned}
LE\,(T_{sn\,1}) &= LE_{sl} + L_i E_s && (62)\\
E_{sl} &= \delta_{sn}\,\rho_a C_{Hs} V_a\,(q_{sat}\,(T_{sn\,1}) - q_a) && (63)\\
E_s &= (1-\delta_{sn})\;\rho_a C_{Hs} V_a\,(q_{sat}\,(T_{sn\,1}) - q_a) && (64)\\
\delta_{sn} &= w_{sl\,1}/w_{sl\,\max 1}\,; \qquad 0 \le \delta_{sn} \le 1 && (65)
\end{aligned}
$$

where evaporation of liquid water is zero when $T_{sn\,1} < T_0$. The transfer coefficient (C_{Hs}) is calculated over the snow covered surface using the same formulation as C_H.

The surface ice fraction is is used to partition the bare soil latent heat flux between evaporation and sublimation, and it is defined as

$$
\delta_i = w_{g\,f}/\,(w_{g\,f} + w_g)\;; \qquad 0 \le \delta_i < 1\;\;. \tag{66}
$$

The relative humidity h_u at the ground surface is related to the superficial soil moisture w_g following

$$
\begin{aligned}
h_u &= \frac{1}{2}\left[1 - cos\left(\frac{w_g}{{w_{fc}}^*}\pi\right)\right]\;,\ \text{if } w_g < {w_{fc}}^* && (67)\\
h_u &= 1 && (68)\\
&,\ \text{if } w_g \ge {w_{fc}}^* && (69)
\end{aligned}
$$

where the field capacity with respect to the liquid water is defined using the modified soil porosity so that ${w_{fc}}^* = w_{fc} w^*_{sat}/w_{sat}$. The humidity for the ice covered portion of the grid box is calculated in a similar fashion as

$$h_{ui} = \frac{1}{2}\left[1 - cos\left(\frac{w_{gf}}{{w_{fc}}^{**}}\pi\right)\right] \text{ , if } w_{gf} < {w_{fc}}^{**} \quad (70)$$

$$h_{ui} = 1 \quad (71)$$

$$\text{, if } w_{gf} \geq {w_{fc}}^{**} \quad (72)$$

where ${w_{fc}}^{**} = w_{fc}(w_{sat} - w_g)/w_{sat}$. In case of dew flux when $q_{sat}(T_s) < q_a$, h_u is also set to 1 (see Mahfouf and Noilhan, 1991 for details). When the flux E_v is positive, the Halstead coefficient h_v takes into account the direct evaporation E_r from the fraction δ of the foliage covered by intercepted water, as well as the transpiration E_{tr} of the remaining part of the leaves:

$$h_v = (1-\delta)R_a/(R_a + R_s) + \delta \quad (73)$$

$$E_r = veg(1 - p_{snv})\frac{\delta}{R_a}\left(q_{sat}(T_s) - q_a\right) \quad (74)$$

$$E_{tr} = veg(1 - p_{snv})\frac{1-\delta}{R_a + R_s}\left(q_{sat}(T_s) - q_a\right) \quad (75)$$

When E_v is negative, the dew flux is supposed to occur at the potential rate, and h_v is taken equal to 1.

Following Deardorff (1978), δ is a power function of the moisture content of the interception reservoir:

$$\delta = (W_r/W_{rmax})^{2/3} \quad (76)$$

The aerodynamic resistance is $R_a = (C_H V_a)^{-1}$. The surface resistance, R_s, depends upon both atmospheric factors and available water in the soil; it is given by:

$$R_s = \frac{R_{smin}}{F_1 F_2 F_3 F_4 LAI} \quad (77)$$

with the limiting factors F_1, F_2, F_3, and F_4:

$$F_1 = \frac{f + R_{smin}/R_{smax}}{1 + f} \quad (78)$$

$$F_2 = \frac{w_2 - w_{wilt}}{w_{fc} - w_{wilt}} \quad and\ 0 \leq F_2 \leq 1 \quad (79)$$

$$F_3 = 1 - \gamma\left(q_{sat}(T_s) - q_a\right) \quad (80)$$

$$F_4 = 1 - 1.6 \times 10^{-3}(T_a - 298.15)^2 \quad (81)$$

where the dimensionless term f represents the incoming photosynthetically active radiation on the foliage, normalized by a species-dependent threshold value:

$$f = 0.55 \frac{R_G}{R_{Gl}} \frac{2}{LAI} \tag{82}$$

Moreover, γ is a species-dependent parameter (see Jacquemin and Noilhan, 1990) and R_{smax} is arbitrarily set to 5000 sm^{-1}.

The surface fluxes of heat, moisture, and momentum can be expressed as

$$(\overline{w'\theta'})_s = \frac{H}{\rho_a c_p T_a/\theta_a} \tag{83}$$

$$(\overline{w'r'_v})_s = \frac{E}{\rho_a(1-q_a)} \tag{84}$$

$$|\overline{w'V'}|_s = C_D|V_a|^2 = u_*^2 \tag{85}$$

where r_v is the water vapor mixing ratio, w is the vertical motion, θ_a is the potential temperature at the lowest atmospheric level. The primes and overbars denote perturbation and average quantities.

For the drag coefficients C_H and C_D, the formulation of Louis (1979) was modified in order to consider different roughness length values for heat z_0 and momentum z_{0h} (Mascart et al., 1995):

$$C_D = C_{DN} F_m \ ; \ C_H = C_{DN} F_h \tag{86}$$

with

$$C_{DN} = \frac{k^2}{[ln(z/z_0)]^2} \tag{87}$$

where k is the Von Karmann constant. Also

$$F_m = 1 - \frac{10Ri}{1 + C_m\sqrt{|Ri|}} \qquad if\ Ri \leq 0 \tag{88}$$

$$F_m = \frac{1}{1 + \frac{10Ri}{\sqrt{1+5Ri}}} \tag{89}$$

$$if\ Ri > 0 \tag{90}$$

and

$$F_h = \left[1 - \frac{15Ri}{1 + C_h\sqrt{|Ri|}}\right] \times \left[\frac{ln(z/z_0)}{ln(z/z_{0h})}\right] \tag{91}$$

$$if\ Ri \leq 0 \tag{92}$$

$$F_h = \frac{1}{1 + 15Ri\sqrt{1+5Ri}} \times \left[\frac{ln(z/z_0)}{ln(z/z_{0h})}\right] \tag{93}$$

$$if\ Ri > 0 \tag{94}$$

where Ri is the gradient Richardson number. The coefficients C_m and C_h of the unstable case are given by

$$C_m = 10{C_m}^* C_{DN}(z/z_0)^{p_m} \quad (95)$$

$$C_h = 15{C_h}^* C_{DN}(z/z_{0h})^{p_h} \times \left[\frac{ln(z/z_0)}{ln(z/z_{0h})}\right] \quad (96)$$

where C_m^*, C_h^*, p_m, and p_h are functions of the ratio $\mu = ln(z_0/z_{0h})$ only:

$$C_h^* = 3.2165 + 4.3431 \times \mu + 0.5360 \times \mu^2 - 0.0781 \times \mu^3 \quad (97)$$

$$C_m^* = 6.8741 + 2.6933 \times \mu - 0.3601 \times \mu^2 + 0.0154 \times \mu^3 \quad (98)$$

$$p_h = 0.5802 - 0.1571 \times \mu + 0.0327 \times \mu^2 - 0.0026 \times \mu^3 \quad (99)$$

$$p_m = 0.5233 - 0.0815 \times \mu + 0.0135 \times \mu^2 - 0.0010 \times \mu^3 \quad (100)$$

2.6 Summary of Useful Parameters

The parameters have been chosen in order to characterize the main physical processes, while attempting to reduce the number of independant variables. They can be divided into two categories: primary parameters needing to be specified by spatial distribution, and secondary parameters which values can be associated with those of the primary parameters.

In the present state of the method, the primary parameters describe the nature of the land surface and its vegetation coverage by means of only four numerical indices: the percentage of sand and clay in the soil, the dominant vegetation type, and the land-sea mask.

The secondary parameters associated with the soil type are evaluated from the sand and clay composition of the soil, according to the continuous formulation discussed in Giordani (1993) and Noilhan et al. (1995) (see 4). These parameters are:

- the saturated volumetric moisture content w_{sat};
- the wilting point volumetric water content w_{wilt}; NoilhanL1995
- the field capacity volumetric water content w_{fc};
- the slope b of the retention curve;
- the soil thermal coefficient at saturation C_{Gsat};
- the value of C_1 at saturation (i.e., C_{1sat});

- the reference value of C_2 for $w_2 = 0.5 w_{sat}$ (i.e., C_{2ref});
- the drainage coefficient C_3 ;
- the diffusion coefficients $C_{4\,ref}$ and C_{4b} ;
- and the coefficients a, p for the w_{geq} formulation.

On the other hand, the parameters associated with the vegetation can either be derived from the dominant vegetation type, or be specified from existing classification or observations. They are

- the fraction of vegetation veg;
- the depth of the soil column d_2 (or the root zone depth);
- the depth of the soil column d_3 (if third soil layer option in use);
- the minimum surface resistance R_{smin};
- the leaf area index LAI;
- the heat capacity C_v of the vegetation;
- the R_{Gl} and γ coefficients found in the formulation of the surface resistance R_s;
- and the roughness length for momentum z_0 and for heat z_{0h}.

Other necessary parameters are

- the albedo α
- the emissivity ϵ.
- and characteristic time scale for phase changes (currently constant) τ_i.

3 Water surfaces

3.1 Simple parameterization

Free water surfaces

For ocean surfaces and over inland waters, all the prognostic variables are kept constant.

The surface fluxes are calculated using Eqs. 55, 56, 58 and Eqs. 83, 84, 85 of Isba, taking the relative humidity of the ocean $hu = 1$, and $veg = p_{sn} = 0$. The roughness length is given by Charnock's relation:

$$z_{0sea} = 0.015\frac{u_*^2}{g} \tag{101}$$

Sea ice

Sea ice is detected in the model when sea surface temperature (SST) is two degrees below 0°C (i.e. 271.15 K). In this case, in order to avoid an overestimation of the evaporation flux, the calculations are performed with the roughness length of flat snow surfaces:

$$z_{0ice} = 10^{-3}m \tag{102}$$

In the same manner, the sea ice albedo is set equal to the fresh snow albedo instead of the free water albedo. This leads to a much brighter surface. This has no effect on the sea ice cover (since there is no evolution of the sea surface parameters), but modifies the lower boundary shortwave flux input for the atmospheric radiative scheme.

Sea surface turbulent fluxes

Various sea surface fluxes parameterizations available in the SURFEX surface scheme. In addition to the direct parameterization from Louis (1979), two iterative parameterizations are avalaible : the COARE3.0 (Fairall et al., 2003) and ECUME (Belamari, 2005) parameterizations. ARPEGE-CLIMAT uses the ECUME parametrization.

Bulk equations

Bulk parameterizations estimate the surface fluxes from mean meteorological gradients in the atmospheric boundary layer. This method 's aim is to determine the transfer coefficients that directly link the surface flux with the meteorological gradients between the surface and a "measurement's height" (Liu et al, 1979).

The surface turbulent fluxes, *i.e.* the stress or the momentum flux τ_{sea}, the sensible heat flux H_{sea} and the latent heat flux LE_{sea} are expressed by:

$$\begin{cases} |\vec{\tau}|_{sea} = \rho_a\overline{w'u'} = -\rho_a u_*^2 \\ H_{sea} = \rho_a c_{p_a}\overline{w'\theta'} = -\rho_a c_{p_a} u_*\theta_* \\ LE_{sea} = \rho_a\mathcal{L}_v\overline{w'q'} = -\rho_a\mathcal{L}_v u_* q_* \end{cases} \tag{103}$$

where u', θ' and q' are the vertical perturbations of wind, temperature potential and specific humidity, u_*, θ_* and q_* are the characteristic scale parameters from Monin-Obukhov.

Considering the bulk parameterizations using transfer coefficients:

$$\begin{cases} |\vec{\tau}|_{sea} = -\rho_a C_D U^2 \\ H_{sea} = \rho_a c_{p_a} C_H U(\theta_s - \theta_a) \\ LE_{sea} = \rho_a \mathcal{L}_v C_E U(q_s - q_a) \end{cases} \tag{104}$$

s indicates sea surface variables whereas a indicates atmospheric variables at first level. U is the mean value of the relative wind. Here, we choose the atmospheric convention, *i. e.* fluxes are defined positive in case of energy benefit for the atmosphere.

From equations (103) and (104), we can write:

$$\begin{cases} C_D = \left(\frac{u_*}{U}\right)^2 \\ C_H = \frac{u_*\theta_*}{U(\theta_a - \theta_s)} \\ C_E = \frac{u_* q_*}{U(q_a - q_s)} \end{cases} \tag{105}$$

In a general way, the transfer coefficient for the X variable is:

$$C_X = \frac{\overline{w'x'}}{U\Delta X} \tag{106}$$

with X equal D for drag, H for heat and E for evaporation and ΔX is the gradient of x ($= u$, θ or q) between the ocean surface and the atmospheric low level.

Each coefficient is divided in two components:

$$C_X = c_x^{\frac{1}{2}} c_d^{\frac{1}{2}} \tag{107}$$

that could be expressed following the Monin-Obukhov's similitude theory as a function of the first atmospheric level height z, of atmospheric stratification with a parameter ζ, of roughness lengths (z_0, z_{0_t} and z_{0_q}) and of the Von Karman's constant κ:

$$c_x^{\frac{1}{2}}(\zeta) = C_{x10n}^{\frac{1}{2}} F_x(\zeta, \kappa, C_{x10n}^{\frac{1}{2}}) \tag{108}$$

$$C_{x10n}^{\frac{1}{2}} = \frac{\kappa}{\ln(\frac{z}{z_{0x}})} \tag{109}$$

Roughness lengths are generally computed thanks to the relationship:

$$z_0 = \frac{\alpha u_*^2}{g} + \frac{\beta \nu}{u_*} \tag{110}$$

where α (also called the Charnock's constant) and β are numerical constants and ν is the dynamical viscosity.

Each of the following parameterizations uses its own closure hypothesis with a theoretical method or resulting from experimentation to determine the exchange coefficients from neutral transfer coefficients at 10m $C_{D_{10n}}$, $C_{H_{10n}}$ and $C_{E_{10n}}$ (*i.e.* for $\zeta = 0$) and from a stability function F_x and roughness lengths (Lebeaupin et al., 2007).

Iterative parameterizations
Bulk equations could be resolve with iterative methods on the stability parameter and the characteristic scale parameters from Monin-Obukhov. Convergence criteria vary according to the parameterizations. They also differ in the representation of various processes as waves effects, sea spray, seawater salinity effect on evaporation, wind gusts and especially in the calculation of the roughness lengths or of the transfer coefficients.

.

The Liu et al (1979) algorithm is the most used iterative algorithm for the turbulent air-sea fluxes computation and was also a base for new parameterizations developments (for example, COARE or the ECUME parameterization).

The ECUME parameterization
The unified parameterization or ECUME (Exchange Coefficients from Unified Multi-campaigns Estimates) is a bulk iterative parameterization developed in order to obtain an optimized parameterization covering a wide range of atmospheric and oceanic conditions.

Based on the LKB algorithm, ECUME includes an estimation of neutral transfer coefficients at 10m from a multi-campaign calibration derived from the ALBATROS database that collects data from five flux measurement campaigns:

- POMME "Programme Océanique Multidisciplinaire à Moyenne Echelle",
- FETCH "Flux, Etat de la mer et Télédetection en Condition de Fetch",
- SEMAPHORE "Structure des Echanges Mer-Atmosphère, Propriétés des Hétérogénéités Océaniques : Recherche Expérimentale",

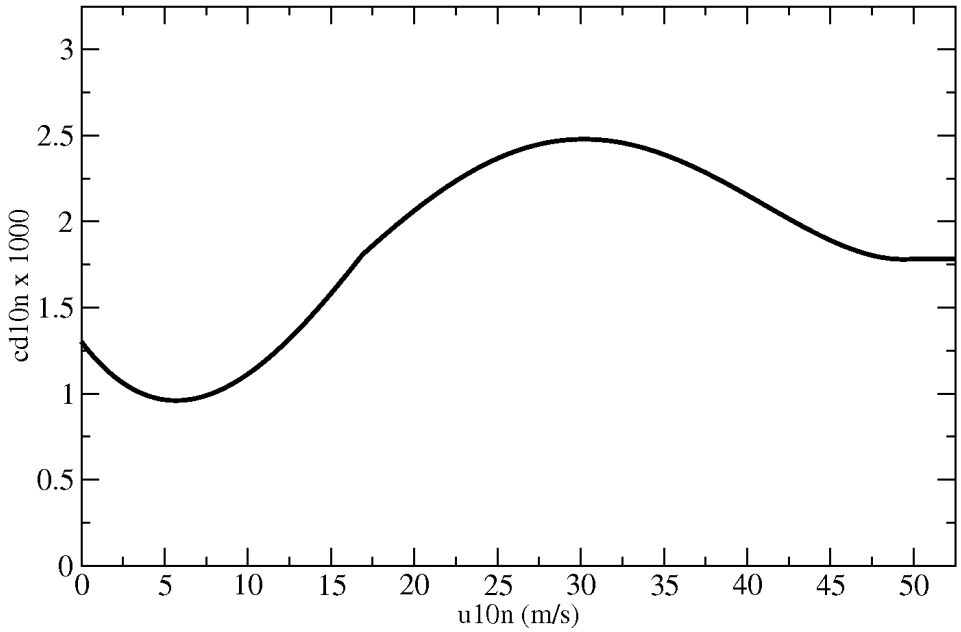

Figure 3: Multi-campaign calibration of the neutral drag coefficient at 10 meters $C_{D_{10n}}$.

- CATCH "Couplage avec l'ATmosphère en Conditions Hivernales",
- EQUALANT99.

A more detailed description of each campaign could be found in Weill et al (2003) and Belamari ().

A similar post-processing was applied to the five campaigns data to derive the drag coefficient $C_{D_{10n}}$, the heat coefficient $C_{H_{10n}}$ and the evaporation coefficient $C_{E_{10n}}$ as neutral 10m-wind functions (Figures 3, 4 and 5).

The ECUME parameterization main characteristic are:

1. An important effort was done on the ECUME algorithm in order to assure the convergence in maximum 20 iterations for every kind of conditions. The iterative sequence is stopped when the difference between the scale parameters between two iterations is inferior to prescribed threshold that are 2.10^{-4} m s^{-1} for u_*, 2.10^{-4} K for θ_* and 2.10^{-7} kg/kg for q_*.

   The closure relationship is the multi-campaign calibration of the neutral transfer coefficients at 10 meters.

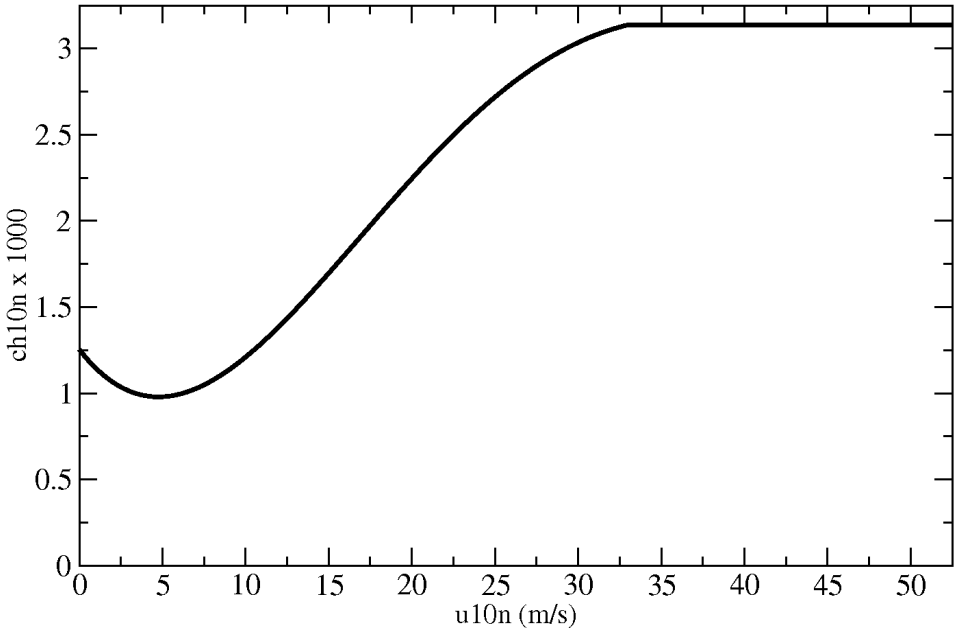

Figure 4: Multi-campaign calibration of the neutral heat coefficient at 10 meters $C_{H_{10n}}$.

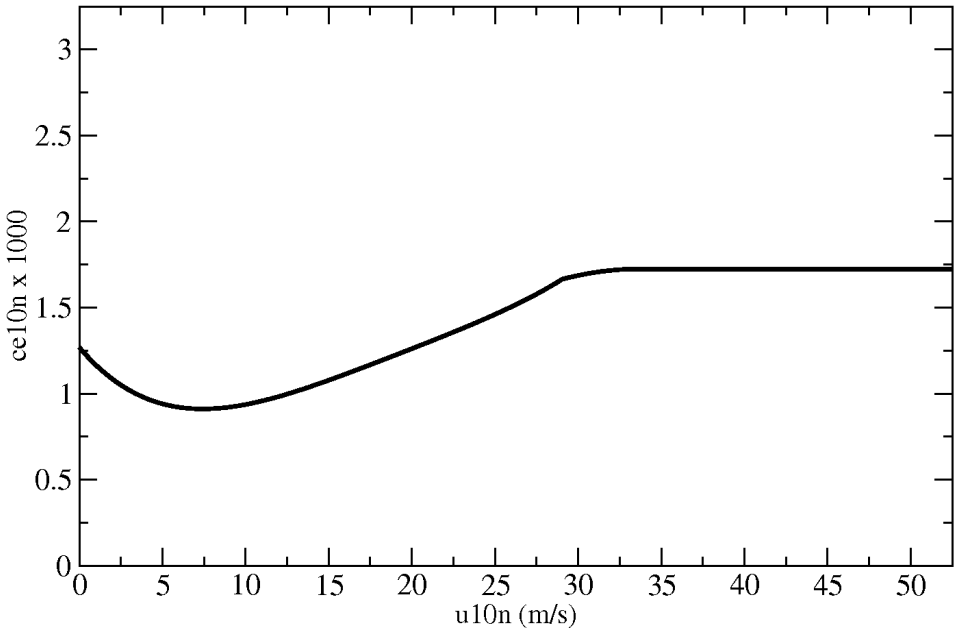

Figure 5: Multi-campaign calibration of the neutral evaporation coefficient at 10 meters $C_{E_{10n}}$.

2. The stability functions are Businger's functions with different coefficients than COARE3.0: ψ_m and ψ_h depend on the Monin-Obukhov's length $\zeta = \frac{z}{L}$ which is computed as described in the following equations:

   - For wind:

   $$ZL = \frac{g\kappa z(T_*(1 + r_0 q) + r_0 T q_*)}{T(1 + r_0 q) \times [MAX(u_*, 1.10^{-9})]^2}$$

   with $r_0 = R_v/R_a - 1$.

   $$si \;\; ZL \geq 0 \quad z/L = MIN(ZL, 0.25) \tag{111}$$
   $$si \;\; ZL < 0 \quad z/L = MAX(ZL, -200) \tag{112}$$

   - For temperature and humidity:

   $$(z/L)_t = z/L \times \frac{z_t}{z} \; ; \qquad (z/L)_q = z/L \times \frac{z_q}{z}$$

   Finally:

$\zeta = \frac{z}{L}$	$\psi_m(\zeta) =$	$\psi_h(\zeta) =$
stable	$-\Gamma\zeta$	$-\Gamma\zeta$
$(\zeta \geq 0)$	$\Gamma = 7$	
unstable:	$(1-f)\psi_{mK} + f\psi_{mC}$	$(1-f)\psi_{hK} + f\psi_{hC}$
$(\zeta < 0)$	$f = \frac{\zeta^2}{(1.0+\zeta^2)}$	
Kansas	$\psi_{mK} = 2ln(\frac{1+x}{2}) + ln(\frac{1+x^2}{2}) - 2arctan(x) + \frac{\pi}{2}$ with $x = (1-16\zeta)^{\frac{1}{4}}$	$\psi_{hK} = 2ln(\frac{1+x}{2})$ with $x = (1-16\zeta)^{\frac{1}{2}}$
Convective	$\psi_{mC} = \frac{3}{2}ln(\frac{y^2+y+1}{3}) - \sqrt{3}arctan(\frac{2y+1}{\sqrt{3}}) + \frac{\pi}{\sqrt{3}}$ with $y = (1-12.87\zeta)^{\frac{1}{3}}$	$\psi_{hC} = \frac{3}{2}ln(\frac{y^2+y+1}{3}) - \sqrt{3}arctan(\frac{2y+1}{\sqrt{3}}) + \frac{\pi}{\sqrt{3}}$ with $y = (1-12.87\zeta)^{\frac{1}{3}}$

3. The roughness length is given by (Eq. 110) with $\alpha = 0.011$ and $\beta = 0.11$.

4. The reduction of 2% of the specific humidity at saturation due to seawater salinity is applied (eq. 113, Kraus (1972).

$$q_s = 0.98 \times q_{sat}(\theta_s) \tag{113}$$

5. The gustiness correction could be applied (Eq. 114).

$$w_g = \beta_{gust}(bf.z_{bl})^{\frac{1}{3}} \tag{114}$$

6. The corrections due to precipitation τ_p and H_p according to Fairall et al. (1996) and Gosnell et al. (1995) could also be computed in the ECUME parameterization (Eq. 115 and 116).

$$\tau_p = \frac{\mathcal{R}U}{3600} \tag{115}$$

$$H_p = \tilde{\mathcal{R}} c_{p_r} \epsilon (T_s - T_a) \left(1 + \frac{1}{B}\right) \tag{116}$$

7. The Webb's correction (LE_{webb}) is a correction applied to the latent heat flux. It is due to air density variations when the humidity vary under the evaporation action. If $\bar{w}$ is the mean value of the vertical perturbations,

$$\overline{w} = 1.61\overline{w'q'} + (1 + 1.61q)\frac{\overline{w'T'}}{T} \tag{117}$$

the Webb's correction expression is:

$$LE_{Webb} = \rho_a \mathcal{L} \overline{w} q \tag{118}$$

where $\mathcal{L}$ is the latent heat of vaporization for water.

8. No waves effects are taking into account in the ECUME parameterization.

4 Parametrization of the surface boundary layer

Diagnostics computed by SURFEX within the routine atmosphere 'ARO_GROUND_DIAG':

- surface humidity
- roughness lenght for momentum
- roughness length for heat
- temperature at 2m
- specific humidity at 2m

- relative humidity at 2m
- zonal wind at 10 m
- meridional wind at 10 m
- longwave budget between Arpege and Surfex
- shortwave budget between Arpege and Surfex
- surface latent heat flux

For more details you can refer to the Scientific Documentation at the http://www.cnrm.meteo.fr/surfex/.

Appendix A: Continuous formulation of the soil secondary parameters

The sand and clay composition (i.e., $SAND$ and $CLAY$) are expressed in percentage.

The saturated volumetric water content ($m^3 m^{-3}$):

$$w_{sat} = (-1.08SAND + 494.305) \times 10^{-3} \tag{119}$$

The wilting point volumetric water content ($m^3 m^{-3}$):

$$w_{wilt} = 37.1342 \times 10^{-3} (CLAY)^{0.5} \tag{120}$$

The field capacity volumetric water content ($m^3 m^{-3}$):

$$w_{fc} = 89.0467 \times 10^{-3} (CLAY)^{0.3496} \tag{121}$$

The slope of the retention curve:

$$b = 0.137CLAY + 3.501 \tag{122}$$

The soil thermal coefficient at saturation ($Km^2 J^{-1}$):

$$C_{Gsat} = -1.557 \times 10^{-2} SAND - 1.441 \times 10^{-2} CLAY + 4.7021 \tag{123}$$

The value of C_1 at saturation:

$$C_{1sat} = (5.58CLAY + 84.88) \times 10^{-2} \tag{124}$$

The value of C_2 for $w_2 = 0.5w_{sat}$:

$$C_{2ref} = 13.815CLAY^{-0.954} \tag{125}$$

The coefficient C_3:

$$C_3 = 5.327CLAY^{-1.043} \tag{126}$$

The coefficient C_{4b}:

$$C_{4b} = 5.14 + 0.115\,CLAY \tag{127}$$

The coefficient $C_{4\,ref}$:

$$C_{4\,ref} = \frac{2(d_3 - d_2)}{(d_2\,{d_3}^2)} \log_{10}{}^{-1}\left[\beta_0 + \sum_{j=1}^{3}\left(\beta_j\,SAND^j + \alpha_j\,CLAY^j\right)\right] \tag{128}$$

where the $\beta_j\,(j = 0, 3)$ coefficients are 4.42×10^{-0}, 4.88×10^{-3}, 5.93×10^{-4} and -6.09×10^{-6}. The $\alpha_j\,(j = 1, 3)$ coefficients are defined as -2.57×10^{-1}, 8.86×10^{-3} and -8.13×10^{-5}.

The coefficients for the w_{geq} formulation:

$$a = 732.42 \times 10^{-3} CLAY^{-0.539} \tag{129}$$

$$p = 0.134CLAY + 3.4 \tag{130}$$

Appendix B: Gaussian formulation for the C_1 coefficient

For dry soils (i.e., $w_g < W_{wilt}$), the C_1 coefficient in Eq. (13) is approximated by the Gaussian distribution:

$$C_1(w) = C_{1max} \exp\left[-\frac{(w_g - w_{max})^2}{2\sigma^2}\right] \tag{131}$$

In this expression,

$$C_{1max} = (1.19w_{wilt} - 5.09) \times 10^{-2}T_s + (-1.464w_{wilt} + 17.86) \quad (132)$$

$$w_{max} = \eta w_{wilt} \quad (133)$$

with

$$\eta = (-1.815 \times 10^{-2}T_s + 6.41)w_{wilt} + (6.5 \times 10^{-3}T_s - 1.4) \quad (134)$$

and

$$\sigma^2 = -\frac{W_{max}^2}{2ln\left(\frac{0.01}{C_{1max}}\right)} \quad (135)$$

15

Ozone

1 Default ozone

When ozone is not a historical variable advected by dynamics and modified by photochemistry, it is simply specified by a climatological monthly file interpolated onto model levels from a climatology coming from University of Reading calculated by Li and Shine (1995). See:

`http://badc.nerc.ac.uk/data/ugamp-o3-climatology/ugamp_help.html`

2 Parameterization of photochemical ozone sources and sinks

The explicit representation of stratospheric photochemistry is too complex to be able to be introduced into a general circulation model. This is why one uses a linearization of the terms of ozone sources and sinks starting from a 2d latitude-pressure model (Cariolle and Déqué, 1986). The 2d model MOBIDYC (64 latitudes and 40 levels pressure) utilized a zonal circulation of stratosphere and 168 chemical reactions concerning 59 components (with in addition 51 reactions of photo-dissociation). The 2d model reaches an equilibrium at the end of 30 years of integration (certain reactions have characteristic times of several years). Stating at the equilibrium situation, one advances one time step ahead in each grid point of the photochemical model, after having disturbed by $\pm 10\%$ the ozone mixing ratio r_{O3}. One thus obtains the derivative of the term of ozone photochemical production or destruction $P - L$ versus r_{O3}. This derivative can be regarded as a relaxation coefficient of the ozone field. Time characteristic of this relaxation

(calculated for each latitude and each level of the model 2d and each month of the year) varies from 0.1 day towards 1 hPa to 1 year at the tropopause. One calculates in same manner the derivative of $P - L$ versus temperature T. Indeed the rates of the chemical reactions (Chapman cycle) depend on temperature. One calculates finally the derivative with respect to ozone thickness above the grid point, Σ_{O3}. When this quantity decreases, ultraviolet flux reaching the point increases, and the production of ozone due to photo-dissociation increases.

The following linear model is thus considered:

$$\begin{aligned}\frac{\partial r_{O3}}{\partial t} &= \overline{P-L} + \overline{\frac{\partial P-L}{\partial r_{O3}}}\,[r_{O3} - \overline{r_{O3}}] \\ &\quad + \overline{\frac{\partial P-L}{\partial T}}\left[T - \overline{T}\right] + \overline{\frac{\partial P-L}{\partial \Sigma_{O3}}}\left[\Sigma_{O3} - \overline{\Sigma_{O3}}\right] \end{aligned} \quad (1)$$

where the over-lined quantities were obtained using the 2d model MOBIDYC. This linear model was substituted for the photochemical model in the 2d model, and the results of the two versions were compared. The relative error remains lower than 10%; the maximum error is in low stratosphere where chemistry is strongly non-linear (just as in troposphere, but the concentrations are weak). The linearized model is thus validated compared to the full model from which it results.

Linear parameterization thus utilizes the 7 coefficients of Equation (1) which are regarded as two-dimensional fields as long as the poles are not tilted, three-dimensional otherwise.

Subroutine ACOZONE calculates initially the ozone quantity above each point:

$$\Sigma_{O3}(l) = \sum_{i=0}^{l-1} \frac{p(\widetilde{i}) - p(\widetilde{i}-1)}{g} r_{O3}(i) \;+\; \frac{p(l) - p(\tilde{l}-1)}{g} r_{O3}(l)$$

The same algorithm is used for term $\overline{\Sigma_{O3}}$ starting from $\overline{r_{O3}}$ to ensure the coherence of the vertical discretization of the model. Then, one calculates the ozone tendency of Equation (1) which is written as:

$$\frac{\partial r_{O3}}{\partial t} = PK_2 + PK_3(r_{O3} - PK_1) + PK_5(T - PK_4) + PK_7(\Sigma_{O3} - \overline{\Sigma_{O3}})$$

with:

$$\overline{\Sigma_{O3}(l)} = \sum_{i=0}^{l-1} \frac{p(\widetilde{i}) - p(\widetilde{i}-1)}{g} PK_1(i) \;+\; \frac{p(l) - p(\tilde{l}-1)}{g} PK_1(l)$$

In fact, the way it is written is less simple as one uses an implicit temporal discretization for the term in r_{O3} (but not for Σ_{O3} because it would be too complicated) to ensure numerical stability with large time steps.

Finally one calculates the ozone flow per vertical integration of the temporal tendencies which one has just calculated and with the assumption of null flow at the top.

3 The effect of chlorine on ozone

Parameterization above does not make it possible to calculate the effect of the application of the Montreal protocol on the reduction of Clx in stratosphere. Heterogeneous chemistry responsible for "ozone hole" is very complex and here a particularly simplified formulation is used. When the solar zenith angle is positive (*i.e.* during daylight) and when temperature is lower than TPSCLIM, namely 195 K, one adds to the PK_3 term the quantity $PK_6\,\mathrm{RCLX}^2$, where PK_6 is a new 2d field and RCLX is a parameter whose temporal evolution is controlled by `namelist`. There is no compatibility with the former versions of the scheme for which fields PK_1 to PK_7 corresponded to other coefficients of Equation (1) (caution: do not mix boundary conditions files!).

4 Parameterization of "mesospheric drag"

The goal of this parameterization is to mitigate the absence of physics in the highest levels of the model (*i.e.* in the mesosphere) when the stratospheric vertical discretization is high. This parameterization consists simply of a linear relaxation of the wind towards 0, of specific moisture towards $q_{min} = 3.725\ 10^{-6}$ (RFMESOQ) to avoid excessive drying and represent chemical sources of H_2O and of the temperature towards the temperature of standard

atmosphere T_{sta} (Fels, 1986) defined in subroutine SUSTA by:

$$\left[\begin{array}{ll} z = 0 & T_{sta} = 288.15\ K \\ 0 < z < 11.0\ km & \dfrac{\partial T_{sta}}{\partial z} = -6.5\ K\ km^{-1} \\ 11.0\ km < z < 20.0\ km & \dfrac{\partial T_{sta}}{\partial z} = 0 \\ 20.0\ km < z < 32.0\ km & \dfrac{\partial T_{sta}}{\partial z} = 1.00\ K\ km^{-1} \\ 32.0\ km < z < 47.4\ km & \dfrac{\partial T_{sta}}{\partial z} = 2.75\ K\ km^{-1} \\ 47.4\ km < z < 51.4\ km & \dfrac{\partial T_{sta}}{\partial z} = 0 \\ 51.4\ km < z < 71.7\ km & \dfrac{\partial T_{sta}}{\partial z} = -2.75\ K\ km^{-1} \\ 71.7\ km < z < 85.7\ km & \dfrac{\partial T_{sta}}{\partial z} = -1.97\ K\ km^{-1} \\ 85.7\ km < z & \dfrac{\partial T_{sta}}{\partial z} = 0 \end{array}\right.$$

The profile of the relaxation coefficients $K(l)$ is defined in subroutine SUTOPH. One chooses for the wind a reference level pressure p_{ref} and a coefficient α. In the same way, for moisture and temperature, one takes another set of coefficients. Profile $K(l)$ is then:

$$K(l) = \alpha\ \max\left(\frac{p_{ref} - p_{sta}(l)}{p_{sta}(l)}, 0\right)$$

where $p_{sta}(l)$ is the standard air pressure at level l. In practice, these two levels are selected above 1 hPa and the constants are adjusted in order to obtain time-constants of a few hours in the highest level.

The writing of linear parameterization is a little complicated by the fact that on the one hand an implicit discretization is used, and that on the other hand one must calculate a flux instead of a tendency. For example, the enthalpy flux at inter-level l is given by:

$$\mathrm{PFRMH} = -\frac{1}{g}\sum_{i=l+1}^{KLEV} \delta p(i)\frac{K(i)}{1 + \Delta t K(i)} c_p(i)(T(i) - T_{sta}(i))$$

where c_p is the specific heat of the air, g gravity, $KLEV$ the number of levels, $\delta p(i)$ the thickness of the layer, Δt the time step of physics and $T(i)$ the temperature. Contrary to fluxes produced by the other parameterizations, this flux is zero at surface. The momentum and energy exchange is done with space and not with earth.

16

Diabatic terms

1 Physical parametrizations

In ARPEGE-CLIMAT, grid point computations at each time step (except post-processing) are carried out in subroutine CPG which calls MF_PHYS. If one excludes horizontal diffusion and nudging terms if any, the diabatic terms of the model equations come from physical parametrizations. This chapter describes what occurs in the model at MF_PHYS level. Subroutine APLPAR is the manager of the physical parametrizations. It takes as input the model prognostic variables at time $t - \Delta t$ and provides vertical fluxes for these variables. Before making calculations of advection, *i.e.* at the origin points of the trajectories, these fluxes are used to evolve the prognostic variables. The next chapters will describe for each parametrization or group of parametrizations how the fluxes are calculated for altitude variables. The surface variables are now computed by SURFEX .

2 Calculation of altitude tendencies

The physical tendencies of the atmospheric variables are calculated from physical fluxes in subroutine CPTEND. We do not take into account here as in the rest of the documentation the option of variable atmospheric mass. See algorithmic documentation of ARPEGE-CLIMAT version 4 for the complete formulas.

2.1 Equation of wind

$$\frac{\partial U}{\partial t} = -g \frac{\partial F_u}{\partial p}$$

$$\frac{\partial V}{\partial t} = -g\frac{\partial F_v}{\partial p}$$

with

$$F_u = F_u^{turb} + F_u^{gwd} + F_u^{conv}$$

$$F_v = F_v^{turb} + F_v^{gwd} + F_v^{conv}$$

2.2 Equation of water vapor

$$\frac{\partial q_v}{\partial t} = -g\left(\frac{\partial\left[F_{q_v}^{turb} + F_{q_v}^{turb\_conv}\right]}{\partial p} + \frac{\partial F_{cond}}{\partial p}\right)$$

with

$$F_{cond} = F_{q_i}^{cond\_conv} + F_{q_l}^{cond\_conv} + F_{q_i}^{cond\_stra} + F_{q_l}^{cond\_stra}$$

Here the condensation fluxes are simply the precipitation fluxes.

2.3 Equation of temperature and enthalpy

In ARPEGE parametrizations, the variable is not temperature, but moist static energy. The equation of change of the temperature is given by:

$$\begin{aligned} c_p\frac{\partial T}{\partial t} &= -g\left[-T\left((c_{p_v}-c_{p_a})\frac{\partial F_{q_v}}{\partial p} + (c_l-c_{p_a})\frac{\partial F_{q_l}}{\partial p} + (c_i-c_{p_a})\frac{\partial F_{q_i}}{\partial p}\right)\right. \\ &\quad + \frac{\partial F_h}{\partial p} - L_l(T)\frac{\partial F_{q_l}^{cond}}{\partial p} - L_i(T)\frac{\partial F_{q_i}^{cond}}{\partial p} \\ &\quad + F_{q_i}^{cond}\frac{\partial}{\partial p}\left((c_l-c_{p_a})T\right) + F_{q_l}^{cond}\frac{\partial}{\partial p}\left((c_i-c_{p_a})T\right) \\ &\quad \left. -\frac{1}{2}\frac{\partial(u^2+v^2)}{\partial t}\right. \end{aligned}$$

with:

$$\frac{\partial \Phi}{\partial t} = 0$$

$$F_{q_v} = F_{q_v}^{turb} + F_{q_v}^{turb\_conv}$$

$$F_{q_i} = F_{q_i}^{turb} + F_{q_i}^{turb\_conv}$$

$$F_{q_l} = F_{q_l}^{turb} + F_{q_l}^{turb\_conv}$$

$$F_h = F_h^{turb} + F_h^{turb\_conv} + F_h^{rayt} + F_h^{rays}$$

Since we do not take into account here the time evolution of liquid and solid water, we have $F_{pi} = F_{q_i}^{cond}$ and $F_{pl} = F_{q_l}^{cond}$.

One names here enthalpy the quantity:

$$h = c_p T + \Phi + \frac{u^2 + v^2}{2}$$

with:

$$c_p = c_{p_a} + (c_{p_v} - c_{p_a})q_v + (c_l - c_{p_a})q_l + (c_i - c_{p_a})q_i$$

After some algebraic calculations, one can arrive at an equation of evolution for enthalpy:

$$\frac{\partial h}{\partial t} = -g\frac{\partial}{\partial p}\left[F_h + F_{hp}\right]$$

with:

$F_{hp} = -L_l(0)F_{ql}^{cond} - L_i(0)F_{qi}^{cond} + F_{pl}\left(c_l - c_{p_a}\right)T + F_{pi}\left(c_i - c_{p_a}\right)T$

where $L_i(0)$ is the latent heat of sublimation to $0\,K$ and $L_l(0)$ the latent heat of vaporization to $0\,K$.

3 Flux of enthalpy due to wet processes

Subroutine CPHPFS calculates fluxes of enthalpy and sensible heat generated by precipitation and condensation.

3.1 Sensible heat flux

$$F_{sl}^{conv} = F_{pl}^{conv}(c_l - c_{p_a})T$$

$$F_{si}^{conv} = F_{pi}^{conv}(c_i - c_{p_a})T$$

$$F_{sl}^{stra} = F_{pl}^{stra}(c_l - c_{p_a})T$$

$$F_{si}^{stra} = F_{pi}^{stra}(c_i - c_{p_a})T$$

3.2 Enthalpy flux related to condensation

$$F_{hl}^{conv} = -L_l(0) F_{q_l}^{cond\_conv}$$

$$F_{hi}^{conv} = -L_i(0) F_{q_i}^{cond\_conv}$$

$$F_{hl}^{stra} = -L_l(0) F_{q_l}^{cond\_stra}$$

$$F_{hi}^{stra} = -L_i(0) F_{q_i}^{cond\_stra}$$

3.3 Total precipitation flux

$$F_p = F_{pl}^{conv} + F_{pi}^{conv} + F_{pl}^{stra} + F_{pi}^{stra}$$

3.4 Total enthalpy flux related to precipitation and condensation

$$\begin{aligned} F_{hp} &= F_{sl}^{conv} + F_{si}^{conv} + F_{sl}^{stra} + F_{si}^{stra} \\ &\quad + F_{hl}^{conv} + F_{hi}^{conv} + F_{hl}^{stra} + F_{hi}^{stra} \end{aligned}$$

4 Time advance in altitude

One modifies the prognostic variables in the atmosphere at time $t + \Delta t$ (index 1): u_1, v_1, T_1, q_{v1}, q_{l1} and q_{i1} by adding to it the physical tendencies in CPUTQY.

4.1 Evolution of wind and of vapor, liquid and solid water

One has:

$$u_1 = u_1 + \Delta t \, \mathrm{PTENDU}$$

$$v_1 = v_1 + \Delta t \, \mathrm{PTENDV}$$

$$q_{v1} = q_{v1} + \Delta t \, \mathrm{PTENDQ}$$

4.2 Evolution of temperature

First of all, enthalpy at $t - \Delta t$ (index 9) is calculated:

$$h_9 = c_{p9} T_9 + \frac{u_9^2 + v_9^2}{2}$$

Then, specific moisture at $t + \Delta t$, due only to physics:

$$q_{v9+\varphi} = q_{v9} + \Delta t \, \mathrm{PTENDQ}$$

$$q_{l9+\varphi} = q_{l9} + \Delta t \, \mathrm{PTENDQL}$$

$$q_{i9+\varphi} = q_{i9} + \Delta t \, \mathrm{PTENDQI}$$

$$c_{p1} = c_{p_a}(1 - q_{v9+\varphi} - q_{l9+\varphi} - q_{i9+\varphi}) + c_l q_{l9+\varphi} + c_i q_{i9+\varphi}$$

as well as kinetic energy at $t + \Delta t$, due to physics:

$$K_1 = \frac{(u_9 + \Delta t \, \mathrm{PTENDU})^2 + (v_9 + \Delta t \, \mathrm{PTENDV})^2}{2}$$

One can thus write the new temperature:

$$T_1 = T_1 + \frac{h_9 - K_1 + \Delta t \, \mathrm{PTENDH}}{c_{p1}} - T_9$$

4.3 Dissipation of the kinetic energy

By definition flux at the top is equal to zero.

$$\mathrm{PFDIS}(l) = \mathrm{PFDIS}(l-1) + \frac{\delta p \, (K_1 - K_9)}{g \, \Delta t}$$

17

Diagnostics

1 Introduction

ARPEGE-CLIMAT calculates a large number of diagnostics during the course of the integration. This software, controlled by the model namelist, is known as "Full Pos". It includes pressure level, model level, and surface instantaneous as well as time accumulated fields. One ARPEGE file and one SURFEX file are created at each postprocessing time step (NFRPOS/NFRSFXHIS), prefixed by PF for the atmosphere and SFX+ for the surface diagnostics. A more detailed description of the "Full Pos" features is available in Yessad (2007e). A comprehensive "Full Pos" User's guide is maintained by Ryad El Khatib who is also in charge of the code development.

In the standard script of ARPEGE-CLIMAT, an additional postprocessing is performed at run time, but it does not use ARPEGE-IFS executable. From the many PF and SFX files generated by the model, a monthly mean file is built (in ARPEGE format) and various ieee-binary files of time series are produced. See the ARPEGE-CLIMAT User's guide for details. In all files, the principles are that IS units are used (Pa for pressure, K for temperature), vectors like wind have their components on the computational sphere and upward fluxes are counted negatively.

2 Post-processable fields

Post-processing can be made on pressure levels, height levels, potential vorticity levels, potential temperature levels or η-levels.

2.1 3D dynamical fields (DYN3D)

Note that availability of some fields depends on the physical parametrizations which have been activated. The standard ARPEGE-CLIMAT does not offer all features.

Non derived:

- Aerosols $AERO$
- Cloud fraction q_a
- Downdraft mesh fraction q_{dal}
- Downdraft vertical velocity q_{dom}
- Equivalent potential temperature Θ_e
- Extra GFL fields
- Geopotential height gz
- Graupel q_g
- Greenhouse gases GHG
- Horizontal wind components U and V
- Ice content q_i
- Liquid water content q_l
- Moist (irreversible) pseudo-adiabatic potential temperature Θ'_w
- Montgomery geopotential Φ_{mg}
- Ozone O_3
- Potential temperature Θ
- Pressure p
- Prognostic pseudo-historic entrainment q_{uen}
- Pseudo-historic convective cloudiness q_{unebh}
- Rain q_r
- Reactive gases GRG
- Relative humidity HU

- Simulated reflectivity
- Snow q_s
- Specific humidity (moisture) q
- Stream function ψ (has to be fitted)
- Temperature T
- Tracers $TRAC$
- Turbulent kinetic energy TKE
- Updraft mesh fraction q_{ual}
- Updraft vertical velocity q_{uom}
- Velocity potential χ (has to be fitted)
- Virtual potential temperature Θ_v
- Wind velocity $\|\vec{u}\|$

Derived:

- Absolute vorticity $\zeta + f$
- Divergence D
- Potential vorticity PV
- Pressure coordinate vertical velocity ω
- Relative vorticity ζ
- Shearing deformation SHD
- Stretching deformation STD

2.2 2D dynamical fields (DYN2D)

Fields marked with ♣ are in the SURFEX file:

- Altitude of isotherm 0
- Altitude of isotherm -10
- Altitude of iso-Θ'_w=0

- Convective available potential energy
- Convective inhibition energy
- ICAO jet meridian component of wind
- ICAO jet zonal component of wind
- ICAO tropopause pressure
- ICAO tropopause temperature
- Interpolated (spectral) model orography
- Logarithm of surface pressure $\ln p_s$
- Mapping factor M
- Maximum relative humidity at 2 m R_x
- Maximum temperature at 2 m T_x ♣
- Mean sea level pressure p_{MSL}
- Minimum relative humidity at 2 m R_n ♣
- Minimum temperature at 2 m T_n ♣
- Moisture convergence
- Planetary boundary layer depth
- Pressure jet
- Pressure of isotherm 0
- Pressure of isotherm -10
- Relative humidity at 2 m R_{cls} ♣
- Specific humidity at 2 m q_{cls} ♣
- Surface pressure p_s
- Temperature at 2 m T_{cls}
- Total water vapor content in a vertical column
- Tropopause folding indicator of the iso-2 PVU surface
- U-component of wind at 10 m U_{cls} ♣
- V-component of wind at 10 m V_{cls} ♣
- Wind velocity at 10 m ♣
- Max Wind velocity at 10 m ♣

2.3 Physical fields (PHYSOL)

These fields are SURFEX fields except for the aerosols and ozone which are archived in the ARPEGE file.

- Aerosols horizontal distribution (continental)
- Aerosols horizontal distribution (desert)
- Aerosols horizontal distribution (marine)
- Aerosols horizontal distribution (soot)
- Aerosols horizontal distribution (sulfate)
- Aerosols horizontal distribution (volcano)
- Anisotropy coefficient of orography
- Anisotropy vector U-momentum
- Anisotropy vector V-momentum
- Budget values
- Climatological relative deep soil wetness
- Climatological relative surface soil wetness
- Deep soil temperature
- Deep soil wetness
- Direction of main axis of orography
- Emissivity
- Free surface fields
- Frozen deep soil wetness
- Frozen surface soil wetness
- Index of vegetation
- Instantaneous surface heat flux
- Instantaneous U-component of surface stress
- Instantaneous V-component of surface stress
- Interception content

- Interpolated dynamic surface $g * z_0$
- Interpolated surface temperature
- Interpolated thermal surface $g * z_0$
- Land/sea mask
- Leaf area index
- Maximum soil depth
- Minimum stomatal resistance
- Output grid-point orography times g
- Ozone horizontal distribution (O3A)
- Ozone horizontal distribution (O3B)
- Ozone horizontal distribution (O3C)
- Percentage of clay within soil
- Percentage of land
- Percentage of sand within soil
- Percentage of urbanization
- Percentage of vegetation
- Relaxation deep soil wetness
- Resistance to evapotranspiration
- Roughness length for heat times g
- Roughness length of bare surface times g
- Snow depth
- Soil depth
- Standard deviation of orography times g
- Surface albedo
- Surface albedo for bare soil
- Surface albedo for snow-free areas
- Surface albedo for soil with vegetation

- Surface relative moisture
- Surface roughness length times g
- Surface snow albedo
- Surface snow density
- Surface soil wetness
- Surface temperature
- Vegetation roughness length times g

2.4 Physical accumulated fluxes

- Contribution of convection to c_pT flux
- Contribution of convection to q flux
- Contribution of convection to U flux
- Contribution of convection to V flux
- Contribution of gravity wave drag U flux
- Contribution of gravity wave drag V flux
- Contribution of turbulence to c_pT flux
- Contribution of turbulence to T flux
- Contribution of turbulence to U flux
- Contribution of turbulence to V flux
- Convective cloud cover
- Convective rainfall
- Convective snow fall
- Deep soil runoff flux
- Evapotranspiration flux
- Filtered duration of total precipitation
- Heat flux in soil
- High cloud cover

- Interception layer runoff flux
- Large scale rainfall (stratiform)
- Large scale snow fall (stratiform)
- Latent heat flux
- Liquid evaporation flux
- Liquid latent heat flux
- Liquid specific moisture
- Low cloud cover
- Medium cloud cover
- Sensible heat flux
- Snow evaporation flux
- Snow mass
- Snow melt flux
- Soil moisture
- Solid latent heat flux
- Solid specific moisture
- Surface clear sky solar radiation flux
- Surface clear sky thermal radiation flux
- Surface downward moon radiation flux
- Surface downward solar flux
- Surface downward thermal flux
- Surface enthalpy flux (due to the dissipation of kinetic energy)
- Surface parallel solar flux
- Surface soil runoff flux
- Surface solar radiation flux
- Surface thermal radiation flux
- Tendency of surface pressure

- Top clear sky solar radiation flux
- Top clear sky thermal radiation flux
- Top mesospheric enthalpy flux (+ dissipation)
- Top parallel solar flux
- Top solar radiation flux
- Top thermal radiation flux
- Total cloud cover
- Total ozone
- Total precipitable water
- Transpiration flux
- Water flux in soil

2.5 Physical instantaneous fluxes

- CAPE
- Cloudiness
- Contribution of convection to c_pT
- Contribution of convection to q
- Contribution of convection to U
- Contribution of convection to V
- Contribution of gravity wave drag to U
- Contribution of gravity wave drag to V
- Contribution of turbulence to c_pT
- Contribution of turbulence to q
- Contribution of turbulence to U
- Contribution of turbulence to V
- Convective cloud cover
- Convective precipitation

- Convective snow fall
- Height of the PBL out of the model
- High cloud cover
- IR clear sky radiance
- IR cloudy sky radiance
- Large scale precipitation
- Large scale snow fall
- Low cloud cover
- Maximum relative humidity at 2 m
- Maximum temperature at 2 m
- Medium cloud cover
- Minimum relative humidity at 2 m
- Minimum temperature at 2 m
- Moisture convergence
- Relative humidity at 2 m
- Specific humidity at 2 m
- Surface solar radiation
- Surface thermal radiation
- Temperature at 2 m
- Top solar radiation
- Top thermal radiation
- Total cloud cover
- U-component of wind at 10 m
- V-component of wind at 10 m
- Wind modulus at 10 m
- WV clear sky radiance
- WV cloudy sky radiance

3 Horizontal interpolations

Horizontal interpolations can be bilinear interpolations or 12-point cubic interpolations.

3.1 Bilinear horizontal interpolations

Horizontal interpolation grid and weights for bi-linear interpolations

A 16-point horizontal grid is defined as it is shown in Figure **??** of Chapter 4. The interpolation point O is between B_1, C_1, B_2 and C_2. Λ and Θ are the longitudes and latitudes on the computational sphere (departure geometry). The following weights are defined as follows:

zonal weight number 1:

$$ZDLO1 = \frac{\Lambda_O - \Lambda_{B_1}}{\Lambda_{C_1} - \Lambda_{B_1}}$$

zonal weight number 2:

$$ZDLO2 = \frac{\Lambda_O - \Lambda_{B_2}}{\Lambda_{C_2} - \Lambda_{B_2}}$$

meridional weight:

$$ZDLAT = \frac{\Theta_O - \Theta_{B_1}}{\Theta_{B_2} - \Theta_{B_1}}$$

Bilinear interpolation

For a quantity X, are computed successively:

a linear interpolation on the longitude number 1:

$$X_1 = X_{B_1} + ZDLO1(X_{C_1} - X_{B_1})$$

a linear interpolation on the longitude number 2:

$$X_2 = X_{B_2} + ZDLO2(X_{C_2} - X_{B_2})$$

a meridional linear interpolation:

$$X_{interpo} = X_1 + ZDLAT(X_2 - X_1)$$

In the FULL-POS code the weights are pre-computed in routines SUHOW2 and SUHOWLSM, so the separation of zonal and meridian interpolations is not visible in the interpolation routines.

3.2 12-point horizontal interpolations

Horizontal interpolation grid and weights for 12-point cubic interpolations

A 16-point horizontal grid is defined as it is shown in Figure **??** of Chapter 4. The interpolation point O is between B_1, C_1, B_2 and C_2. The following weights are defined as follows:

zonal weight number 0:

$$ZDLO0 = \frac{\Lambda_O - \Lambda_{B_0}}{\Lambda_{C_0} - \Lambda_{B_0}}$$

zonal weight number 1:

$$ZDLO1 = \frac{\Lambda_O - \Lambda_{B_1}}{\Lambda_{C_1} - \Lambda_{B_1}}$$

zonal weight number 2:

$$ZDLO2 = \frac{\Lambda_O - \Lambda_{B_2}}{\Lambda_{C_2} - \Lambda_{B_2}}$$

zonal weight number 3:

$$ZDLO3 = \frac{\Lambda_O - \Lambda_{B_3}}{\Lambda_{C_3} - \Lambda_{B_3}}$$

meridional weights:

$$ZCLA2 = \frac{(\Theta_O - \Theta_{B_0})(\Theta_O - \Theta_{B_2})(\Theta_O - \Theta_{B_3})}{(\Theta_{B_1} - \Theta_{B_0})(\Theta_{B_1} - \Theta_{B_2})(\Theta_{B_1} - \Theta_{B_3})}$$

$$ZCLA3 = \frac{(\Theta_O - \Theta_{B_0})(\Theta_O - \Theta_{B_1})(\Theta_O - \Theta_{B_3})}{(\Theta_{B_2} - \Theta_{B_0})(\Theta_{B_2} - \Theta_{B_1})(\Theta_{B_2} - \Theta_{B_3})}$$

$$ZCLA4 = \frac{(\Theta_O - \Theta_{B_0})(\Theta_O - \Theta_{B_1})(\Theta_O - \Theta_{B_2})}{(\Theta_{B_3} - \Theta_{B_0})(\Theta_{B_3} - \Theta_{B_1})(\Theta_{B_3} - \Theta_{B_2})}$$

Horizontal 12-point interpolation

Let us define:

$$\begin{aligned} f_2(\alpha) &= (\alpha+1)(\alpha-2)(\alpha-1)/2 \\ f_3(\alpha) &= -(\alpha+1)(\alpha-2)\alpha/2 \\ f_4(\alpha) &= \alpha(\alpha-1)(\alpha+1)/6 \end{aligned}$$

For a quantity X, are computed successively:

a linear interpolation on longitude number 0:

$$X_0 = X_{B_0} + ZDLO0(X_{C_0} - X_{B_0})$$

a cubic 4-point interpolation on longitude number 1:

$$X_1 = X_{A_1} + f_2(ZDLO1)(X_{B_1} - X_{A_1}) + f_3(ZDLO1)(X_{C_1} - X_{A_1}) +$$

$$f_4(ZDLO1)(X_{D_1} - X_{A_1})$$

a cubic 4-point interpolation on longitude number 2:

$$X_2 = X_{A_2} + f_2(ZDLO2)(X_{B_2} - X_{A_2}) + f_3(ZDLO2)(X_{C_2} - X_{A_2}) +$$

$$f_4(ZDLO2)(X_{D_2} - X_{A_2})$$

a linear interpolation on longitude number 3:

$$X_3 = X_{B_3} + ZDLO3(X_{C_3} - X_{B_3})$$

a meridional cubic 4-point interpolation:

$$X_{interpo} = X_0 + ZCLA2(X_1 - X_0) + ZCLA3(X_2 - X_0) + ZCLA4(X_3 - X_0)$$

In the FULL-POS code the weights are pre-computed in routines SUHOW2 and SUHOWLSM, so the separation of zonal and meridian interpolations is not visible in the interpolation routines.

4 Vertical interpolations and extrapolations

4.1 General considerations

For 3D variables to be vertically interpolated, vertical interpolations are generally linear interpolations between the layers where are defined model variables. The treatment of the extrapolations above the highest layer, the extrapolations below the lowest layer or the surface depend on the variable considered. In particular cases some variables can be diagnosed using the vertically interpolated value of some other variables.

4.2 Notations

- $\left[\frac{dT}{dz}\right]_{ST}$: standard atmosphere vertical gradient of the temperature in the troposphere ($0.0065\,K\,m^{-1}$)
- R_d: dry air constant
- g: gravity acceleration
- L: number of layers of the model

4.3 More details for 3D dynamical variables

Wind components, wind velocity

Way of interpolating (subroutine PPUV):

- Linear interpolation between layer 2 and the lowest layer.
- The coordinate used for linear interpolation is the logarithm of the pressure.
- Linear interpolation between layer 1 and layer 2 using the values of layers 1, 2 and 3.
- Linear interpolation between the top and layer 1 using the values of the top, layers 1 and 2; the value of the top is obtained by a linear extrapolation from the values of layers 1 and 2.
- Extrapolation below the middle of the lowest layer and below the surface assumes that the quantity is constant.

Temperature

Applies to temperature if the vertical coordinate of post-processing is not the potential vorticity, otherwise see routine PP2DINT.

Way of interpolating (subroutine PPT):

- Quadratic interpolation between the middles of the upper and lowest layers.
- Quadratic interpolation between the top and the middle of the highest layer: the top value of the temperature is assumed to be equal to the value of the middle of the highest layer; due to the fact that the interpolation is a quadratic one, that does not mean that the temperature is constant in this atmosphere depth.
- The coordinate used for quadratic interpolation is the logarithm of pressure.
- A surface temperature T_{SURF} is computed by SURFEX on land surface and the ocean model on sea surface.

Geopotential height

Applies to geopotential height if the vertical coordinate of post-processing is not the potential vorticity, otherwise see routine PP2DINT.

Way of interpolating (subroutine PPGEOP):

- The variable interpolated is a geopotential height departure from a reference defined by a standard atmosphere without any orography. After the interpolation an increment is added, sum of the surface orography and the "standard" geopotential height depth between the pressure level of interpolation and the actual surface. This method avoids to introduce interpolations for the standard component of the geopotential height which can be computed analytically (in routine PPSTA).
- Quadratic interpolation between the middles of the upper and lowest layers.
- Quadratic interpolation between the top and the middle of the highest layer.
- The coordinate used for quadratic interpolation is the logarithm of pressure. The interpolation is a quadratic analytic expression of the logarithm of pressure of the same type as the one used to post-process the temperature.

- Linear interpolation between the lowest layer and the surface
- Extrapolation below surface uses the surface temperature T_{SURF} of Equation (**??**).

$$gz_{extrapo} = \Phi_s - R_d T_{SURF} \ln\left(\frac{p_s}{p_L}\right)\left(1 + \frac{y}{2} + \frac{y^2}{6}\right) \quad (1)$$

where y is defined by formula (**??**) with $\Gamma = \left[\frac{dT}{dz}\right]_{ST}$ in all cases.

Variables interpolated using routine PP2DINT

List of variables:

- Geopotential height gz if vertical coordinate is potential vorticity
- Temperature T if vertical coordinate is potential vorticity
- Relative vorticity ζ
- Divergence D
- Potential temperature Θ if vertical coordinate is not potential temperature
- Velocity potential χ
- Stream function ψ
- Equivalent potential temperature Θ_e
- Absolute vorticity $\zeta + f$
- Stretching deformation STD
- Shearing deformation SHD
- Potential vorticity PV

Way of interpolating:

- Linear interpolation (between the upper and the lowest layer for quantities defined on the middle of layers, between the layer 1 and the surface for quantities defined on inter-layers).
- The coordinate used for linear interpolation is the pressure.
- Extrapolation above the middle of the highest layer assumes that the quantity is constant.
- Extrapolation below the middle of the lowest layer and below the surface assumes that the quantity is constant.

GFL variables (moisture, ...)

These variables use subroutine PPQ.

- Linear interpolation (between the upper and the lowest layer).
- The coordinate used for linear interpolation is the pressure.
- Extrapolation above the middle of the highest layer assumes that the quantity is constant.
- Extrapolation below the middle of the lowest layer and below the surface assumes that the quantity is constant.

Relative humidity

This variable uses subroutine PPRH.

- Linear interpolation (between the upper and the lowest layer).
- The coordinate used for linear interpolation is the pressure.
- Extrapolation above the middle of the highest layer assumes that the quantity is constant.
- Extrapolation below the middle of the lowest layer and below the surface assumes that the quantity is constant.

Pressure coordinate vertical velocity ω

This variable uses subroutine PPVVEL.

- Linear interpolation (between the upper and the lowest layer).
- The coordinate used for linear interpolation is the pressure.
- Extrapolation above the middle of the highest layer is a linear interpolation between a zero value at the top and the value of the highest layer.
- Extrapolation between the middle of the lowest layer and the surface assumes that the quantity is constant.
- Extrapolation below the surface assumes that the quantity is zero.

Moist (irreversible) pseudo-adiabatic potential temperature Θ'_w

Subroutine PPTHPW provides this diagnostic. It takes as input the vertically post-processed pressure, temperature, moisture, liquid water and ice and computes Θ'_w at the post-processing levels using a diagnostic (and rather complicated) algorithm.

4.4 2D dynamical variables which need extrapolations

Mean sea level pressure p_{MSL}

Subroutine PPPMER provides this diagnostic. It takes as input the vertically If $\mid \Phi_s \mid$ is lower than $0.001\, J\, kg^{-1}$ the mean sea level pressure is set to the surface pressure. In the other cases one uses the following algorithm:

- One computes the surface temperature T_{SURF} of Equation (**??**) and the mean sea level temperature $T_0 = T_{SURF} + \left[\frac{dT}{dz}\right]_{ST} \frac{\Phi_s}{g}$.
- To avoid extrapolation of too low pressures over high and warm surfaces the following modifications are done:
  - if $T_0 > 290.5\ K$ and $T_{SURF} \leq 290.5\ K$, Γ is defined by:
    $$\Gamma = (290.5 - T_{SURF})\frac{g}{\Phi_s} \tag{2}$$
  - if $T_0 > 290.5\ K$ and $T_{SURF} > 290.5\ K$, Γ is set to 0, T_{SURF} is modified and set to $0.5 * (290.5\ K$ + old value of $T_{SURF})$.
- To avoid extrapolation of too high pressures over cold surfaces the following modifications are done when $T_{SURF} < 255\ K$: Γ is set to $\left[\frac{dT}{dz}\right]_{ST}$ and T_{SURF} is modified and set to $0.5 * (255\ K$ + old value of $T_{SURF})$.
- In the other cases Γ is set to $\left[\frac{dT}{dz}\right]_{ST}$.
- Mean sea level pressure is computed as follows:
  $$p_{MSL} = p_s \exp\left[\frac{\Phi_s}{R_d T_{SURF}}\left(1 - \frac{x}{2} + \frac{x^2}{3}\right)\right] \tag{3}$$
  where:
  $$x = \frac{\Gamma \Phi_s}{g T_{SURF}} \tag{4}$$

5 Filtering in spectral space

Filtering is done in routine SPOS and processed differently on derivative and non-derivative fields.

5.1 THX filtering on derivatives

Cases where this filtering is used: This filtering applies in the spectral space to absolute vorticity, relative vorticity, divergence, vertical velocity, stretching and shearing deformations, and potential vorticity (and extends to all variables if the vertical coordinate of post-processing is the potential vorticity). This filter is active if:

- CFPFMT is not 'MODEL' in namelist NAMFPC
- LFPFIL=.TRUE. in namelist NAMFPF
- Variable NFMAX is smaller than the equivalent unstretched sphere truncation N_c (in practical N_c is between $1.1\,c\,N_s$ and $1.2\,c\,N_s$, where c is the stretching factor)

If one wishes to keep these fields unfiltered, then just set LFPFIL=.FALSE. (namelist NAMFPF). On the other hand, you can keep the filter active but you can tune the filtering function.

Function of filtering: This function looks like a smoothed step function; for a given total wave-number n in the unstretched spectral space (i.e. the spectral space of the equivalent unstretched sphere of truncation N_c), the formula is:

$$f_{THX}(n) = \frac{1 - \tanh(e^{-k}(n - n_0))}{2} \tag{5}$$

(The use of the function hyperbolic tangent is the reason of the nickname THX for this filter). It means that this function equals roughly 1 if n is less than n_0, and 0 if it is greater than n_0.

Tunable parameters in the previous function: k and n_0 are tunable parameters:

- n_0 is in the variable NFMAX. If CFPFMT='GAUSS' or 'MODEL' in namelist NAMFPC, the default value is NFPMAX*FPSTRET; else, it is the truncation of the Gaussian grid which would have been defined by NLAT latitudes and NLON longitudes with default so that $3 * NFMAX + 1 = \min(NLAT, NLON)$

- k is stored in variable RFPBED

Operations done in SPOS for this filtering: One assumes that CFPFMT is not 'MODEL'.

- LFPFIL=.T. and $N_s < N_c$: the previous function $f_{THX}(n)$ is computed in the equivalent unstretched sphere of truncation N_c, so reading dilatation and contraction matrices respectively denoted by $\mathcal{D}$ and $\mathcal{C}$ (computed by the configuration 911) is necessary. The operator applied to spectral fields in the computational sphere is a matrix operator $\mathcal{C}\, f_{THX}(n)\, \mathcal{D}$ pre-computed in the routine FPFILTER (called by SU3FPOS) and stored in the array RFPMAT. In SPOS the initially unfiltered fields are in SPDFP and the filtered fields are put in SPBFP. Filtering is done only if NFMAX $< N_c$, elsewhere there is a simple copy of SPDFP in SPBFP without filtering.

- LFPFIL=.T. and $N_s = N_c$: identity $N_s = N_c$ is satisfied if the model resolution has no stretching. $f_{THX}(n)$ is stored in the array RFPFIL. This function is directly applied in SPOS to SPDFP and the filtered fields are put in SPBFP. Filtering is done only if NFMAX $< N_s$, elsewhere there is a simple copy of SPDFP in SPBFP without filtering.

- LFPFIL=.F.: no filtering, simple copy of SPDFP in SPBFP.

5.2 Bell-shaped filtering on non-derivative fields

Way of filtering: It is also possible to filter the non-derivative post-processed fields through bell-shaped filters. Separate bell-shaped filters are available for geopotential height, temperature, mean sea level pressure, relative humidity and all other non-derivatives. By default, these filters are active for geopotential height, temperature, mean sea level pressure and relative humidity. For a given wave-number n in the stretched spectral space, the formula is:

$$f_{bs}(n) = \exp\left(-\frac{k}{2}\left[\frac{n}{N_s}\right]^2\right) \tag{6}$$

where N_s is the model truncation (NSMAX) and k a tunable variable. In SPOS, the bell-shaped filtering is done by multiplying the array SPAFP by $f_{bs}(n)$, the result is still in SPAFP.

Variables controlling bell-shaped filtering:

- Switches LFPBEG for geopotential height, LFPBET for temperature, LFPBEH for relative humidity, LFPBEP for mean sea level pressure, LFPBEL for other non-derivatives,: .TRUE. if filtering, .FALSE. if no filtering.
- Variables RFPBEG for geopotential height, RFPBET for temperature, RFPBEH for relative humidity, RFPBEP for mean sea level pressure, RFPBEL for other non-derivatives, : to control the intensity of the filtering (variable k of formula (6)).

References

- Belamari, S. (2005). Report on uncertainty estimates of an optimal bulk formulation for surface turbulent fluxes. *MERSEA IP Deliverable*, D.4.1.2:29.
- Best, M., Beljaars, A., Polcher, J., and Viterbo, P. (2004). A proposed structure for coupling tiled surfaces with the planetary boundary layer. *Journal of hydrometeorology*, 5:1271–1278.
- Betts, A. (1973). Non-precipitating cumulus convection and its parameterization. *Quart. J. Roy. Meteor. Soc.*, 99:178–196.
- Beven, K. and Kirkby, M. (1979). A physically-based variable contributing area model of basin hydrology. *Hydrol. Sci.*, 24:43–69.
- Bhumralkar, C. (1975). Numerical experiments on the computation of the ground surface temperature in an atmospheric general circulation model. *J. Appl. Meteorol.*, 14:1246–1258.
- Blackadar, A. (1976). Modelling the nocturnal boundary layer. *Proceedings of the third symposium on atmospheric turbulence diffusion and air quality*, Boston. American Meteorological Society:43–49.
- Blanke, B. and Delecluse, P. (1993). Low frequency variability of the tropical atlantic ocean simulated by a general circulation model with mixed layer physics. *J. Phys. Oceanogr.*, 23:1363–1388.
- Boone, A., Calvet, J.-C., and Noilhan, J. (1999). Inclusion of a third soil layer in a land-surface scheme using the force-restore method. *J. Appl. Meteorol.*, 38:1611–1630.
- Boone, A. and Etchevers, P. (2001). An intercomparison of three snow schemes of varying complexity coupled to the same land-surface and macroscale hydrologic models. *J. Hydrometeor*, 2:374–394.
- Boone, A., Masson, V., Meyers, T., and Noilhan, J. (2000). The influence of the inclusion of soil freezing on simulations by a soil-atmosphere-transfer scheme. *J. Hydrometeor*, 39:1544–1569.

- Bossuet, C., Déqué, M., and Cariolle, D. (1998). Impact of a simple parameterization of convective gravity wave drag in a stratosphere-troposphere general circulation model and its sensitivity to vertical resolution. *Annales Geophysicae*, 16:238–249.

- Boucher, O. and Pham, M. (2002). History of sulfate aerosol radiative forcings. *Geophys. Res. Letters*, 29:10.1029/2001GL014048.

- Bougeault, P. (1981). Modeling the trade-wind cumulus boundary layer. part i: testing the ensemble cloud relations against numerical data. *J. Atmos. Sci.*, 38:2414–2428.

- Bougeault, P. (1982). Cloud ensemble relations based on the gamma probability distribution for the higher-order models of the planetery boundary layer. *J. Atmos. Sci.*, 39:2691–2700.

- Bougeault, P. (1985). A simple parameterization of the large-scale effects of cumulus convection. *Mon. Wea. Rev.*, 113:2108–2121.

- Bougeault, P. and Lacarrère, P. (1989). Parameterization of orography-induced in a mesobeta-scale model,. *Mon. Wea. Rev.*, 117:1872–1891.

- Braud, I., Noilhan, J., Bessemoulin, P., Mascart, P., Haverkamp, R., and Vauclin, M. (1993). Bare-ground surface heat and water exchanges under dry conditions: Observations and parameterization. *Bound.-Layer Meteor.*, 66:173–200.

- Caballero, Y., Voirin-Morel, S., Habets, F., Noilhan, J., LeMoigne, P., Lehenaff, A., and Boone, A. (2007). Hydrological sensitivity of the adour-garonne river basin to climate change. *Water Resour. Res.*, 43:19pp.

- Cariolle, D. and Déqué, M. (1986). Southern hemisphere medium-scale waves and total ozone disturbances in a spectral general circulation model. *J. Geophys. Res.*, 91:10825–10846.

- Cariolle, D. and Teyssédre, H. (2007). A revised linear ozone photochemistry parameterization for use in transport and general circulation models: multi-annual simulations. *Atmospheric chemistry and physics*, 7:2183–2196.

- Clapp, R. and Hornberger, G. (1978). Empirical equations for some hydraulic properties. *Water Resour. Res.*, 14:601–604.

- Clark, T. and Peltier, W. (1977). On the evolution and stability of finite amplitude mountain waves. *J. Atmos. Sci.*, 34:1715–1730.

- Clough, S. and Iacono, M. (1995). Line-by-line calculation of atmospheric fluxes and cooling rates. application to carbon dioxide, ozone, methane, nitrous oxide and the halocarbons. *J. Geophys. Res.*, 100D:16519–16536.

- Clough, S., Iacono, M., and Moncet, J. (1992). Line-by-line calculation of atmospheric fluxes and cooling rates: Application to water vapor. *J. Geophys. Res.*, 97D:15761–15786.

- Clough, S., Kneizys, F., and Davies, R. (1989). Line shape and the water vapor continuum. *Atmos. Res.*, 23:229–241.

- Coakley, J. and Chylek, J. (1975). The two-stream approximation in radiation transfer: Including the angle of the incident radiation. *J. Atmos. Sci.*, 32:409–418.

- Courtier, P. and Geleyn, J. (1988). A global numerical weather prediction model with variable resolution: Application to the shallow water equations. *Quart. J. Roy. Meteor. Soc.*, 114:1321–1346.

- Deardorff, J. (1977). A parameterization of ground surface moisture content for use in atmospheric prediction models. *J. Appl. Meteorol.*, 16:1182–1185.

- Deardorff, J. (1978). Efficient prediction of ground temperature and moisture with inclusion of a layer of vegetation. *J. Geophys. Res.*, 83:1889–1903.

- Decharme, B. and Douville, H. (2006). Introduction of a sub-grid hydrology in the isba land surface model. *Climate Dyn.*, 26:65–78.

- Decharme, B. and Douville, H. (2007). Global validation of the isba sub-grid hydrology. *Climate Dyn.*, 29:21–37.

- Decharme, B., Douville, H., Boone, A., Habets, F., and Noilhan, J. (2006). Impact of an exponential profile of saturated hydraulic conductivity within the ISBA LSM: simulations over the rhone basin. *J. Hydrometeor*, 7:61–80.

- Deschamps, P., Herman, M., and Tanré, D. (1983). Modélisation du rayonnement solaire réfléchi par l'atmosphère et la terre, entre 0,35 et 4 microns. *Rapport ESA 4393/80/F/DD(SC)*, 156 pp.

- Dickinson, R. (1984). Modeling evapotranspiration for three-dimensional global climate models. *Climate Processes and Climate sensitivity. American Geophysical Union. Geophys. Monog.*, 29:58–72.

- Donald, A. M. and Haugen, J. (1992). A two-time-level, three-dimensional semi-lagrangian, semi-implicit, limited-area grid-point model of the primitive equations. *Mon. Wea. Rev.*, 120:2603–2621.
- Douville, H., Royer, J., and Mahfouf, J. (1995a). A new snow parameterization for the météo-france climate model. Part I: Validation and stand alone experiment. *Climate Dynamics*, 12:21–35.
- Douville, H., Royer, J., and Mahfouf, J. (1995b). A new snow parameterization for the météo-france climate model. part ii: Validation in a 3d gcm experiment. *Climate Dynamics*, 12:37–52.
- Dubuisson, P., Buriez, J., and Fouquart, Y. (1996). High spectral resolution solar radiative transfer in absorbing and scattering media: application to the satellite simulation. *J. Quant. Spectrosc. Radiat. Transfer*, 55:103–126.
- Dumenil, H. and Todoni, E. (1992). A rainfall-runoff scheme for use in the hamburg climate model. *Adv. Theor. Hydrol.*, 9:129–157.
- Dyer, A. (1974). A review of flux-profile relationships. *Boundary Layer Meteorology*, 7:363–372.
- Ebert, E. and Curry, E. (1992). A parameterization of ice cloud optical properties for climate models. *J. Geophys. Res.*, 97D:3831–3836.
- Fairall, C., Bradley, E., Hare, J., Grachev, A., and Edson, J. (2003). Bulk parameterization of air-sea fluxes : Updates and verification for the coare algorithm. *J. Climate*, 16:571–591.
- Fairall, C., Bradley, E., Rogers, D. P., Edson, J. B., , and Young, G. S. (1996). Bulk parameterization of air-sea fluxes for tropical ocean-global atmosphere coupled-ocean atmosphere response experiment. *J. Geophys. Res.*, 101:3747–3764.
- Fan, Y., Wood, E., Baeck, M., and Smith, J. (1996). The fractional coverage of rainfall over a grid: Analyses of nexrad data over the southern plains. *Water Resour. Res.*, 32:2787–2802.
- Fels, S. (1986). Analytic representations of standard atmosphere temperature profiles. *J. Atmos. Sci.*, 43:219–221.
- Fouquart, Y. (1974). Utilisation des approximants de padé pour l'étude des largeurs équivalentes des raies formes en atmosphèrere diffusante. *J. Quant. Spectrosc. Radiat. Transfer*, 14:497–506.
- Fouquart, Y. and Bonnel, B. (1980). Computations of solar heating of the earth's atmosphere: A new parametrization. *Beitr. Phys. Atmosph.*, 53:35–62.

- Fu, Q. (1996). An accurate parameterization of the solar radiative properties of cirrus clouds for climate models. *J. Climate*, 9:2058–2082.
- Fu, Q. and Liou, K. (1992). On the correlated k-distribution method for radiative transfer in non homogeneous atmospheres. *J. Atmos. Sci.*, 49:2139–2156.
- Fu, Q. and Liou, K. (1993). Parameterization of the radiative properties of cirrus clouds. *J. Atmos. Sci.*, 50:2008–2008.
- Fu, Q. and Sun, W. (2001). Retrieval of cirrus particle sizes using a split-window technique: a sensitivity study. *J. Quant. Spectrosc. Radiat. Transfer*, 68:725–736.
- Fu, Q., Yang, P., and Sun, W. (1998). An accurate parametrization of the infrared radiative properties of cirrus clouds of climate models. *J. Climate*, 11:2223–2237.
- Galperin, B., Kantha, L., Hassid, S., and Rosati, A. (1988). A quasi-equilibrium turbulent energy for geophysical flows. *J. Atmos. Sci.*, 45:55–62.
- Geleyn, J. (1988). Interpolation of wind, temperature and humidity values from model levels to the height of measurement. *Tellus*, 40A:347–351.
- Geleyn, J., Girard, C., and Louis, J. (1982). A simple parameterization of moist convection for large-scale atmospheric models. *Beitr. Phys. Atmosph.*, 55:325–334.
- Geleyn, J. and Hollingsworth, A. (1979). An economical analytic method for the computation of the interaction between scattering and line absorption of radiation. *Beitr. Phys. Atmosph.*, 52:1–16.
- Gent, P. and Williams, J. M. (1990). Isopycnal mixing in ocean circulation models. *J. Phys. Oceanogr.*, 20:150–155.
- Giordani, H. (1993). Expériences de validation unidimensionnelles du schéma de surface NP89 aux normes Arpège sur trois sites de la campagne EFEDA 91. *Note de travail du CNRM*, 24.
- Gosnell, R., Fairall, C., and Webster, P. J. (1995). The sensible heat of rainfall in the tropical ocean. *J. Geophys. Res.*, 100:18437–18442.
- Gourdin, A. and Boumarhat, M. (1983). Méthodes numériques appliquées. *Technique et documentation*, 423 pp.
- Habets, F. (2008). The SAFRAN-ISBA-MODCOU hydrometeorological model applied over France. *J. Geophys. Res.*, 113

- Habets, F. and Saulnier, G. (2001). Subgrid runoff parameterization. *Physics and Chemistry of the Earth, Part B: Hydrology, Oceans and Atmosphere*, 26 Issues 5-6:455–459.

- Helfand, H. and Labraga, J. (1988). Design of the non singular level 2.5 second order closure model for the prediction of atmospheric turbulence. *J. Atmos. Sci.*, 45:113–132.

- Holtslag, A. and Boville, B. (1993). Local versus non-local boundary diffusion in a global climate model. *J. Climate*, 6:1825–1842.

- Hortal, M. (1996). Experiments with the linear gaussian grid at ecmwf. *Research Activities in Atmospheric and Oceanic Modelling*, 23:17–19.

- Hortal, M. (2002). The development and testing of a new two-time-level semi-lagrangian scheme (SETTLS) in the ECMWF forecast model. *Quart. J. Roy. Meteor. Soc.*, 128:1671–1687.

- Hortal, M. and Simmons, A. (1991). Use of reduced gaussian grids in spectral models. *Mon. Wea. Rev.*, 119:1057–1074.

- Jacquemin, B. and Noilhan, J. (1990). Validation of a land surface parameterization using the hapex-mobilhy data set. *Bound.-Layer Meteor.*, 52:93–134.

- Jarvis, P. (1976). The interpretation of the variations in the leaf water potential and stomatal conductance found in canopies in the field. *Philos. Trans. Roy. Soc. London*, 273B:593–610.

- Joseph, J., Wiscombe, W., and Weinman, J. (1976). The Delta-Eddington approximation for radiative flux transfer. *J. Atmos. Sci.*, 33:2452–2459.

- Kershaw, R. and Gregory, D. (1997). Parameterization of momentum transport by convection - I: Theory and cloud modelling results. *Quart. J. Roy. Meteor. Soc.*, 123:1133–1151.

- Kessler, E. (1969). On distribution and continuity of water substance in atmospheric circulations. *Met. Mon. American. Met. Soc. 10*, 32:84 pp.

- Kraus, E. (1972). Atmosphere-ocean interactions. *London Oxford University press.*

- Lacis, A. and Oinas, V. (1991). A description of the correlated k distribution method for modeling nongray gaseous absorption, thermal emission, and multiple scattering in vertically inhomogeneous atmospheres. *J. Geophys. Res.*, 96D:9027–9063.

- Large, W., Williams, J. M., and Doney, S. (1994). Oceanic vertical mixing - a review and a model with a nonlocal boundary layer parameterization. *Reviews of Geophysics*, 32:363–404.
- Lebeaupin-Brossier, C. (2007). Etude du couplage océan-atmosphère associé aux épisodes de pluies intenses en région méditerranéenne. *PhD thesis, University Paul Sabatier, TOULOUSE, France*, 228pp.
- Lenderink, G. and Holtslag, M. (2004). An updated length-scale formulation for turbulent mixing in clear and cloudy boundary layers. *Quart. J. Roy. Meteor. Soc.*, 130:3405–3427.
- Lilly, D. (1968). Models of cloud-topped mixed layers under a strong inversion. *Quart. J. Roy. Meteor. Soc.*, 94:292–309.
- Lindner, T. and Li, J. (2000). Parametrization of the optical properties for water clouds in the infrared. *J. Climate*, 13:1797–1805.
- Liu, W., Katsaros, K., and Businger, J. (1979). Bulk parameterization of the air-sea exchange of heat and water vapor including the molecular constraints at the interface. *J. Atmos. Sci.*, 36:1722–1735.
- Lott, F. and Miller, M. (1995). A new sub-grid scale orographic drag parameterization: its formulation and testing. *Report to the Scientific Advisory Commitee*, ECMWF:31 pp.
- Louis, J. (1979). A parametric model of vertical eddy fluxes in the atmosphere. *Boundary Layer Meteorology*, 17:187–202.
- Louis, J., Tiedtke, M., and Geleyn, J. (1982). A short history of the operational PBL-parameterization at ECMWF. *Proceedings of ECMWF workshop on planetary boundary layer parameterization. 25-27 November 1981*, 59–80.
- Madec, G. (2008). Nemo reference manual, ocean dynamics component: Nemo-opa preliminary version. *Note du Pole de modélisation, Institut Pierre-Simon Laplace, ISSN 1288-1619*, 27
- Mahfouf, J. and J.-F., J. N. (1991). Comparative study of various formulations of evaporation from bare soil using in situ data. *J. Appl. Meteorol.*, 9:1354–1365.
- Mahfouf, J. and J.-F., J. N. (1996). Inclusion of gravitational drainage in a land surface scheme based on the force restore method. *J. Appl. Meteorol.*, 35:987–992.
- Mahfouf, J., Noilhan, J., and Péris, P. (1994). Simulations du bilan hydrique avec ISBA: Application au cycle annuel dans le cadre de PILPS. *Atelier de modélisation de l'atmosphère - CNRM/Météo-France*, 83–92.

- Martin, G., Johnson, D., and Spice, A. (1994). The measurement and parameterization of effective radius of droplets in warm stratocumulus. *J. Atmos. Sci.*, 51:1823–1842.

- Mascart, P., Noilhan, J., and Giordani, H. (1995). A modified parameterization of the surface layer flux-profile relationships using different roughness length values for heat and momentum. *Boundary Layer Meteorology*, 72:331–344.

- Masson, V., Champeaux, J., Chauvin, F., Meringuet, C., and Lacaze, R. (2003). A global database of land surface parameters at 1 km resolution in meteorological and climate models. *J. Climate*, 16:1261–1282.

- Matveev, L. (1984). Clouds dynamics. *Atmosph. Science Library. Reidel Publ. Comp.*, 340 pp.

- Mellor, G. (1977). The gaussian cloud model relation. *J. Atmos. Sci.*, 34:356–358corrigenda1483–1484.

- Mellor, G. and Yamada, T. (1974). A hierarchy of turbulence closure models for planetary boundary layers. *J. Atmos. Sci.*, 31:1791–1806.

- Mellor, G. and Yamada, T. (1982). Development of a turbulence closure model for geophysical fluid problems. *Reviews of Geophysical Physics and Space Physics*, 20:851–875.

- Mlawer, E., Taubman, S., Brown, P., Iacono, M., and Clough, S. (1997). Radiative transfer for inhomogeneous atmospheres: RRTM, a validated correlated-k model for the longwave. *J. Geophys. Res.*, 102D:16663–16682.

- Noihlan, J. and Planton, S. (1989). A simple parameterization of land surface processes for meteorological models. *Mon. Wea. Rev.*, 117:536–549.

- Noilhan, J. and Lacarrère, P. (1995). GCM gridscale evaporation from mesoscale modelling. *J. Climate*, 8:206–223.

- Noilhan, J. and Mahfouf, J. (1996). The ISBA land surface parameterisation scheme. *Global and Planetary Change*, 13-Issues 1-4:145–159.

- Ou, S. and Liou, K. (1995). Ice microphysics and climatic temperature feedback. *Atmos. Res.*, 35:127–138.

- Pacanowski, R. and Philander, S. (1981). Parameterization of vertical mixing in numerical models of tropical oceans. *J. Phys. Oceanogr.*, 11:1443–1451.

- Parol, F., Buriez, J., Brogniez, G., and Fouquart, Y. (1991). Information content of AVHRR channels 4 and 5 with respect to the effective radius of cirrus cloud particles. *J. of Applied Meteorology*, 30:973–984.

- Polcher, J., McAveney, B., Viterbo, P., Gaertner, M.-A., Hahmann, A., Mahfouf, J.-F., Noilhan, J., Phillips, T., Pitman, A., Schlosser, C., Schulz, J.-P., Timbal, B., Verseghy, D., and Xue, Y. (1998). A proposal for a general interface between land-surface schemes and general circulation models. *Global and Planetary Change*, 19:261–276.

- Quaas, J. and Boucher, O. (2005). Constraining the first aerosol indirect radiative forcing in the LMDZ GCM using POLDER and MODIS satellite data. *Geophys. Res. Letters*, 32

- Ricard, J. (1992). Etude d'un schéma statistique de génération de nuages et son introduction dans le modèle de circulation générale emeraude. *Thèse de doctorat*, Université Paul Sabatier Toulouse III:230 pp.

- Ricard, J. and Royer, J. (1993). A statistical cloud scheme for use in an agcm. *Annales Geophysicae*, 11:1095–1115.

- Ritchie, H. and Tanguay, M. (1996). A comparison of spatially-averaged eulerian and semi-lagrangian treatments of mountains. *Mon. Wea. Rev.*, 124:167–181.

- Robert, A. (1981). A stable numerical integration scheme for the primitive meteorological equations. *Atm. Ocean*, 19:35–46.

- Rochas, M. and Courtier, P. (1992). La méthode spectrale en météorologie. *Note de Travail ARPEGE*, 30:58 pp.

- Rockel, B., Raschke, E., and Weyres, B. (1991). A parameterization of broad band radiative transfer properties of water, ice, and mixed layer clouds. *Beitr. Phys. Atmosph.*, 64:1–12.

- Rodgers, C. (1967). The radiative heat budget of the troposphere and lower stratosphere. *Planetary Circulation Project. Dept. of Meteorology. Mass. Instit. Techn.*, A2:99 pp.

- Rothman, L., Gamache, R., Goldman, A., Brown, L., Toth, R., Pickett, H., Poynter, R., Flaud, J., Camy-Peyret, C., Barbe, A., Husson, N., Rinsland, C., and Smith, M. (1987). The HITRAN database, 1986 edition. *Appl. Optics*, 26:4058–4097.

- Rothman, L., Gamache, R., Tipping, R., and et al., C. R. (1992). The hitran database, editions of 1991 and 1992. *J. Quant. Spectrosc. Radiat. Transfer*, 48:469–507.

- Savijarvi, H. and Raisanen, P. (1997). Long-wave optical properties of water clouds and rain. *Tellus*, 50-A:1–11.

- Schulz, M. (2007). Constraining model estimates of the aerosol radiative forcing. *Habilitation Thesis, Université Pierre et Marie Curie*

- Shettle, E. and Weinman, J. (1970). The transfer of solar irradiance through inhomogeneous turbid atmospheres evaluated by Eddington's approximation. *J. Atmos. Sci.*, 27:1048–1055.

- Silvapalan, M., Beven, K., and Wood, E. (1987). On hydrologic similarity: 2. a scaled model of storm runoff production. *Water Resour. Res.*, 23:2266–2278.

- Simmons, A. and Burridge, D. (1981). An energy and angular momentum conserving vertical finite-difference scheme and hybrid vertical coordinate. *Mon. Wea. Rev.*, 109:758–766.

- Slingo, A. (1989). A GCM parameterization for the shortwave radiative properties of water clouds. *J. Atmos. Sci.*, 46:1419–1427.

- Smith, E. and Shi, A. L. (1992). Surface forcing of the infrared cooling profile over the tibetan plateau. Part I: Influence of relative longwave radiative heating at high altitude. *J. Atmos. Sci.*, 49:805–822.

- Smith, R. (1990). A scheme for predicting layer clouds and their water content in a general circulation model. *Quart. J. Roy. Meteor. Soc.*, 116:435–460.

- Sommeria, G. and Deardorff, J. (1977). Subgrid-scale condensation in models of non precipitating clouds. *J. Atmos. Sci.*, 34:344–355.

- Sun, Z. and Rikus, L. (1999). Parametrization of effective sizes of cirrus-cloud particles and its verification against observations. *Quart. J. Roy. Meteor. Soc.*, 125:3037–3055.

- Sundqvist, H. (1978). A parameterization scheme for non-convective condensation including prediction of cloud water content. *Quart. J. Roy. Meteor. Soc.*, 104:677–690.

- Tegen, I., Hollrig, P., Chin, M., Fung, I., Jacob, D., and Penner, J. (1997). Contribution of different aerosol species to the global aerosol extinction optical thickness: estimates from model results. *J. Geophys. Res.*, 102:23895–23915.

- Temperton, C. (1991). On scalar and vector transform methods for global spectral models. *Mon. Wea. Rev.*, 119:1303–1307.

- Tréguier, A., Held, I., and Larichev, V. (1997). Parameterization of quasigeostrophic eddies in primitive equation ocean models. *J. Phys. Oceanogr.*, 27:567–580.

- Troen, I. and Mahrt, L. (1986). A simple model of the atmosphere boundary layer; sensitivity to surface evaporation. *Boundary Layer Meteorology*, 37:129–148.

- Valcke, S. (2006). Oasis3 user guide (prism 2-5). *PRISM Support Initiative*, 3:68 pp.

- Verseghy, D. (1991). CLASS - a Canadian Land Surface Scheme for GCMs. 1. Soil model. *Int. J. Climatol.*, 11:111–133.

- Weill, A., Eymard, L., Caniaux, G., Hauser, D., Planaton, S., Dupuis, H., Brut, A., C.Guerin, P.Nacass, Butet, A., Cloché, S., Pedreros, R., Durand, P., Bourras, D., Giordani, H., Lachaud, G., and Bouhours, G. (2003). Toward a better determination of turbulent air-sea fluxes from several experiments. *Journal of Climate*, 16:600–618.

- Williamson, D. and Rosinski, J. (2000). Accuracy of reduced grid calculations. *Quart. J. Roy. Meteor. Soc.*, 126:1619–1640.

- Yamada, T. and Mellor, G. (1975). A simulation of the wangara atmospheric boundary layer data. *J. Atmos. Sci.*, 32:2309–2329.

- Yessad, K. (2007a). Full-pos in the cycle 32 of ARPEGE/IFS. *ARPEGE Technical Documentation*, 79 pp.

- Yessad, K. (2007b). Horizontal diffusion computations in the cycle 32 of ARPEGE/IFS. *ARPEGE Technical Documentation*, 21 pp.

- Yessad, K. (2007c). Semi-implicit spectral computations and predictor-corrector schemes in the cycle 32 of ARPEGE/IFS. *ARPEGE Technical Documentation*, 42 pp.

- Yessad, K. (2007d). Semi-lagrangian computations in the cycle 32 of ARPEGE/IFS. *ARPEGE Technical Documentation*, 100 pp.

- Yessad, K. (2007e). Spectral transforms in the cycle 32 of ARPEGE/IFS. *ARPEGE Technical Documentation*, 32 pp.